DOT/FAA/AR-00/56

Office of Aviation Research
Washington, D.C. 20591

Vertical Drop Test of a Narrow-Body Transport Fuselage Section With a Conformable Auxiliary Fuel Tank Onboard

Allan Abromowitz
Timothy G. Smith
Dr. Tong Vu

September 2000

Final Report

This document is available to the U.S. public through the National Technical Information Service (NTIS), Springfield, Virginia 22161.

U.S. Department of Transportation
Federal Aviation Administration

NOTICE

Technical Report Documentation Page

1. Report No.	2. Government Accession No.	3. Recipient's Catalog No.
DOT/FAA/AR-00/56		

4. Title and Subtitle	5. Report Date
VERTICAL DROP TEST OF A NARROW-BODY TRANSPORT FUSELAGE SECTION WITH A CONFORMABLE AUXILIARY FUEL TANK ONBOARD	September 2000
	6. Performing Organization Code
7. Author(s) Allan Abramowitz, Timothy G. Smith, and Dr. Tong Vu	8. Performing Organization Report No.
9. Performing Organization Name and Address Federal Aviation Administration Airframe Structures Section, AAR-431 William J. Hughes Technical Center Atlantic City International Airport, NJ 08405	10. Work Unit No. (TRAIS) 11. Contract or Grant No.
12. Sponsoring Agency Name and Address U.S. Department of Transportation Federal Aviation Administration Office of Aviation Research Washington, DC 20591	13. Type of Report and Period Covered Final Report July 1999-July 2000 14. Sponsoring Agency Code ANM-100

15. Supplementary Notes

The FAA William J. Hughes Technical Center Crashworthiness Project Manager was Gary Frings

16. Abstract

A narrow-body transport airplane fuselage section was subjected to a vertical impact drop test at the Federal Aviation Administration (FAA) William J. Hughes Technical Center located at the Atlantic City International Airport, New Jersey. The objective of the test was to determine the interaction between a typical transport airplane fuselage, particularly its floor structure, and a conformable auxiliary fuel tank under severe, but survivable, impact conditions. The fuel tank used in this test is representative of tanks being installed in narrow-body transport airplanes. A 10-foot airframe section from a Boeing 737-200 airplane was dropped from a height of 14 feet, generating a vertical impact velocity of 30 ft/sec. The airframe test section, at a weight of 8780 pounds, simulated the load density at the maximum takeoff weight condition. The weight included cabin seats, dummy occupants, and simulated fuel in the 500-gallon fuel tank. Structural response data were obtained during the impact from instrumentation installed on the fuselage structure, floor structure, and the fuel tank.

The fuselage test section sustained severe damage after the test. Portions of the cabin floor were damaged due to the impact with the auxiliary fuel tank located in the cargo compartment. The bottom of the fuel tank was punctured in numerous locations resulting in fuel spillage. The strength and rigidity of the fuel tank limited the inherent ability of the fuselage structure to absorb energy crushing during the impact.

17. Key Words	18. Distribution Statement
Crash testing, Vertical impact, Drop test, Auxiliary fuel tank, Dynamic testing, Acceleration, Airplane	This document is available to the public through the National Technical Information Service (NTIS) Springfield, Virginia 22161.

19. Security Classif. (of this report)	20. Security Classif. (of this page)	21. No. of Pages	22. Price
Unclassified	Unclassified	147	

Form DOT F1700.7 (8-72) Reproduction of completed page authorized

ACKNOWLEDGMENTS

The authors would like to thank Mr. Stephen Soltis, the Federal Aviation Administration's National Resource Specialist for Crash Dynamics, for his technical direction during this test.

They would also like to thank Mr. Anthony Dang, airframe and powerplant technician, for his invaluable assistance.

TABLE OF CONTENTS

LIST OF ILLUSTRATIONS

LIST OF TABLES

EXECUTIVE SUMMARY

A narrow-body transport airplane fuselage section was subjected to a vertical impact drop test at the Federal Aviation Administration (FAA) William J. Hughes Technical Center located at the Atlantic City International Airport, New Jersey. The objective of the test was to determine the interaction between a typical transport airplane fuselage, particularly its floor structure, and a conformable auxiliary fuel tank under severe, but survivable, impact conditions. The fuel tank used in this test is representative of tanks being installed in narrow-body transport airplanes. A 10-foot airframe section from a Boeing 737-200 airplane was dropped from a height of 14 feet, generating a vertical impact velocity of 30 ft/sec. The airframe test section weight of 8780 pounds simulated the load density at the maximum takeoff weight condition. The weight included cabin seats, dummy occupants, and simulated fuel in the 500-gallon fuel tank. Structural response data were obtained during the impact from instrumentation installed on the fuselage structure, floor structure, and the fuel tank. Seventeen cameras recorded the test.

The fuselage test section sustained severe damage after the test. Portions of the cabin floor were damaged due to the impact with the auxiliary fuel tank located in the cargo compartment. Portions of the fuselage bottom were crushed by approximately 2 feet. The bottom of the fuel tank was punctured in numerous locations causing fuel to leak out. The strength and rigidity of the fuel tank limited the inherent ability of the fuselage structure to absorb energy crushing during the impact.

INTRODUCTION

This report presents the results of a vertical drop test of a narrow-body transport airplane fuselage section conducted at the Federal Aviation Administration (FAA) William J. Hughes Technical Center at Atlantic City International Airport, New Jersey. The objective of the test was to determine the interaction between a typical transport airplane fuselage, particularly its floor structure, and a conformable auxiliary fuel tank under severe, but survivable, impact conditions. The fuel tank used in this test is representative of tanks being installed in narrow-body transport airplanes. A 10-foot airframe section from a Boeing 737-200 was dropped from a height of 14 feet to simulate an impact velocity of 30 ft/sec. This is consistent with the vertical velocity change found in the Seat Dynamic Performance Standard in 14 CFR Part 25 paragraph 25.562(b)(1) [1]. The airframe section was configured to simulate the load density at the maximum takeoff weight condition. The weight included cabin seats, dummy occupants, and simulated fuel in a 500-gallon conformable auxiliary fuel tank. Structural response data were obtained during impact from instrumentation installed on the fuselage structure, floor structure, and the fuel tank.

BACKGROUND

The FAA has developed a Crash Dynamics and Engineering Development Program [2]. This vertical drop test is one of a series of transport airframe section tests conducted in support of the FAA's program. Such tests included the vertical drop test of a transport airframe section [3], the longitudinal impact test of a transport airframe section [4], the longitudinal acceleration test of overhead stowage bins in a transport airframe section [5], the vertical drop test of a transport fuselage section with overhead stowage bins and auxiliary fuel tank on board [6], and the longitudinal acceleration tests of overhead stowage bins and auxiliary fuel tank in a transport airplane airframe section [7]. All the tests were conducted under severe but survivable impact conditions. The vertical drop test [3] and the longitudinal impact test [4] determined the interaction between the transport airplane fuselage section, floor structure, and cabin interior components. The longitudinal test [5] identified the interaction between a transport airplane fuselage section and the overhead stowage bins. The vertical impact test [6] showed the dynamic response characteristics of the fuselage section, the onboard overhead stowage bins, and the double-wall auxiliary fuel tank system. The longitudinal test [7] presented the structural response and interaction between a transport airplane fuselage section, overhead stowage bins, and conformable auxiliary fuel tank system.

DESCRIPTION OF TEST FACILITY AND TEST ARTICLE

TEST FACILITY.

The drop test facility is comprised of two 57-foot vertical steel towers connected at the top by a horizontal platform (figures 1 and 2). An electrically powered winch, mounted on the platform and attached to a reeved hoisting cable, is used to raise and lower the test article. A sheave block assembly hanging from the free end of the reeved cable is attached to a solenoid-operated release hook. The airplane is connected to the release hook by a cable/turnbuckle assembly which is bolted to the fuselage section at four locations. Located below the winch cable assembly and

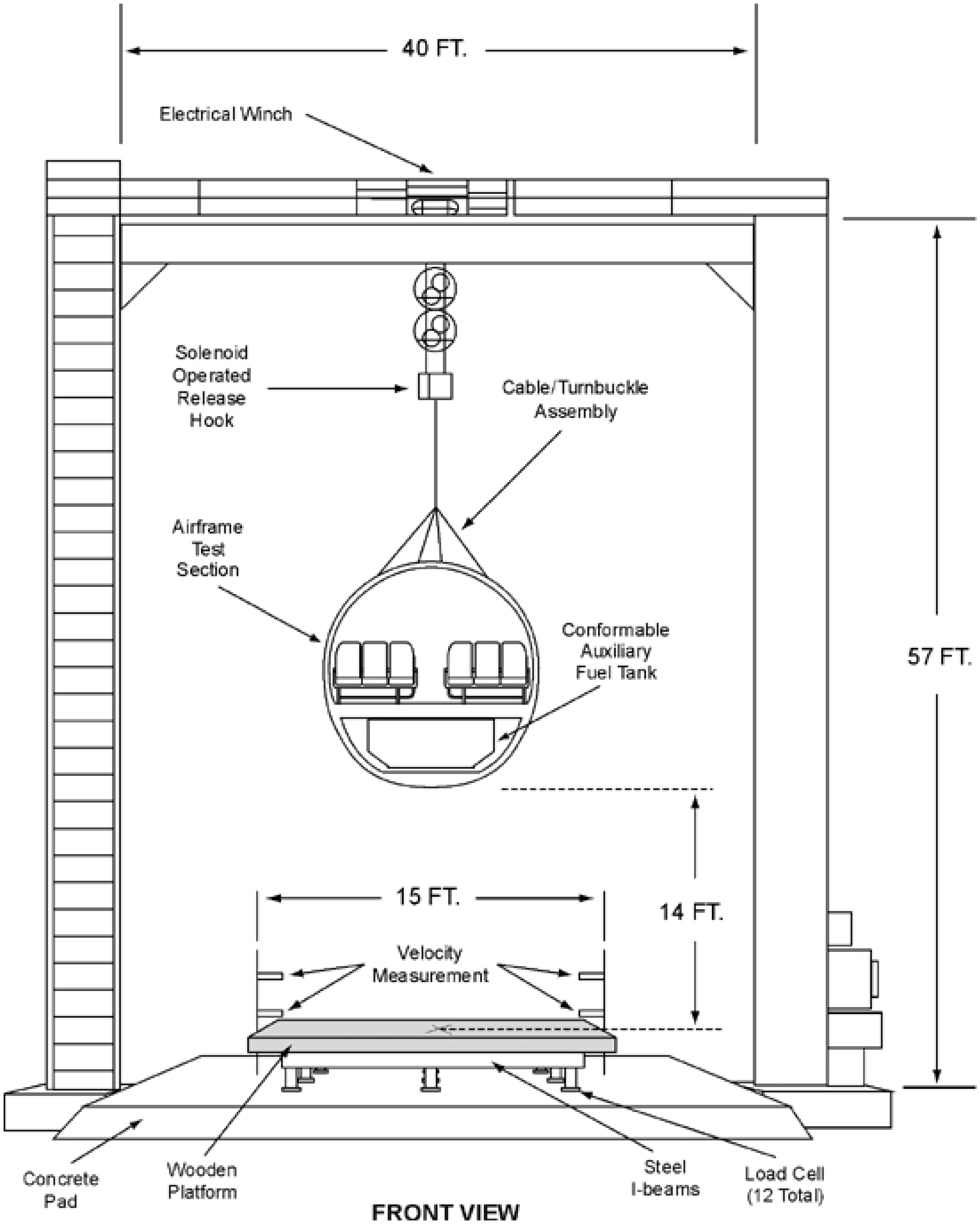

FIGURE 1. DYNAMIC DROP TEST FACILITY DIAGRAM

between the tower legs is a 15 by 36.5-foot wooden platform which rests upon steel I-beams and is supported by 12 load cells.

FIGURE 2. DYNAMIC DROP TEST FACILITY

TEST ARTICLE.

The test article was a 10-foot section cut from fuselage station (FS) 400 to FS 500A from a Boeing 737-200 transport airplane (figure 3). The test section included a below-floor cargo compartment with an access door located on the right (copilot) side (figure 4). The outer floor beams at each of end of the test section were reinforced (figure 4) to minimize the open-end effects, i.e., to simulate the reaction that would be seen if an entire aircraft fuselage was tested. Nonstructural interior liners and insulation were removed from the airframe test section. The section was equipped with typical cabin seats and a conformable auxiliary fuel tank system.

The cabin section was configured with six triple cabin seats placed in three rows. Two different cabin seats were used in the test. UOP seats (model 830-820B-3R) were installed on the right side at a 36-inch pitch, and Weber Aircraft seats (part # 829633-405) were mounted on the left side at a 35-inch pitch. For the purpose of this report, the seats were numbered as shown in figure 5. All the seats were “9 g-rated seats” and contained a mannequin or an anthropomorphic test dummy (ATD). The ATDs are of the Hybrid II type, manufactured to represent the 50th percentile male adult passenger. Table 1 gives the description of the seats and the ATD locations by fuselage station. The seats, dummies, and mannequins were used to achieve the desired test section weight and provide comparative data to other tests; they were not of primary interest in this test.

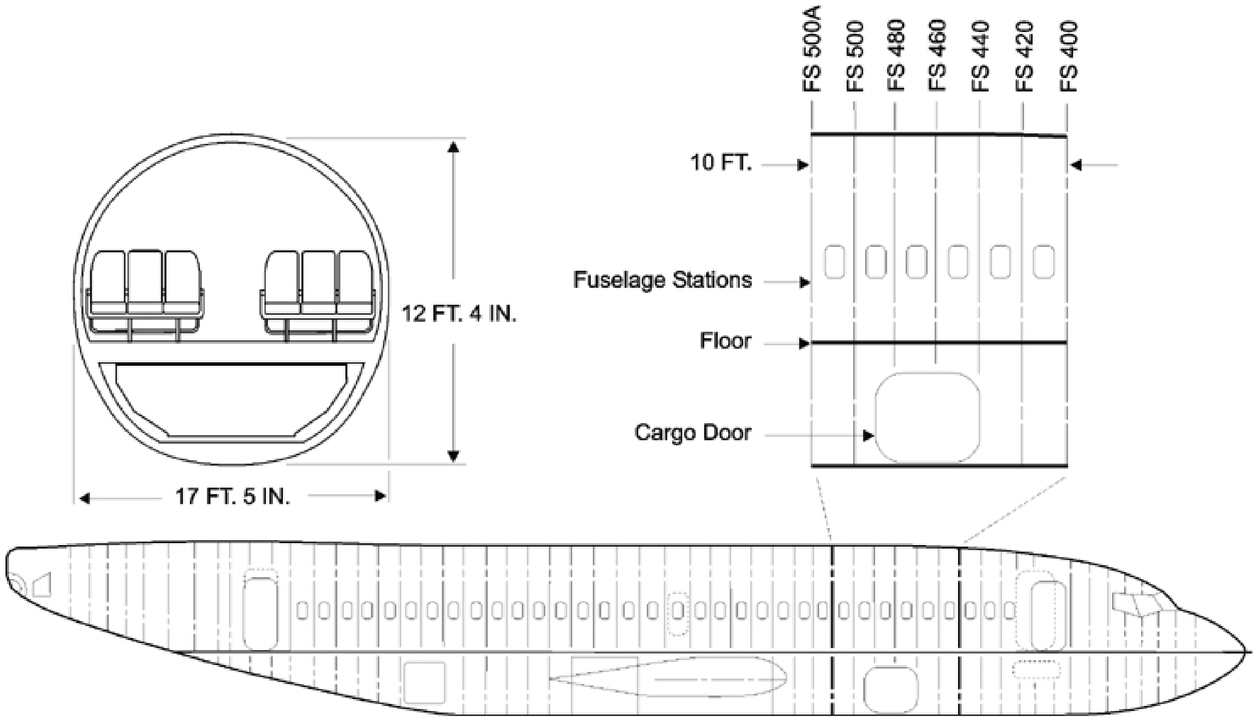

FIGURE 3. AIRFRAME TEST SECTION
(From a Boeing 737-200 Airplane)

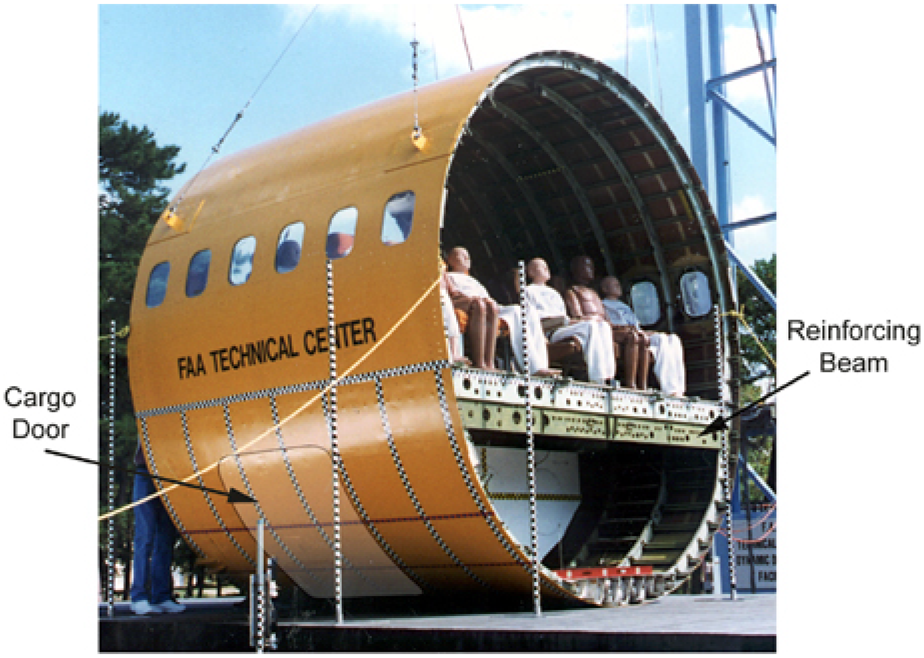

FIGURE 4. TEST SECTION—SHOWING CARGO DOOR AND REINFORCING BEAM

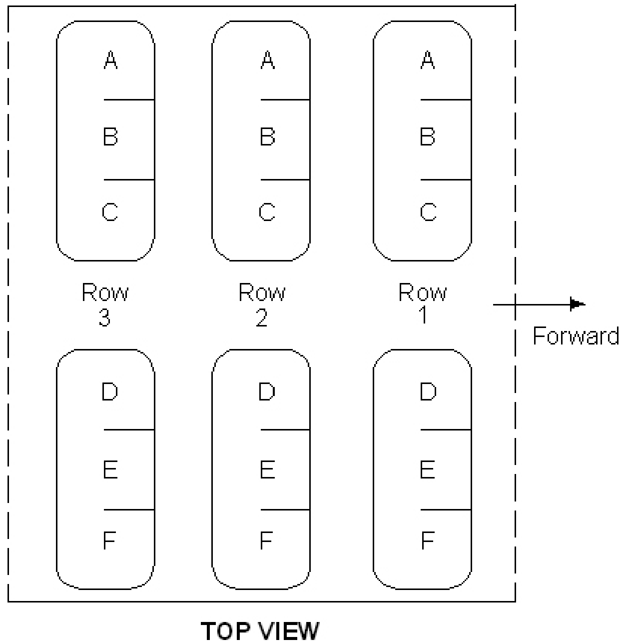

FIGURE 5. TEST SECTION—SEAT NUMBERING SCHEME

TABLE 1. SEAT AND ANTHROPOMORPHIC TEST DUMMY LOCATIONS

Location	Seat Description	Seat Number	Occupants
FS 426 (Row 1)	Left Side Weber Aircraft Seat	A	Mannequin
		B	ATD #1
		C	Mannequin
	Right Side UOP Seat	D	Mannequin
		E	ATD #2
		F	Mannequin
FS 462 (Row 2)	Left Side Weber Aircraft Seat	A	Mannequin
		B	ATD #3
		C	Mannequin
	Right Side UOP Seat	D	Mannequin
		E	ATD #4
		F	Mannequin
FS 498 (Row 3)	Left Side Weber Aircraft Seat	A	Mannequin
		B	ATD #5
		C	Mannequin
	Right Side UOP Seat	D	Mannequin
		E	ATD #6
		F	Mannequin

The auxiliary fuel tank system consisted of a 500-gallon conformable tank (figure 6), two longitudinal mounting rails, and two longitudinal aluminum straps. The rails were located on the right and left sides, mounted to the underside of the cabin floor beams at FS 440 through FS 500.

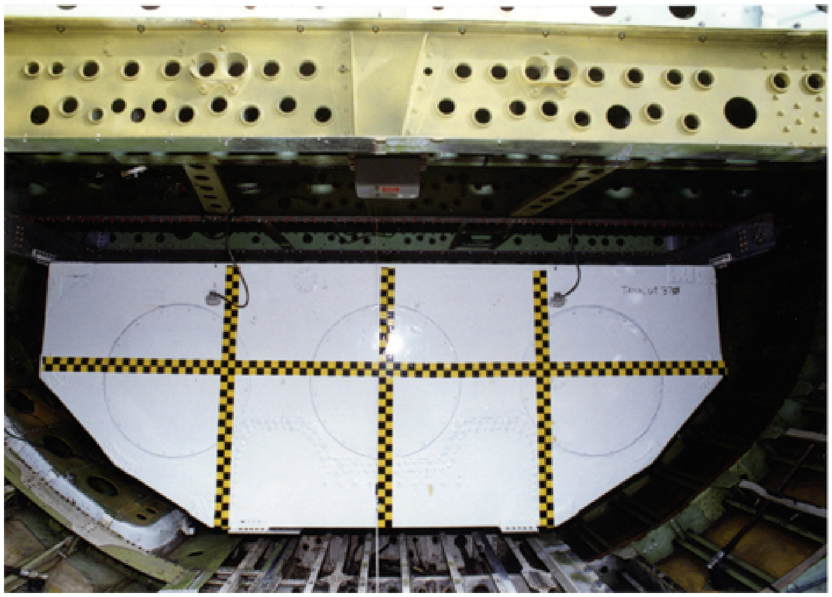

FIGURE 6. FIVE HUNDRED-GALLON CONFORMABLE AUXILIARY FUEL TANK

The fuel tank hung from the rails (figures 7, 8, 9, and 10) and was suspended between FS 446 and FS 489. The tank was prevented from moving by the bearing blocks (figure 11) mounted on the rails at FS 445 and FS 490 and the two aluminum straps. One end of the strap was attached to the bottom of the tank; the other end was mounted to the cargo compartment floor. The tank contained 404 gallons of water to simulate the weight of a full tank of fuel and was pressurized to 1.0 psi. All fuel ports on the tank were capped. No fuel lines were used in the test.

The test article also contained four onboard cameras and one onboard data acquisition system which are discussed in the instrumentation section.

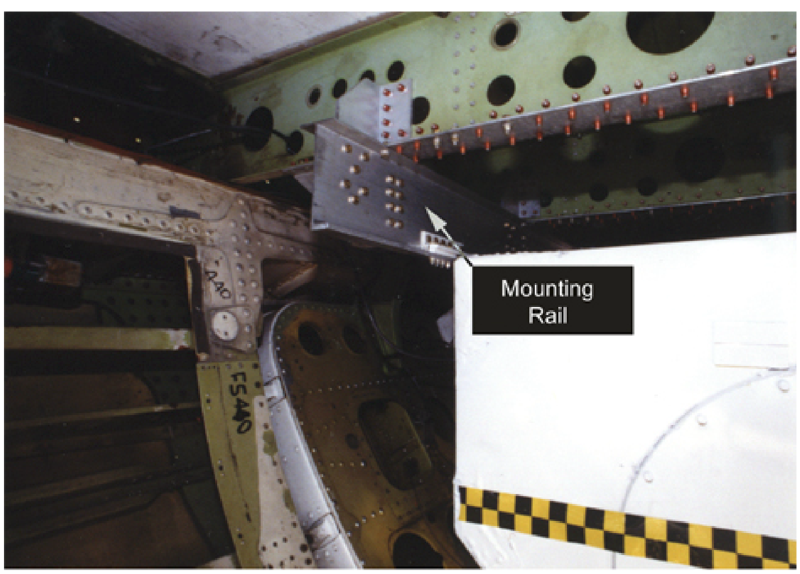

FIGURE 7. FUEL TANK MOUNTING SYSTEM—RIGHT FRONT

FIGURE 8. FUEL TANK MOUNTING SYSTEM—LEFT FRONT

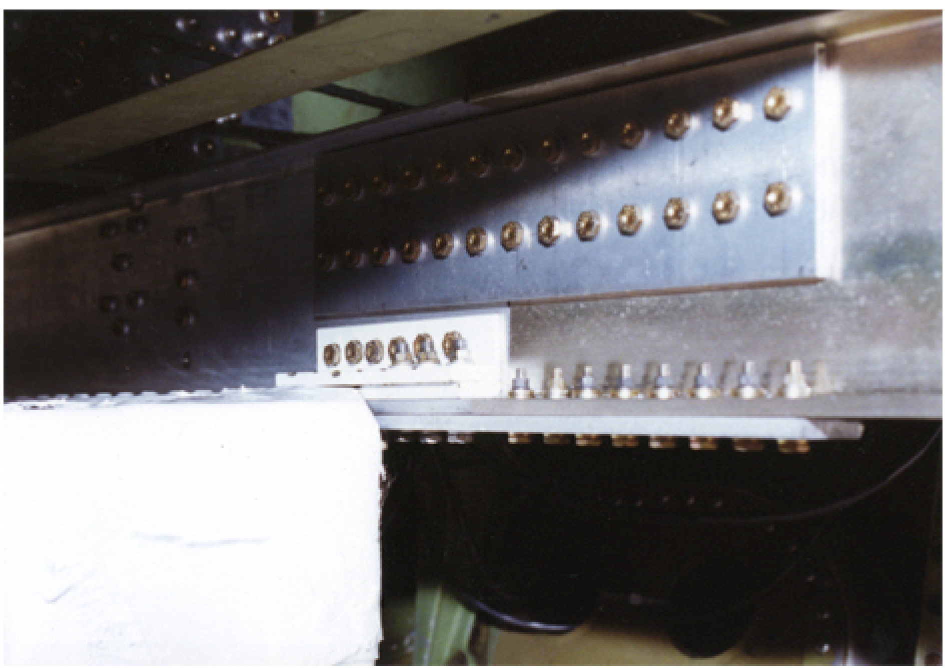

FIGURE 9. FUEL TANK MOUNTING SYSTEM—RIGHT REAR

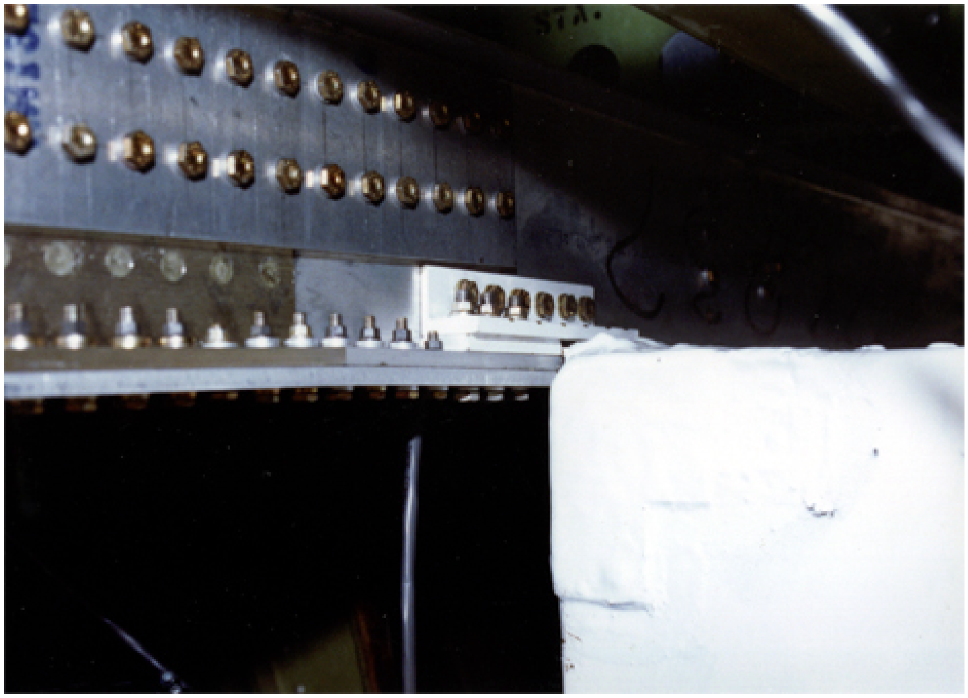

FIGURE 10. FUEL TANK MOUNTING SYSTEM—LEFT REAR

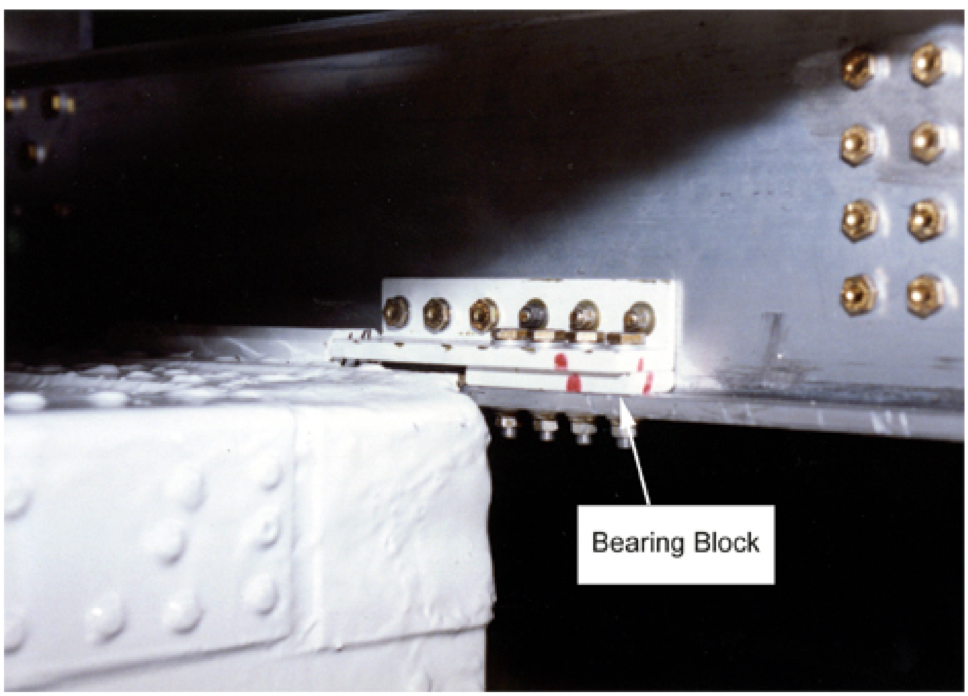

FIGURE 11. FUEL TANK MOUNTING SYSTEM—CLOSE-UP

The total weight of the test article was 8780 pounds. The individual item weights are presented in table 2.

TABLE 2. TEST ARTICLE WEIGHT

Item	Weight (lb)	Quantity	Total (lb)
ATD	170	6	1020
Mannequin	161	12	1932
Cameras	22	4	88
UOP Seat	80	3	240
Weber Aircraft Seat	68	3	204
Fuel Tank (empty)	370	1	370
Fuel (water)	8.342/gal.	404 gal.	3370
Fuselage	1317	1	1317
Camera mounting plate	45	1	45
Data Acquisition System and mount	36	1	36
Miscellaneous	158	1	158
TOTAL			8780

TEST ARTICLE AND DROP TEST PLATFORM ORIENTATION.

The test article and drop test platform were centered below the drop tower. The coordinate systems for both were referenced while standing in and looking toward the front of test article. The fuselage coordinate system is per manufacturer's specifications; and a location is represented by the distance (inches) from a reference. Thus, FS 420 is denoted as being located +420 inches from the reference point. In this particular test article, the last frame is technically denoted as FS 500A. This corresponds to a distance of +520 inches from the reference point. Distances measured in the lateral direction (left -x and right +x) are referenced from the longitudinal centerline. The relative height is referenced from the surface of the cabin floor (above floor +z, below -z). The reference point for the platform is the intersection of the geometric center of its length and width, and the surface of the platform (corresponding to the x, y, and z-axes, respectively). Positive directions are forward (+x), right (+y), and up (+z).

TEST INITIATION

Prior to the test, the four supporting cable/turnbuckle assemblies were adjusted to level the fuselage forward to aft and left to right. The fuel tank was pressurized with air to 1.0 psi to simulate operating conditions. The data acquisition systems were started and the test article was raised 14 feet above the surface of the platform (measured from the bottom of the fuselage). Four guide ropes, manned by members of the drop test team, steadied the airplane while it hung above the platform. When the test article was steady and level, the automatic timing sequence was started. The high-speed film cameras and video cameras were activated and two seconds later, the test article was released. The wind prior to and during the test was calm.

INSTRUMENTATION

FUSELAGE.

The descriptions and locations of all the instrumentation used during the test are shown in figures 12 and 13 and listed in table 3. The fuselage was divided into two areas: the cargo area, which consists of the area beneath the cabin floor including the floor beams, and the cabin area consisting of the cabin floor and the area above it. The fuselage instrumentation for this test included 57 Endevco model 7231C-750 accelerometers and two Celesco model PT 101-0040 string potentiometers. The accelerometers in the cargo area were located on the fuselage sidewall frames, cargo floor, and cabin floor beams (figure 12). The string potentiometers were mounted to the cabin floor beams and attached to the cargo floor frames to measure the distance associated with the cargo floor crushing. The accelerometers in the cabin area were located on the sidewall frame sections at three levels: floor level—one inch above the floor, lower level—12 inches above the floor, and the upper level—64 or 70 inches above the floor. The upper accelerometers were located in the area where the overhead stowage bin mounting brackets would normally be located. Two accelerometers were mounted at the crown area of the fuselage. The sensor locations selected were deemed to be the most suitable to characterize the fuselage response and its affect on the occupants, provide comparative data with other tests, and support crash modeling research. The following sensors supplied data for the two latter objectives: crown accelerometers, cabin area—floor-level accelerometers, and cargo area ceiling accelerometers located at FS 420 and FS 500 (not above the fuel tank).

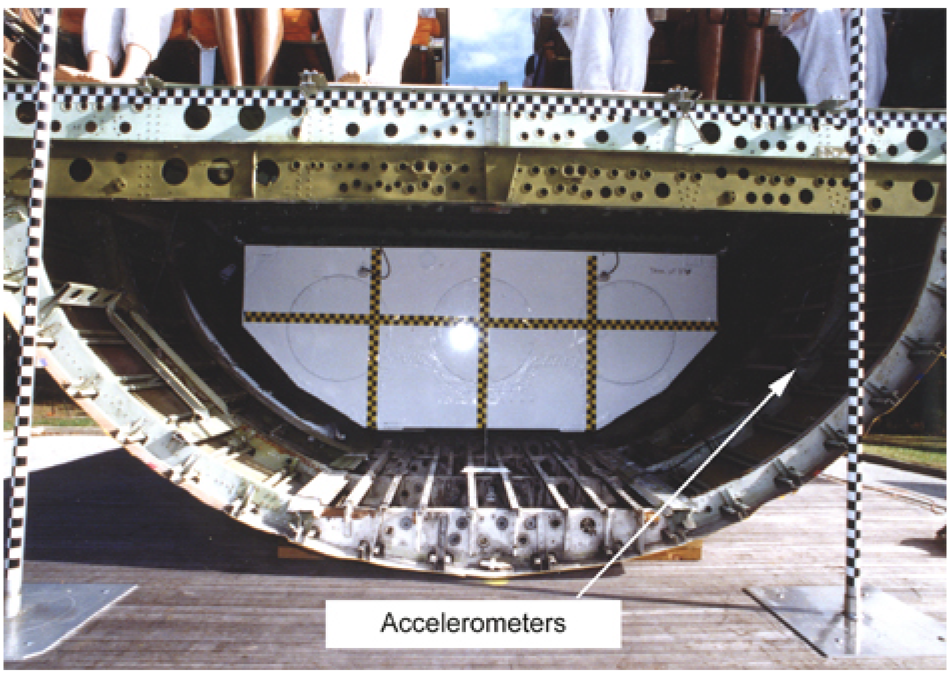

FIGURE 12. CARGO AREA ACCELEROMETER LOCATION

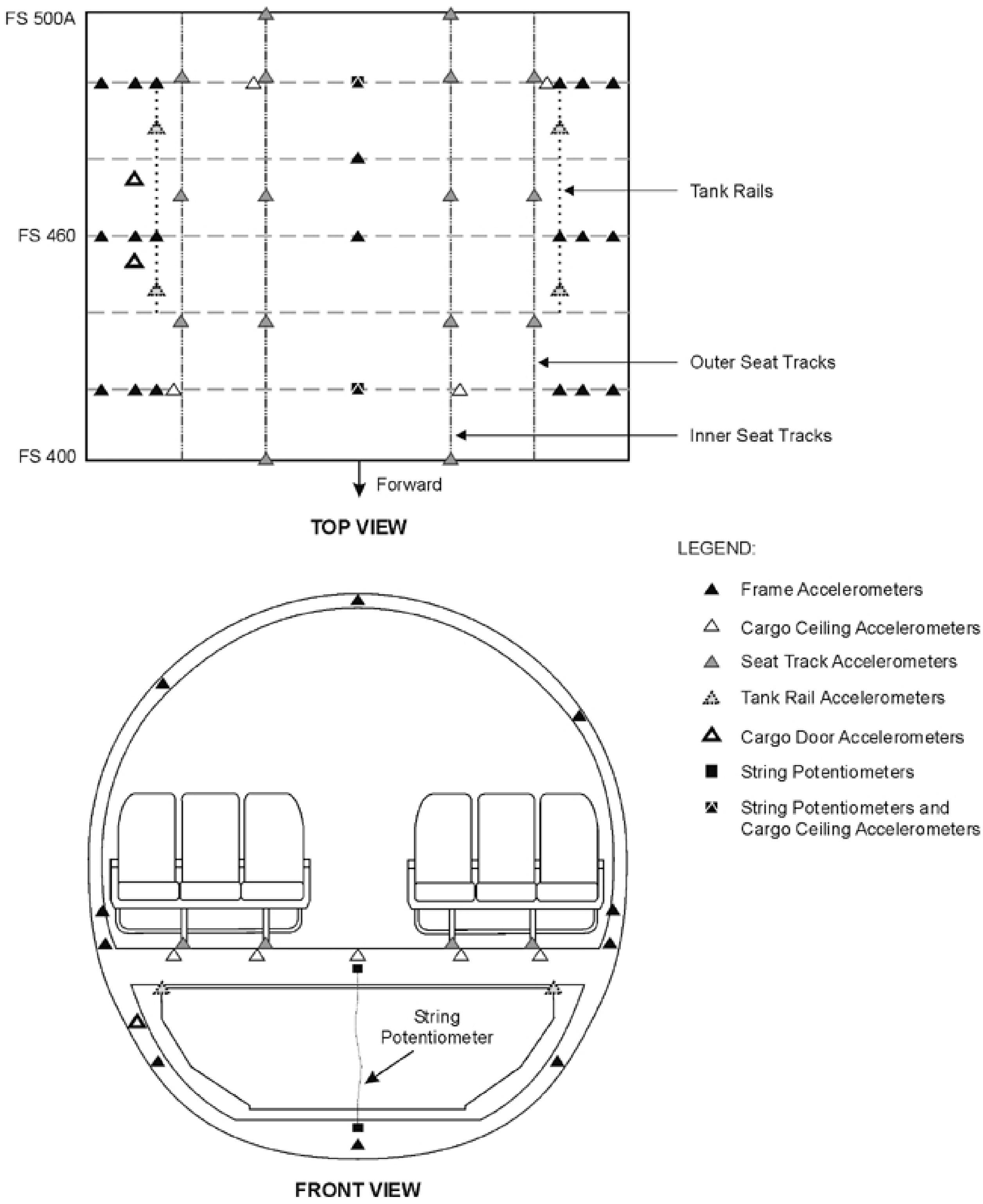

FIGURE 13. TEST ARTICLE SENSOR LOCATIONS

TABLE 3. DATA ACQUISITION SYSTEMS—CONFIGURATIONS AND SENSOR LOCATIONS

Channel NEFF 490	Description	Sensor Mfg-Model	Range ±	Unit	Location		
					X	Y	Z
101	FS 420 CA-L SW	Endevco 7231C-750	201	g	420	-52	-34
102	FS 420 CA-C Floor	Endevco 7231C-750	203	g	420	0	-54
103	FS 420 CA-C String Pot	Celesco PT 101-0020	20	inch	420	0	-10/-51
104	FS 420 CA-R SW	Endevco 7231C-750	200	g	420	52	-34
109	FS 460 CA-L SW	Endevco 7231C-750	195	g	460	-52	-34
110	FS 487 CA-L Rail	Endevco 7231C-750	139	g	487	-51	-11
111	FS 500 CA-L Ceiling	Endevco 7231C-750	206	g	500	-45	-1
112	FS 446 CA-L Front Tank	Endevco 7231C-750	198	g	446	-24	-17
113	FS 457 CA-R Side Tank	Endevco 7231C-750	206	g	457	48	-18
114	FS 478 CA-L Side Tank	Endevco 7231C-750	206	g	478	-48	-18
115	FS 489 CA-R Rear Tank	Endevco 7231C-750	203	g	489	24	-17
201	Platform Accel. #1	Endevco 2262A-200	200	g	18' 2"	-5' 6"	-11"
202	Platform String Pot #1	Celesco PT 101-0020	10	inch	18' 2"	-5' 6"	-11"/-3'2"
203	Platform Loadcell #1B	Sensotec 41	50000	lb	18' 2"	-5'	-2' 8"
204	Platform Accel. #2	Endevco 2262A-200	200	g	18' 2"	-4"	-11"
205	Platform Accel. #3	Endevco 2262A-200	200	g	18' 2"	5' 6"	-11"
206	Platform String Pot #2	Celesco PT 101-0020	10	inch	18' 2"	5' 6"	-11"/-3'2"
207	Platform Loadcell #3B	Sensotec 41	50000	lb	18' 2"	5'	-2' 8"
208	Platform Loadcell #2B	Sensotec 41	50000	lb	18' 2"	0	-2' 8"
209	Platform Accel. #6	Endevco 2262A-200	200	g	6'	5' 6"	-11"
210	Platform Loadcell #6A	Interface 1231 BMZ	100000	lb	6'	5'	-2' 8"
211	Platform Loadcell #6B	Interface 1231BMZ	100000	lb	6'	5'	-2' 8"
212	Platform Accel #9	Endevco 2262A-200	200	g	-6'	5' 6"	-11"
213	Platform Accel #4	Endevco 2262A-200	200	g	6'	-5' 6"	-11"
214	Platform Loadcell #4A	Interface 1231BMZ	100000	lb	6'	-5'	-2' 8"
215	Platform Loadcell #4B	Interface 1231BMZ	100000	lb	6'	-5'	-2' 8"
216	Platform Accel #5	Endevco 2262A-200	200	g	6' 5"	-4"	-11"
217	Platform String Pot #3	Celesco PT 101-0020	5	inch	6' 5"	-4"	-11"/-3'2"
218	Platform Loadcell #5A	Interface 1241BMZ	250000	lb	6'	0	-2' 8"
219	Platform Loadcell #5B	Interface 1241BMZ	250000	lb	6'	0	-2' 8"
220	Platform Accel #8	Endevco 2262A-200	200	g	-6' 5"	-4"	-11"
221	Platform String Pot #4	Celesco PT 101-0020	5	inch	-6' 5"	-4"	-11"/-3'2"
222	Platform Loadcell #8A	Interface 1241 BMZ	250000	lb	-6'	0	-2' 8"
223	Platform Loadcell #8B	Interface 1241BMZ	250000	lb	-6'	0	-2' 8"
224	Platform Accel #7	Endevco 2262A-200	200	g	-6'	-5' 6"	-11"
225	Platform Loadcell #9B	Interface 1231 BMZ	100000	lb	-6'	5'	-2' 8"
226	Platform Loadcell #7B	Interface 1231BMZ	100000	lb	-6'	-5'	-2' 8"
227	Platform Loadcell #9A	Interface 1231BMZ	100000	lb	-6'	5'	-2' 8"
228	FS 420 CB-L Upper SW	Endevco 7231C-750	202	g	420	-57	64
229	FS 420 CB-L Lower SW	Endevco 7231C-750	167	g	420	-68	13
230	FS 420 CB-L Floor	Endevco 7231C-750	144	g	420	-67	1
231	FS 438 CB-L Inner ST	Endevco 7231C-750	175	g	438	-23	1

TABLE 3. DATA ACQUISITION SYSTEMS—CONFIGURATIONS AND SENSOR LOCATIONS (Continued)

Channel NEFF 490	Description	Sensor Mfg-Model	Range ±	Unit	Location X	Y	Z
301	FS 400 CB-R Inner ST	Endevco 7231C-750	189	g	400	23	1
302	FS 420 CB-C Crown	Endevco 7231C-750	143	g	420	0	93
303	FS 426 CB-R ATD #2 LDCL	R. Denton 1707	5000	lb	426	36	24
304	FS 426 CB-R ATD #2	Endevco 7231C-750	133	g	426	36	20
305	FS 420 CB-R Floor	Endevco 7231C-750	190	g	420	67	1
306	FS 420 CB-R Lower SW	Endevco 7231C-750	199	g	420	68	12
307	FS 420 CB-R Upper SW	Endevco 7231C-750	199	g	420	51	70
308	FS 438 CB-R Outer ST	Endevco 7231C-750	134	g	438	44	1
309	FS 460 CB-L Upper SW	Endevco 7231C-750	234	g	460	-57	64
310	FS 460 CB-L Lower SW Y-Dir	Endevco 7231C-750	200	g	460	-68	12
311	FS 460 CB-L Lower SW	Endevco 7231C-750	143	g	460	-68	13
312	FS 460 CB-L Floor	Endevco 7231C-750	197	g	460	-67	2
313	FS 462 CB-L ATD #3 LDCL	R. Denton 1708	5000	lb	462	-36	24
314	FS 463 CB-L ATD #3	Endevco 7231C-750	140	g	462	-36	20
315	Wind Speed Anemometer	Micro Response 2031					
401	FS 472 CB-L Outer ST X-Dir	Endevco 7231C-750	145	g	472	-44	1
402	FS 472 CB-L Outer ST Y-Dir	Endevco 7231C-750	202	g	472	-44	1
403	FS 472 CB-L Inner ST	Endevco 7231C-750	200	g	472	-23	1
404	FS 500 CB-L Floor	Endevco 7231C-750	199	g	500	-67	1
405	FS 472 CB-R Outer ST	Endevco 7231C-750	203	g	472	44	1
406	FS 500 CB-R Upper SW	Endevco 7231C-750	214	g	500	51	70
407	FS 500 CB-R Lower SW	Endevco 7231C-750	189	g	500	68	13
408	FS 500 CB-R Floor	Endevco 7231C-750	115	g	500	67	1
409	FS 504 CB-L Outer ST	Endevco 7231C-750	200	g	504	-44	1
410	FS 497 CB-L ATD #5 LDCL	R. Denton 1708	5000	lb	497	-36	24
411	FS 497 CB-L ATD #5	Endevco 7231C-750	145	g	497	-36	20
412	FS 518 CB-L Inner ST	Endevco 7231C-750	203	g	518	-23	1
413	FS 504 CB-R Inner ST	Endevco 7231C-750	192	g	504	23	1
414	FS 498 CB-R ATD #6 LDCL	R. Denton 1708	5000	lb	498	36	24
415	FS 498 CB-R ATD #6	Endevco 7231C-750	144	g	498	36	20
416	FS 456 CA-R Door	Endevco 7231C-750	201	g	456	57	-24
417	FS 476 CA-R Door	Endevco 7231C-750	202	g	476	57	-24
418	FS 500 CA-R SW	Endevco 7231C-750	197	g	500	52	-34
419	IRIG Generator 1PPS	True Time					
420	FS 420 CA-L Ceiling	Endevco 7231C-750	203	g	420	-25	-1
421	FS 420 CA-R Ceiling	Endevco 7231C-750	191	g	420	45	-1
422	FS 447 CA-R Rail	Endevco 7231C-750	199	g	447	51	-11
423	FS 460 CA-C Ceiling	Endevco 7231C-750	197	g	460	0	-7
424	Platform Accel #12	Endevco 2262A-200	200	g	-18' 2"	5' 6"	-11"/-3'2"
425	Platform String Pot #6	Celesco PT 101-0020	10	inch	-18' 2"	5' 6"	-2' 8"
426	Platform Loadcell #12B	Sensotec 41	50000	lb	-18' 2"	5'	-2' 8"
427	Platform Loadcell #11B	Sensotec 41	50000	lb	-18' 2"	0	-11"
428	Platform Accel #10	Endevco 2262A-200	200	g	-18' 2"	-5' 6"	-11"
429	Platform String Pot #5	Celesco PT 101-0020	10	inch	-18' 2"	-5' 6"	-11"/-3'2"
430	Platform Loadcell #10B	Sensotec 41	50000	lb	-18' 2"	-5'	-2' 8"
431	Platform Accel #11	Endevco 2262A-200	200	g	-18' 2"	-4"	-11"

TABLE 3. DATA ACQUISITION SYSTEMS—CONFIGURATIONS AND SENSOR LOCATIONS (Continued)

Channel DAS-48S	Description	Sensor Mfg/Model	Range ±	Unit	Location X	Location Y	Location Z
1	FS 400 CB-L Inner ST	Endevco 7231C-750	200	g	400	-23	1
2	IRIG Generator 1PPS	True Time					
3	FS 427 CB-L ATD #1	Endevco 7231C-750	100	g	427	-36	20
4	FS 438 CB-L Outer ST	Endevco 7231C-750	200	g	438	-44	1
5	FS 438 CB-R Inner ST	Endevco 7231C-750	200	g	438	23	1
6	FS 462 CB-R ATD #4 LDCL	Endevco 7231C-750	5000	lb	462	36	24
7	FS 463 CB-R ATD #4	Endevco 7231C-750	100	g	462	36	20
8	FS 460 CB-R Floor	Endevco 7231C-750	200	g	460	67	1
9	FS 460 CB-R Lower SW Y-Dir	Endevco 7231C-750	200	g	460	68	12
10	FS 460 CB-R Lower SW	Endevco 7231C-750	200	g	460	68	13
11	FS 460 CB-R Upper SW	Endevco 7231C-750	200	g	460	51	70
12	FS 472 CB-L Outer ST	Endevco 7231C-750	200	g	472	-44	1
13	FS 472 CB-R Inner ST	Endevco 7231C-750	200	g	472	23	1
14	FS 472 CB-R Outer ST X-Dir	Endevco 7231C-750	200	g	472	44	1
15	FS 472 CB-R Outer ST Y-Dir	Endevco 7231C-750	200	g	472	44	1
16	FS 500 CB-C Crown	Endevco 7231C-750	200	g	500	0	93
17	FS 500 CB-L Upper SW	Endevco 7231C-750	200	g	500	-57	64
18	FS 500 CB-L Lower SW	Endevco 7231C-750	200	g	500	-68	13
19	FS 504 CB-L Inner ST	Endevco 7231C-750	200	g	504	-23	1
20	FS 504 CB-R Outer ST	Endevco 7231C-750	200	g	504	44	1
21	FS 518 CB-R Inner ST	Endevco 7231C-750	200	g	518	23	1
22	FS 447 CA-L Rail	Endevco 7231C-750	200	g	447	-51	-11
23	FS 480 CA-C Ceiling	Endevco 7231C-750	200	g	480	0	-7
24	FS 487 CA-R Rail	Endevco 7231C-750	200	g	487	51	-11
25	FS 500 CA-L SW	Endevco 7231C-750	200	g	500	-52	-34
26	FS 500 CA-C Floor	Endevco 7231C-750	200	g	500	0	-54
27	FS 500 CA-R Ceiling	Endevco 7231C-750	200	g	500	25	-1
28	FS 446 CA-R Front Tank	Endevco 7231C-750	200	g	446	24	-17
29	FS 457 CA-L Side Tank	Endevco 7231C-750	200	g	457	-49	-18
30	FS 478 CA-R Side Tank	Endevco 7231C-750	200	g	478	49	-18
31	FS 489 CA-L Rear Tank	Endevco 7231C-750	200	g	489	-24	-17
32	FS 501 CA-C String Pot	Celesco PT 101-0020	2.7	inch	501	0	-10/-51
33	FS 427 CB-L ATD #1 LDCL	R. Denton 1708	5000	lb	427	-36	24

Note: Sensor excitation voltage equals 10 volts. See Test Article and Platform Orientation section for details on each coordinate system. All accelerometers are mounted in the z-direction unless otherwise noted. The units designating the distances from the reference are in inches unless otherwise noted. Platform locations are indicated with the inch (″) and foot symbol (′) to help differentiate them from the fuselage locations.

CB = Cabin Area   ST = Seat Track   L = Left   C = Center   R = Right
CA = Cargo Area   LDCL = Load Cell   SW = Sidewall

ANTHROPOMORPHIC TEST DUMMIES.

There were six 50th percentile Hybrid II anthropomorphic test dummies onboard. All of the ATDs were instrumented with load cells (Denton model 1708) to measure spinal column axial loading at the lumbar area and accelerometers (Endevco model 7231C-750) to measure g forces in the pelvic region. The ATDs were located in the center seats (B and E) at FS 426, 462, and 498 as noted in table 1 and shown in figures 14 and 15.

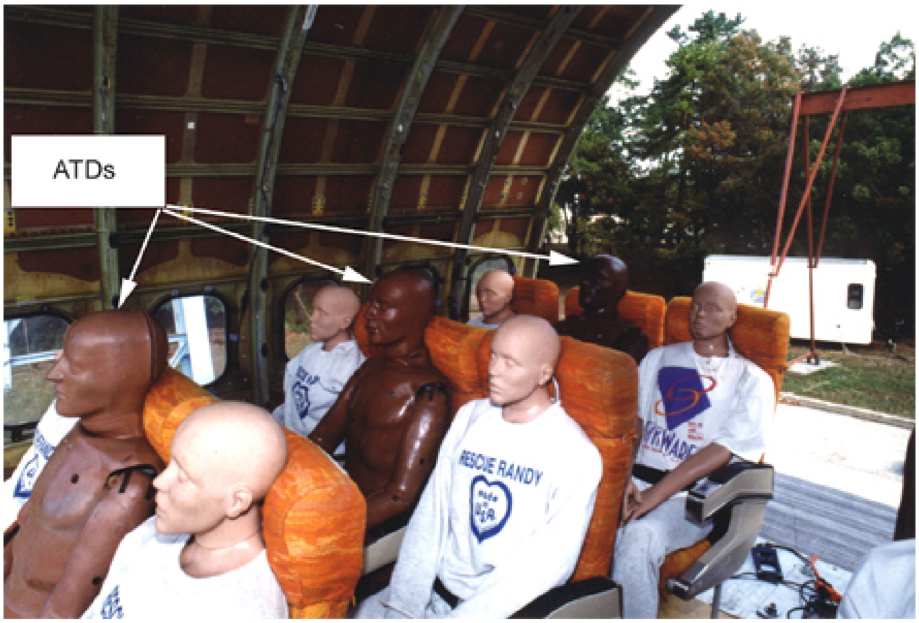

FIGURE 14. ATD LOCATION—RIGHT SIDE

FIGURE 15. ATD LOCATION—LEFT SIDE

DROP TEST PLATFORM.

The platform rested on six Sensotec model 41, four Interface model 1231, and two Interface model 1241 load cells with load capacities of 50,000, 100,000, and 200,000 pounds, respectively. All platform load cells were dual-output, denoted as A and B. The load cell locations are shown in figure 16. Prior to the drop test, the platform was leveled and the tare weight was electronically zero-balanced. The platform load cells were used to measure the impact loads and determine their distribution. The reaction forces generated during the impact of the airplane can then be determined from the data.

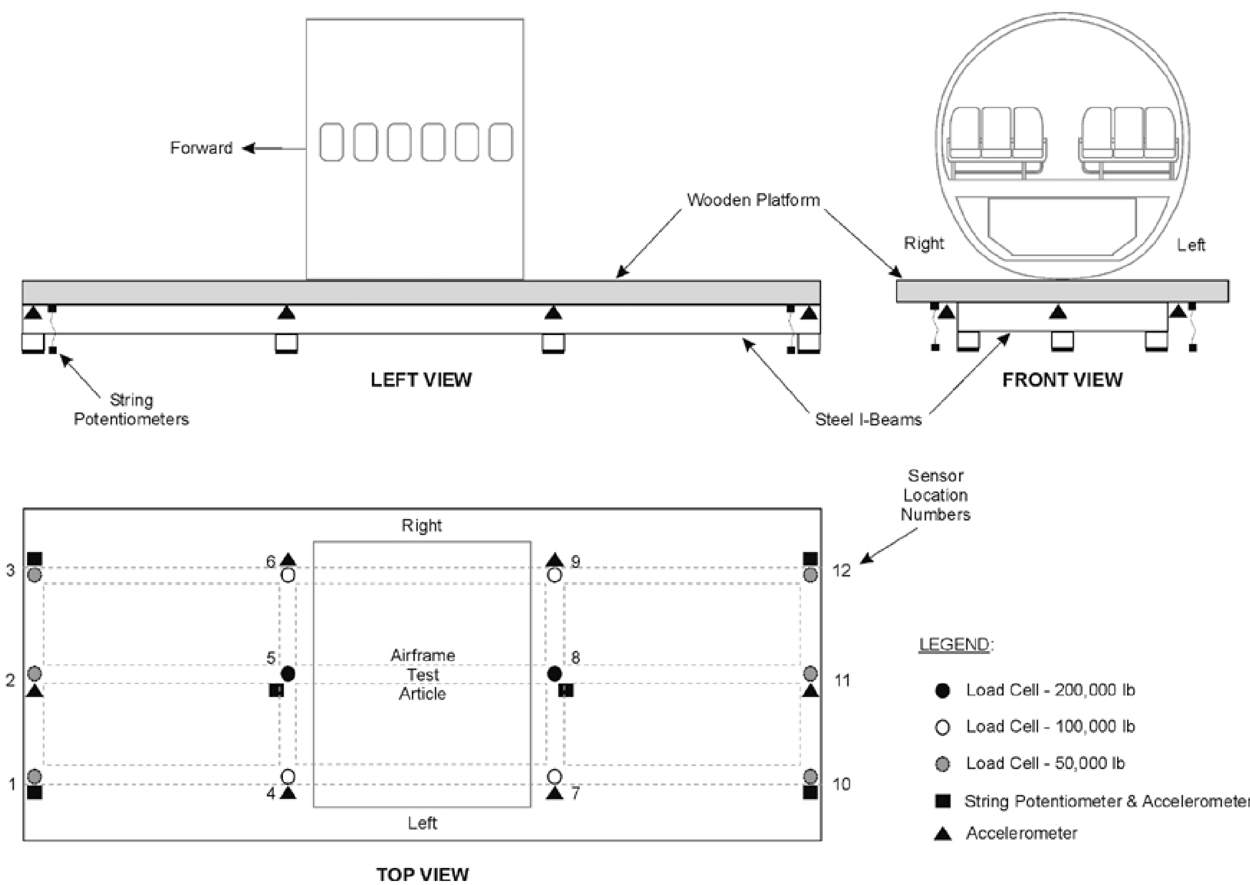

FIGURE 16. DROP TEST PLATFORM INSTRUMENTATION

Twelve Endevco model 2262A-200 accelerometers, numbered 1 through 12, were mounted on the bottom of the platform to characterize the platform response to the impact (figure 16). Platform response was measured because of the potential influence it may have on fuselage accelerometer readings.

Six Celesco model PT101-020 string potentiometers were attached to the platform to measure platform displacement (figure 16).

CONFORMABLE AUXILIARY FUEL TANK AND MOUNTING RAILS.

The fuel tank and rails were instrumented with 12 Endevco model 7231C-750 accelerometers. Two accelerometers were located on each side of the tank and two accelerometers were mounted on each rail. Each rail accelerometer was adjacent to a bearing block that secured the tank in place (figure 17). The fuel tank was pressurized via a portable air compressor. A dial-type pressure gage mounted on the tank was used to determine tank pressure.

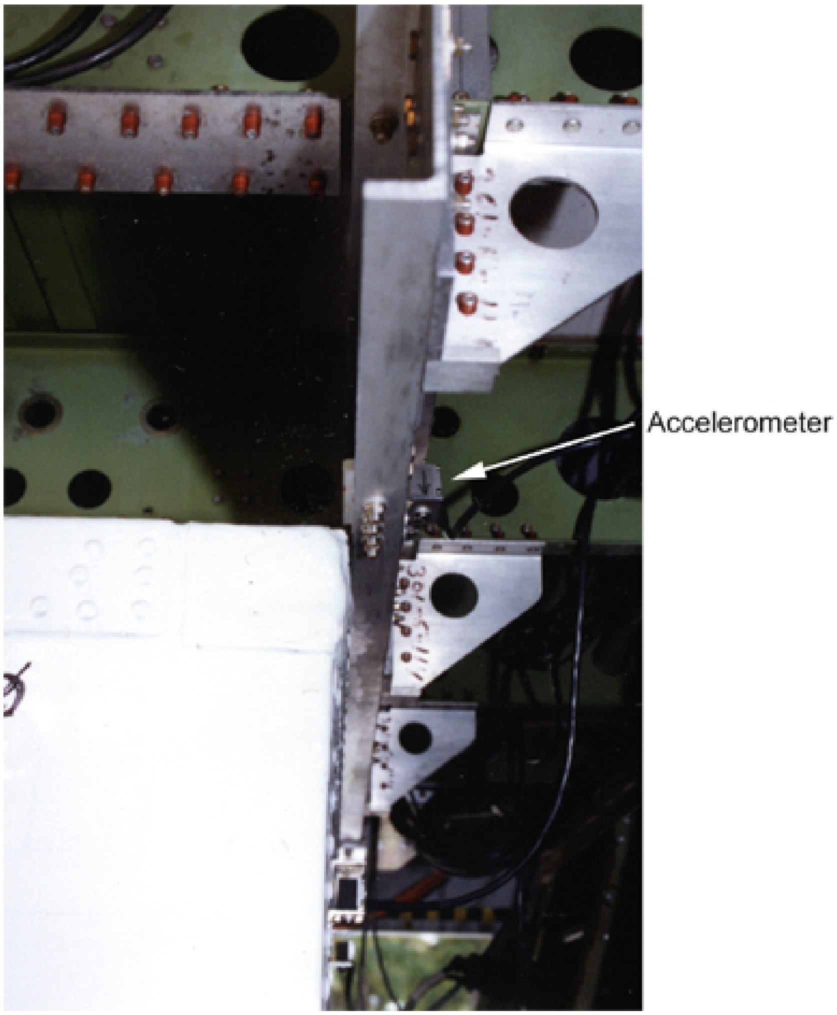

FIGURE 17. TANK RAIL ACCELEROMETER

HIGH-SPEED FILM AND VIDEO CAMERAS.

Nine high-speed (H/S) film cameras were used to record the test at 500 frames per second. Four of these cameras were onboard the airplane to record the internal impact reactions. The remaining five cameras were located around the exterior of the airplane. All the cameras recorded IRIG time, which was continuously supplied by a satellite-based time code receiver. This allowed for the precision time stamping of each frame of film and provided a means to correlate the data between cameras as well as the recorded data.

Three H/S video (500 frames per second) and five standard video cameras (30 frames per second) were also used to record the test. All eight video cameras were located around the exterior of the airplane in order to capture a variety of views. The camera locations are shown in figure 18.

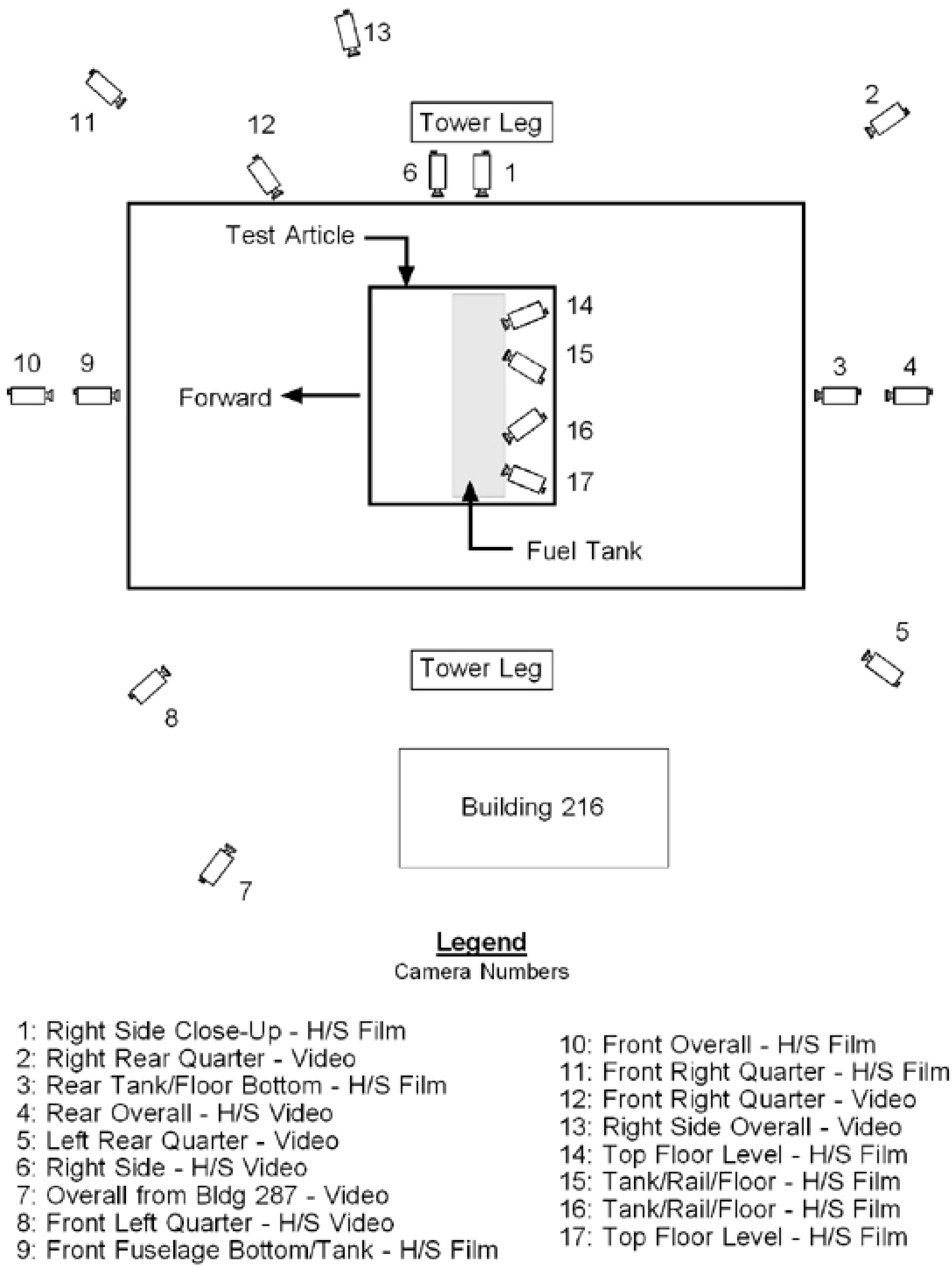

FIGURE 18. CAMERA LOCATIONS

DATA ACQUISITION AND REDUCTION

DATA ACQUISITION SYSTEMS.

A Neff 490 (figure 19) and an EME DAS-48S (figure 20) data acquisition system were used to collect the test data. They were controlled by two independent personal computers (PC). A synchronization pulse, generated by a satellite-based time code receiver, was recorded to synchronize the two systems to the H/S film and each other. A list of sensor locations for both systems is given in table 3.

NEFF 490. The NEFF 490 is a H/S data acquisition system with the capability to sample and record data at sampling rates of up to 100 kHz per channel. The system consists of 92 channels. Each channel includes a 12-bit analog-to-digital (A/D) converter, and a 6-pole Bessel antialias filter with four programmable cutoff frequencies (100, 200, 1000, and 2000 Hz). Analog input is fed to a differential input amplifier with 12 programmable gain steps. Full-scale range inputs are selectable from ±5 mV to ±10.24 V.

FIGURE 19. NEFF 490 DATA ACQUISITION SYSTEM

For the test, the system was set to sample and record 88 channels of data simultaneously at 10,000 samples per second per channel. All data channels were prefiltered at a cutoff frequency of 1 kHz. The collected data were temporarily stored in onboard 256 k word DRAM memory during the test. Test data were then transferred to a PC by an IEEE-488 interface for further analysis. The full-scale range for each channel was selected to be consistent with the expected output of the sensor.

EME DAS-48S. The EME DAS-48S is a H/S, small, flexible, ruggedized portable data acquisition system. The system can acquire analog and digital data at rates up to 20 kHz per channel. The system consists of 48 analog channels and 24 digital channels of data; all channels are simultaneously sampled. The system has a 12-bit A/D converter and a 6-pole Butterworth antialias filter with a programmable cutoff frequency (from 10 Hz to 20 kHz). Analog input is fed to a differential input amplifier with variable gain of 1 to 1000. The maximum input voltage is ±2.5 volts.

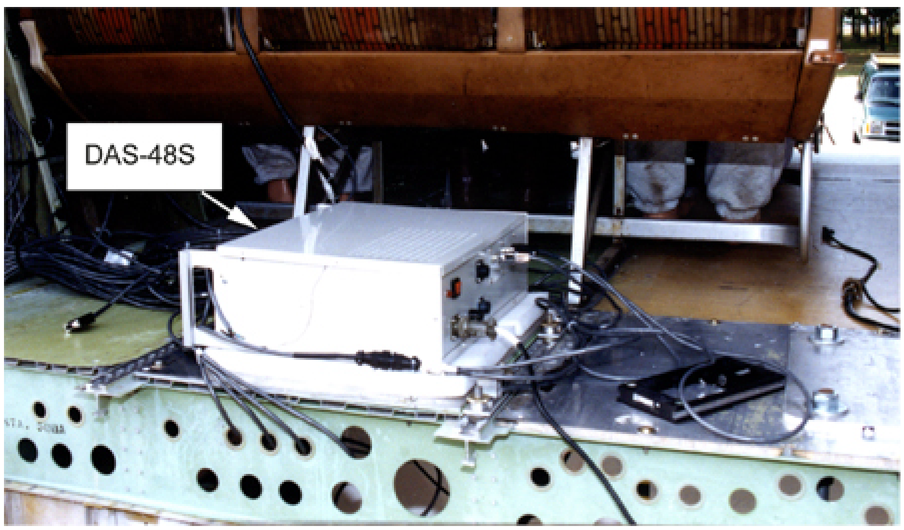

FIGURE 20. EME DAS-480S DATA ACQUISITION SYSTEM

For the test, the system was set to sample and record 33 channels of data simultaneously at 10,000 samples per second per channel. All data channels were prefiltered at a cutoff frequency of 1 kHz. The collected data was temporarily stored in the 32 megabyte of onboard memory during the test. Test data were then transferred to a PC by an RS-232/422 interface for further analysis. The gain value for each channel was selected to be consistent with the expected output of the sensor.

DATA COLLECTION.

Before the test, the bridge output voltage for each channel's sensor was zero-balanced to compensate for any variation in the zero state of the sensor. The channels were then calibrated. All phases of balancing the bridge output voltage, calibrating the channels, measuring sensitivity, and determining conversion coefficients for calculating engineering units were controlled by the data acquisition system software based upon user inputs.

The two systems were programmed to collect data in a pretrigger mode, a technique that allows the continuous sampling and storing of data in a buffer prior to the test trigger. The two data systems collected and saved the data 2 seconds prior to and 8 seconds after hook separation. The data acquisition systems were enabled prior to the hoisting of the aircraft thus insuring that data would be collected in the event of an inadvertent hook release. A Bowen 10-channel sequencer was used to initiate the test sequence including hook release, control all the video, camera equipment, and accessories.

DATA REDUCTION.

DSP Development Corporation's DADiSP data analysis software was used to analyze the data. All accelerometers and platform load cell sensors were filtered with a Society of Automotive Engineers (SAE) J211class 60 digital filter [9]. For the purposes of this test time zero (T_0) was defined as the moment of impact as observed on the H/S video and confirmed via the recorded data. This time corresponds to an IRIG date and time of October 21, 1999, at 17:30:34.797.

DATA ANALYSIS

TIME TO IMPACT.

The expected free fall time of the airplane, 0.933 second, was calculated using the equation

$$t = \sqrt{2h / g} \tag{1}$$

where t is time, h is the drop test distance (14 ft), and g is the acceleration due to gravity (32.2 ft/sec^2). The calculated time was close to the observed free fall time (t = 0.935 sec) determined from the H/S films of the front view and quarter view cameras, which were equipped with IRIG B timing devices.

IMPACT VELOCITY.

The theoretical impact velocity was calculated using the kinematic equation

$$v_t = \sqrt{2gh} \tag{2}$$

where v_t is the final theoretical velocity, g is the acceleration due to gravity, and h is the drop test distance. Using this equation, the theoretical impact velocity was 30 ft/sec. The theoretical velocity was compared to the observed and measured velocities.

The observed impact velocity was calculated using the kinematic linear motion equation

$$v_b - v_0 = gt \tag{3}$$

where v_b is the final observed velocity, v_0 is the initial velocity (0 ft/sec), g is the acceleration due to gravity, and t is the observed free fall time. The resulting observed velocity was 30 ft/sec.

The measured impact velocity was determined by adding the average velocity and a correction factor (cf). The average velocity was measured by the velocity measuring system (figure 21). The cf was used to compensate for sensor height above the platform and the conversion of the average velocity to a final velocity. The measured velocity (30 ft/sec) was calculated using the equation

$$v_m = \frac{\Delta d}{\Delta t} + cf \tag{4}$$

where v_m is the measured velocity, Δd = 1 ft, Δt equals the measured elapsed time (0.0347 sec), and cf = 0.8 ft/sec.

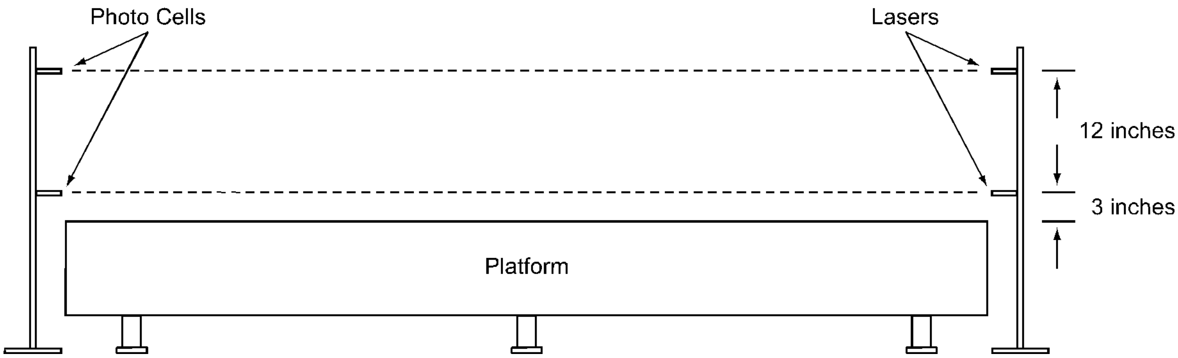

FIGURE 21. VELOCITY MEASURING SYSTEM

Table 4 shows the drop test velocities obtained using the above different methodologies.

TABLE 4. IMPACT VELOCITY

Methodology	Velocity (ft/sec)
Theoretical	30
Observed	30
Measured	30

SEQUENCE OF EVENTS.

A time line was developed from the H/S film to denote the significant occurrences during the test. This information is superimposed on each of the graphs in appendix B. A description is outlined below.

1. T_0 - Time of impact.
2. T_{15} - 15 ms after T_0, the bottom of the tank impacts the cargo bay floor.
3. T_{50} - 50 ms after T_0, cabin floor beams impact the top of the tank.

TEST ARTICLE ACCELERATION AND STRING POTENTIOMETER DATA.

The airframe acceleration data are presented in seven groups, divided into two areas: cargo area and cabin area. Cargo area includes sidewall accelerations, ceiling accelerations, and fuel tank accelerations. Cabin area includes upper sidewall accelerations, lower sidewall accelerations, inner seat track accelerations, and outer seat track accelerations. The data can be found in tables 5 through 11, respectively. All other airframe accelerometer measurements were acquired for supporting research. Filtered data for all the channels can be found in appendix B. Acceleration data is given in terms of three or four parameters: peak acceleration (G_{peak}), pulse duration, time of peak acceleration, and time of pulse onset. The data in the tables were selected to contain the necessary information to understand the events occurring at that particular location. In many instances the values of the two observed significant pulses were given. All accelerometers are mounted in the z-direction unless otherwise noted.

CARGO AREA SIDEWALL ACCELERATIONS. The accelerometer data from the cargo area left sidewall locations were unusable since the fuselage frames broke during crushing and proper accelerometer orientation was not maintained. The reinforced cargo doorframe located on the right side supplied sufficient support to limit fuselage crushing on that side. The data is listed in table 5 and is comprised of two significant readings per location. During the first reading, a peak acceleration of 68 g at 14 ms after T_0 was recorded on the sidewall, while a peak acceleration of 51 g at 29 ms after T_0 was recorded on the door. The sidewall values were higher and occurred earlier than those measured on the door, as the door frame acted as a load path which reduced and delayed the load to the door. Comparable times for the second significant reading may be due to the impact between the cabin floor beam and the fuel tank.

TABLE 5. CARGO AREA SIDEWALL ACCELERATIONS

	Left Side						Right Side					
	First Pulse			Second Pulse			First Pulse			Second Pulse		
Location	G_{peak} (g)	Pulse Duration (ms)	Peak Time (ms)	G_{peak} (g)	Pulse Duration (ms)	Peak Time (ms)	G_{peak} (g)	Pulse Duration (ms)	Peak Time (ms)	G_{peak} (g)	Pulse Duration (ms)	Peak Time (ms)
FS 420	----	----	----	----	----	----	68	6	14	33	21	63
FS 456 DOOR	----	----	----	----	----	----	51	8	29	60	11	61
FS 476 DOOR	----	----	----	----	----	----	31	17	39	66	13	61
FS 500	----	----	----	----	----	----	56	5	12	55	31	64

CARGO AREA CEILING ACCELERATIONS. The two ceiling accelerometers placed directly above the fuel tank along the longitudinal centerline of the fuselage were used to record the time of impact between the tank and the floor as well as the resulting g forces. The data is listed in table 6. The recorded time for impact between the tank and the cabin floor is approximately 50 seconds after T_0 and correlates closely with observations of several different views of the H/S film.

TABLE 6. CARGO AREA CEILING ACCELERATIONS

Location	Accelerometer Data			
	G_{peak} (g)	Pulse Duration (ms)	Peak Time (ms)	Onset Time (ms)
FS 460	78	9	54	51
FS 480	77	9	56	51

CARGO AREA FUEL TANK AND RAIL ACCELERATIONS. The fuel tank accelerations occur as early as 12 ms after T_0. This time coincides closely with the observations of the H/S film (15 ms). Maximum accelerations occur approximately 30 seconds later. The readings on the fuselage right side appear to occur earlier than those on the left and are of slightly lower magnitude (table 7). This may be attributed to the protruding reinforced lip on the lower edge of the doorframe, which would have contacted the right side of the fuel tank prior to the left side. The lip remained intact, causing the fuel tank and its contents to roll to the left, which caused a nonsymmetrical impact.

Analysis of the H/S film indicated that the fuselage was flexing laterally to the right just prior to the tank impacting the floor. The tank, however, continued to drop vertically. Visual inspection of the fuel tank rails confirmed that the right rail sustained little damage while the left side was bent and twisted. Thus, the data from the left rail was unusable. The rail data on the right side at FS 447 was comparable to that seen by the cargo area ceiling accelerometers.

TABLE 7. CARGO AREA FUEL TANK AND RAIL ACCELERATIONS

Location	Left Side			Right Side		
	G_{peak} (g)	Pulse Duration (ms)	Peak Time (ms)	G_{peak} (g)	Pulse Duration (ms)	Peak Time (ms)
FS 446 FRONT	52	51	42	47	51	39
FS 457 SIDE	51	46	37	48	38	35
FS 478 SIDE	77	45	38	55	44	35
FS 489 REAR	77	44	42	75	38	40
FS 447 RAIL	----	----	----	83	9	55
FS 487 RAIL	----	----	----	----	----	----

Note: The cable at FS 487 on the right side was severed 35 ms into the test.

CARGO AREA STRING POTENTIOMETER DATA. The data from both string potentiometers are shown in appendix B. Posttest inspection indicated that both the strings were snagged by broken metal brackets protruding from the fuselage floor. Consequentially, the initial readings are valid while those readings after approximately 20 ms are invalid.

CABIN AREA—UPPER SIDEWALL DATA. The cabin area, upper sidewall accelerometers were mounted on the fuselage frames located approximately 67 inches above the floor. This location provides sidewall data for comparison with previous tests and for future tests. Review of the photographic films show significant upper fuselage lateral movement. The data are shown in table 8.

TABLE 8. CABIN AREA—UPPER SIDEWALL ACCELERATIONS

Location	Left Side						Right Side					
	First Pulse			Second Pulse			First Pulse			Second Pulse		
	G_{peak} (g)	Pulse Duration (ms)	Peak Time (ms)	G_{peak} (g)	Pulse Duration (ms)	Peak Time (ms)	G_{peak} (g)	Pulse Duration (ms)	Peak Time (ms)	G_{peak} (g)	Pulse Duration (ms)	Peak Time (ms)
FS 420	29	18	43	28	25	105	34	13	37	48	19	71
FS 460	31	17	41	30	32	99	28	16	33	42	22	77
FS 500	30	19	42	55	30	100	40	20	39	50	17	71

<u>CABIN AREA—LOWER SIDEWALL DATA</u>. The cabin area, lower sidewall accelerometers were mounted on the fuselage frames located approximately 12 inches above the floor. This location provided sidewall accelerations while minimizing the effect of the fuselage sidewall sway. Compared to the left side, the data on the right side contained sharper and cleaner pulses. They are characterized by two well-defined pulses as opposed to one. This difference is attributed to the continued crushing on the left side and breaking of the floor beams on the left side. The data are shown in table 9. A comparison between the cabin area floor-level sidewall accelerations and the cabin area lower sidewall accelerations shows that they are comparable.

TABLE 9. CABIN AREA—LOWER SIDEWALL ACCELERATIONS

Location	Left Side						Right Side					
	First Pulse			Second Pulse			First Pulse			Second Pulse		
	G_{peak} (g)	Pulse Duration (ms)	Peak Time (ms)	G_{peak} (g)	Pulse Duration (ms)	Peak Time (ms)	G_{peak} (g)	Pulse Duration (ms)	Peak Time (ms)	G_{peak} (g)	Pulse Duration (ms)	Peak Time (ms)
FS 420	31	13	40	9	8	61	32	17	28	36	26	61
FS 460	33	15	40	29	5	62	30	24	30	31	28	59
FS 500	35	14	38	24	7	61	40	24	31	42	28	59
FS 460 Y-DIR	-46	11	58	39	12	62	52	7	55	-30	8	65

<u>CABIN AREA—INNER AND OUTER SEAT TRACK DATA</u>. Inner and outer seat track data are found in tables 10 and 11. Analysis of the inner and outer seat track data showed that the peak pulse at FS 472 (accelerometer above tank) occurred at approximately 56 ms after T_0 with an initial onset time of 50 ms. This is comparable to the times seen on the cargo area floor beam accelerometers (50-51 ms). These are in close agreement to the time obtained from the H/S photographic coverage and the cargo area floor beam accelerometers. As previously noted, accelerometer signals from the right side are generally characterized by sharper and cleaner pulses than those from the left side. The maximum measured accelerations were those recorded above the fuel tank at FS 472. The posttest investigation showed that the left side seat track was broken at several locations while the right side remained intact. This accounted for the higher reading on the right side (129 g vs 82 g). A significant negative reading was noted on the left seat track at FS 438, starting at 106 ms after T_0 and peaking at 110 ms after T_0. The signal from

the accelerometer located at the left outer seat track was ended at approximately 106 ms after T_0, due to a torn cable.

TABLE 10. CABIN AREA—INNER SEAT TRACK ACCELERATIONS

Location	Left Side						Right Side					
	First Pulse			Second Pulse			First Pulse			Second Pulse		
	G_{peak} (g)	Pulse Duration (ms)	Peak Time (ms)	G_{peak} (g)	Pulse Duration (ms)	Peak Time (ms)	G_{peak} (g)	Pulse Duration (ms)	Peak Time (ms)	G_{peak} (g)	Pulse Duration (ms)	Peak Time (ms)
FS 400	50	9	66	34	10	80	65	11	65	----	----	----
FS 438	55	10	59	53	12	68	65	8	57	62	10	69
FS 472	82	10	59	58	7	66	129	8	55	----	----	----
FS 504	58	10	63	----	----	----	34	15	71	----	----	----
FS 518	34	15	71	----	----	----	51	24	65	----	----	----

TABLE 11. CABIN AREA—OUTER SEAT TRACK ACCELERATIONS

Location	Left Side						Right Side					
	First Pulse			Second Pulse			First Pulse			Second Pulse		
	G_{peak} (g)	Pulse Duration (ms)	Peak Time (ms)	G_{peak} (g)	Pulse Duration (ms)	Peak Time (ms)	G_{peak} (g)	Pulse Duration (ms)	Peak Time (ms)	G_{peak} (g)	Pulse Duration (ms)	Peak Time (ms)
FS 438	45	7	59	23	6	66	50	8	57	51	17	69
FS 472	----	----	----	----	----	----	101	8	56	----	----	----
FS 504	57	10	63	----	----	----	63	13	60	----	----	----
FS 472 X-DIR	-25	6	72	15	12	79	22	6	41	45	3	-6
FS 472 Y-DIR	-28	9	57	24	11	7	19	12	54	-12	4	58

Note: The z-direction data at FS 472 left side was not considered valid due to the suspicious offset observed in the signal.

DROP TEST PLATFORM DATA.

PLATFORM LOAD CELL DATA. The platform load cell data are presented in appendix B. A linear momentum energy balance was performed to verify the measured results. The energy was balanced by applying the principle of linear impulse and momentum for a rigid body using equation 5.

$$\int_{t_1}^{t_2} F\,dt = mv_1 - mv_2 \tag{5}$$

where F is the sum of the 12 load cells minus the weight of the test article (8780 lb), m is the mass of the test article, v_1 and v_2 are the velocities of the test article just prior to impact and at rest after impact (30 ft/sec and 0 ft/sec, respectively); t_1 and t_2 are defined as the time of impact and 800 ms after impact. The integrated value from the measured loads was 7953 slug-ft/sec.

This compares favorably to the value of 8180 slug-ft/sec, which was calculated using the mass and velocities (v_1 and v_2) of the test section.

DROP TEST PLATFORM ACCELERATION DATA. The platform acceleration data are presented in appendix B. Analysis indicated that there was no significant platform response superimposed on the airframe data. The platform data was symmetric between the forward and aft locations along the platform centerline.

ANTHROPOMORPHIC TEST DUMMIES.

Six ATDs were used to measure loads and accelerations in their respective lumbar and pelvic areas. The ATD data are presented in table 12 and appendix B for reference value only. The impact caused the ATDs to shift in their seats due to the fracturing of the seats and the seat tracks; therefore, ATD lumbar load cell and acceleration data were not usable.

TABLE 12. ANTHROPOMORPHIC TEST DUMMY DATA

ATD No.	Location	Lumber Load (lb)	Accelerometer Data	
			G_{peak} (g)	Pulse Duration (ms)
1	FS 427 LS	1804	17.4	49
2	FS 426 RS	906	17.3	48
3	FS 462 LS	1734	34	32
4	FS 462 RS	1269	21	55
5	FS 497 LS	1247	27	61
6	FS 498 RS	961	17	18

RESULTS AND DISCUSSION

FUSELAGE STRUCTURE.

Analysis of the films indicates that the conformable auxiliary fuel tank was very rigid and stiff. The fuselage moved laterally to the right prior to the impact of the cabin floor beams with the fuel tank. The interaction of the fuselage with the fuel tank and its mounting system caused the floor beams at FS 460 and FS 480 to fracture. The fracturing of the floor beams led to the failure of the seat tracks at FS 421, FS 438, FS 460, and FS 483. In addition, the effects of the rigidity and stiffness of the frame surrounding the cargo door resulted in nonsymmetric crushing of the fuselage section.

EXTERNAL.

The test section experienced permanent deformation of the cargo area due to the platform impact (figure 22 and table 13). The left side experienced 21.7 inches of crush in the front and 20.7 inches of crush in the aft end. The right side experienced 10.7 inches of crush in the front and 10.5 inches of crush in the aft end. The difference was due to the support provided by the rigid and stiff reinforced cargo doorframe, located on the right side and slightly offset to the rear of the test section spanning FS 443 through FS 490. A review of the H/S film showed that the test article impacted the platform at a level attitude; and then the forward section pivoted downward. Such a motion would account for the larger crush measurements in the forward area. The deformation measurements were taken from the four corners of the cabin floor to the surface of the drop test platform.

FIGURE 22. FRONT VIEW—LOWER FUSELAGE CRUSH

TABLE 13. LOWER FUSELAGE CRUSH MEASUREMENTS

Measurement	Left Side		Right Side	
	Forward	Aft	Forward	Aft
Pretest (in)	59.2	59.2	59.2	59.2
Posttest (in)	37.5	38.5	48.5	48.7
Crush (in)	21.7	20.7	10.7	10.5

INTERNAL.

The most noticeable deformation in the cabin area of the fuselage structure was the upward intrusion of the floor into the passenger cabin. The damage was localized in the floor area above and surrounding the fuel tank. However, a survivable volume was maintained and the passengers would have been able to exit the aircraft. Permanent deformations in the cabin at the longitudinal centerline and the left end of the floor beam at FS 460 and FS 480 were approximately 3 and 6 inches respectively. H/S photography showed that, during the event, the dynamic deformation might have been twice as large.

CABIN FLOOR BEAMS AND FUEL TANK RAILS. The cabin floor, seat tracks, and fuel tank mounting rails experienced significant deformation. As discussed in the Data Analysis section, the fuselage frame flexed laterally to the right while the fuel tank continued to drop vertically. During this time, the fuel tank slid off the right rail and loaded the left tank mounting system and floor beams. As the fuselage shifted to the right and continued crushing, the floor beams located at FS 460 and FS 480 impacted the top of the fuel tank. This impact provided sufficient energy to push the floor beams up into the cabin area and buckled the floor. Figure 23 shows the damage to the cabin floor beams and fuel tank rail mounting bracket. The left fuel tank mounting rail was bent in a U-shape, with the apex of the U near location FS 470. All four of the mounting brackets that secured the rails to the beams remained attached to the rail. Only the mounting brackets at FS 500 remained attached to the floor beam. In the other three locations where the mounting brackets were attached, they separated from and fractured the beam. The floor beams located at FS 460 and FS 480 fractured. The floor beams at FS 440 and FS 500 remained intact.

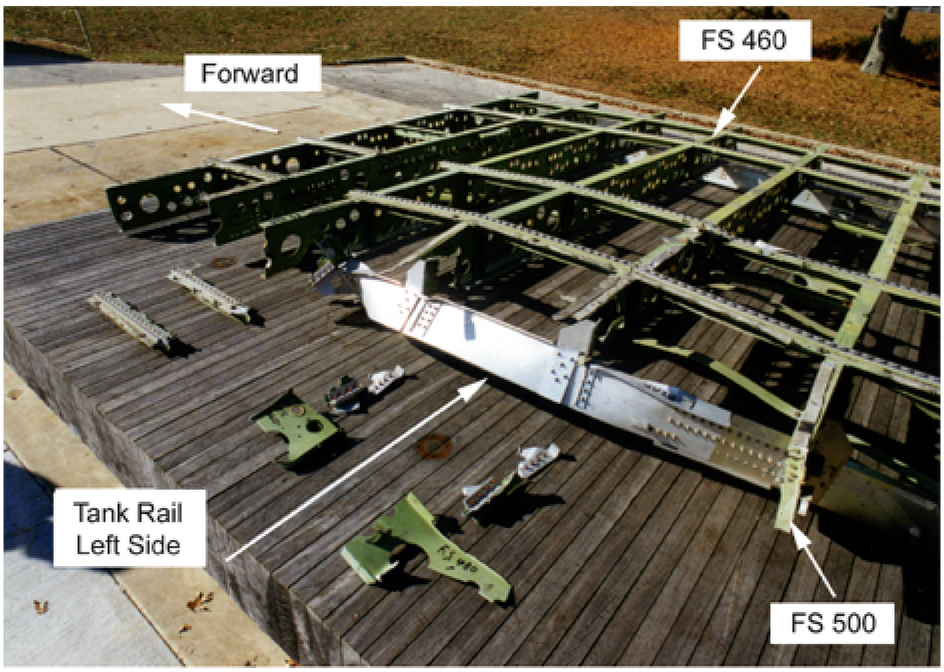

FIGURE 23. CABIN FLOOR BEAMS AND FUEL TANK RAIL MOUNTING BRACKET DAMAGE

CABIN FLOOR SEAT TRACKS. The cabin floor seat tracks are an integral part of the fuselage structure. Running the length of the cabin floor, they connect each of the adjacent floor beams. In this test section, the seat tracks are composed of two lengths of track. The first length extends from FS 400 to FS 480 and the second is from FS 480 to FS 500A. The inner and outer seat tracks are spaced 23 inches and 44 inches, respectively, from the longitudinal centerline of the test section on both sides.

When the floor beams impacted the tank, the floor sustained a dynamic deformation in excess of 3 inches at the longitudinal centerline and 6 inches near the left sidewall at FS 460 and FS 480.

The loading due to the impact's resultant deformation caused cracking of the upper face of the inner and outer left side seat tracks at FS 460. No damage was observed at FS 480 where the two lengths of seat track were spliced. There were no visible cracks on the inner or outer seat tracks located on the right side of the cabin. The inner and outer seat tracks at FS 420 and FS 438 on the left side were fractured and separated from the floor (figure 24). This resulted in the rear legs of the first row seat displacing into the cargo area (figures 25, 26, and 27). The fracturing was due to the loading from the seat legs of Seats A, B, and C of Row 1 and the loading imposed by the tank below. The legs of the mannequins and the ATDs located in Rows 2 and 3 supported the seat backs in Rows 1 and 2, respectively (figures 28 and 29). The seat track fractured where the cross-sectional area was minimal (figure 30). A similar fracture and separation was also observed at the inner left side seat track at FS 483 (Seats B/C Row 3). The outer left side seat track was not fractured (Seats A/B Row 3). Analysis of the H/S film in conjunction with the postcrash inspection indicated that the cross tube supporting Seat A row 3 bent and separated during the test. The reduced loading of the seat leg on the outer left side seat track and the loading due to the deformation of the floor were not sufficient to fracture the seat track.

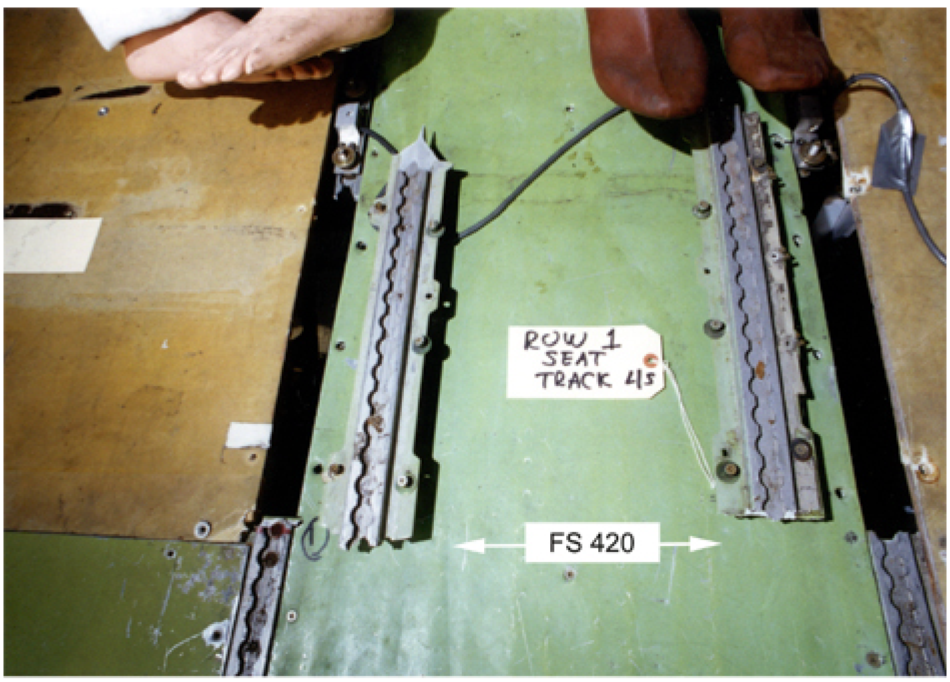

FIGURE 24. FRACTURED SEAT TRACKS

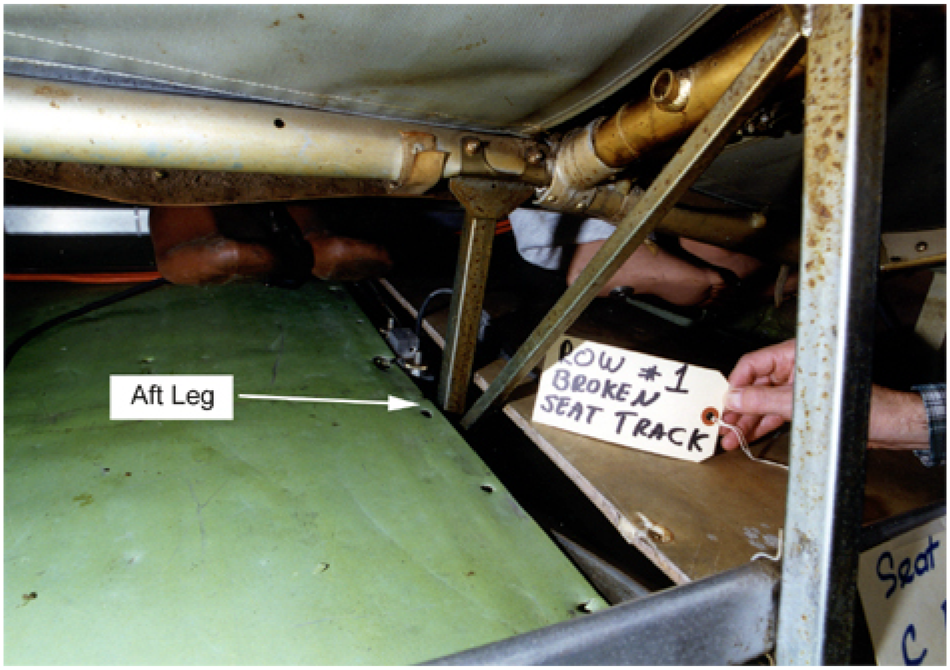

FIGURE 25. REAR LEGS OF FIRST ROW SEATS DISPLACED THROUGH FLOOR

FIGURE 26. DISPLACEMENT OF OUTER SEAT TRACK INTO CARGO AREA

FIGURE 27. DISPLACEMENT OF INNER SEAT TRACK INTO CARGO AREA

FIGURE 28. POSTTEST—LEFT SIDE SEATS

FIGURE 29. POSTTEST—RIGHT SIDE SEATS

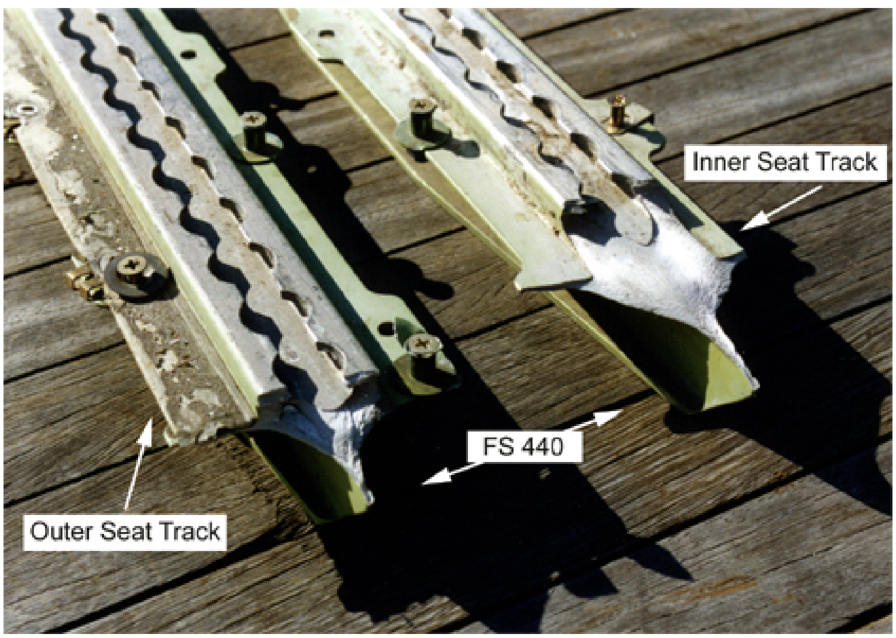

FIGURE 30. FRACTURED SEAT TRACKS

FUEL TANK.

The fuel tank sustained no noticeable change to its physical dimensions (figure 31). The tank was viewed as a stiff, rigid, reinforced structure that proved capable of retaining its shape despite intense compressive loading. An inspection of the inside of the tank revealed that a stiffening member supporting the right side was bent (figure 31).

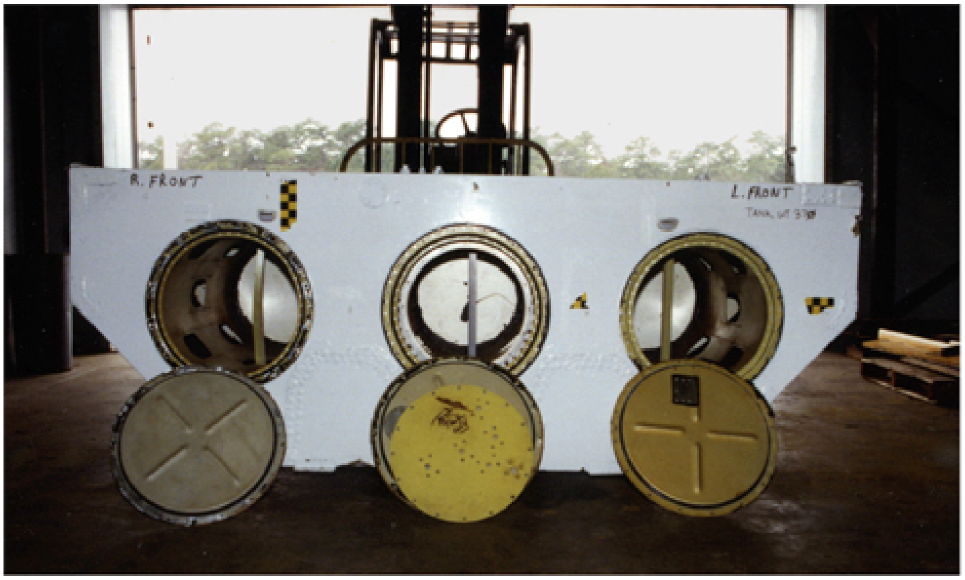

FIGURE 31. POSTCRASH—CONFORMABLE AUXILIARY FUEL TANK

The bent member was attributed to the fuel tank side wall impacting the reinforced lip on the lower edge of the doorframe. The bottom of the tank sustained substantial damage. The fuselage cargo floor frames, metal members, and cargo floor tracks (figure 32) penetrated the bottom of the tank (figures 33 and 34). This damage resulted in significant simulated fuel leaking from the tank.

FIGURE 32. FUEL TANK CRUSHING CARGO FLOOR

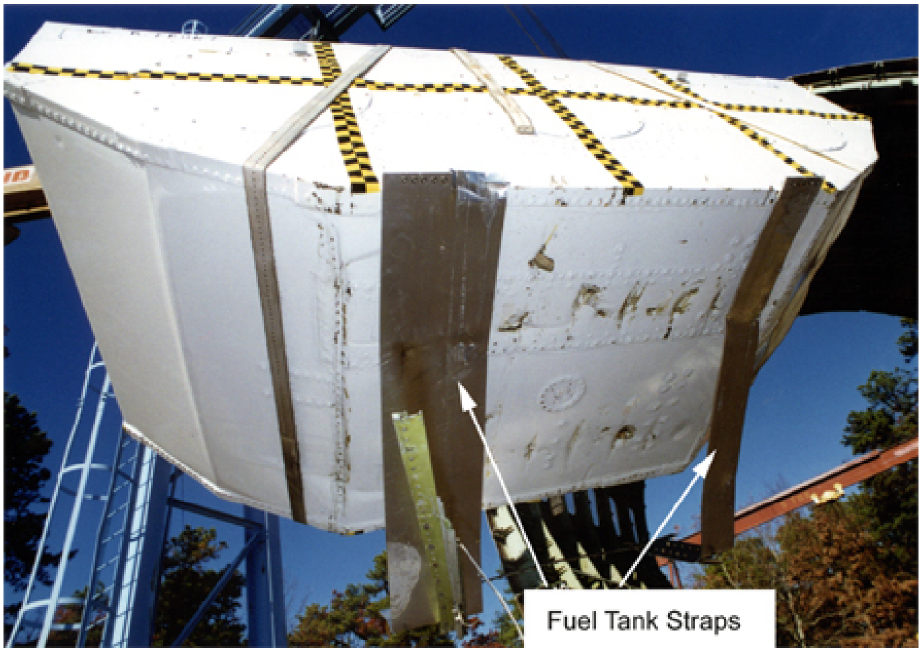

FIGURE 33. POSTCRASH—TANK BOTTOM

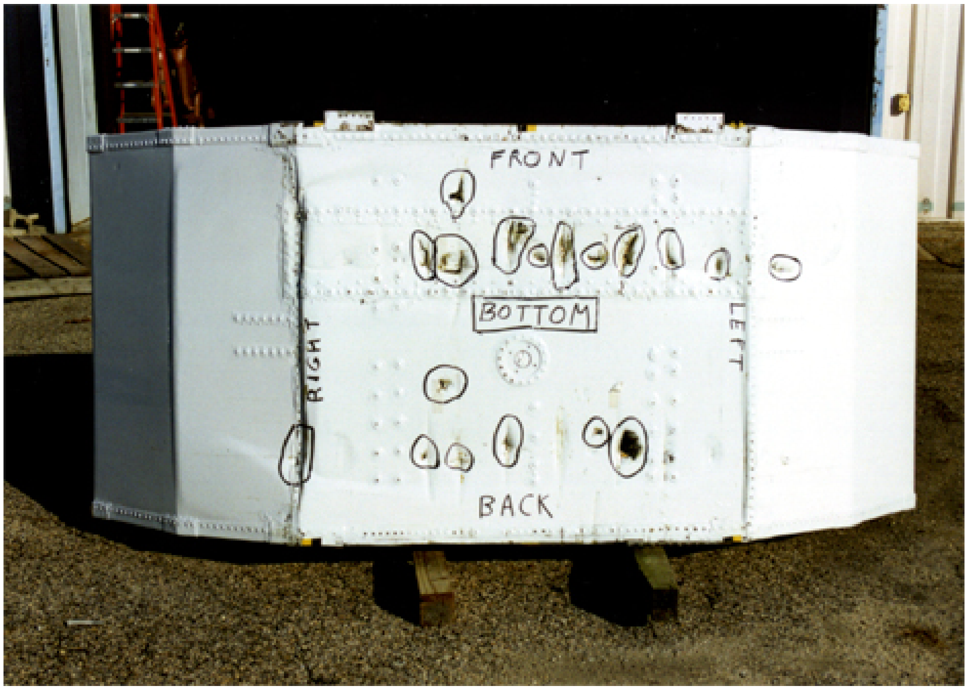

FIGURE 34. POSTCRASH—FUEL TANK DAMAGE

SEATS.

A postcrash inspection determined that all seat pans remained intact; all seat legs remained attached to the seat tracks; and only four seats located in the last row sustained seat back damage (i.e., excessive reclining). The legs of the mannequins and the ATDs, located in Rows 2 and 3, supported the seat backs in Rows 1 and 2 respectively. A camera mounted on the floor closely behind the back of the UOP aisle seat, located in the last row, provided sufficient support to prevent seat back damage. The Weber seat located in the last row at position A did not sustain seat back damage. This was attributed to the bending of the cross tube support and subsequent separation of the seat from the frame. Seat damage was remarkably different for the two types of seats. The UOP seat predominately suffered from the bending of the leg supports (figures 35 through 40). The Weber seat suffered from bending and severing of the cross tubes and spreader tubes (figures 41 through 46). A list of the seat damage is found in table 14. As was previously mentioned, the seats were not of primary interest in this test. The test was primarily structured to be a fuel tank test. An actual crash impact imparts a longitudinal drag load on the aircraft that will significantly change the load distribution in a seat. Thus, the seat fracture modes observed in this test are not necessarily reflective of what may occur in service. Therefore, special consideration must be given when considering the results of seat test data obtained from this vertical drop test.

TABLE 14. SEAT DAMAGE

Left Side - Weber Seats					
Row	Seat Legs	Seat Frames	Aisle Seat Back	Center Seat Back	Window Seat Back
1	Intact	Fractured	Upright	Upright	Upright
2	Intact	Fractured	Upright	Upright	Upright
3	Intact	Fractured	Reclined	Reclined	Upright
Right Side - UOP Seats					
Row	Seat Legs	Seat Frames	Aisle Seat Back	Center Seat Back	Window Seat Back
1	Fractured	Intact	Upright	Upright	Upright
2	Fractured	Intact	Upright	Upright	Upright
3	Fractured	Intact	Upright	Reclined	Reclined

FIGURE 35. POSTCRASH—ROW 1, UOP SEAT, BOTTOM VIEW

FIGURE 36. POSTCRASH—ROW 2, UOP SEAT, BOTTOM VIEW

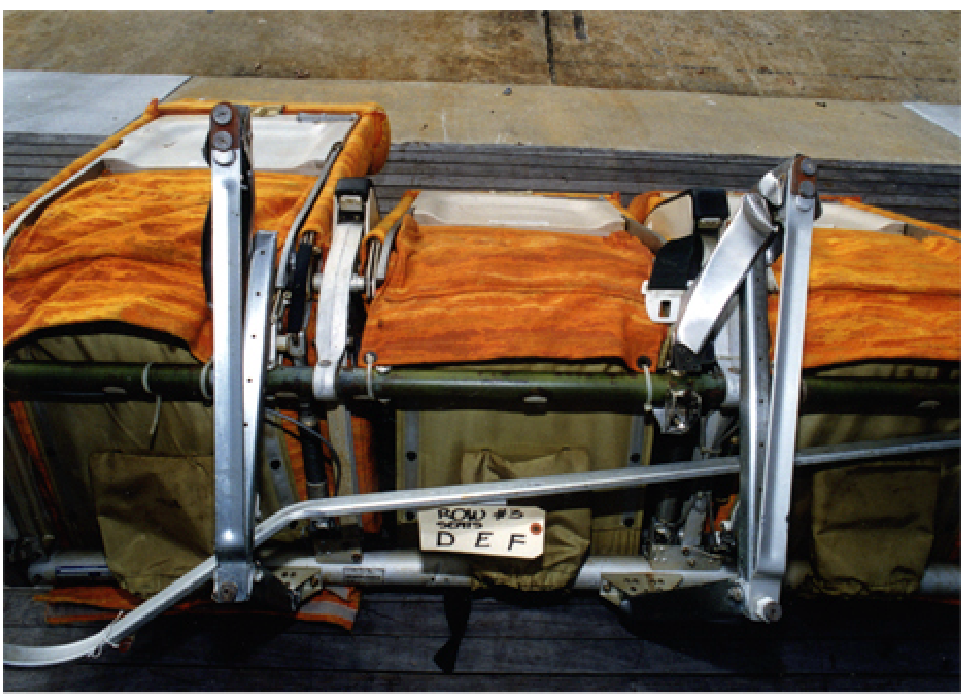

FIGURE 37. POSTCRASH—ROW 3, UOP SEAT, BOTTOM VIEW

FIGURE 38. POSTCRASH—ROW 1, UOP SEAT

FIGURE 39. POSTCRASH—ROW 2, UOP SEAT

FIGURE 40. POSTCRASH—ROW 3, UOP SEAT

FIGURE 41. POSTCRASH—ROW 1, WEBER SEAT, BOTTOM VIEW

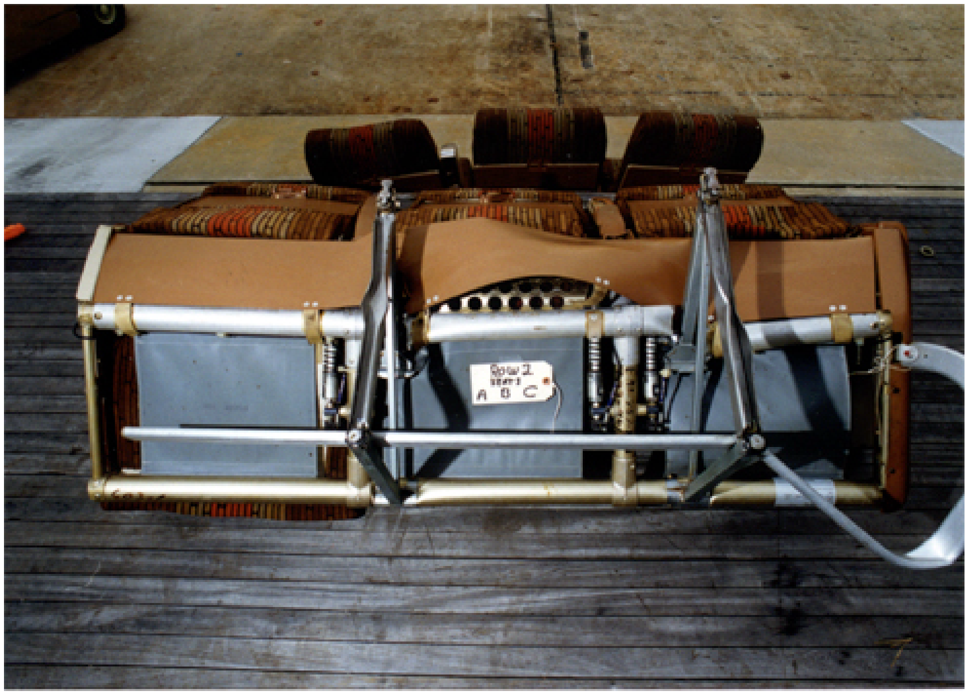

FIGURE 42. POSTCRASH—ROW 2, WEBER SEAT, BOTTOM VIEW

FIGURE 43. POSTCRASH—ROW 3, WEBER SEAT, BOTTOM VIEW

FIGURE 44. POSTCRASH—ROW 1, WEBER SEAT

FIGURE 45. POSTCRASH—ROW 2, WEBER SEAT

FIGURE 46. POSTCRASH—ROW 3, WEBER SEAT

CONCLUSIONS

Postcrash fuel-fed fires are a major contributor to the fatal accident rate. The FAA has been conducting research to better understand and minimize these fires. On October 23, 1999, a fully instrumented narrow-body transport airplane fuselage section with an onboard conformable auxiliary fuel tank was subjected to a vertical impact drop test at the FAA William J. Hughes Technical Center located at the Atlantic City International Airport, New Jersey. The objective of the test was to determine the interaction between a typical transport airplane fuselage, particularly its floor structure, and this type of fuel tank under severe, but survivable, impact conditions. The fuel tank used in this test is representative of tanks being installed in narrow-body transport airplanes. Fuselage damage was as expected; however, portions of the cabin floor were severely damaged due to its impact with the auxiliary fuel tank located in the cargo compartment. Consequently, some of the seat tracks broke. The bottom of the fuel tank was punctured in numerous locations resulting in fuel spillage.

1. A narrow-body transport fuselage section with an onboard conformable auxiliary fuel tank was dropped from a height of 14 feet resulting in a vertical velocity of 30 feet per second. This resulted in what may be considered a severe, but survivable, impact condition.

2. Two acceleration pulses characterized the reaction of the fuselage to the impact. The first pulse corresponds to the initial impact of the fuselage with the drop test platform, the second pulse corresponds to the impact of the cabin floor beams with the auxiliary fuel

tank. The energy levels associated with each impact corresponded to velocity changes of 9 ft/s and 15 ft/s, respectively. The pulse amplitudes and pulse durations were 35 g, 22 ms and 34 g, 19 ms respectively.

3. The ten-foot-long fuselage test section sustained severe nonsymmetric damage. The left side crushed almost 2 feet; the right side less than 1 foot. A cargo door and its associated reinforced doorframe located on the right side of the test section helped support the right side, resulting in less damage. A portion of the cabin floor on the left side was severed loose by its impact with the auxiliary fuel tank. This may have contributed to the fracture of the seat tracks on that side.

4. The acceleration levels and pulse durations on the left side seat tracks were 50 g and 10 ms while the right side seat tracks experienced 67 g and 12 ms.

5. The bottom of the conformable auxiliary fuel tank was punctured in numerous locations resulting in simulated fuel spillage. The fuel tank was very strong and rigid in its construction thus allowing it to maintain its structure. This resulted in the fuel tank fracturing the floor beams directly above it; consequently, the floor beams penetrated the passenger cabin.

6. The seats were not a primary focus of this test. However, the seats experienced major structural damage.

7. It appears that the use of such fuel tanks limits the inherent ability of the fuselage structure to absorb energy resulting in a more severe crash condition for the occupants.

REFERENCES

1. Federal Aviation Regulations, 14 CFR Part 25 paragraph 25.562, January 1, 1999.

2. Crash Dynamics and Engineering Development Program, Federal Register, Volume 49, No. 185, September 21, 1984.

3. Johnson, R. and Wilson, A., "Vertical Drop Test of a Transport Airframe Section," FAA Report DOT/FAA/CT-TN86/34, October 1986.

4. Johnson, R. and Wade, B., "Longitudinal Impact Test of a Transport Airframe Section," FAA Report DOT/FAA/CT-87/26, July 1988.

5. Ault, D., "Longitudinal Acceleration Test of Overhead Luggage Bins in a Transport Airframe Section," FAA Report DOT/FAA/CT-92/9, November 1992.

6. Logue, T., McGuire, R., Reinhardt, J., and Vu, T., "Vertical Drop Test of a Narrow-Body Fuselage Section With Overhead Stowage Bins and Auxiliary Fuel Tank on Board," FAA Report DOT/FAA/CT-94/116, April 1995.

7. McGuire, R. and Macy, T., "Longitudinal Acceleration Tests of Overhead Luggage Bins and Auxiliary Fuel Tank in a Transport Airplane Airframe Section," FAA Report DOT/FAA/AR-99/4, June 1999.

8. Aircraft Crash Survival Design Guide, Volume II. December 1989, Simula Inc., Phoenix, AZ, 85044.

9. SAE International, "Surface Vehicle Recommended Practice," SAE J211/1, Revised March 1995.

APPENDIX A—PHOTOGRAPHIC DOCUMENTATION

PRETEST PHOTOS (FIGURES A-1 TO A-4)

POSTTEST PHOTOS (FIGURES A-5 TO A-67)

PRETEST PHOTOS

FIGURE A-1. DYNAMIC DROP TEST FACILITY

FIGURE A-2. TEST SECTION—FRONT VIEW

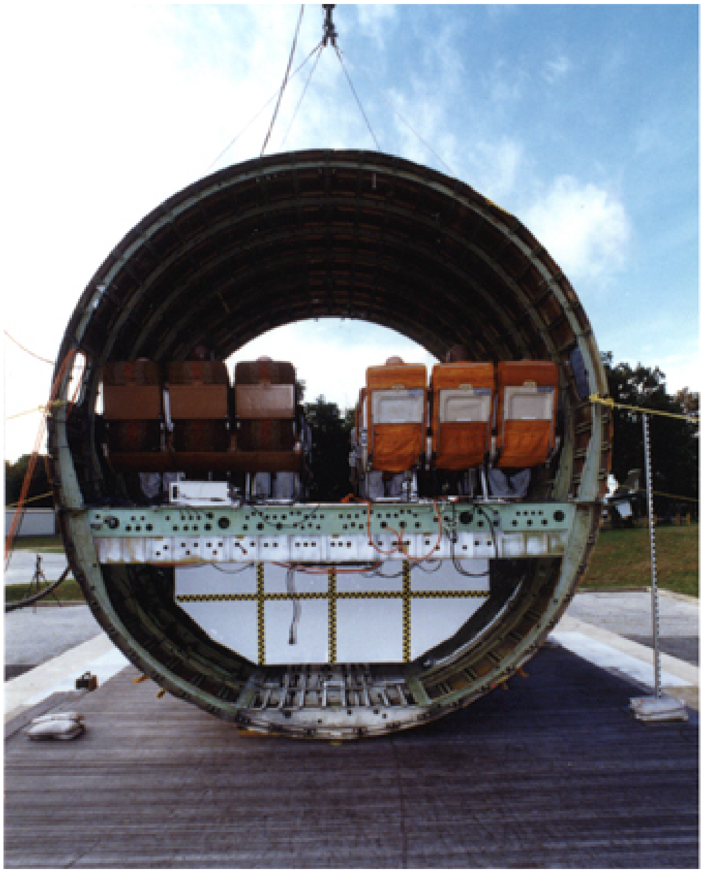

FIGURE A-3. TEST SECTION—REAR VIEW

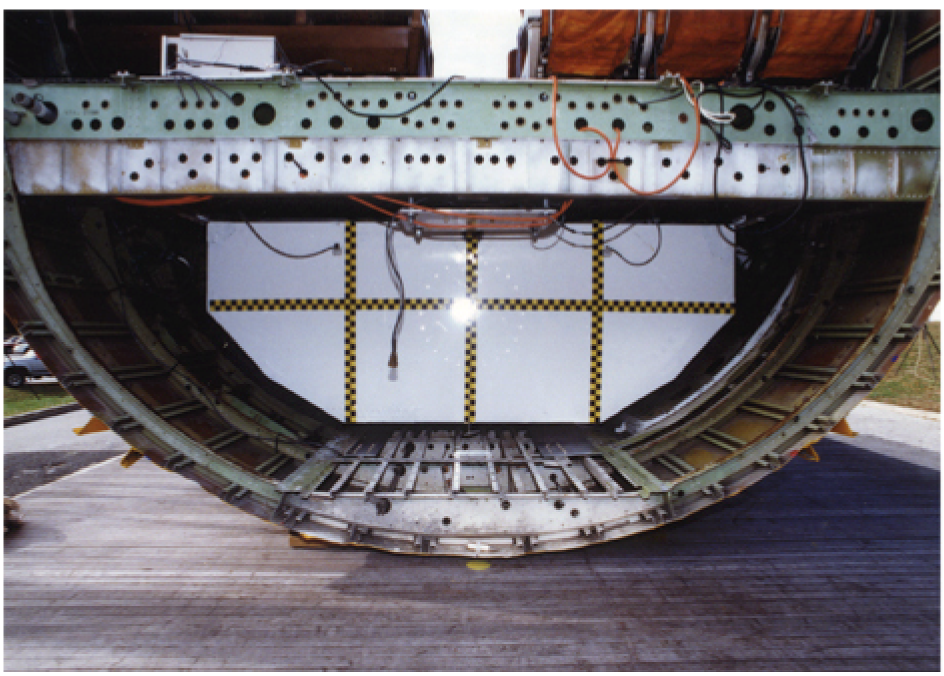

FIGURE A-4. CONFORMABLE AUXILIARY FUEL TANK—REAR VIEW

POSTTEST PHOTOS

FIGURE A-5. TEST SECTION—REAR VIEW

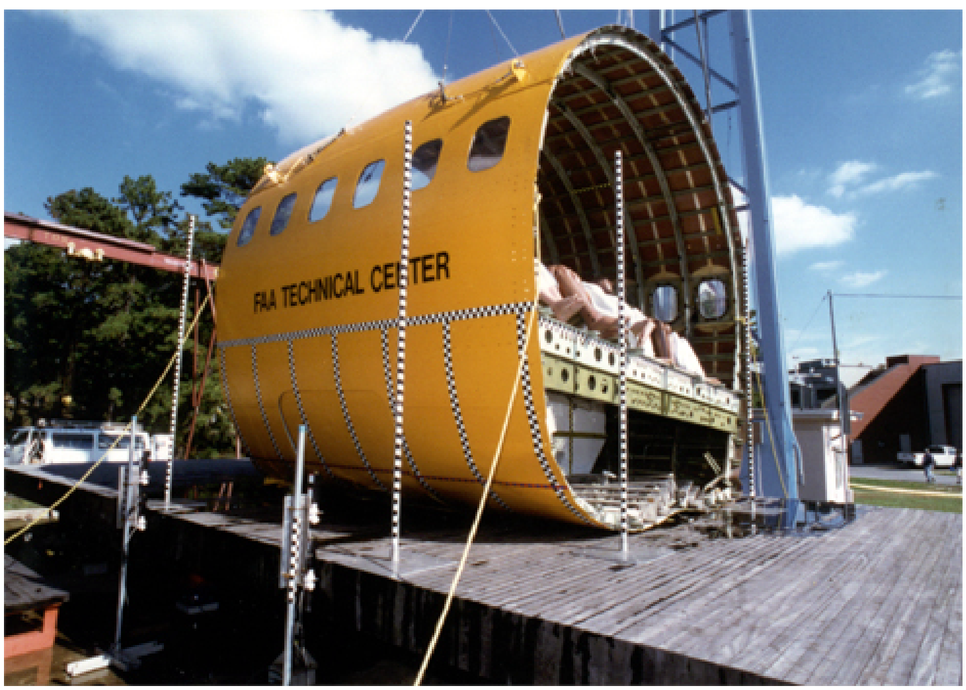

FIGURE A-6. RIGHT FRONT QUARTER VIEW

FIGURE A-7. LEFT FRONT QUARTER VIEW

FIGURE A-8. RIGHT REAR QUARTER VIEW

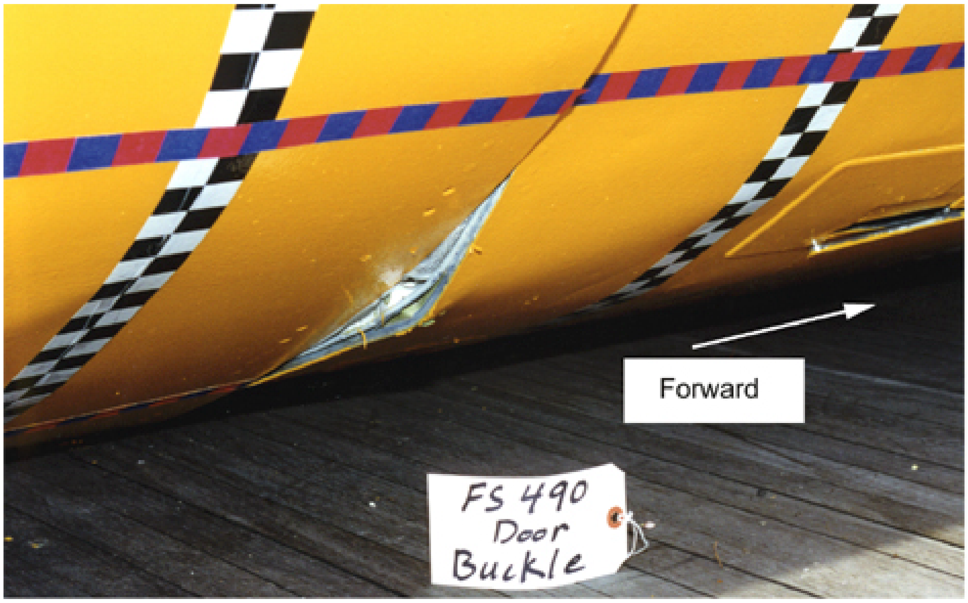

FIGURE A-9. FUSELAGE STATION 490 DOOR BUCKLE

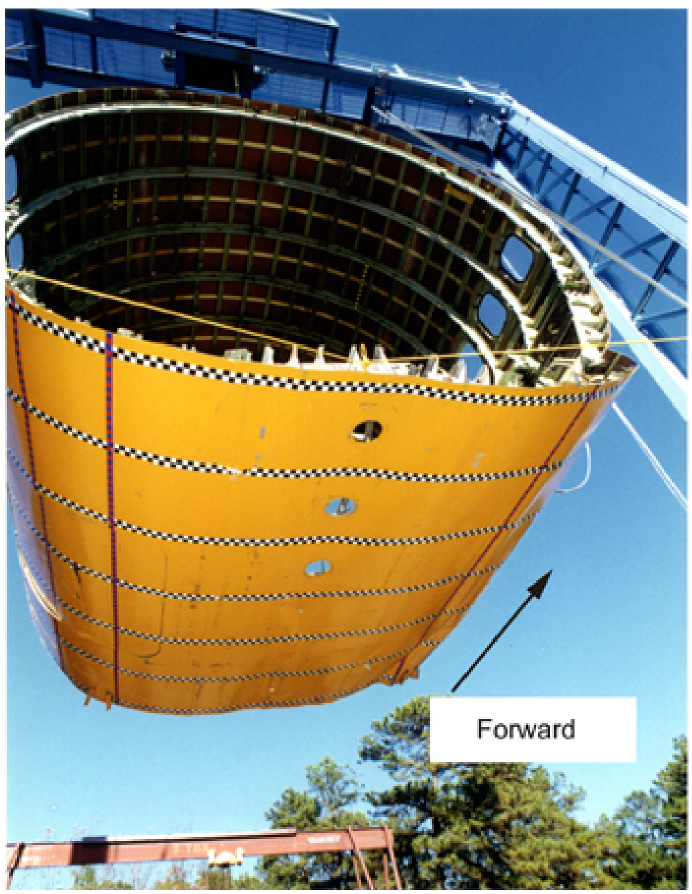

FIGURE A-10. TEST SECTION—BOTTOM VIEW

FIGURE A-11. RIGHT FRONT FRAMES—CARGO AREA

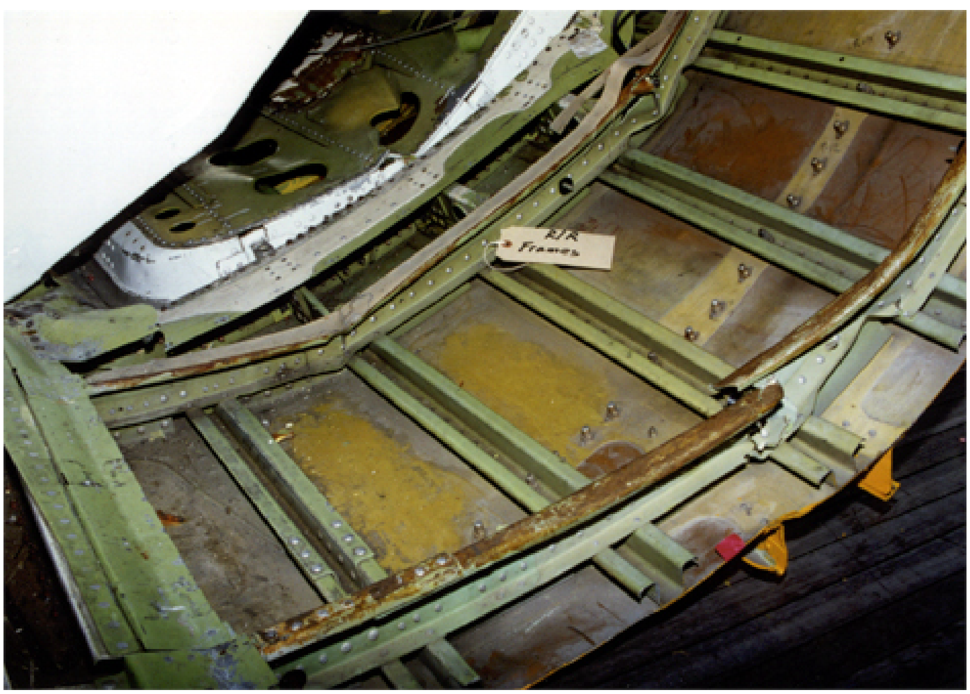

FIGURE A-12. RIGHT REAR FRAMES—CARGO AREA

FIGURE A-13. LEFT FRONT FRAMES—CARGO AREA

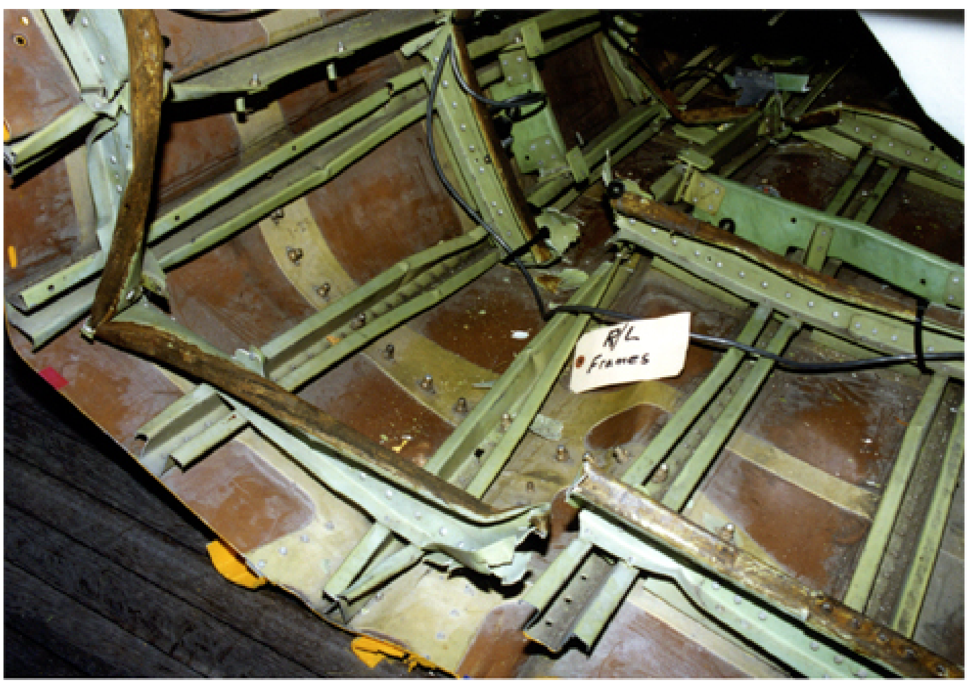

FIGURE A-14. LEFT REAR FRAMES—CARGO AREA

FIGURE A-15. CENTER REAR FRAMES—CARGO AREA

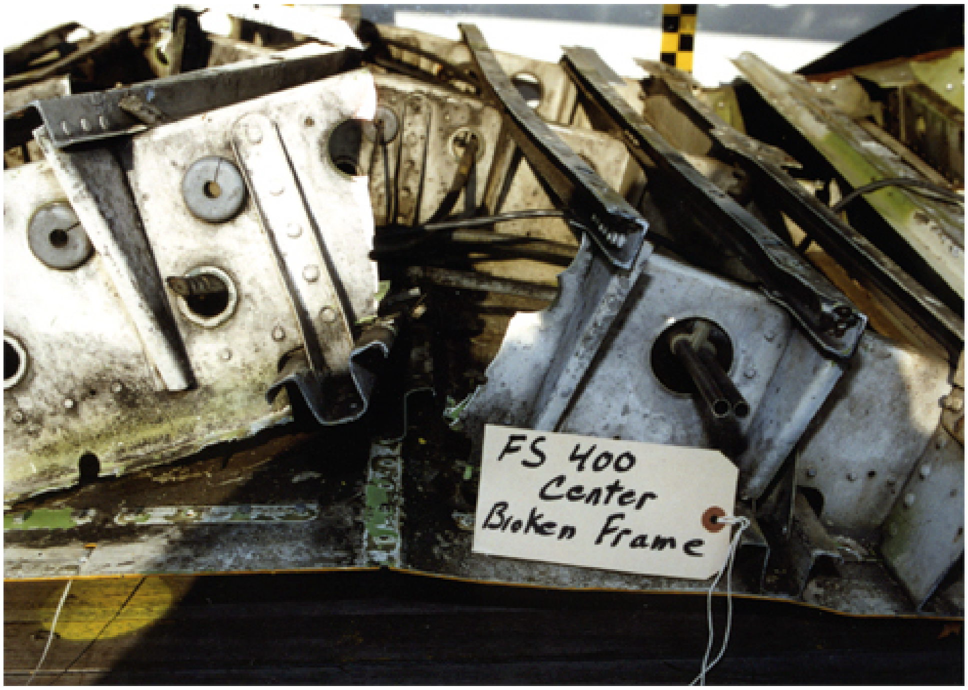

FIGURE A-16. FUSELAGE STATION 400 CENTER FRONT FRAME—CLOSE-UP

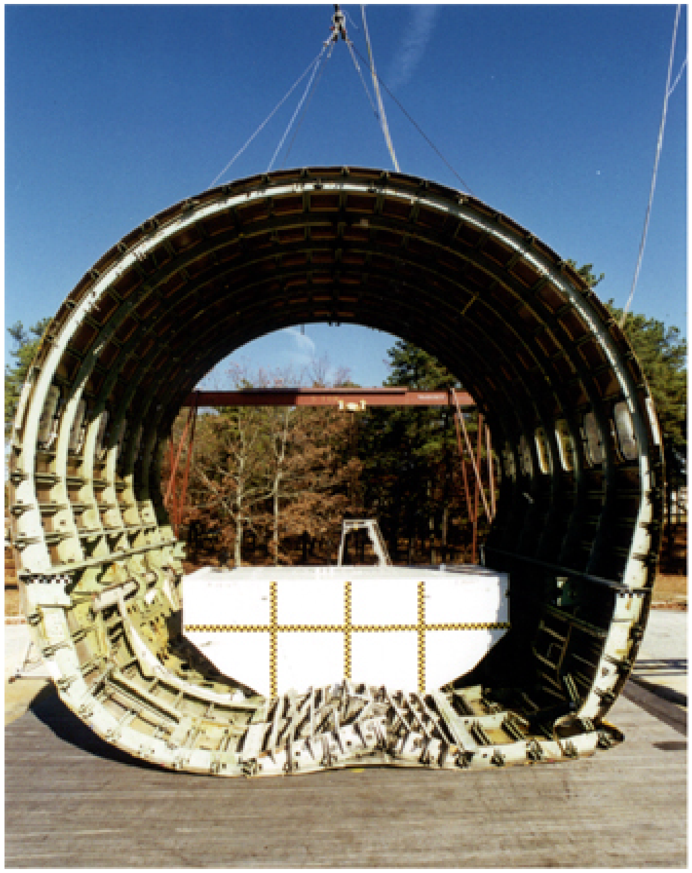

FIGURE A-17. CABIN FLOOR REMOVED—FRONT VIEW

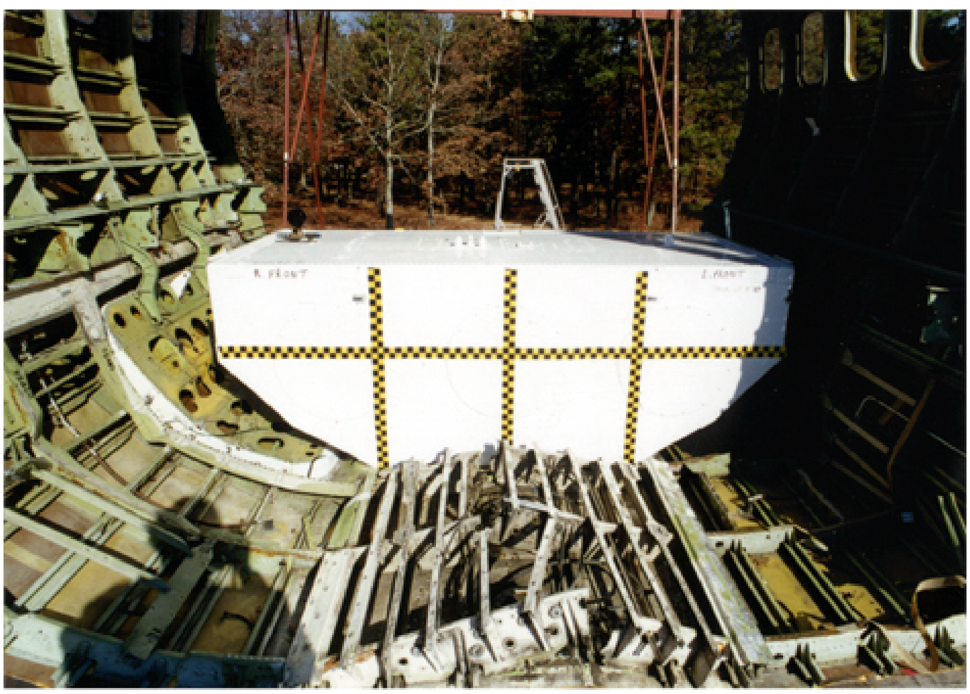

FIGURE A-18. CARGO AREA FLOOR BUCKLE—FRONT VIEW

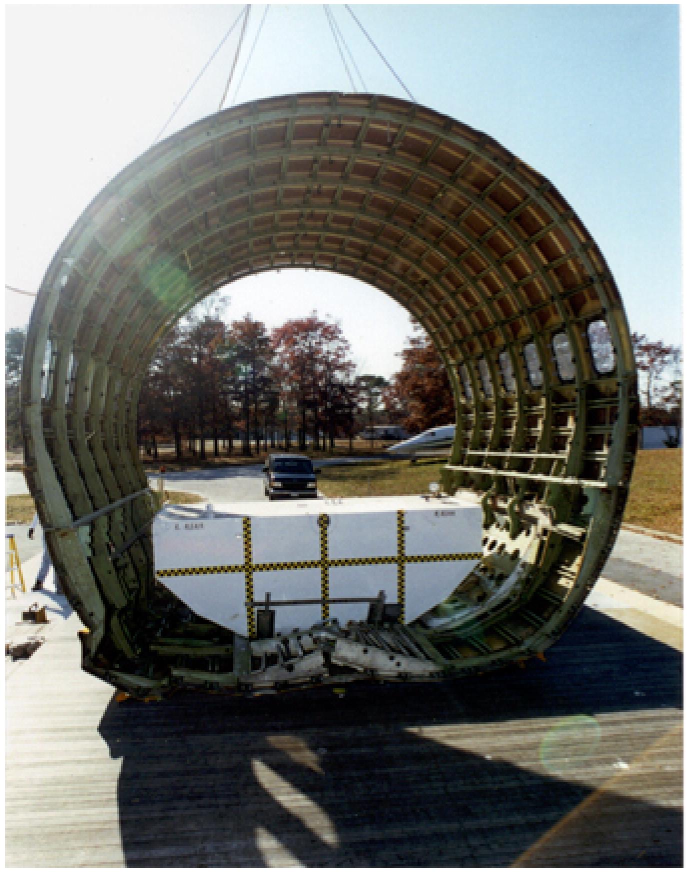

FIGURE A-19. CABIN FLOOR REMOVED—REAR VIEW

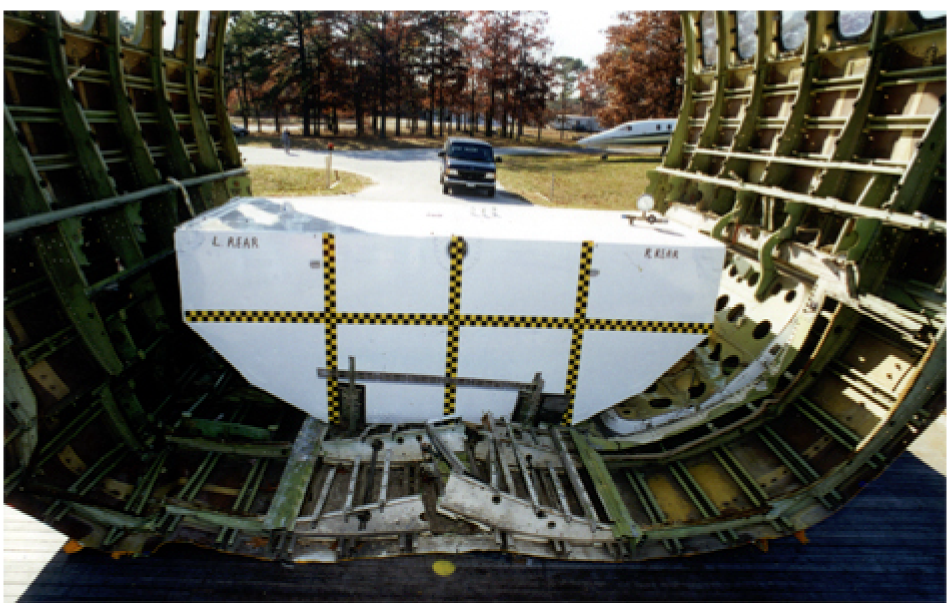

FIGURE A-20. CARGO AREA FLOOR BUCKLE—REAR VIEW

FIGURE A-21. CONFORMABLE AUXILIARY FUEL TANK—RIGHT SIDE

FIGURE A-22. CONFORMABLE AUXILIARY FUEL TANK—LEFT SIDE

FIGURE A-23. CONFORMABLE AUXILIARY FUEL TANK—BOTTOM

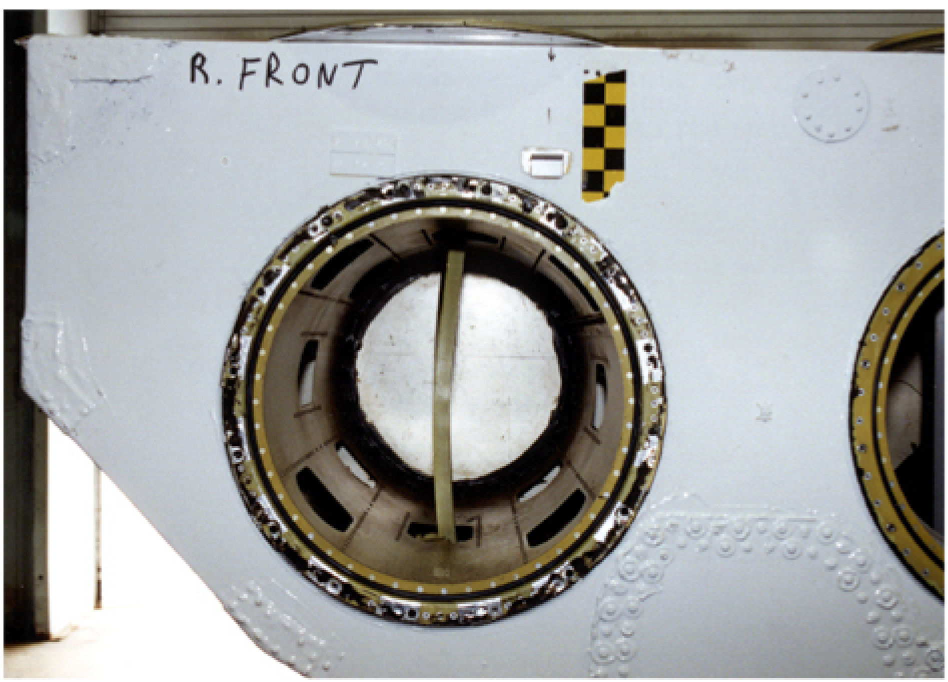

FIGURE A-24. FUEL TANK, BENT STIFFENING MEMBER—RIGHT SIDE

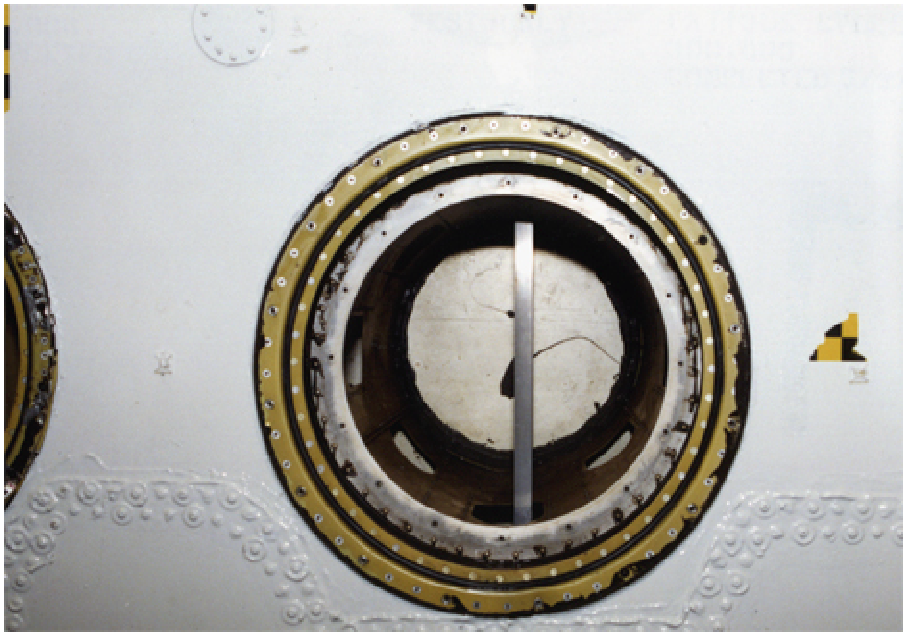

FIGURE A-25. FUEL TANK, STIFFENING MEMBER—CENTER

FIGURE A-26. FUEL TANK, STIFFENING MEMBER—LEFT SIDE

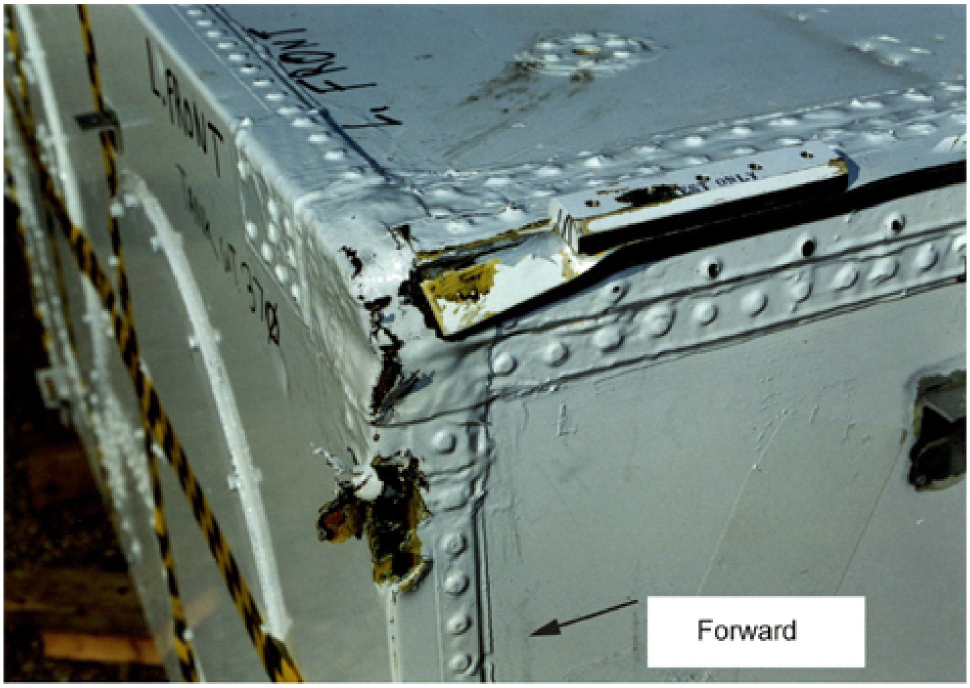

FIGURE A-27. FUEL TANK DAMAGE—LEFT FRONT

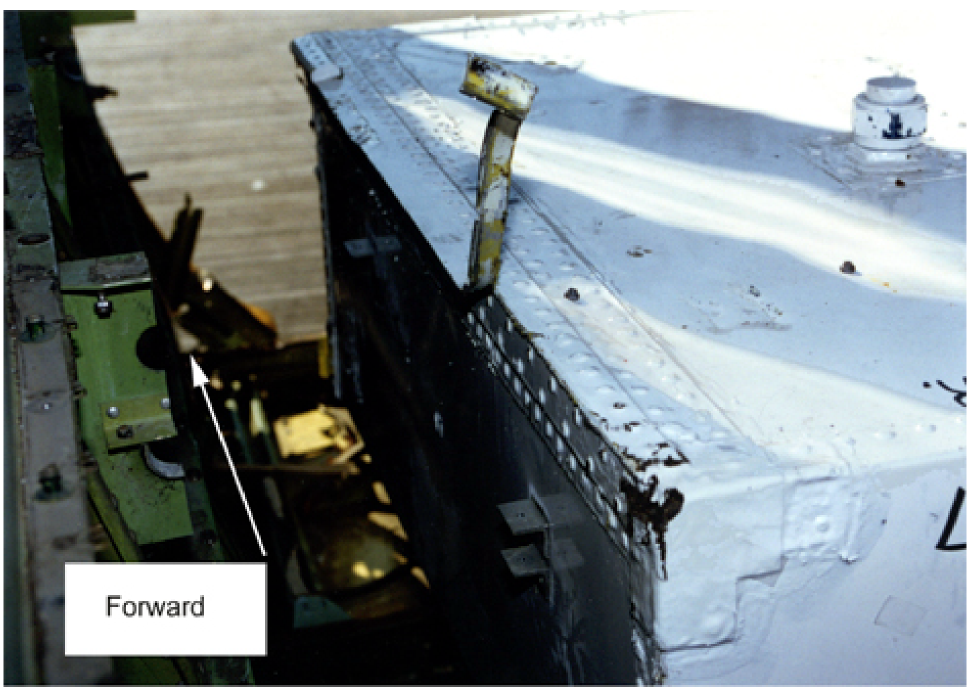

FIGURE A-28. FUEL TANK DAMAGE—LEFT REAR

FIGURE A-29. BENT RIGHT TANK RAIL

FIGURE A-30. FUEL TANK—BOTTOM, LEFT REAR

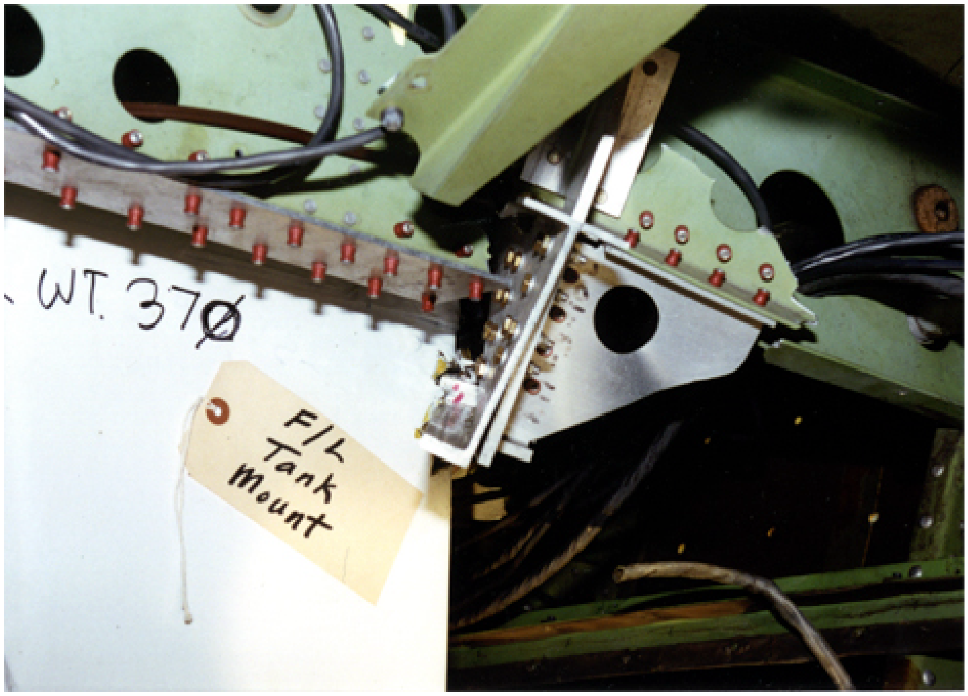

FIGURE A-31. FUEL TANK MOUNT—LEFT FRONT

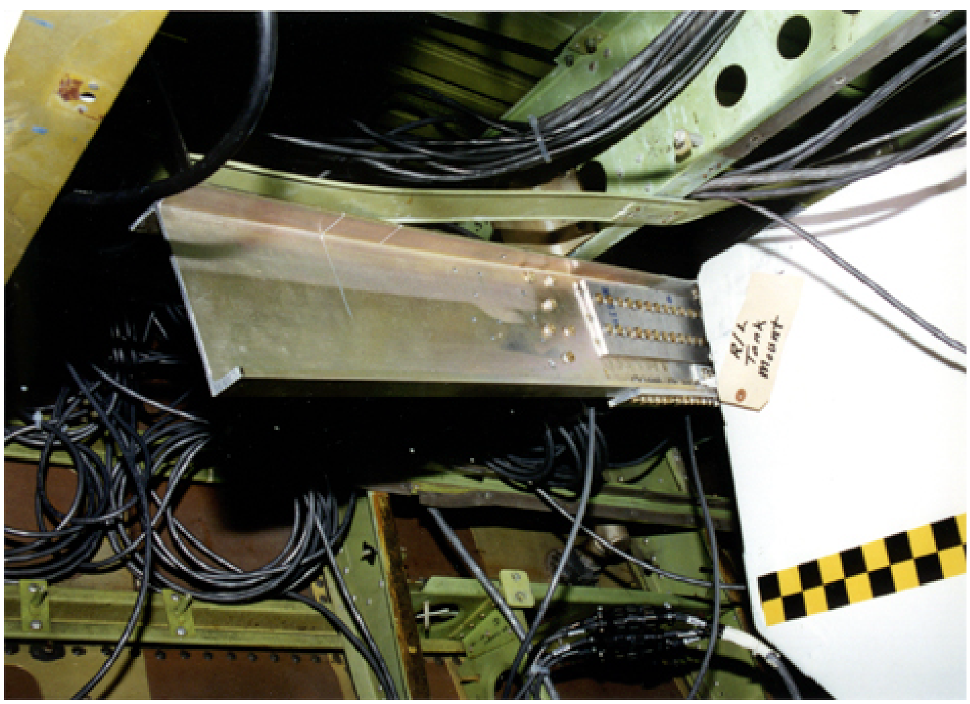

FIGURE A-32. FUEL TANK MOUNT—LEFT REAR

FIGURE A-33. FUEL TANK MOUNT—RIGHT FRONT

FIGURE A-34. FUEL TANK MOUNT—RIGHT REAR

FIGURE A-35. FUEL TANK—LEFT FRONT

FIGURE A-36. FUEL TANK—LEFT REAR

FIGURE A-37. FUEL TANK—RIGHT FRONT

FIGURE A-38. FUEL TANK—RIGHT REAR

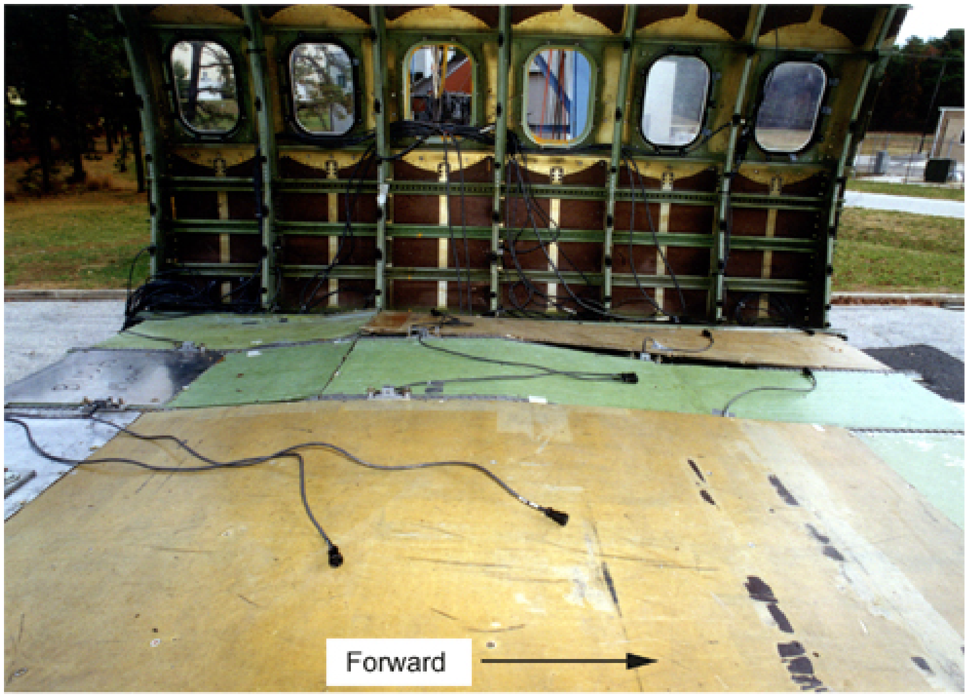

FIGURE A-39. CABIN FLOOR BUCKLE

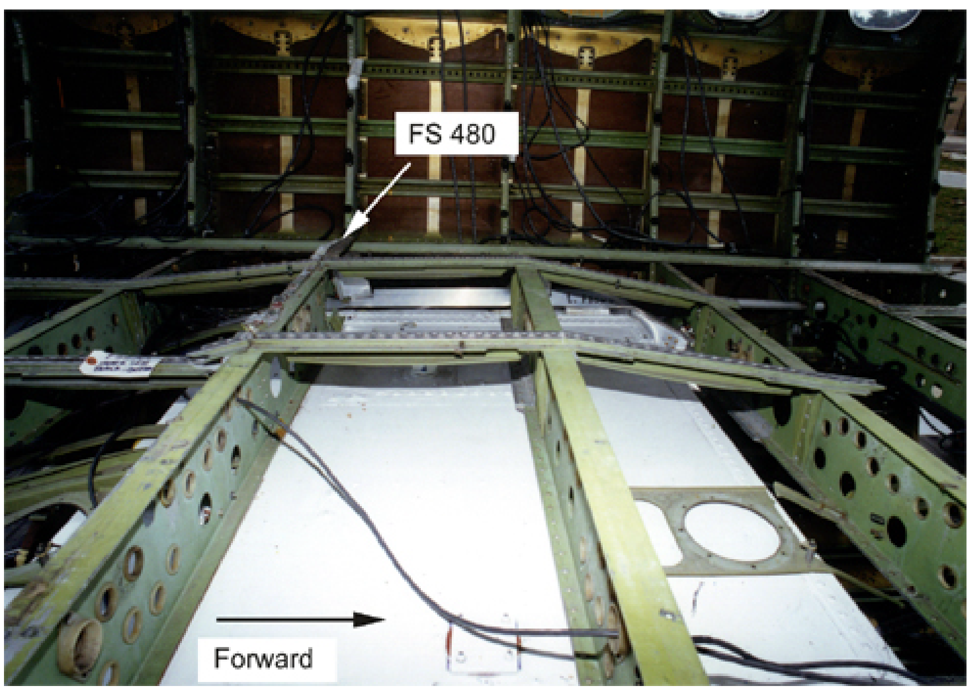

FIGURE A-40. BROKEN SEAT TRACKS—LEFT SIDE

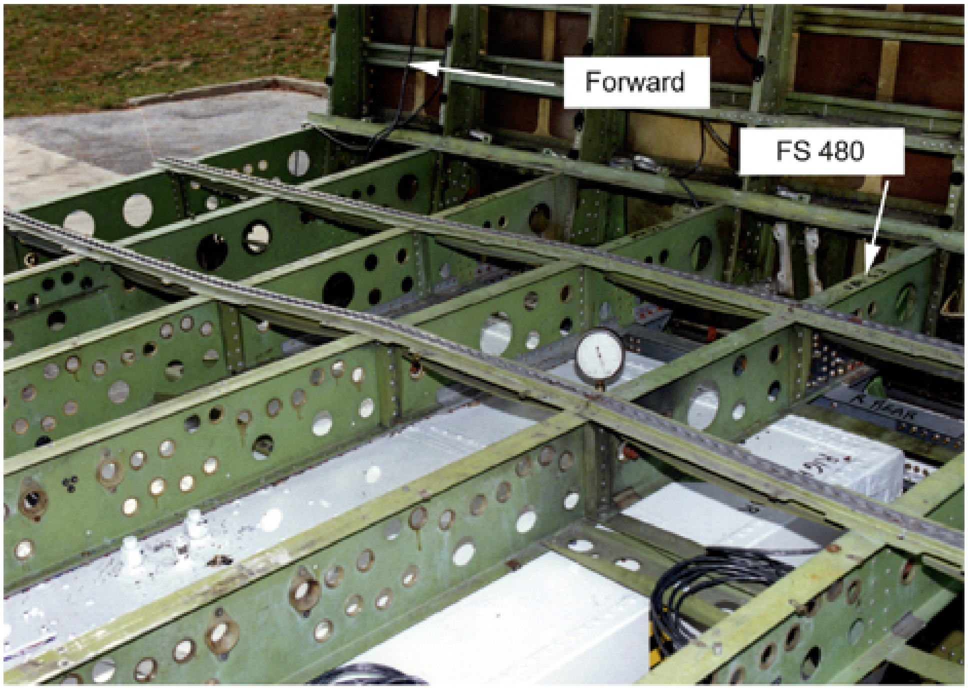

FIGURE A-41. BENT SEAT TRACKS—RIGHT SIDE

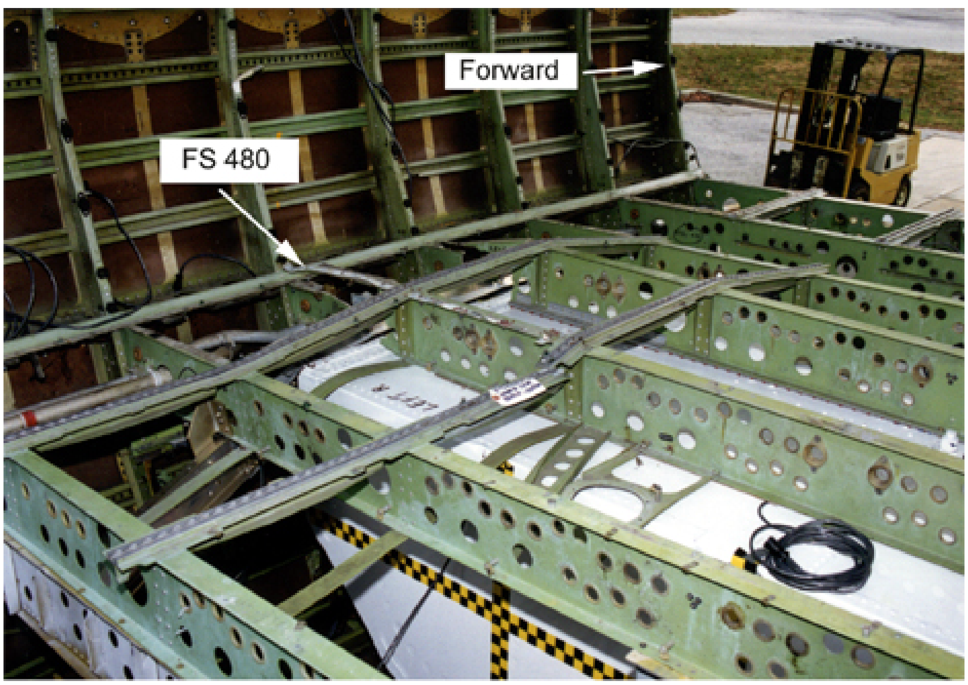

FIGURE A-42. BROKEN SEAT TRACKS—LEFT SIDE

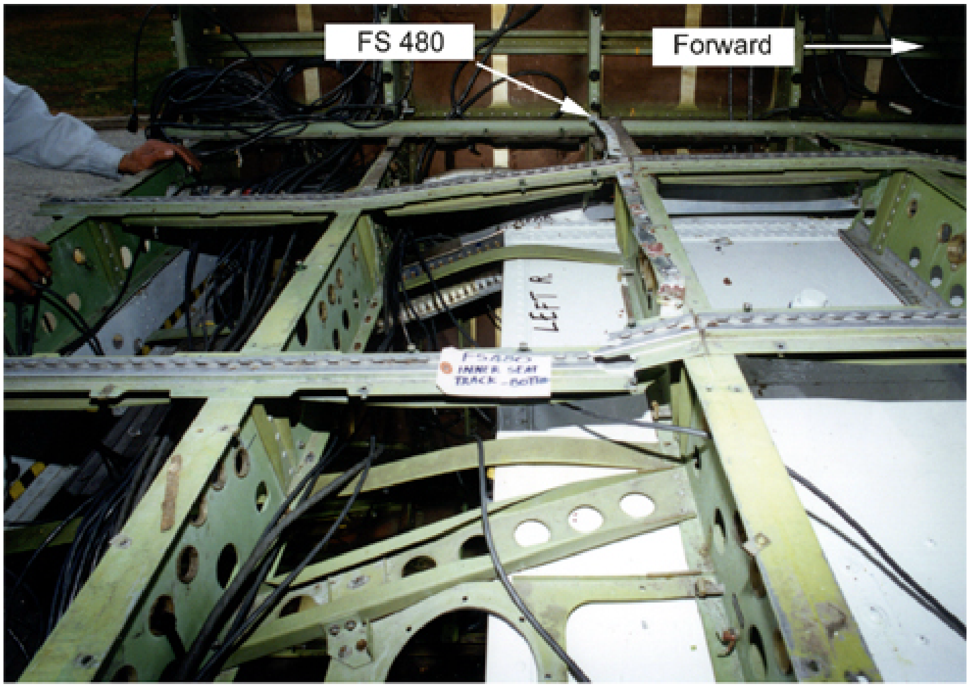

FIGURE A-43. BROKEN SEAT TRACKS—LEFT REAR

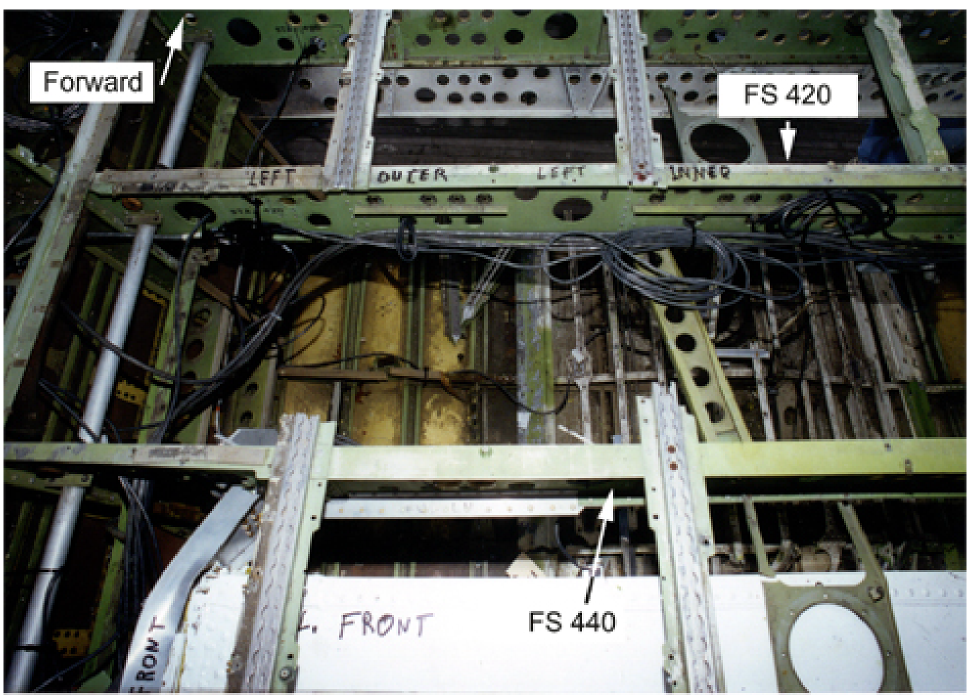

FIGURE A-44. BROKEN SEAT TRACKS—LEFT FRONT

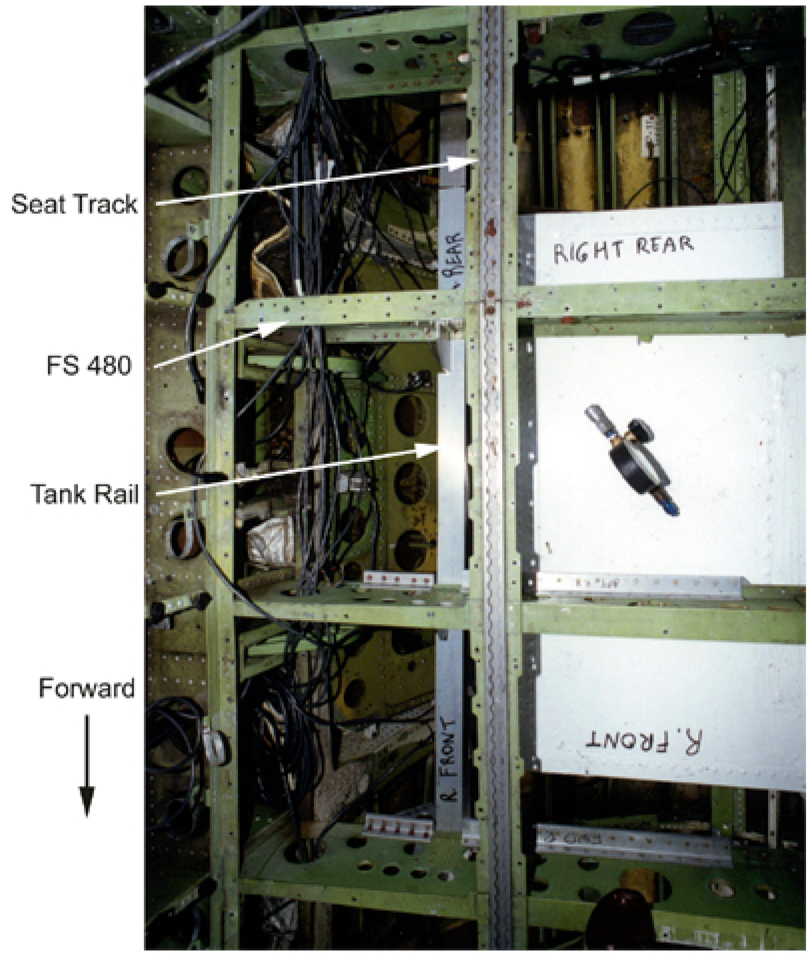

FIGURE A-45. OUTER SEAT TRACK AND TANK RAIL—RIGHT SIDE, VIEW LOOKING DOWN

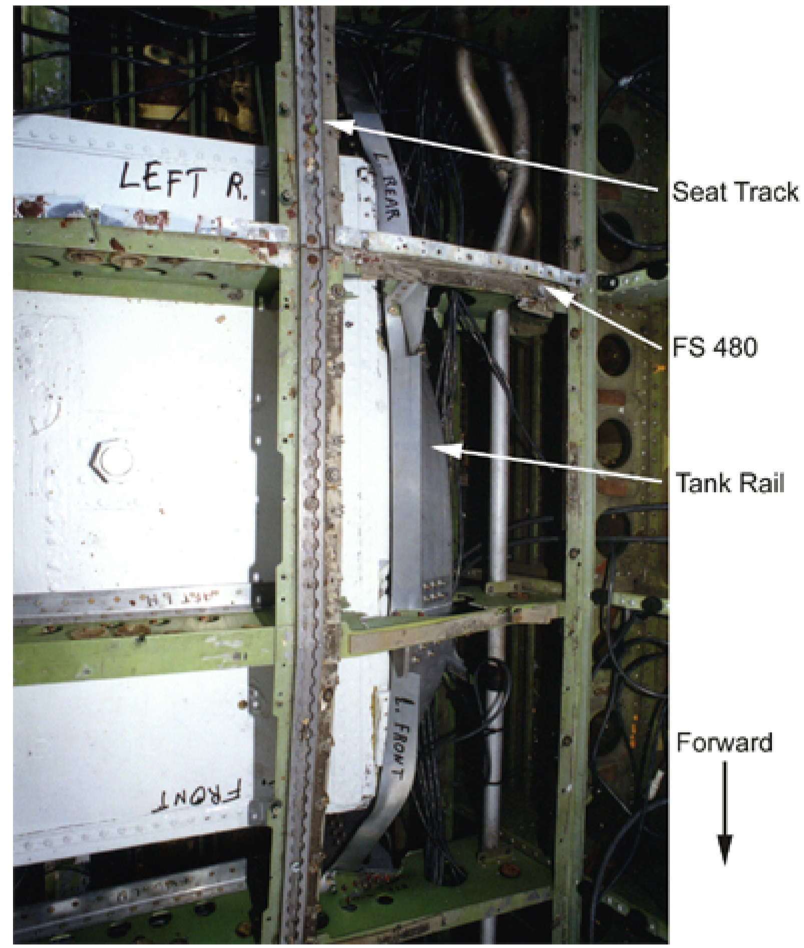

FIGURE A-46. OUTER SEAT TRACK AND TANK RAIL—LEFT SIDE, VIEW LOOKING DOWN

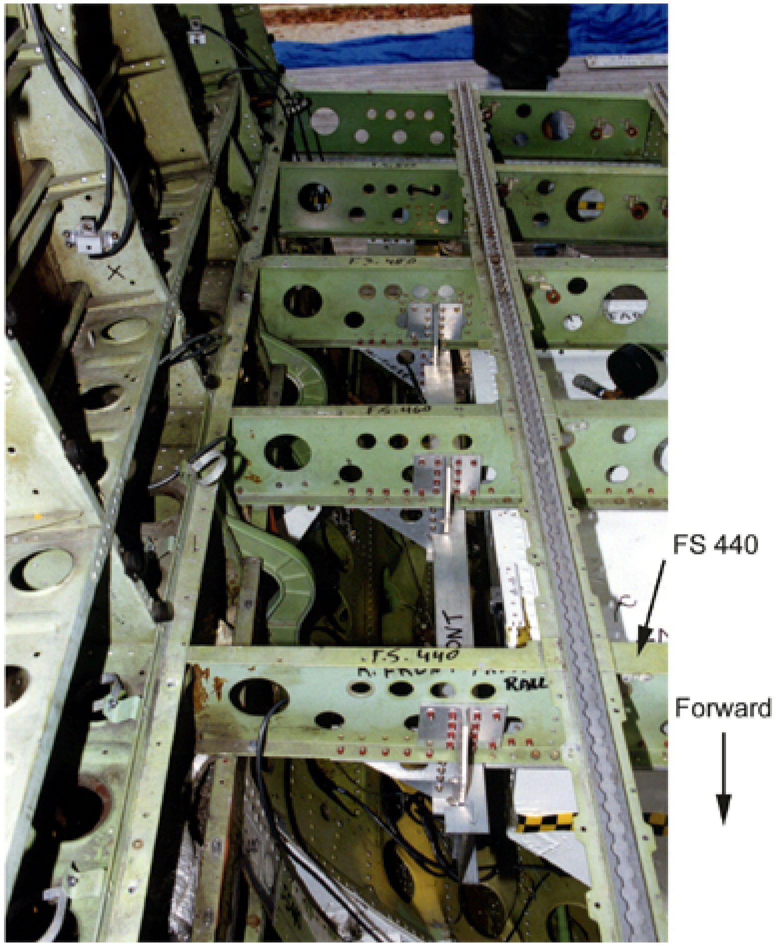

FIGURE A-47. OUTER SEAT TRACK AND TANK RAIL—RIGHT SIDE, VIEW LOOKING AFT

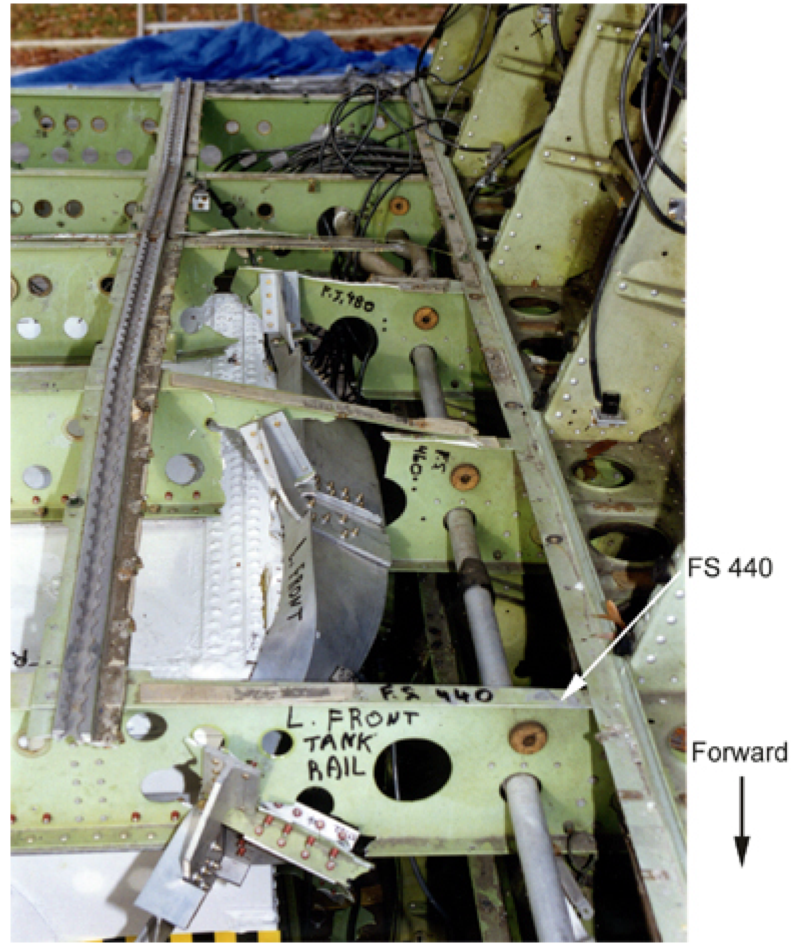

FIGURE A-48. OUTER SEAT TRACK AND TANK RAIL—LEFT SIDE, VIEW LOOKING AFT

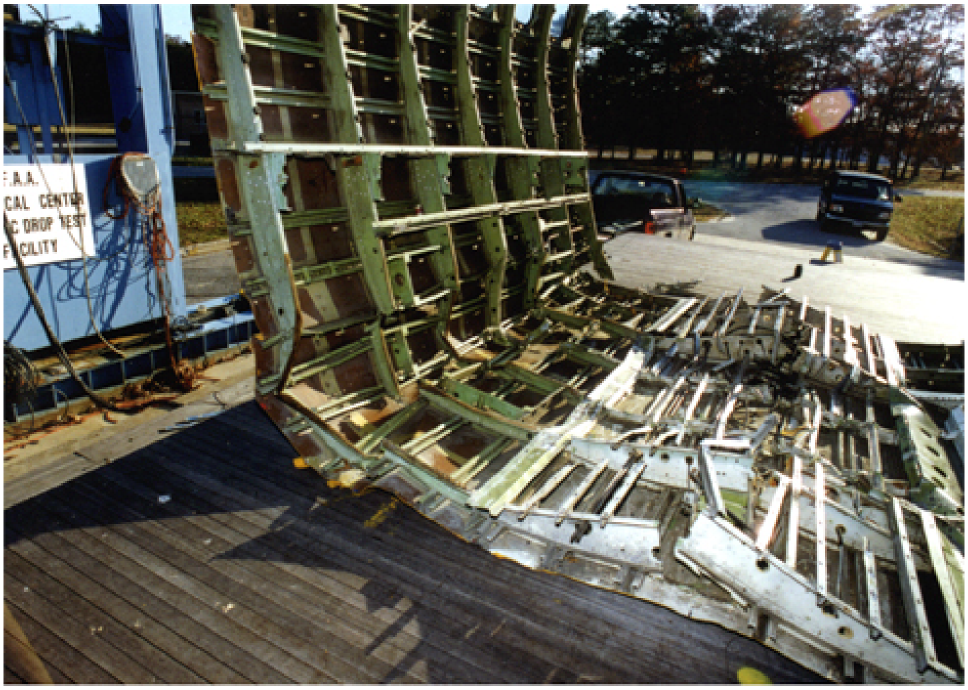

FIGURE A-49. FUSELAGE CRUSH WITH CABIN FLOOR REMOVED—LEFT SIDE, VIEW LOOKING FORWARD

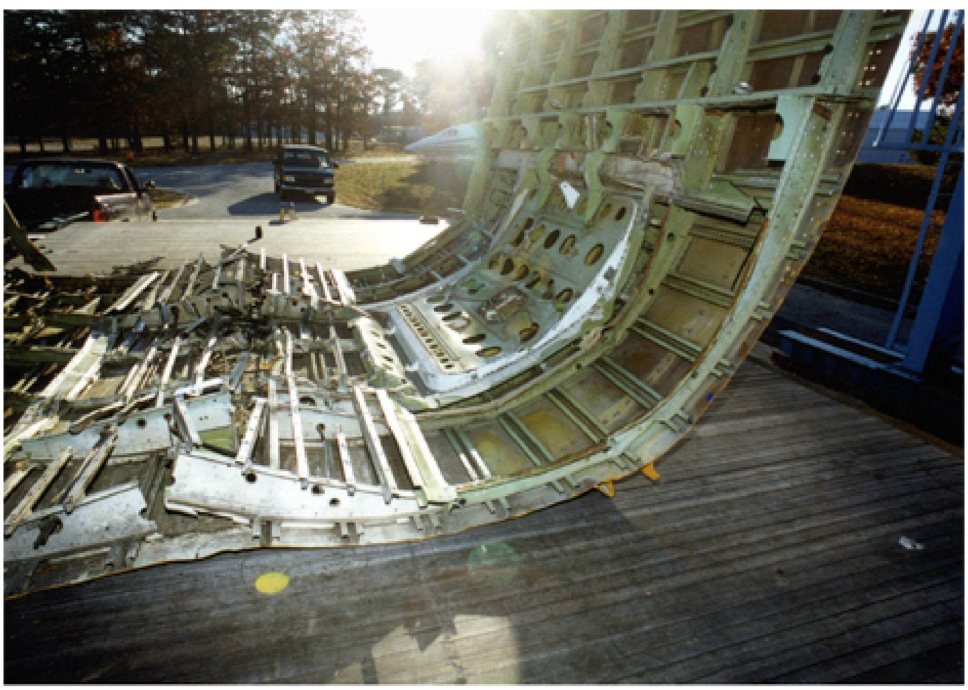

FIGURE A-50. FUSELAGE CRUSH WITH CABIN FLOOR REMOVED—RIGHT SIDE, VIEW LOOKING FORWARD

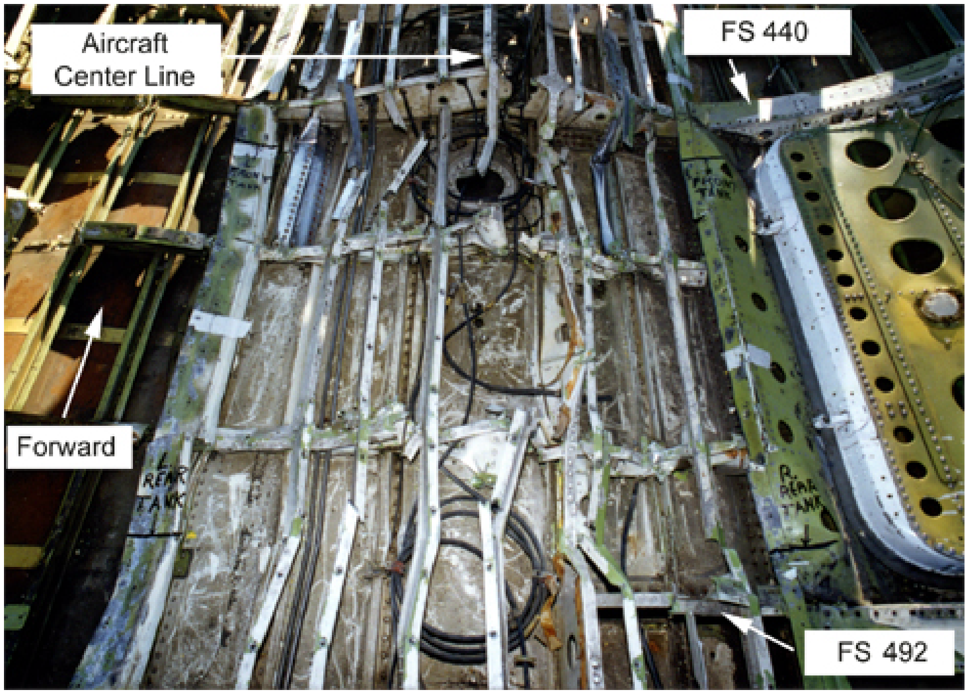

FIGURE A-51. CARGO FLOOR CRUSHED BY FUEL TANK

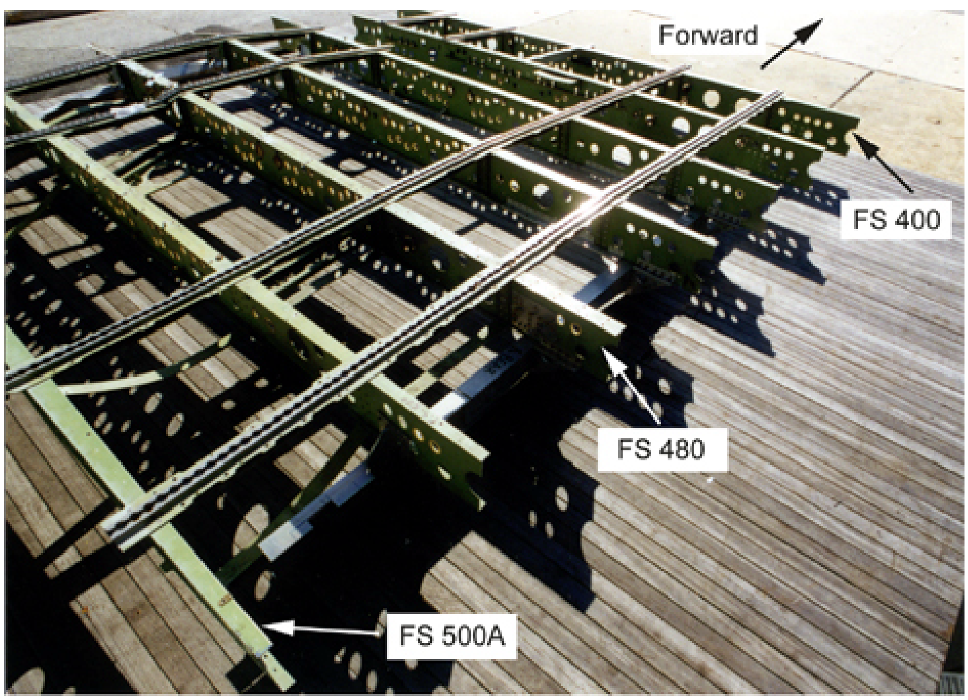

FIGURE A-52. FLOOR BEAMS AND SEAT TRACKS

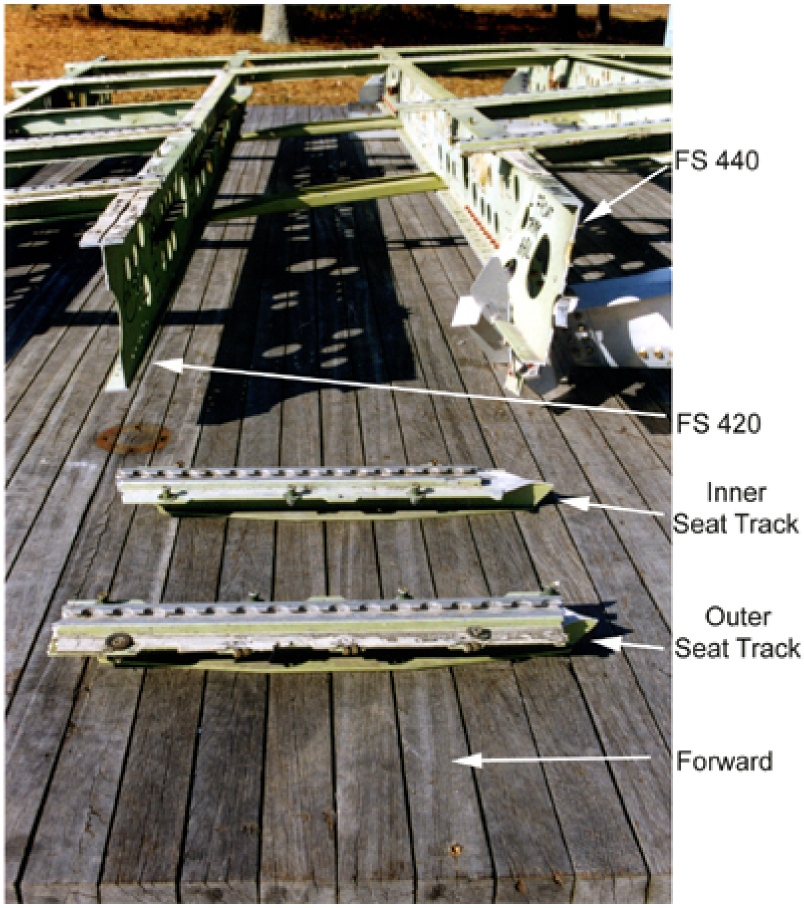

FIGURE A-53. BROKEN SEAT TRACKS—LEFT SIDE

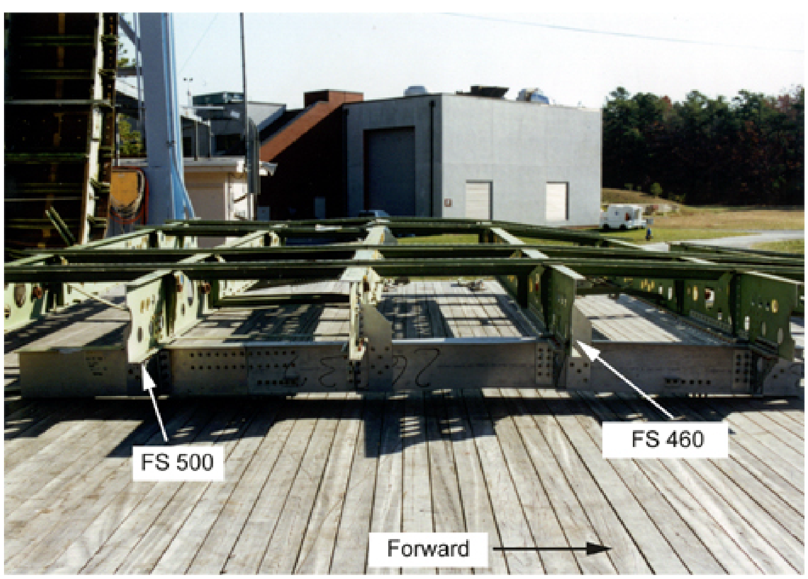

FIGURE A-54. FLOOR BEAMS, SEAT TRACKS, FUEL TANK RAIL—RIGHT SIDE

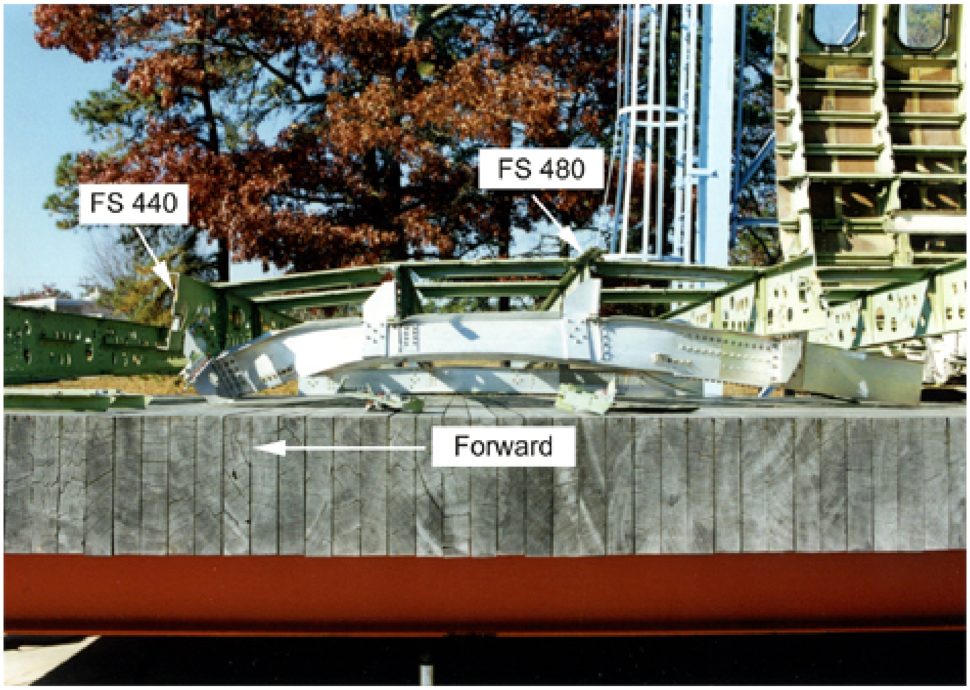

FIGURE A-55. FLOOR BEAMS, SEAT TRACKS, FUEL TANK RAIL—LEFT SIDE

FIGURE A-56. ROW 1, UOP SEAT, DUMMIES—RIGHT SIDE

FIGURE A-57. ROW 2, UOP SEAT, DUMMIES—RIGHT SIDE

FIGURE A-58. ROW 3, UOP SEAT, DUMMIES—RIGHT SIDE

FIGURE A-59. ROW 1, UOP SEAT—RIGHT SIDE

FIGURE A-60. ROW 2, UOP SEAT—RIGHT SIDE

FIGURE A-61. ROW 3, UOP SEAT—RIGHT SIDE

FIGURE A-62. ROW 1, WEBER SEAT, DUMMIES—LEFT SIDE

FIGURE A-63. ROW 2, WEBER SEAT, DUMMIES—LEFT SIDE

FIGURE A-64. ROW 3, WEBER SEAT, DUMMIES—LEFT SIDE

FIGURE A-65. ROW 1, WEBER SEAT—LEFT SIDE

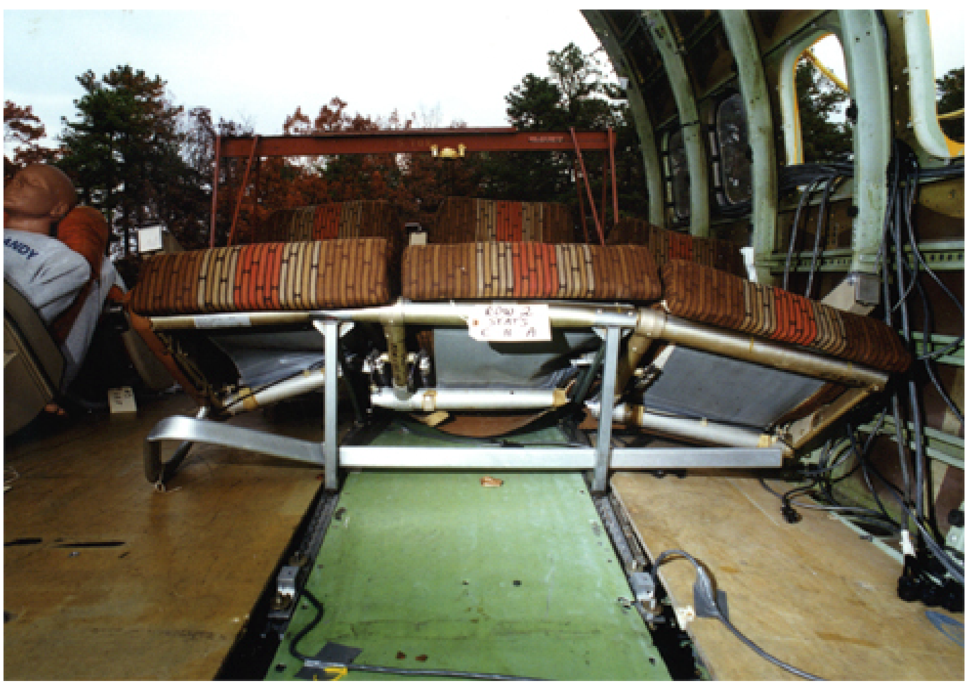

FIGURE A-66. ROW 2, WEBER SEAT—LEFT SIDE

FIGURE A-67. ROW 3, WEBER SEAT—LEFT SIDE

APPENDIX B—TEST DATA

ANTHROPOMORPHIC TEST DUMMY DATA (FIGURES B-1 TO B-12)

CABIN AREA FUSELAGE DATA (FIGURES B-13 TO B-54)

CARGO AREA FUSELAGE DATA (FIGURES B-55 TO B-83)

DROP TEST PLATFORM DATA (FIGURES B-84 TO B-113)

ANTHROPOMORPHIC TEST DUMMY DATA

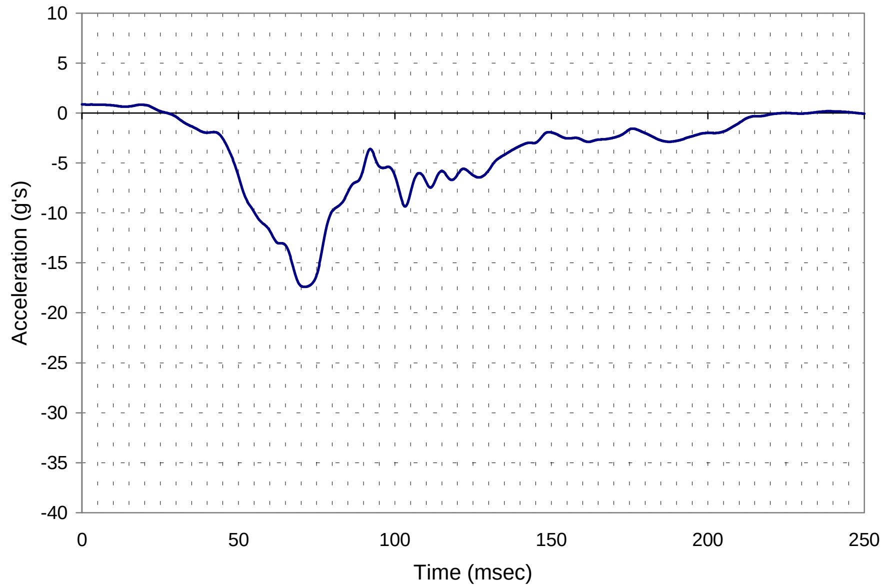

FIGURE B-1. FS 427 ATD #1, ACCELEROMETER Z-DIRECTION, ROW 1 SEAT B
(DAS-48S Channel 3)

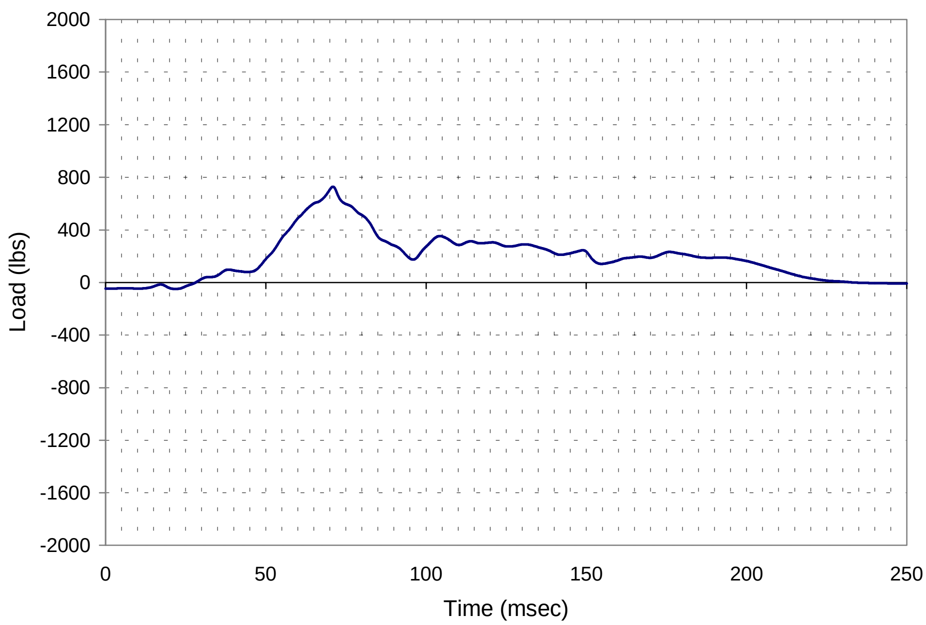

FIGURE B-2. FS 427 ATD #1, LOAD CELL, ROW 1 SEAT B
(DAS-48S Channel 33)

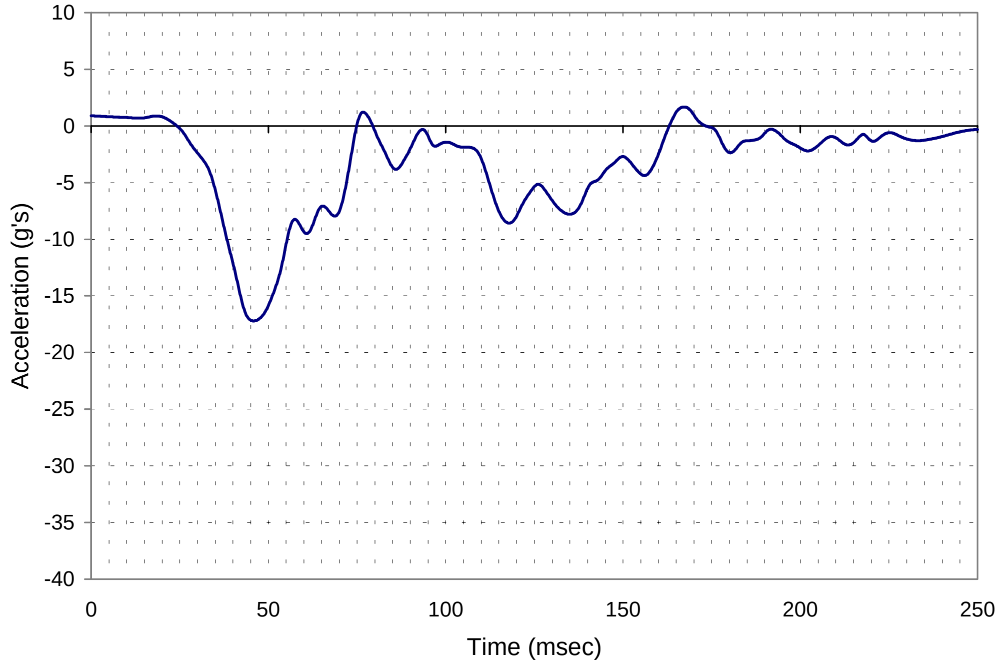

FIGURE B-3. FS 426 ATD #2, ACCELEROMETER Z-DIRECTION, ROW 1 SEAT E
(NEFF Channel 304)

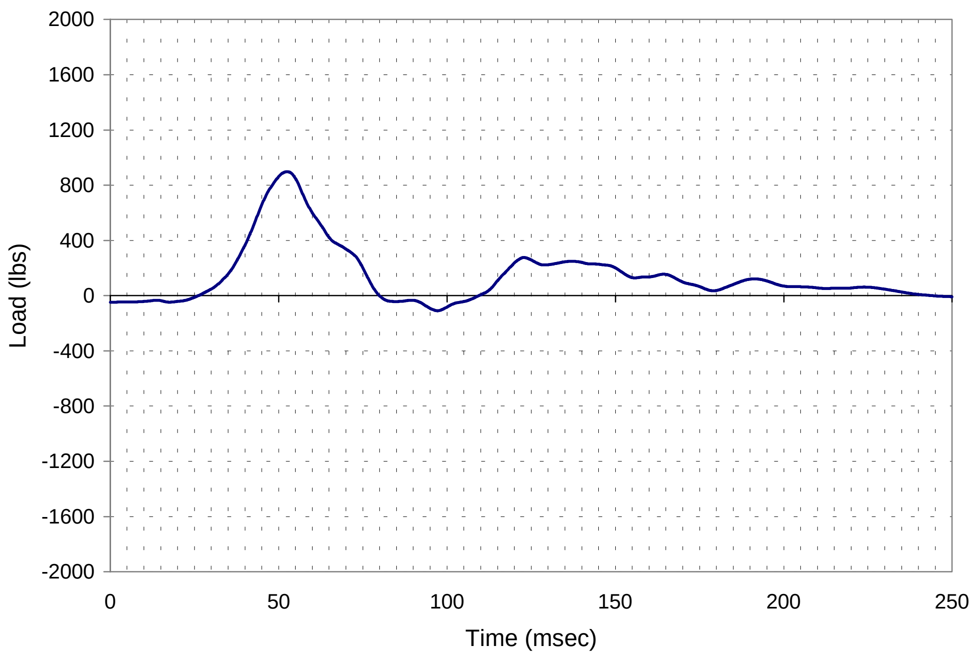

FIGURE B-4. FS 426 ATD #2, LOAD CELL, ROW 1 SEAT E
(NEFF Channel 303)

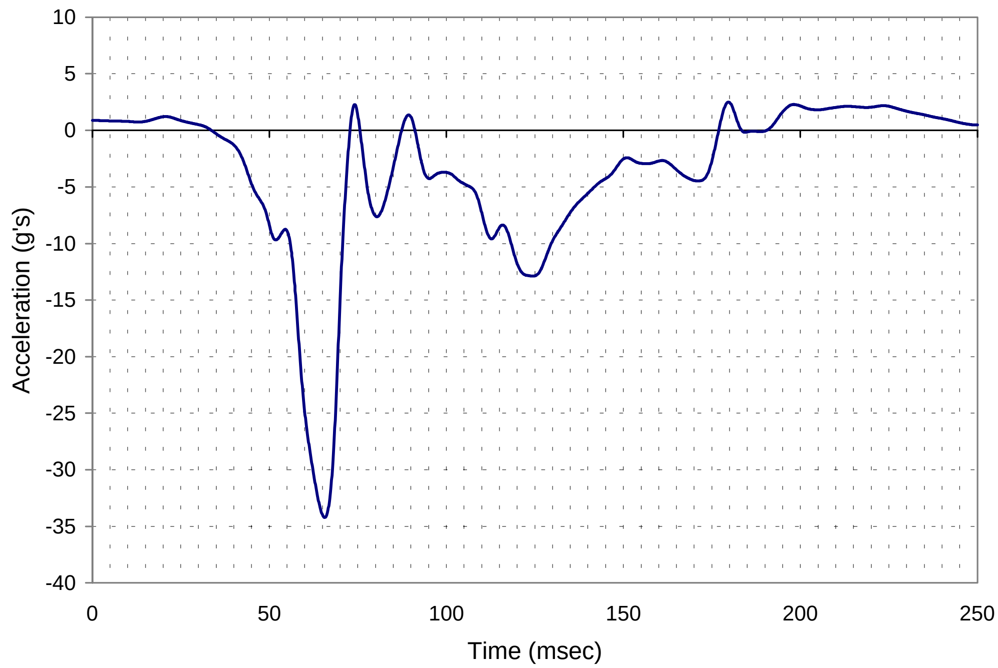

FIGURE B-5. FS 462 ATD #3, ACCELEROMETER Z-DIRECTION, ROW 2 SEAT B
(NEFF Channel 314)

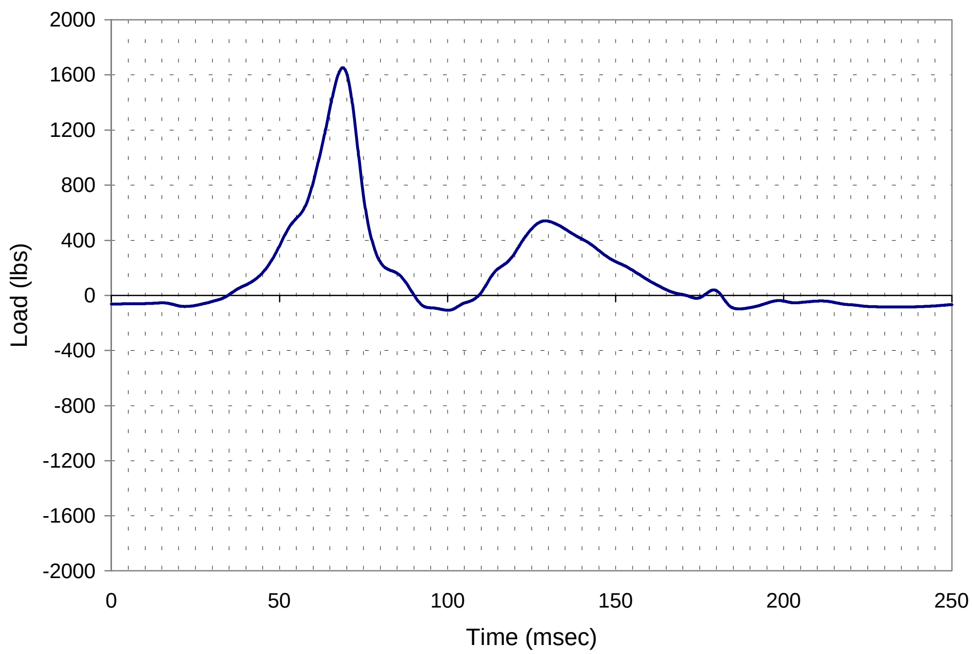

FIGURE B-6. FS 462 ATD #3, LOAD CELL, ROW 2 SEAT B
(NEFF Channel 313)

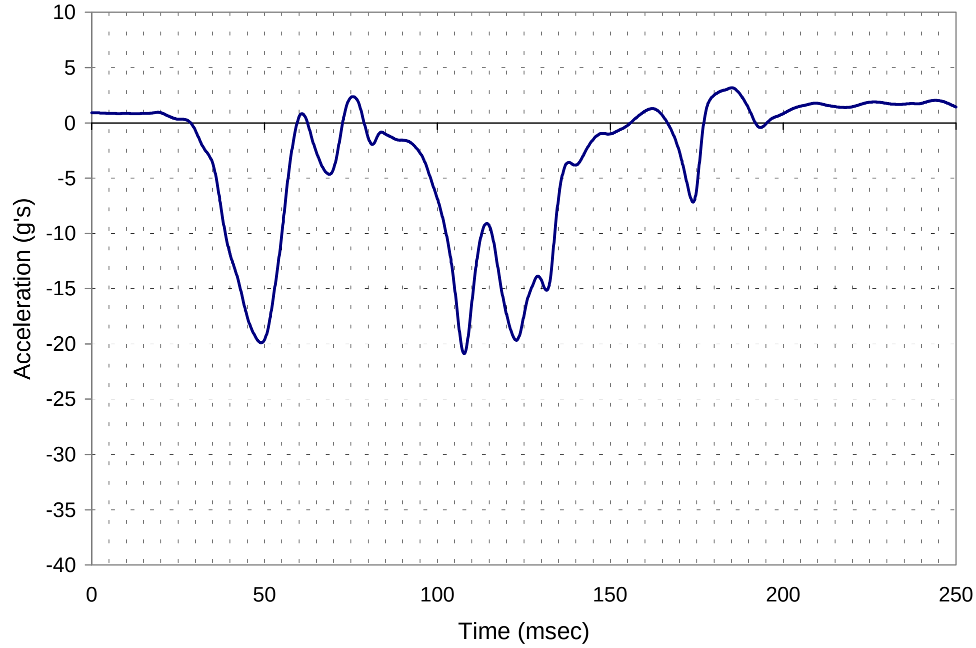

FIGURE B-7. FS 462 ATD #4, ACCELEROMETER Z-DIRECTION, ROW 2 SEAT E
(DAS-48S Channel 7)

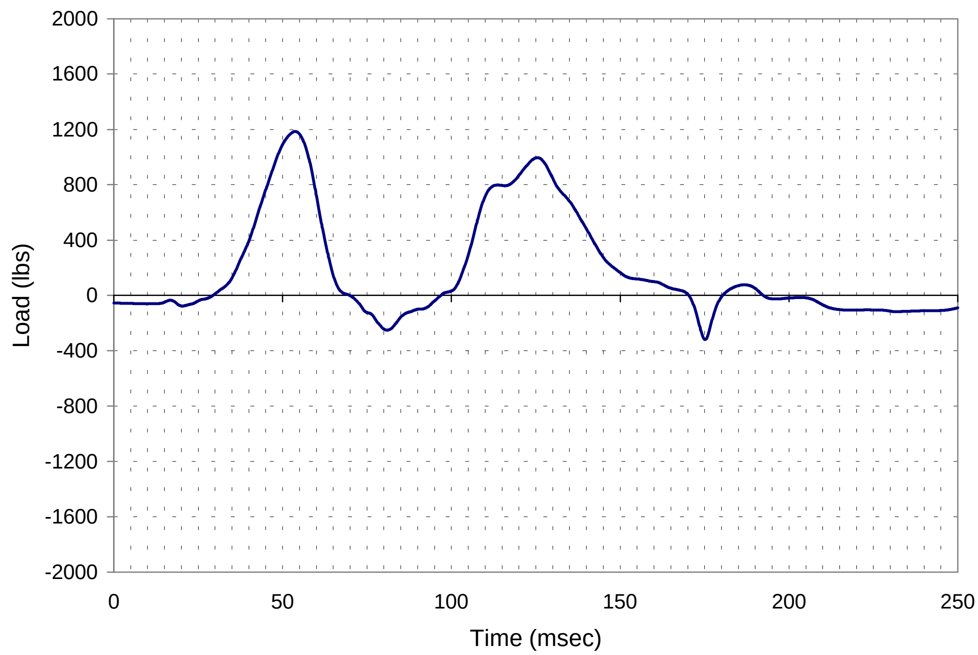

FIGURE B-8. FS 462 ATD #4, LOAD CELL, ROW 2 SEAT E
(DAS-48S Channel 6)

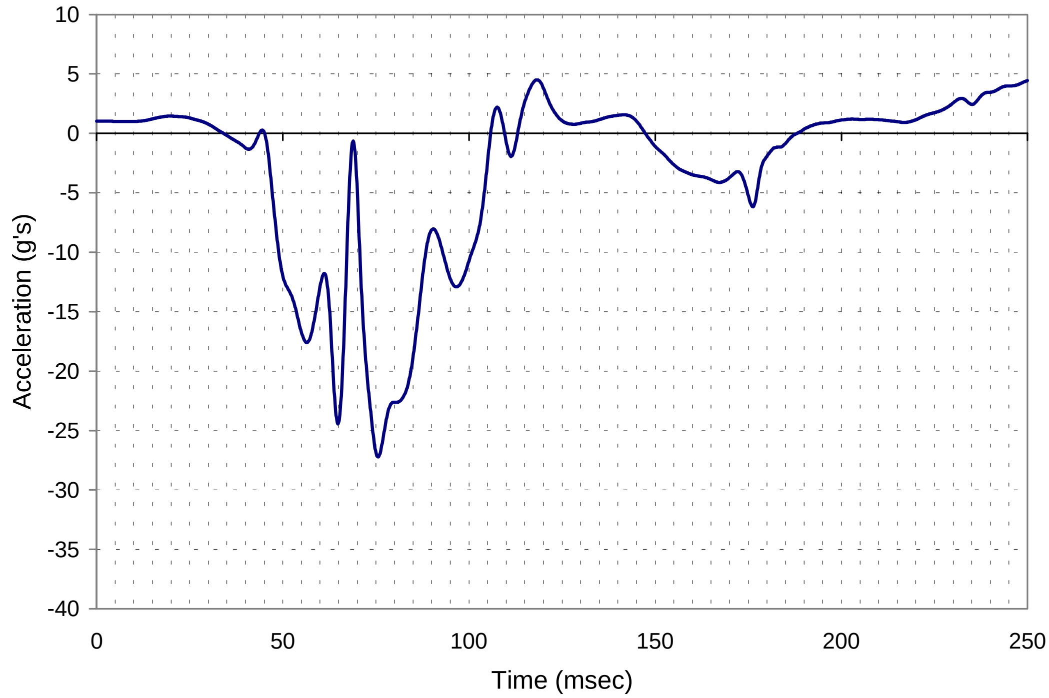

FIGURE B-9. FS 497 ATD #5, ACCELEROMETER Z-DIRECTION, ROW 3 SEAT B
(NEFF Channel 411)

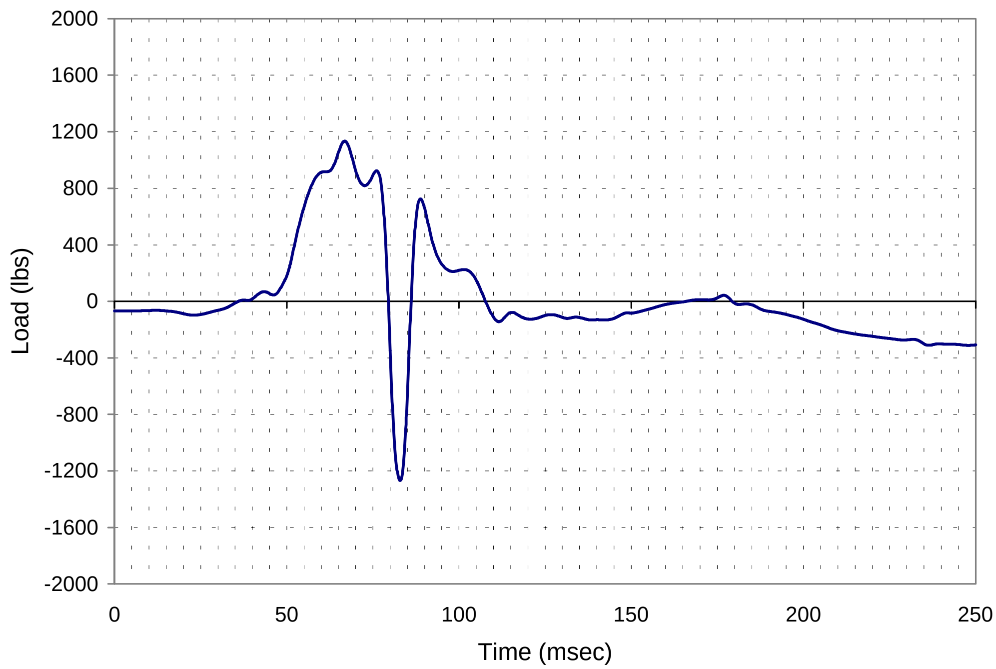

FIGURE B-10. FS 497 ATD #5, LOAD CELL, ROW 3 SEAT B
(NEFF Channel 410)

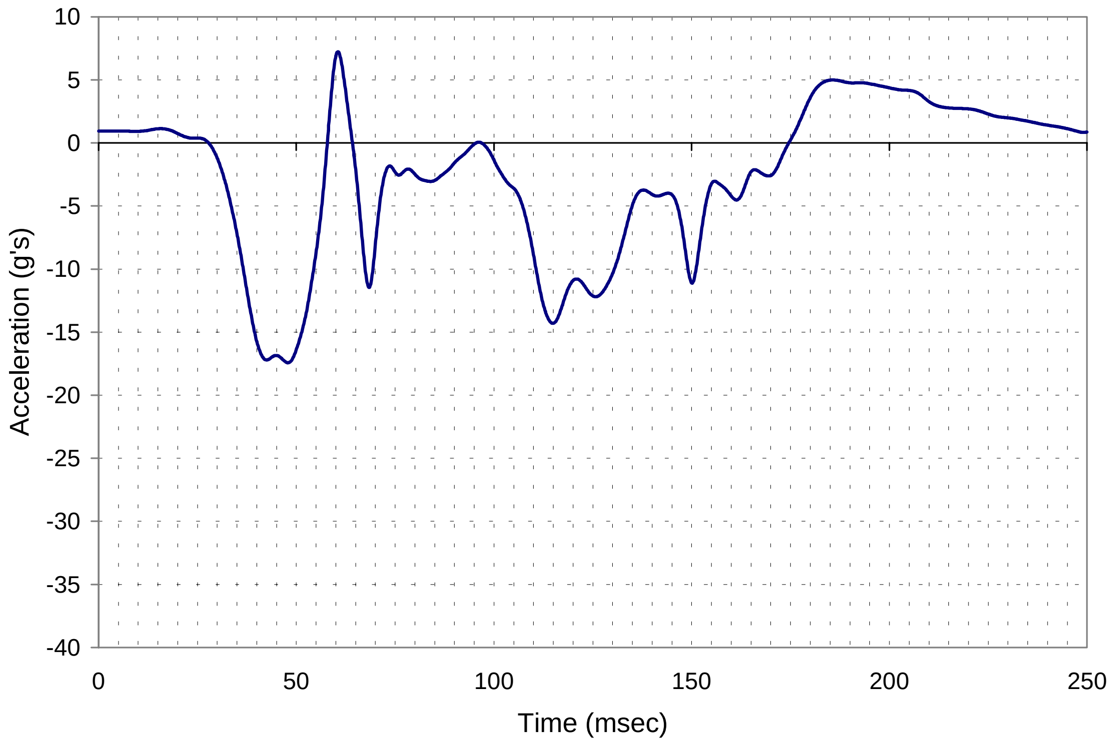

FIGURE B-11. FS 498 ATD #6, ACCELEROMETER Z-DIRECTION, ROW 3 SEAT E
(NEFF Channel 415)

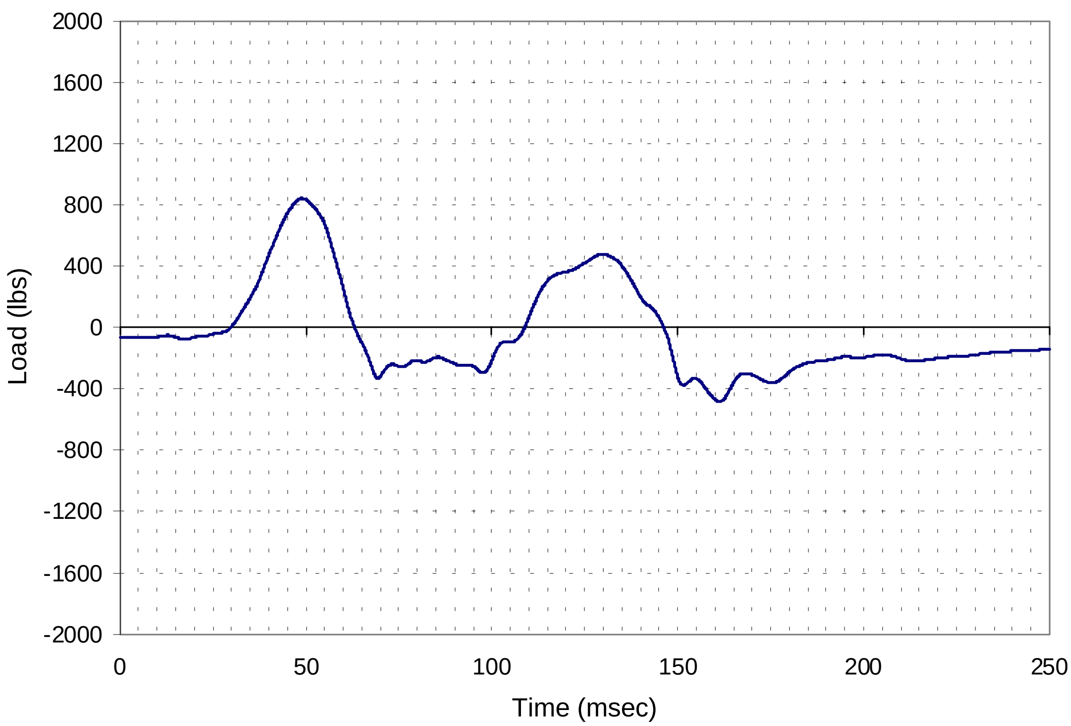

FIGURE B-12. FS 498 ATD #6, LOAD CELL, ROW 3 SEAT E
(NEFF Channel 414)

CABIN AREA FUSELAGE DATA

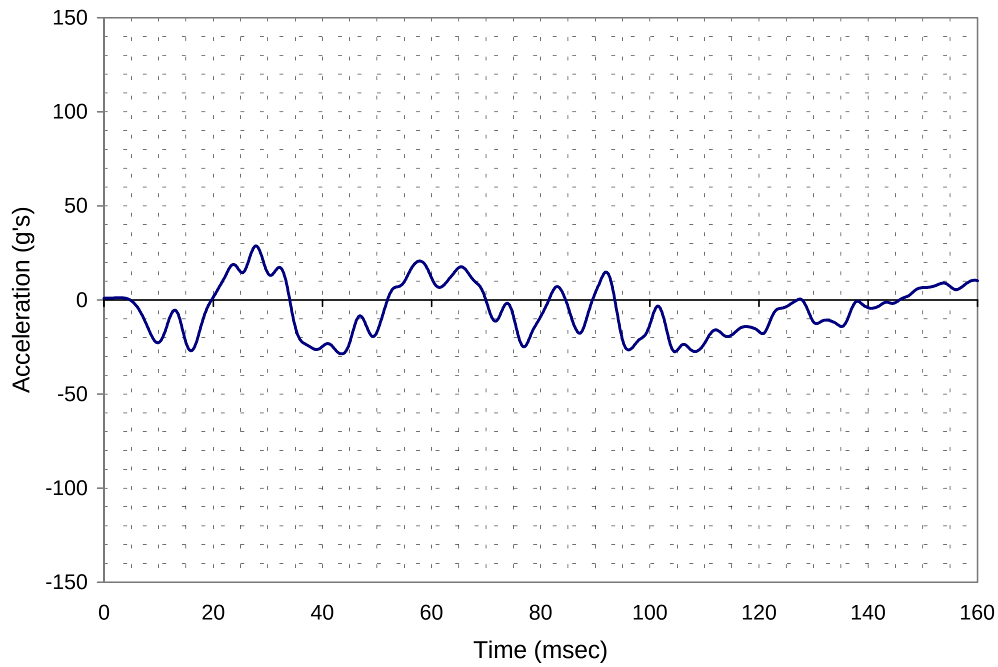

FIGURE B-13. FS 420 LEFT UPPER SIDEWALL, ACCELEROMETER Z-DIRECTION
(NEFF Channel 228)

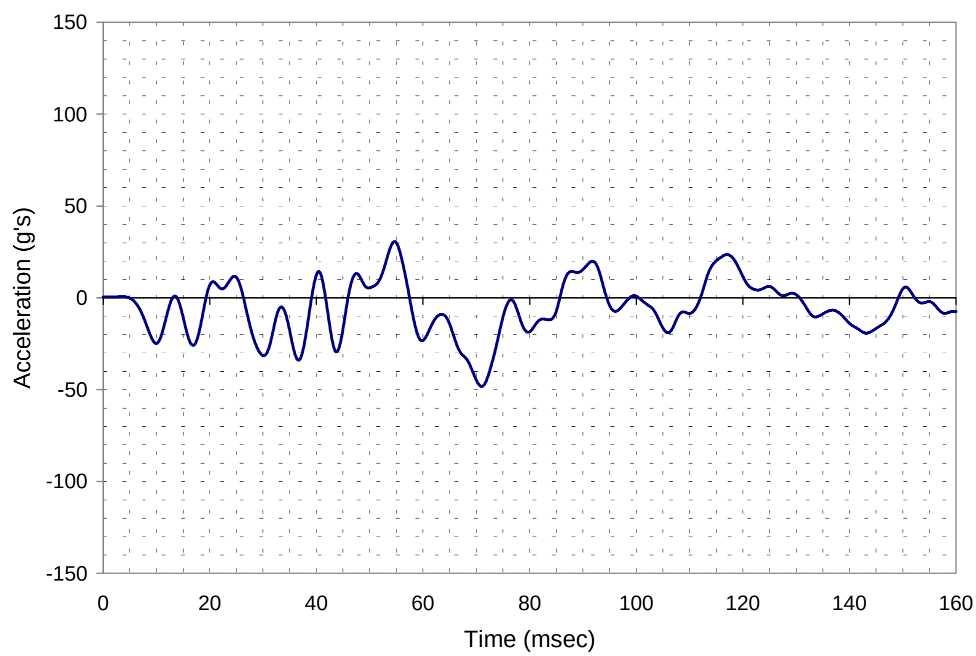

FIGURE B-14. FS 420 RIGHT UPPER SIDEWALL, ACCELEROMETER Z-DIRECTION
(NEFF Channel 307)

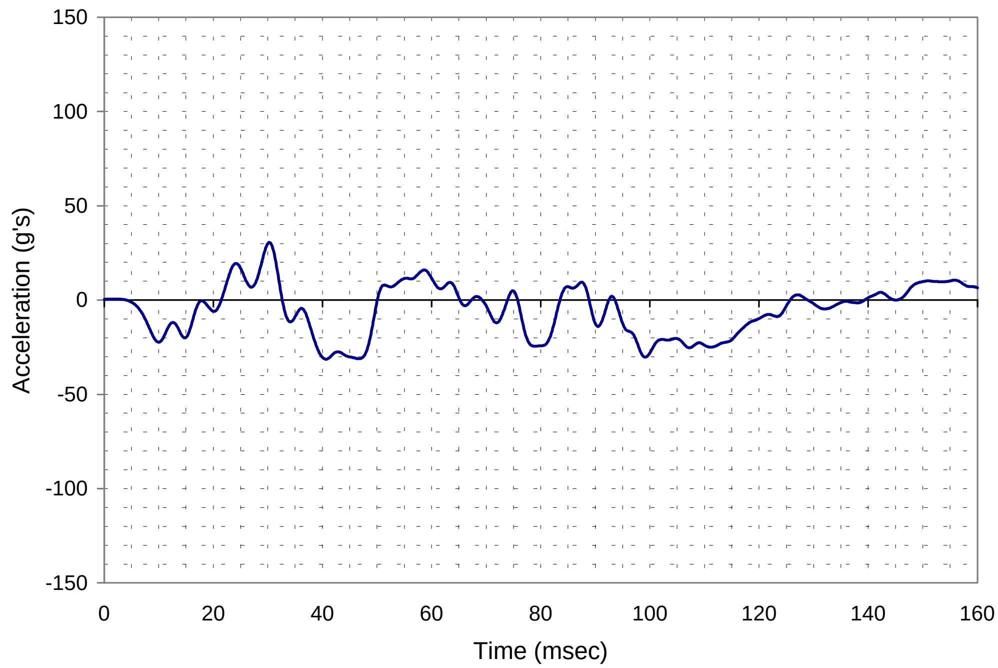

FIGURE B-15. FS 460 LEFT UPPER SIDEWALL, ACCELEROMETER Z-DIRECTION (NEFF Channel 309)

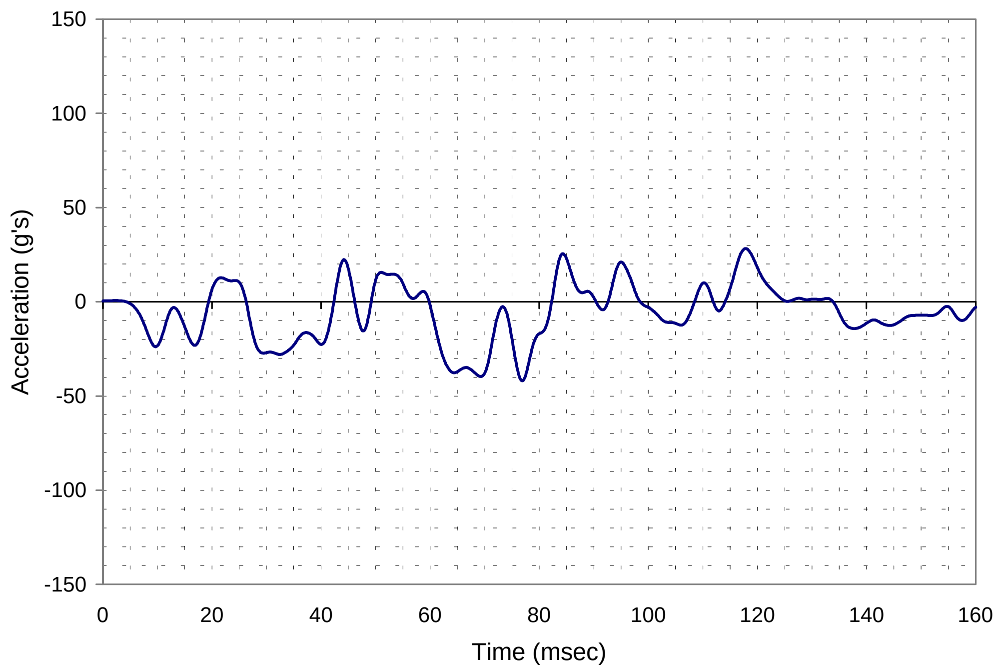

FIGURE B-16. FS 460 RIGHT UPPER SIDEWALL, ACCELEROMETER Z-DIRECTION (DAS-48S Channel 11)

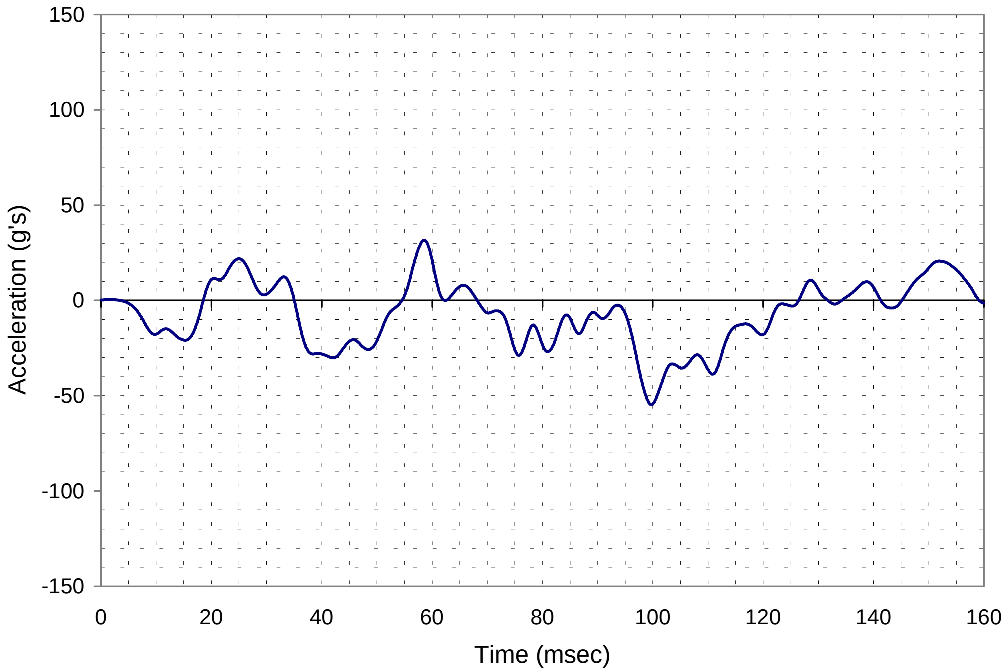

FIGURE B-17. FS 500 LEFT UPPER SIDEWALL, ACCELEROMETER Z-DIRECTION (DAS-48S Channel 17)

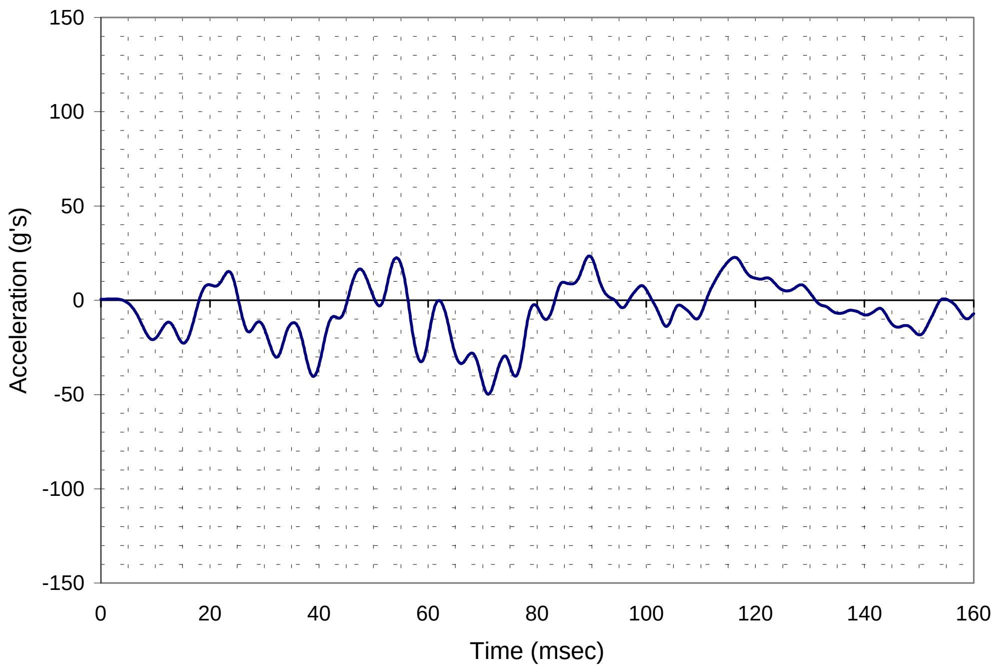

FIGURE B-18. FS 500 RIGHT UPPER SIDEWALL, ACCELEROMETER Z-DIRECTION (NEFF Channel 406)

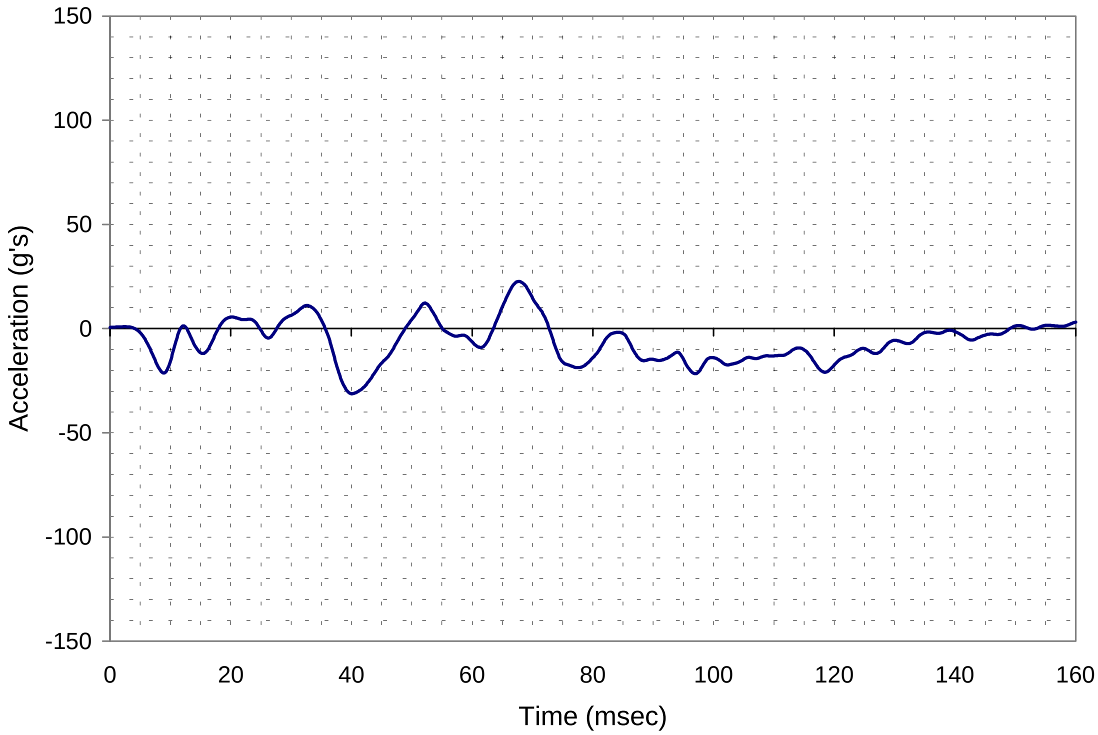

FIGURE B-19. FS 420 LEFT LOWER SIDEWALL, ACCELEROMETER Z-DIRECTION
(NEFF Channel 229)

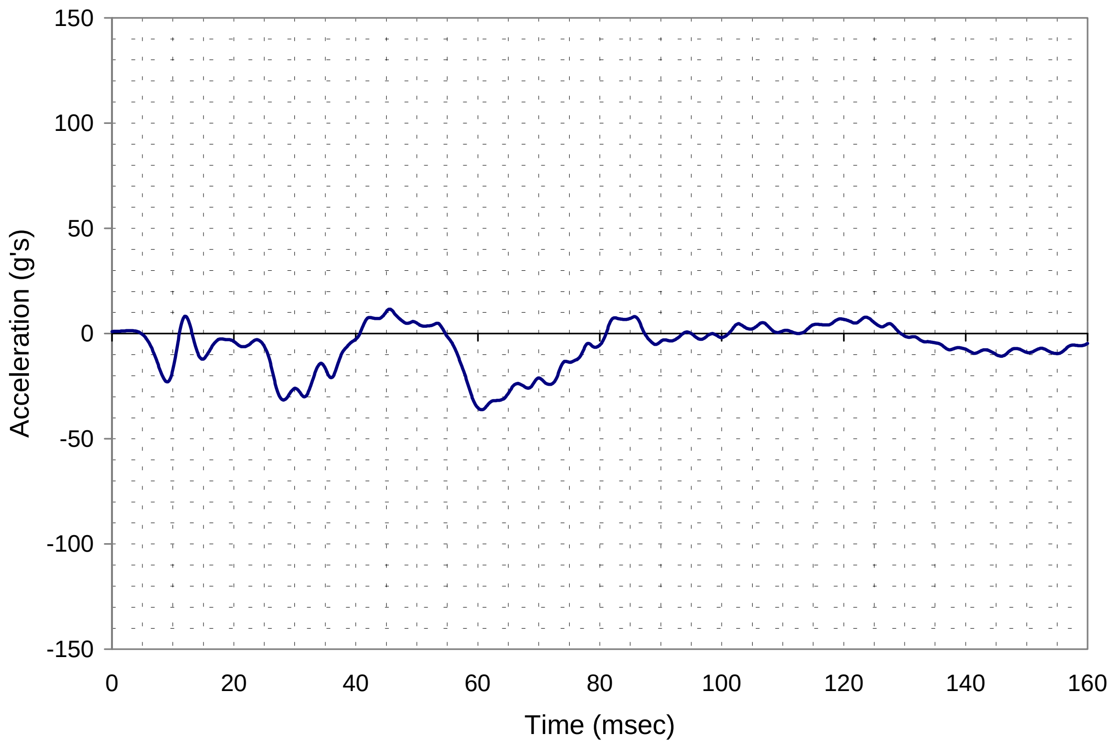

FIGURE B-20. FS 420 RIGHT LOWER SIDEWALL, ACCELEROMETER Z-DIRECTION
(NEFF Channel 306)

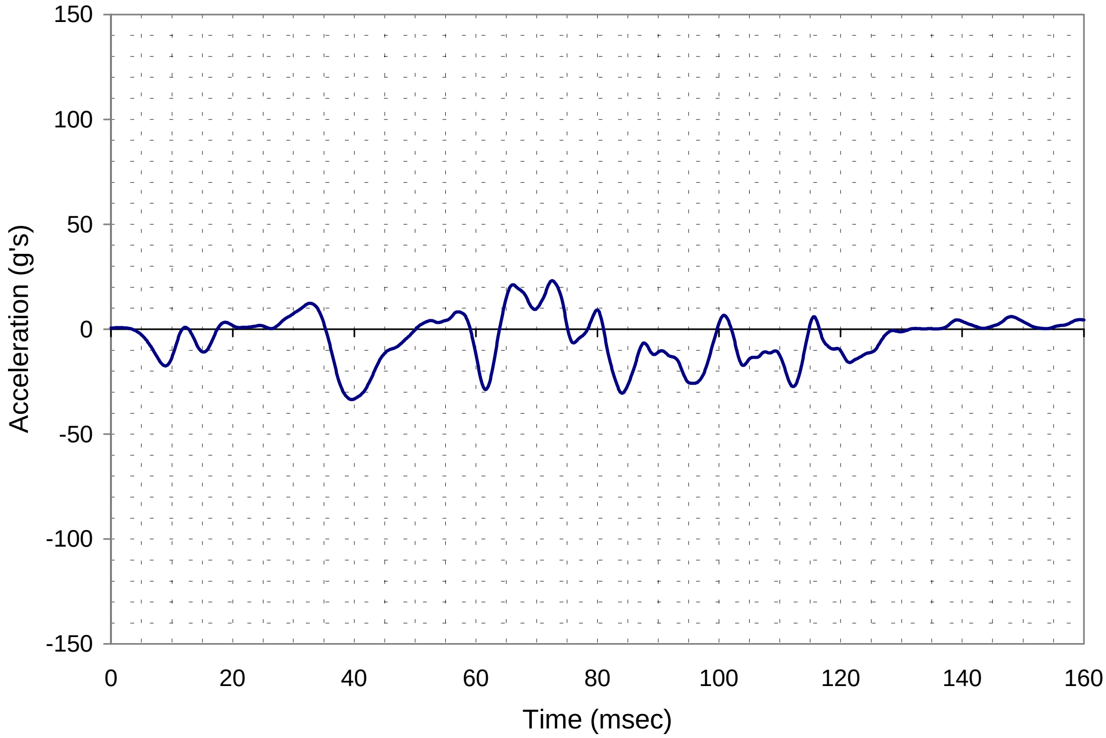

FIGURE B-21. FS 460 LEFT LOWER SIDEWALL, ACCELEROMETER Z-DIRECTION (NEFF Channel 311)

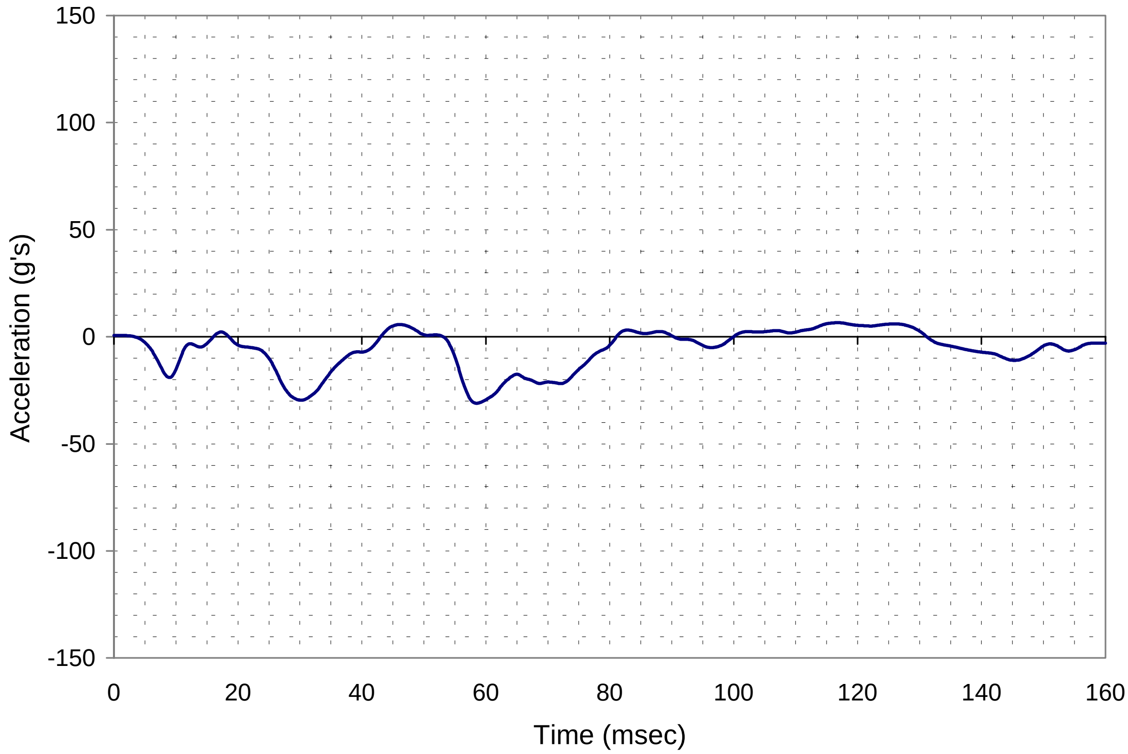

FIGURE B-22. FS 460 RIGHT LOWER SIDEWALL, ACCELEROMETER Z-DIRECTION (DAS-48S Channel 10)

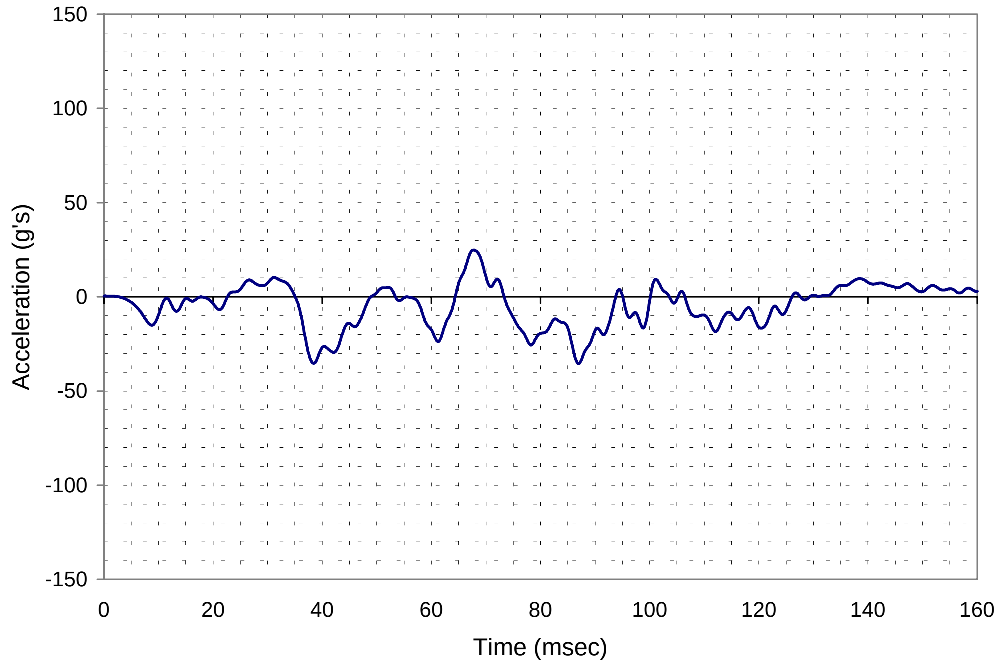

FIGURE B-23. FS 500 LEFT LOWER SIDEWALL, ACCELEROMETER Z-DIRECTION
(DAS-48S Channel 18)

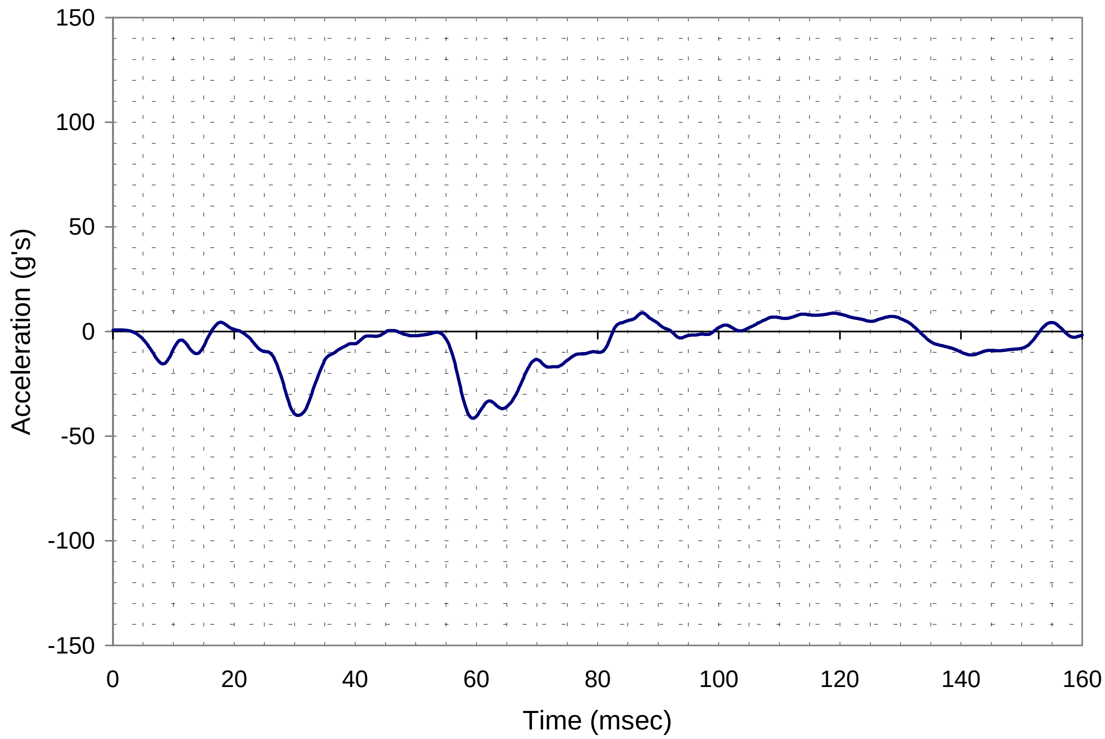

FIGURE B-24. FS 500 RIGHT LOWER SIDEWALL, ACCELEROMETER Z-DIRECTION
(NEFF Channel 407)

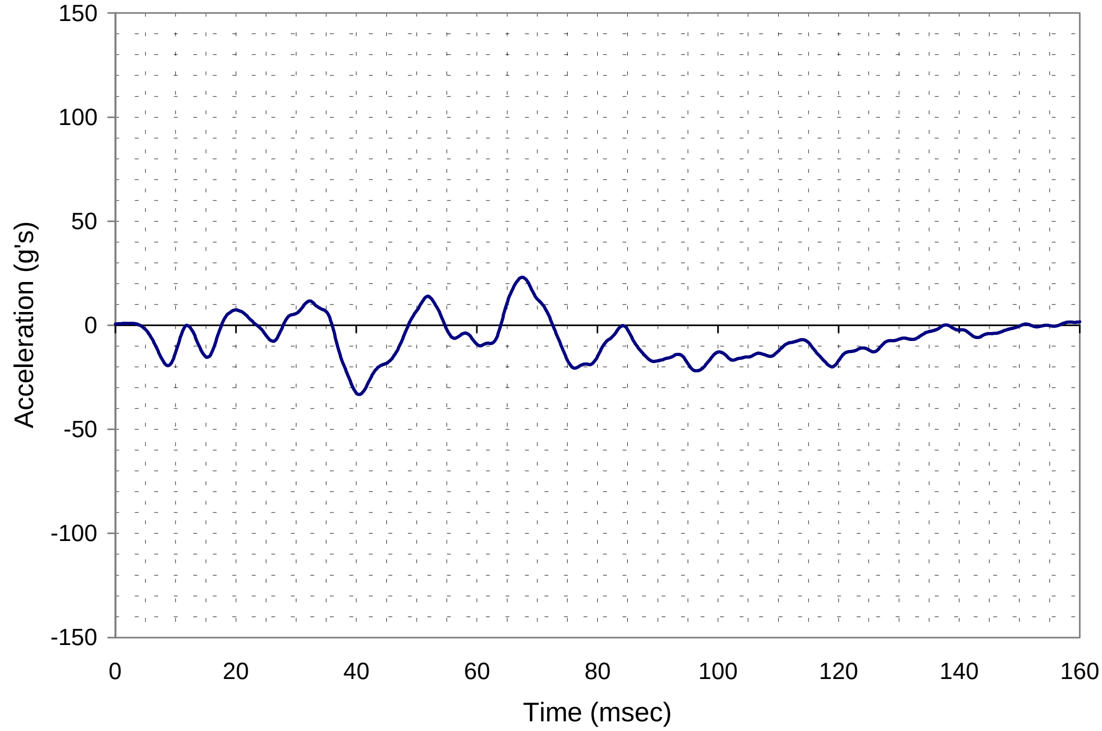

FIGURE B-25. FS 420 LEFT FLOOR, ACCELEROMETER Z-DIRECTION
(NEFF Channel 230)

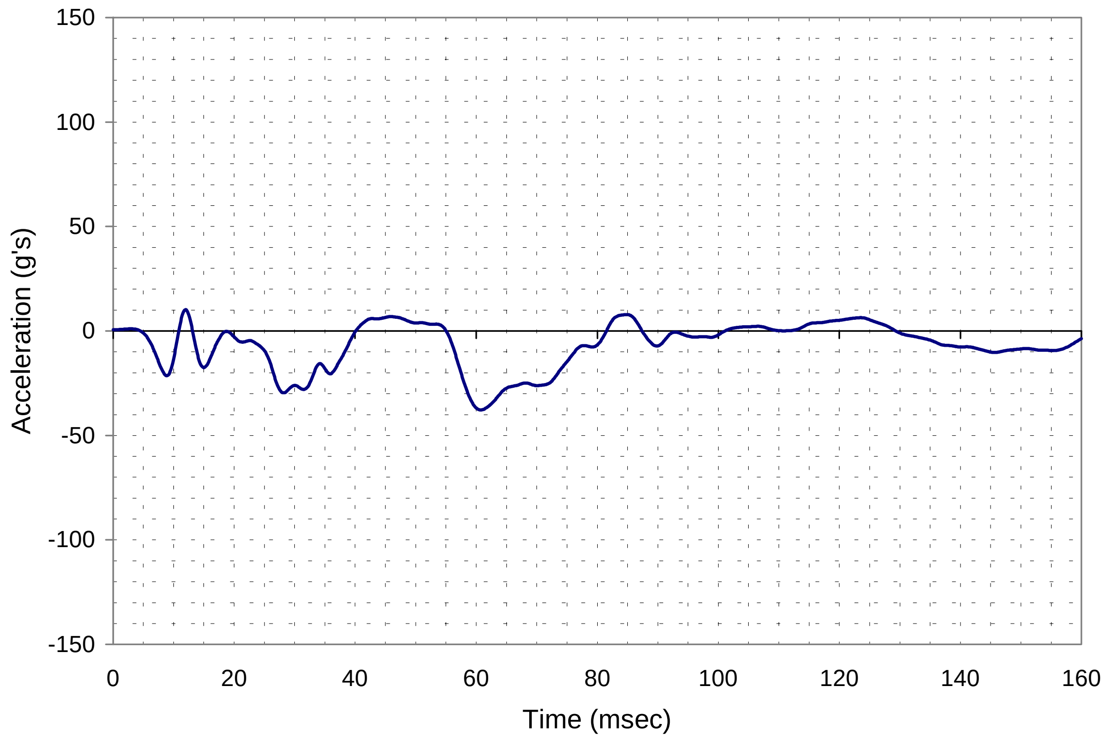

FIGURE B-26. FS 420 RIGHT FLOOR, ACCELEROMETER Z-DIRECTION
(NEFF Channel 305)

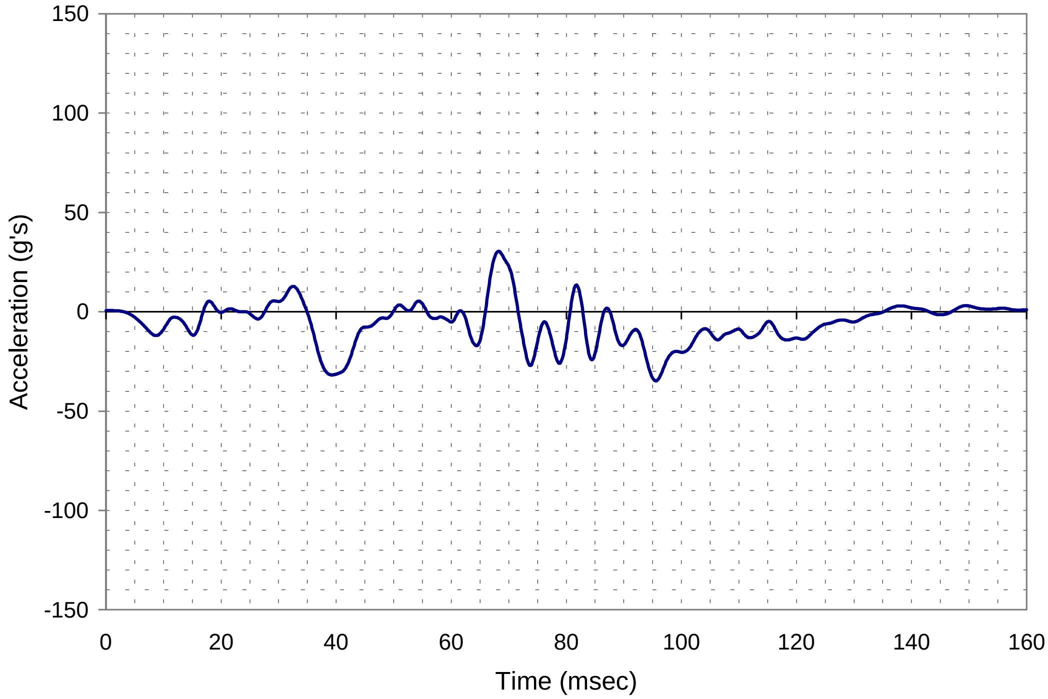

FIGURE B-27. FS 460 LEFT FLOOR, ACCELEROMETER Z-DIRECTION
(NEFF Channel 312)

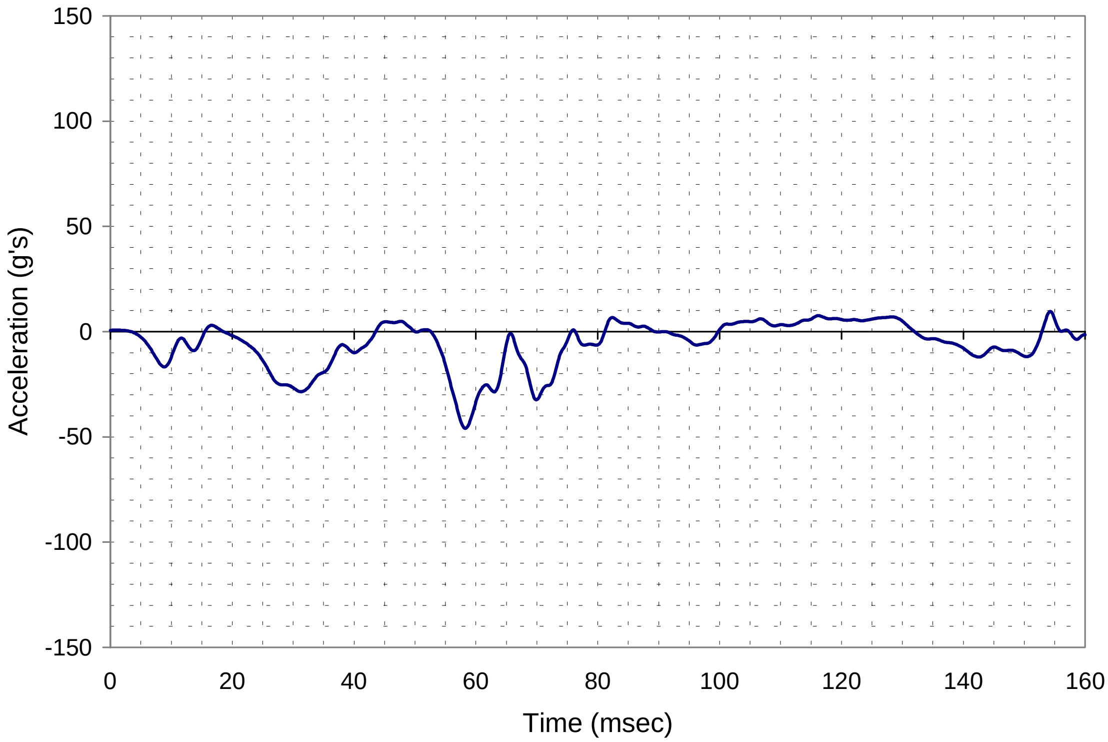

FIGURE B-28. FS 460 RIGHT FLOOR, ACCELEROMETER Z-DIRECTION
(DAS-28S Channel 8)

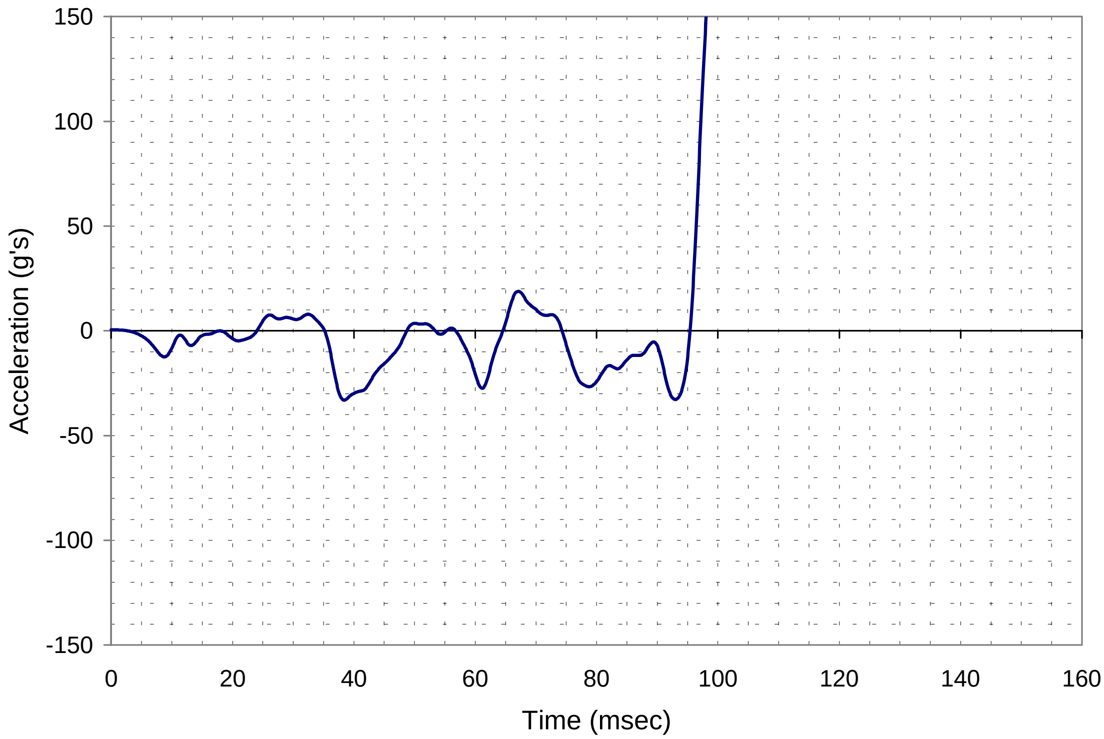

FIGURE B-29. FS 500 LEFT FLOOR, ACCELEROMETER Z-DIRECTION
(NEFF Channel 404)

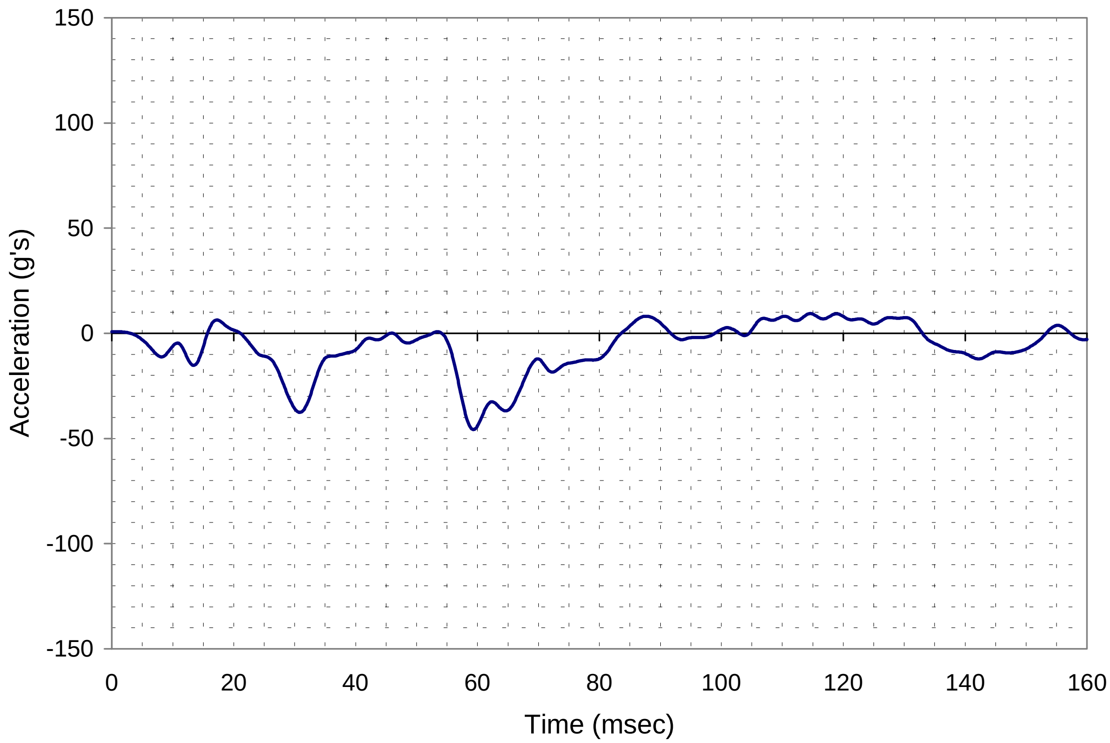

FIGURE B-30. FS 500 RIGHT FLOOR, ACCELEROMETER Z-DIRECTION
(NEFF Channel 408)

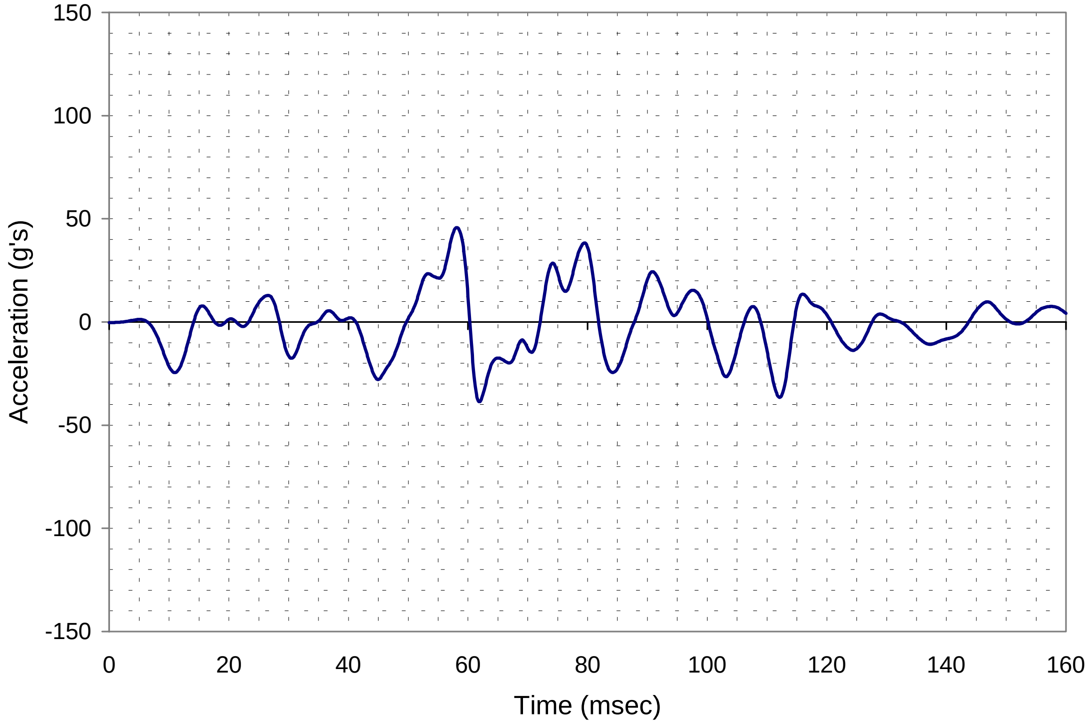

FIGURE B-31. FS 460 LEFT LOWER SIDEWALL, ACCELEROMETER Y-DIRECTION
(NEFF Channel 310)

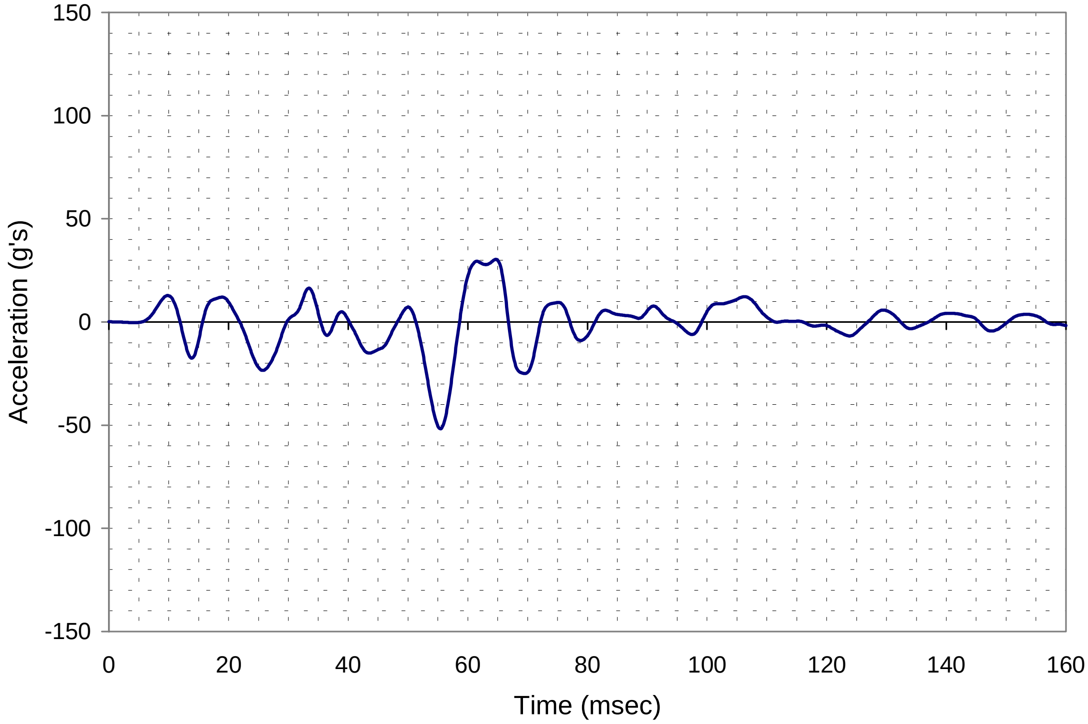

FIGURE B-32. FS 420 RIGHT LOWER SIDEWALL, ACCELEROMETER Y-DIRECTION
(DAS-48S Channel 9)

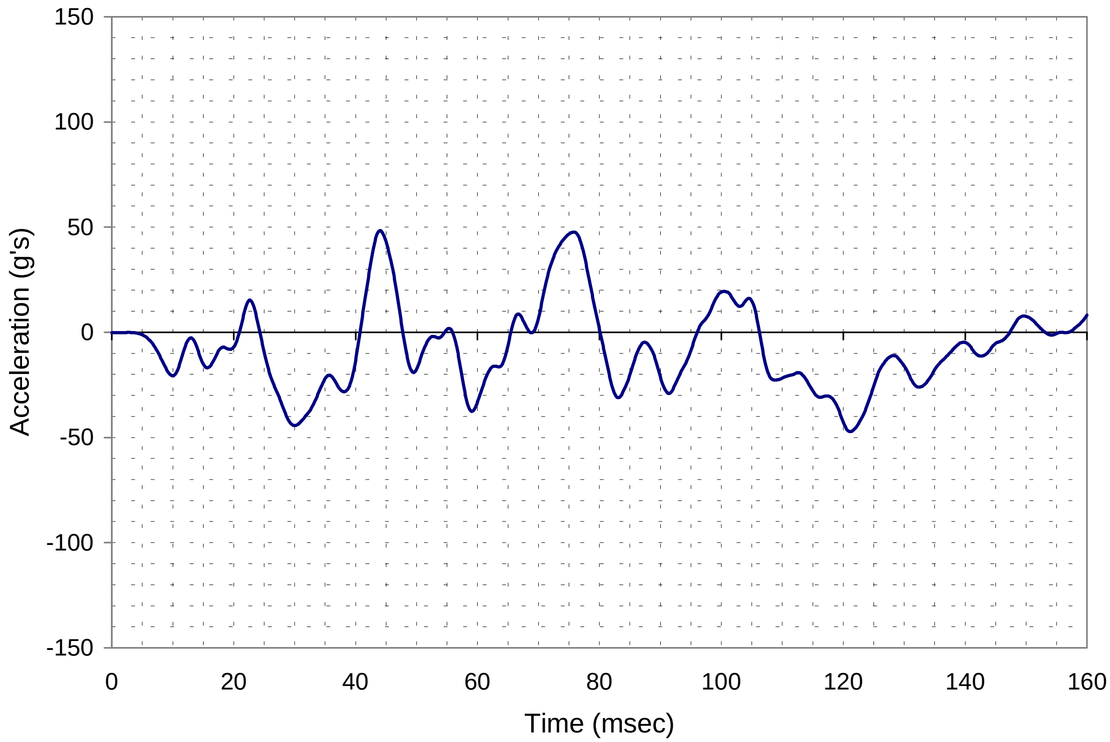

FIGURE B-33. FS 420 CENTER CROWN, ACCELEROMETER Z-DIRECTION
(NEFF Channel 302)

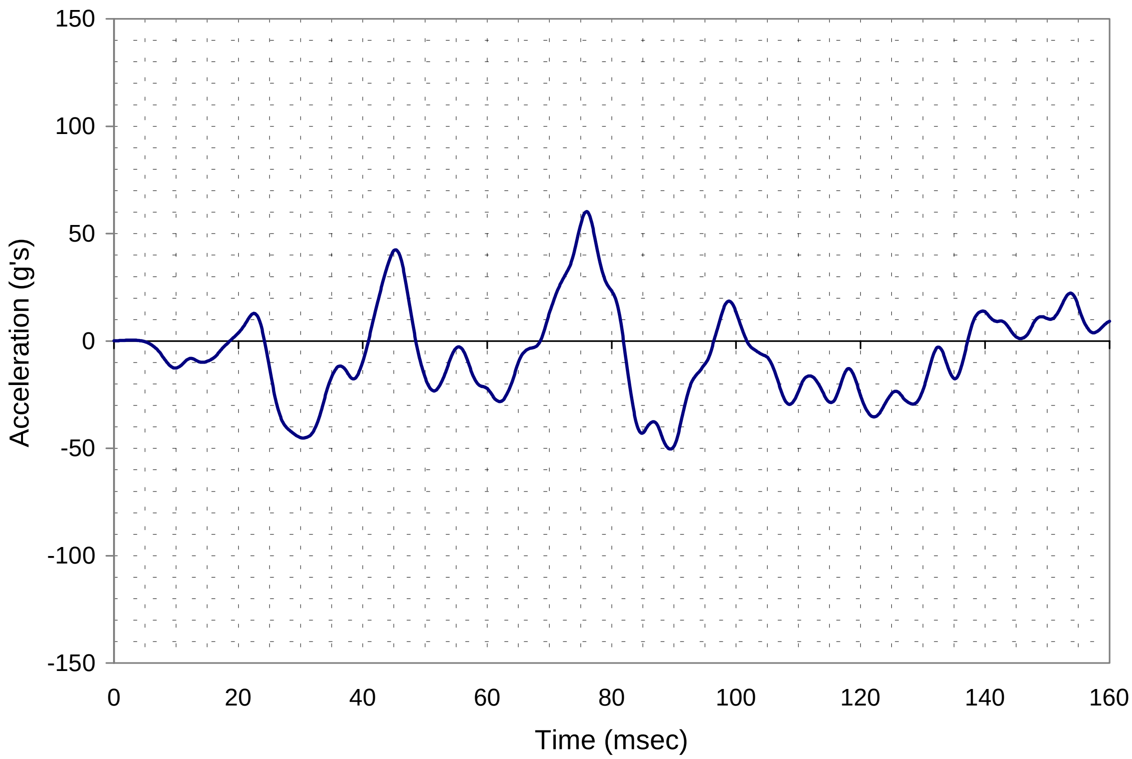

FIGURE B-34. FS 500 CENTER CROWN, ACCELEROMETER Z-DIRECTION
(DAS-48S Channel 16)

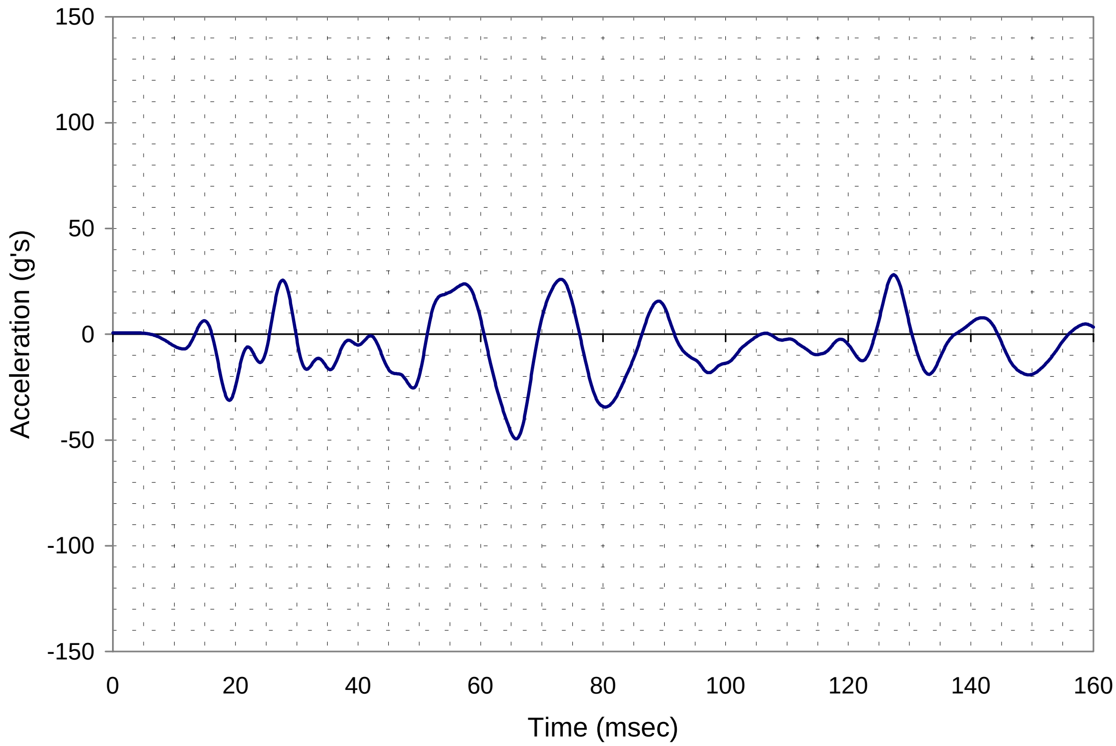

FIGURE B-35. FS 400 LEFT INNER SEAT TRACK, ACCELEROMETER Z-DIRECTION
(DAS-48S Channel 1)

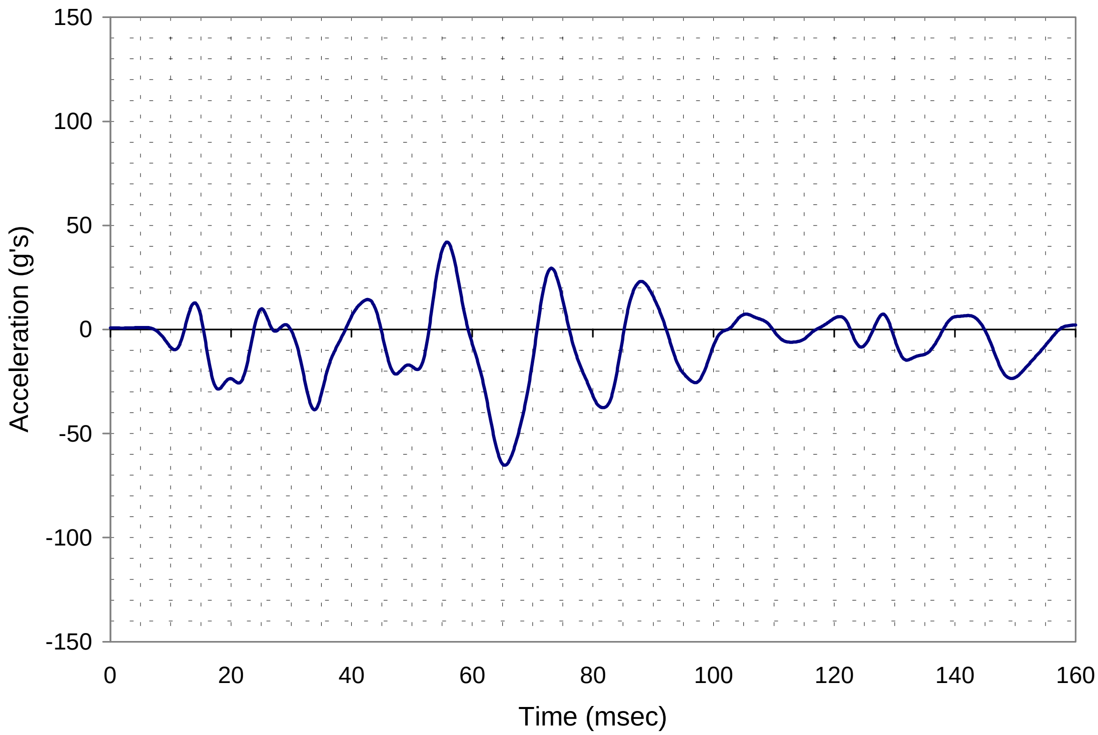

FIGURE B-36. FS 400 RIGHT INNER SEAT TRACK, ACCELEROMETER Z-DIRECTION
(NEFF Channel 301)

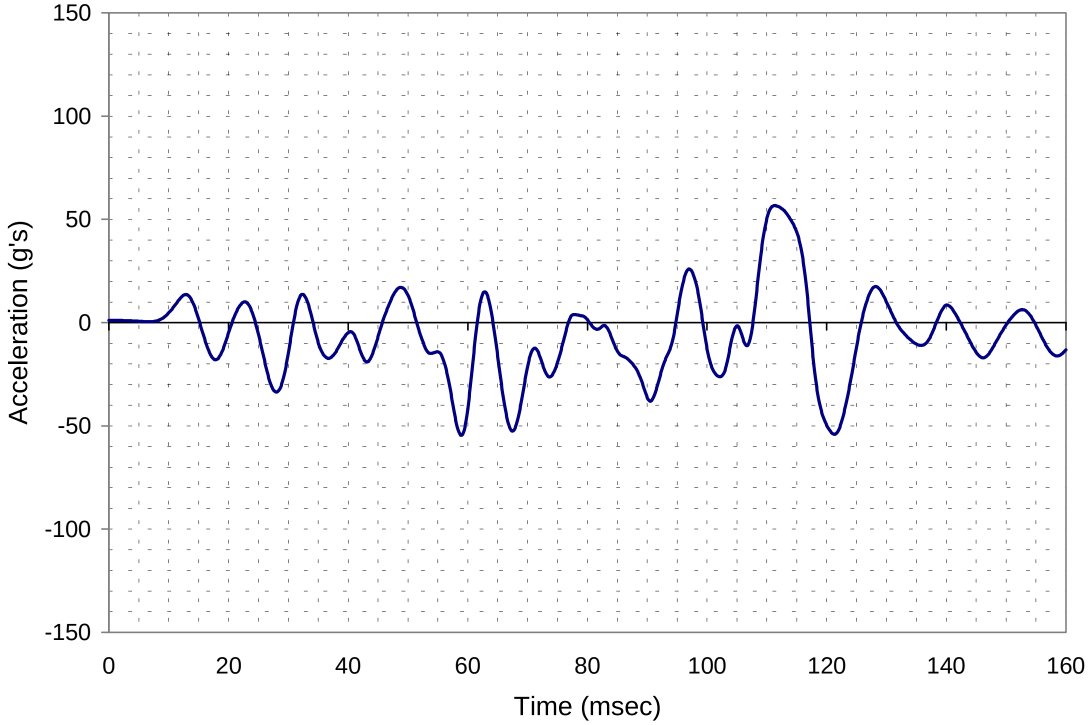

FIGURE B-37. FS 438 LEFT INNER SEAT TRACK, ACCELEROMETER Z-DIRECTION
(NEFF Channel 231)

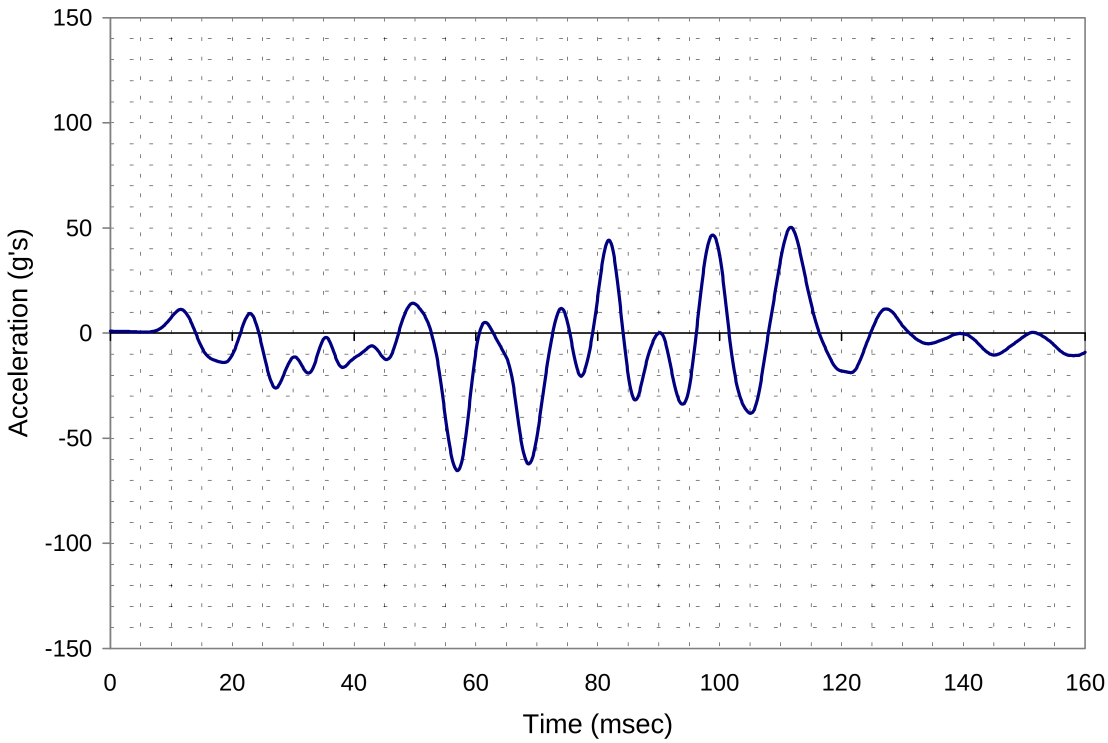

FIGURE B-38. FS 438 RIGHT INNER SEAT TRACK, ACCELEROMETER Z-DIRECTION
(DAS-48S Channel 5)

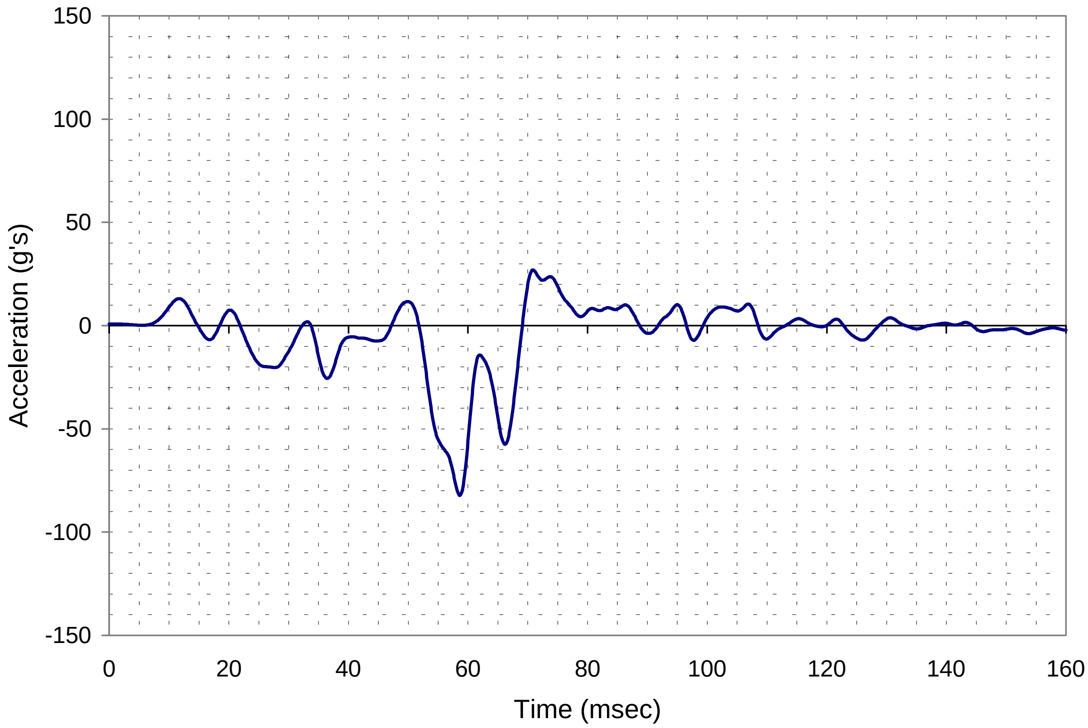

FIGURE B-39. FS 472 LEFT INNER SEAT TRACK, ACCELEROMETER Z-DIRECTION
(NEFF Channel 403)

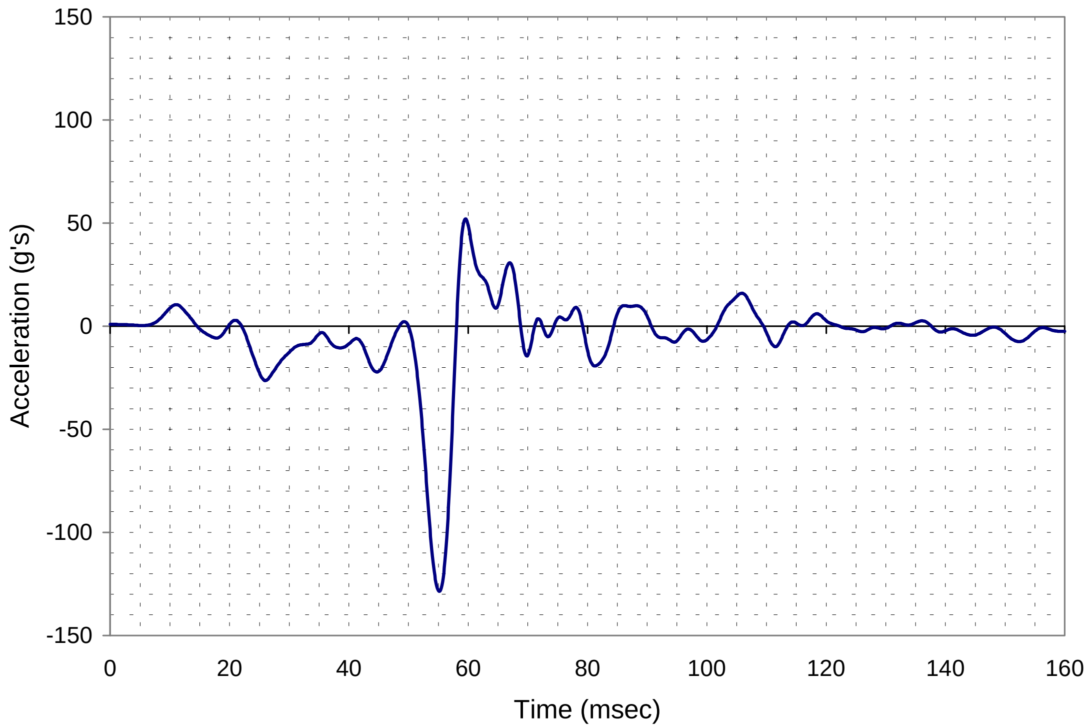

FIGURE B-40. FS 472 RIGHT INNER SEAT TRACK, ACCELEROMETER Z-DIRECTION
(DAS-48S Channel 13)

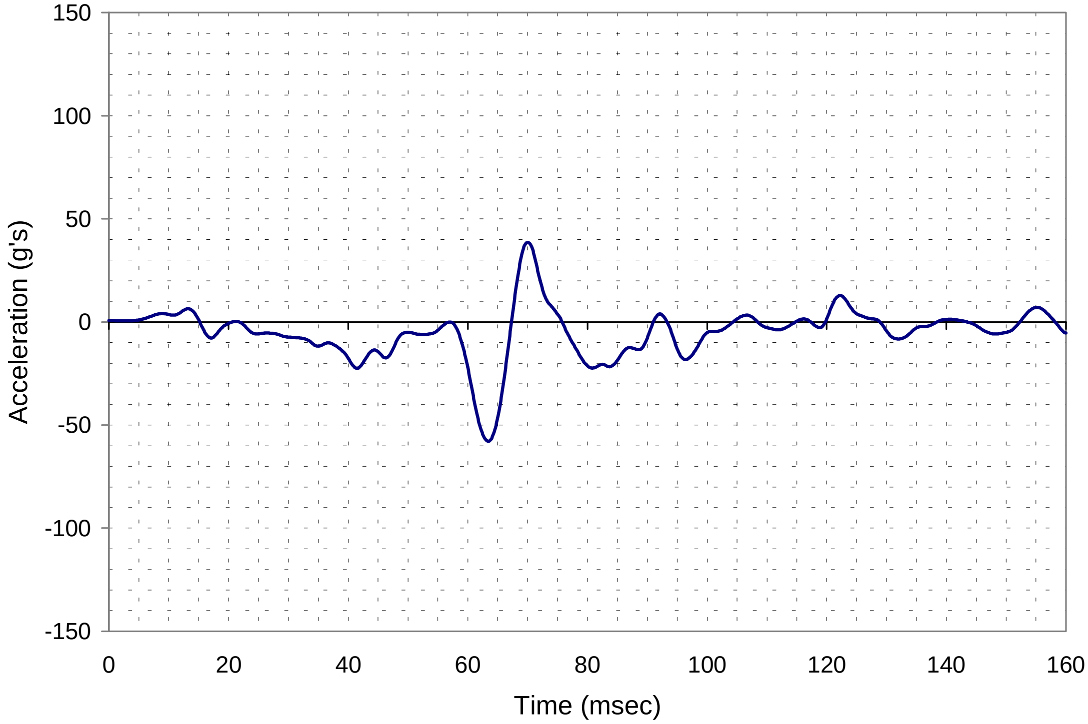

FIGURE B-41. FS 504 LEFT INNER SEAT TRACK, ACCELEROMETER Z-DIRECTION
(DAS-48S Channel 19)

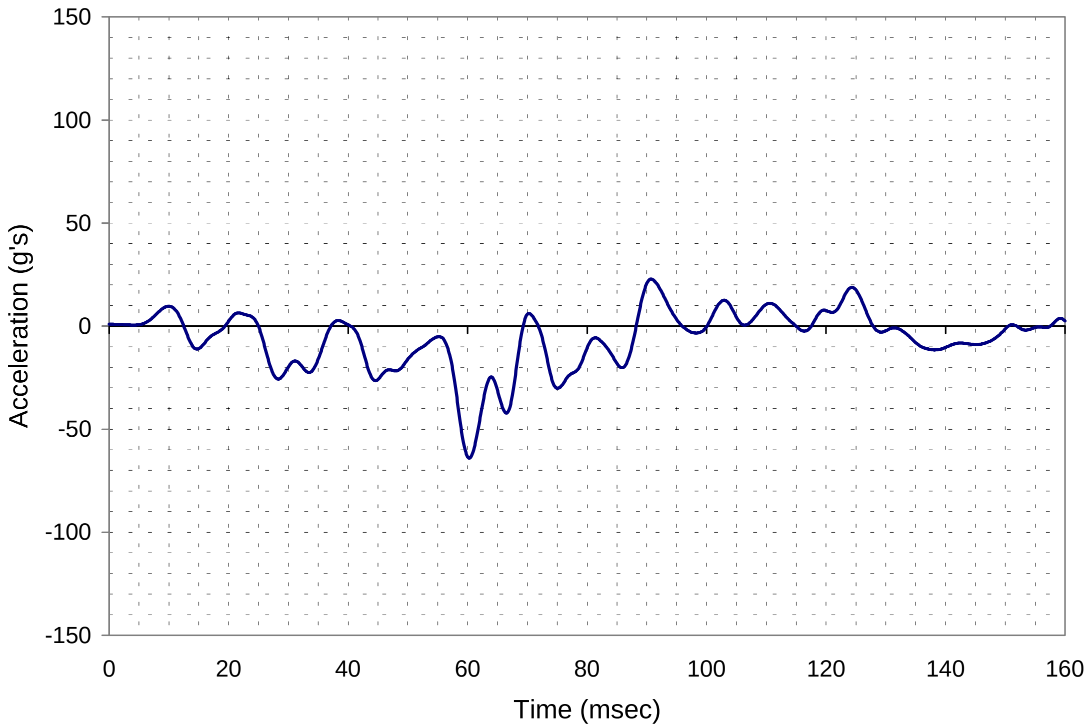

FIGURE B-42. FS 504 RIGHT INNER SEAT TRACK, ACCELEROMETER Z-DIRECTION
(NEFF Channel 413)

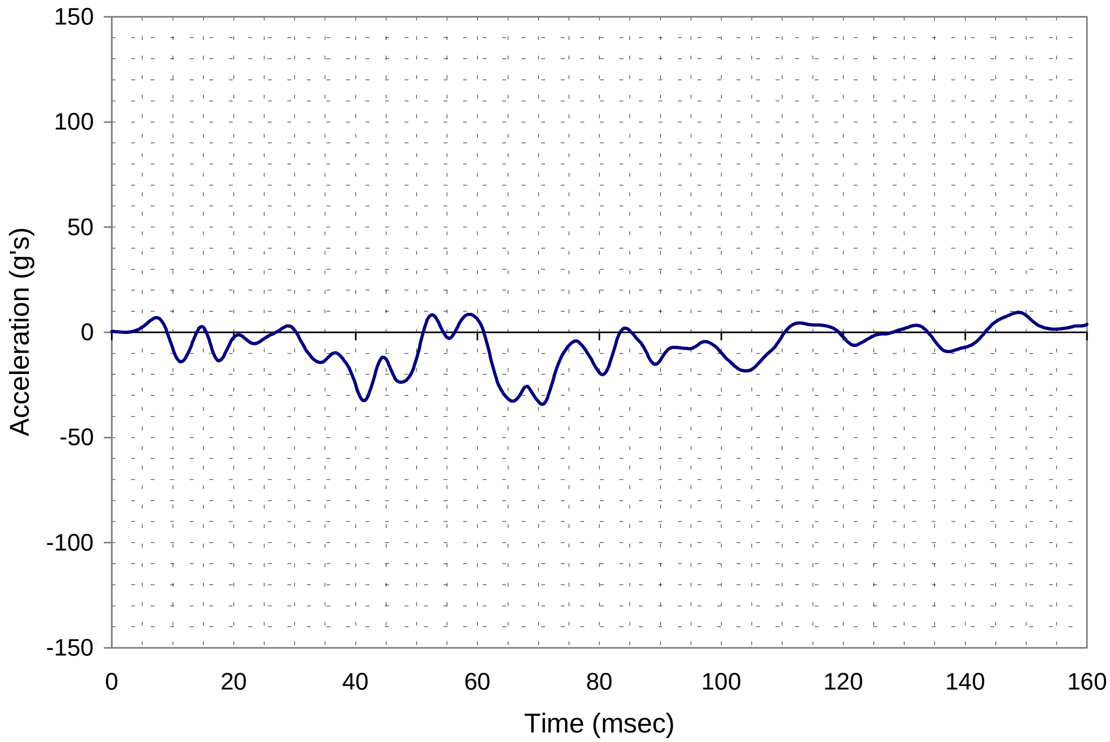

FIGURE B-43. FS 518 LEFT INNER SEAT TRACK, ACCELEROMETER Z-DIRECTION
(NEFF Channel 412)

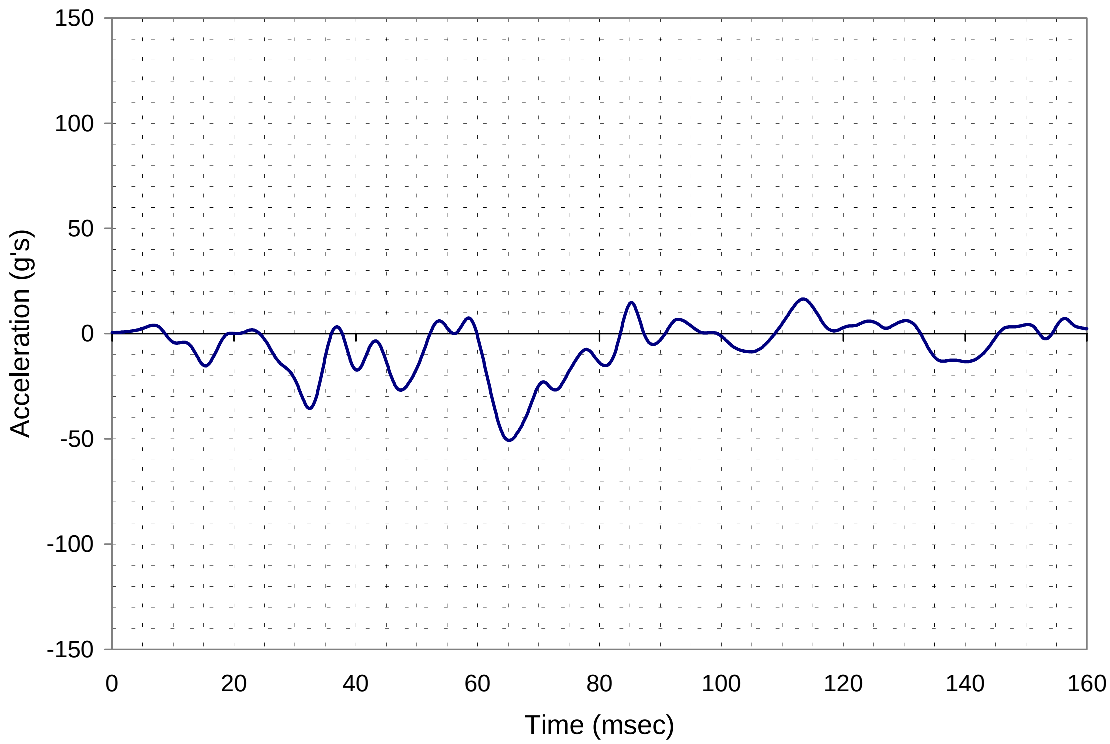

FIGURE B-44. FS 518 RIGHT INNER SEAT TRACK, ACCELEROMETER Z-DIRECTION
(DAS-48S Channel 21)

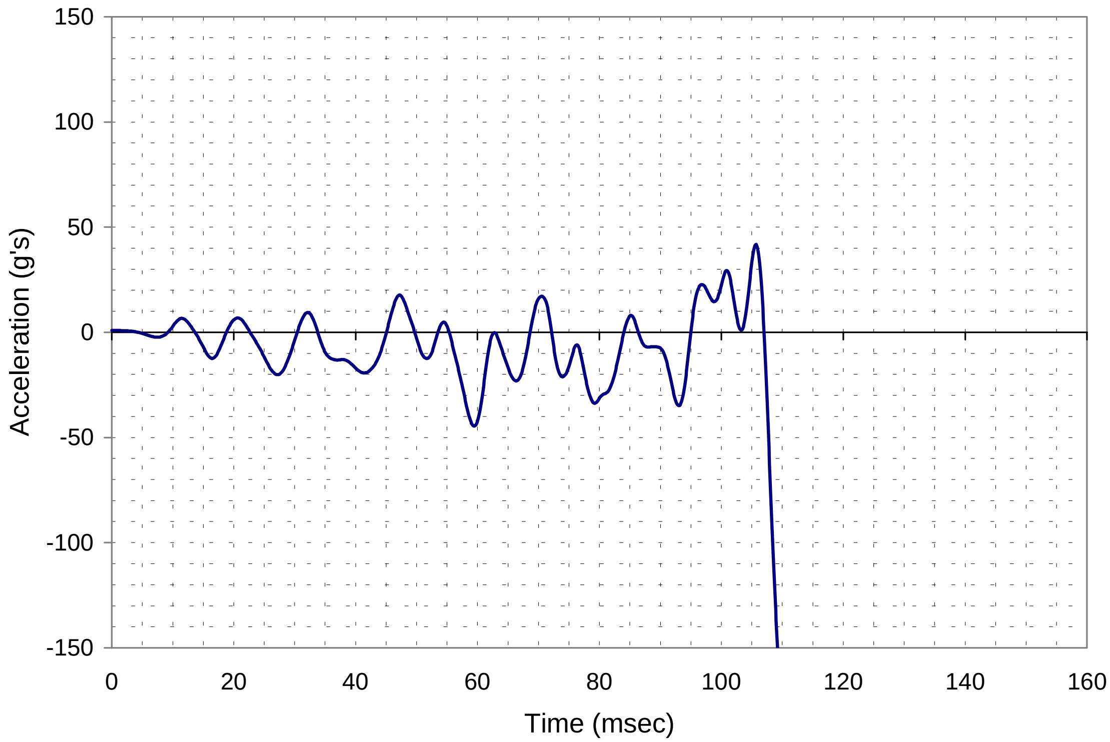

FIGURE B-45. FS 438 LEFT OUTER SEAT TRACK, ACCELEROMETER Z-DIRECTION
(DAS-48S Channel 4)

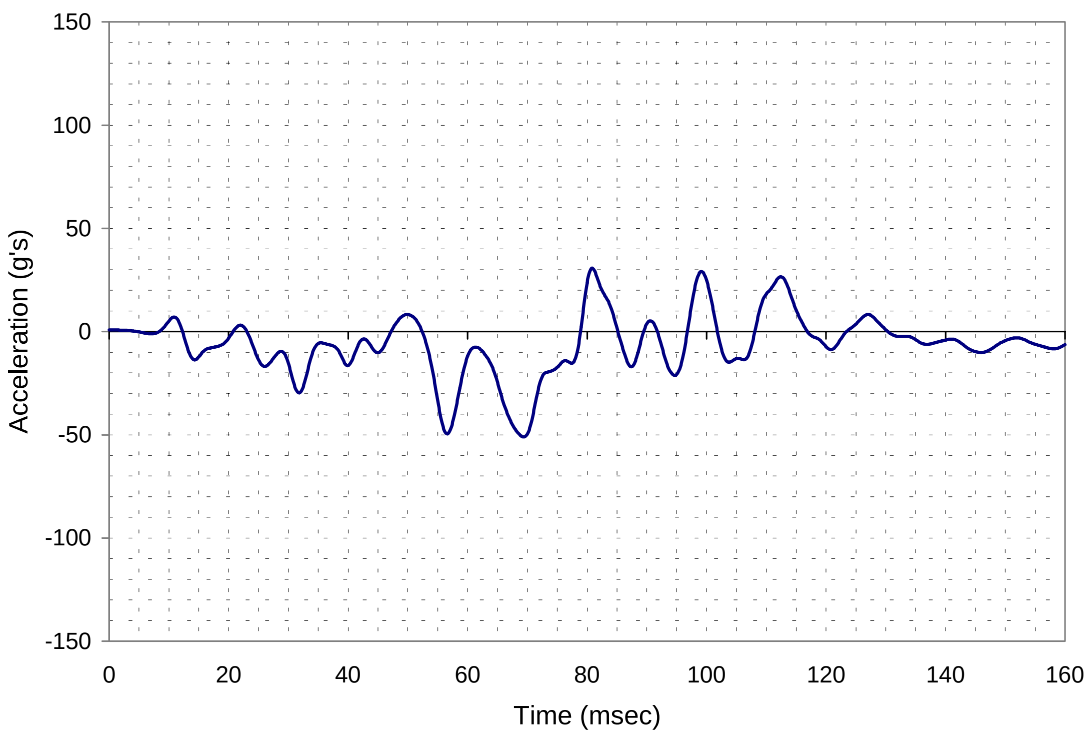

FIGURE B-46. FS 438 RIGHT OUTER SEAT TRACK, ACCELEROMETER Z-DIRECTION
(NEFF Channel 308)

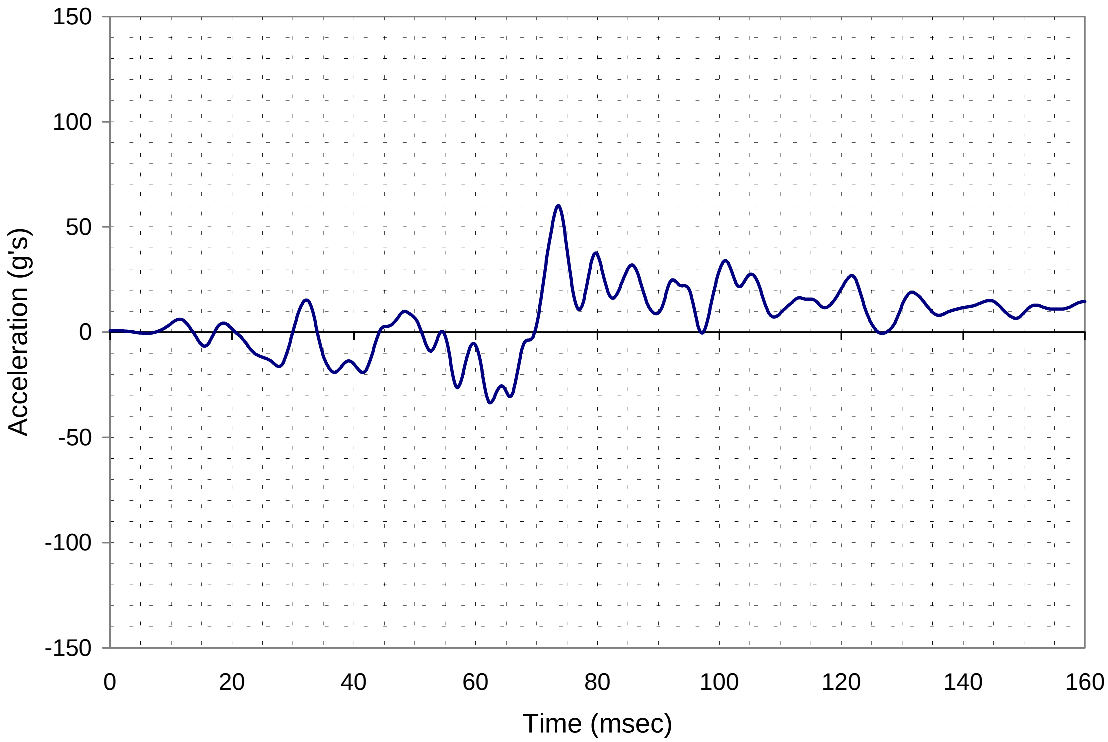

FIGURE B-47. FS 472 LEFT OUTER SEAT TRACK, ACCELEROMETER Z-DIRECTION
(DAS-48S Channel 12)

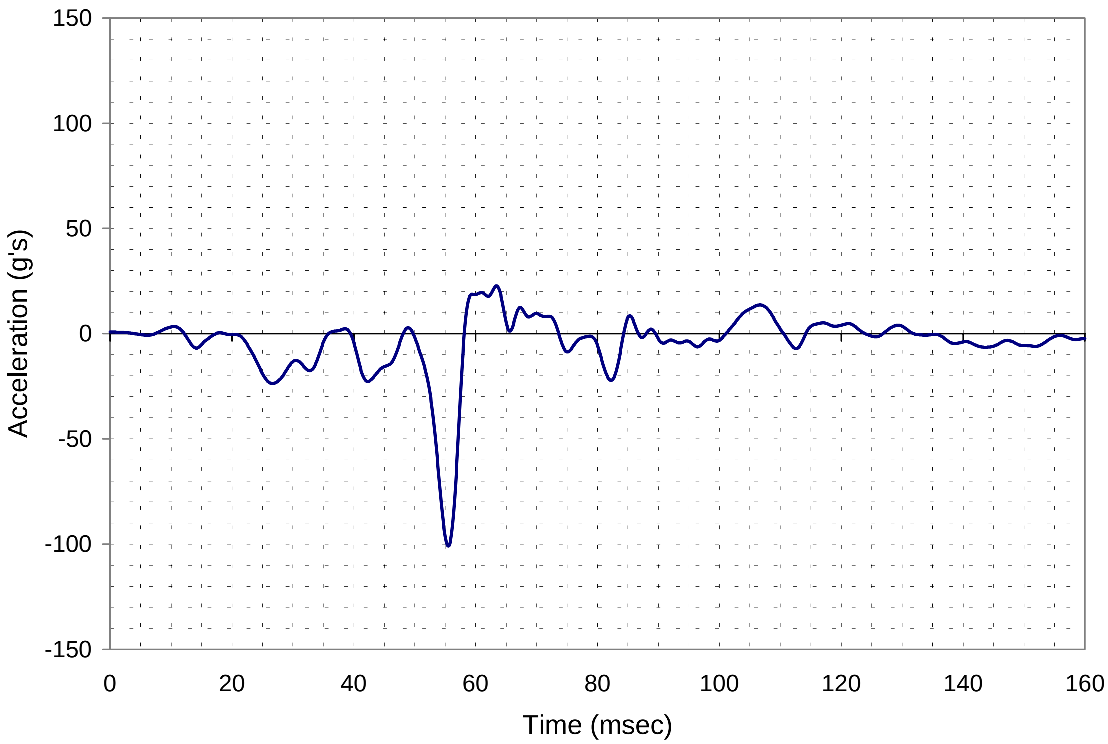

FIGURE B-48. FS 472 RIGHT OUTER SEAT TRACK, ACCELEROMETER Z-DIRECTION
(NEFF Channel 405)

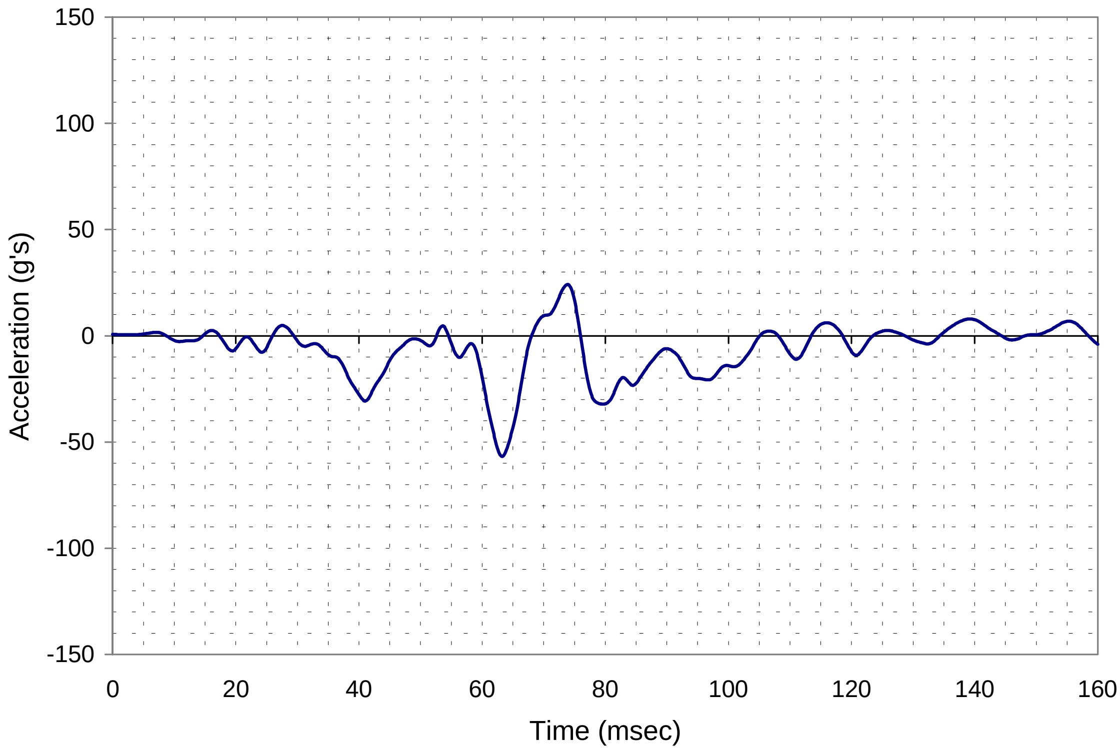

FIGURE B-49. FS 504 LEFT OUTER SEAT TRACK, ACCELEROMETER Z-DIRECTION
(NEFF Channel 409)

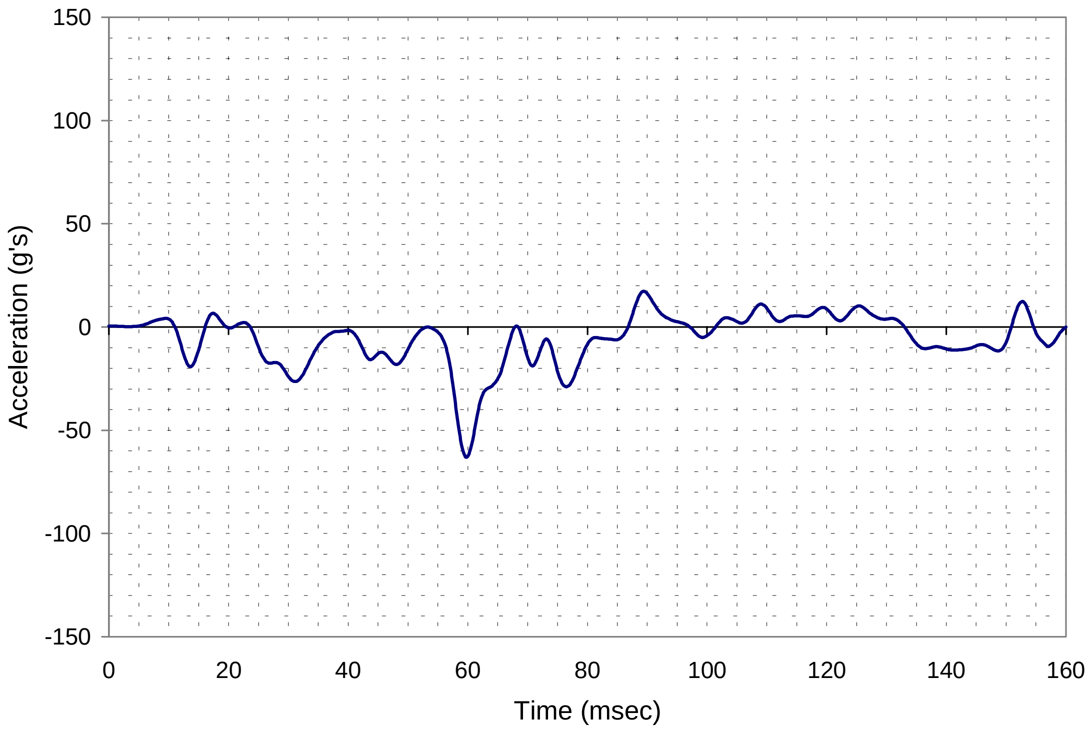

FIGURE B-50. FS 504 RIGHT OUTER SEAT TRACK, ACCELEROMETER Z-DIRECTION
(DAS-48S Channel 20)

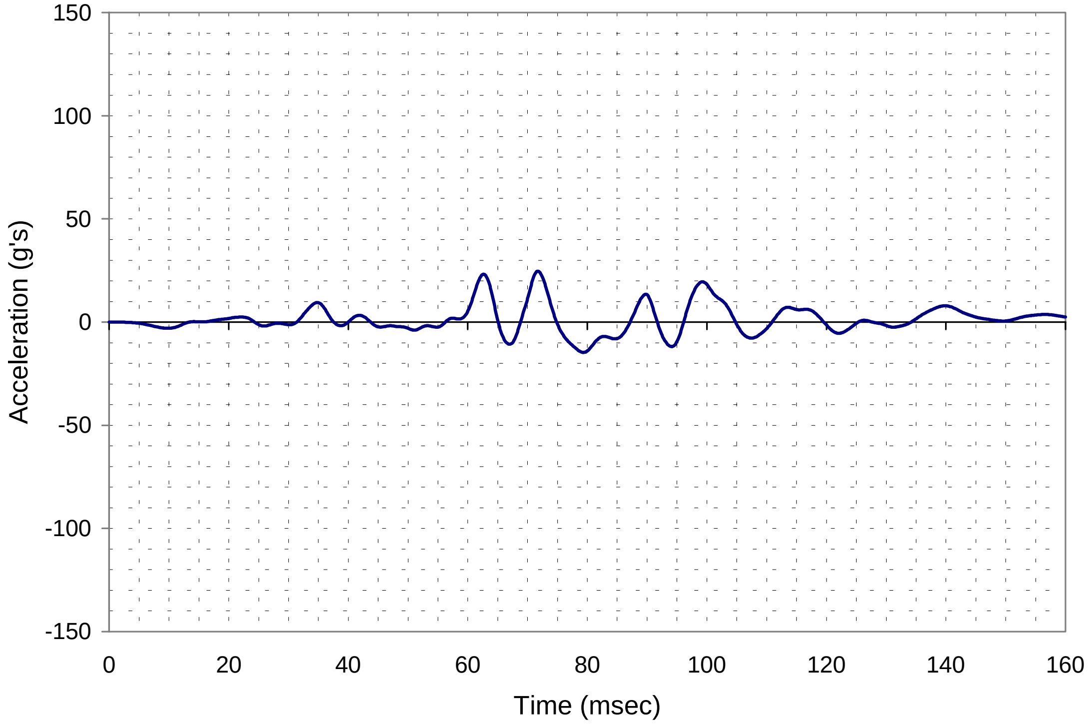

FIGURE B-51. FS 472 LEFT OUTER SEAT TRACK, ACCELEROMETER X-DIRECTION
(NEFF Channel 401)

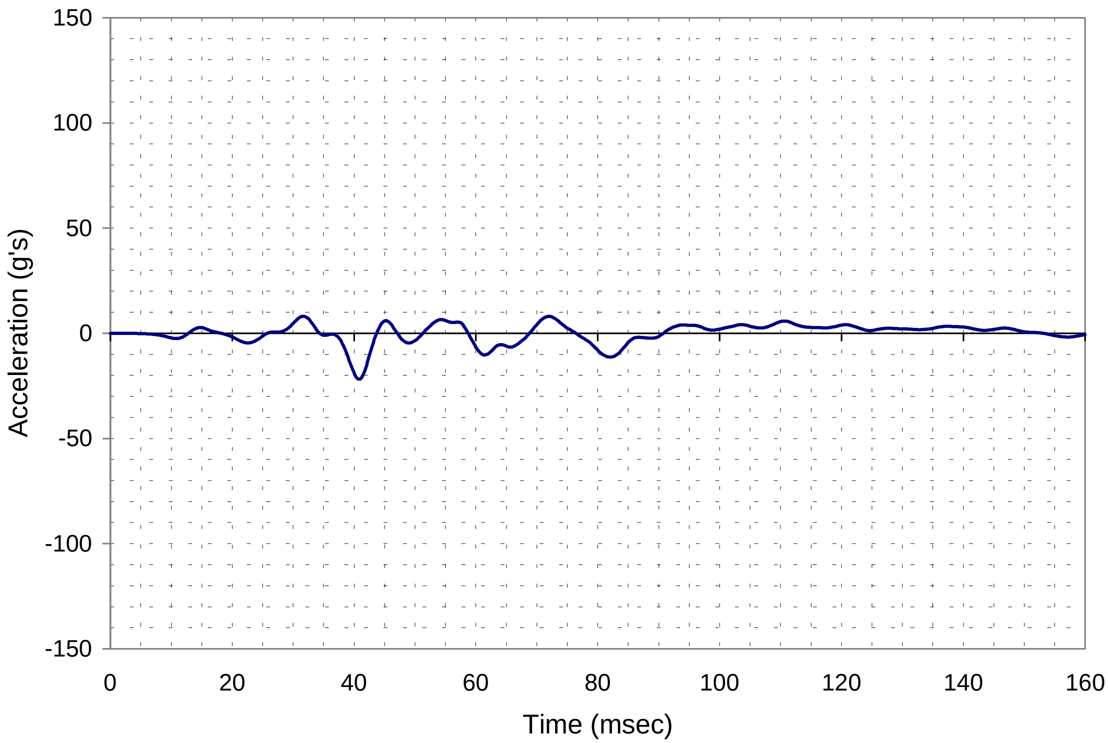

FIGURE 52. FS 472 RIGHT OUTER SEAT TRACK, ACCELEROMETER X-DIRECTION
(DAS-48S Channel 14)

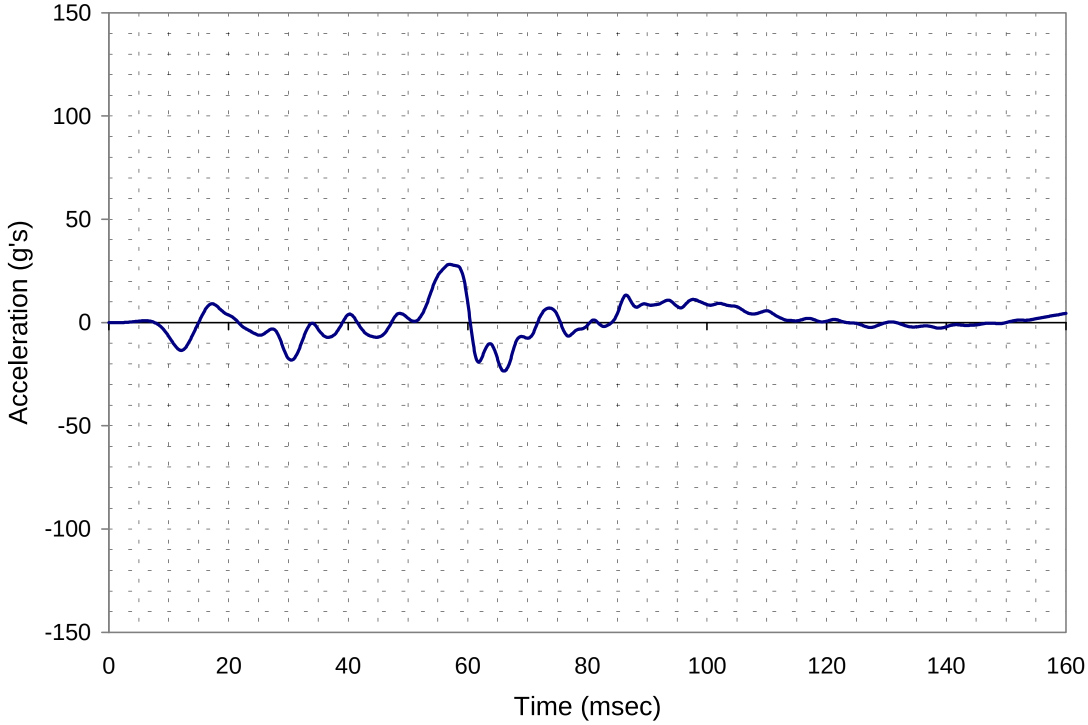

FIGURE B-53. FS 472 LEFT OUTER SEAT TRACK, ACCELEROMETER Y-DIRECTION (NEFF Channel 402)

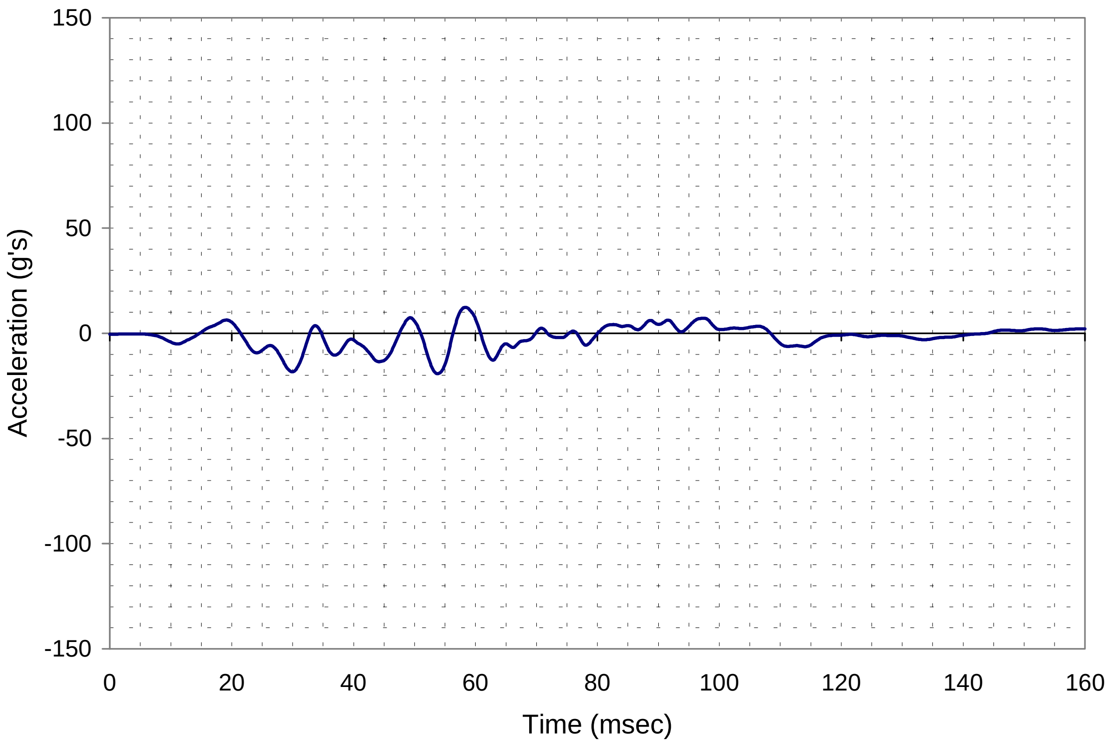

FIGURE B-54. FS 472 RIGHT OUTER SEAT TRACK, ACCELEROMETER Y-DIRECTION (DAS-48S Channel 15)

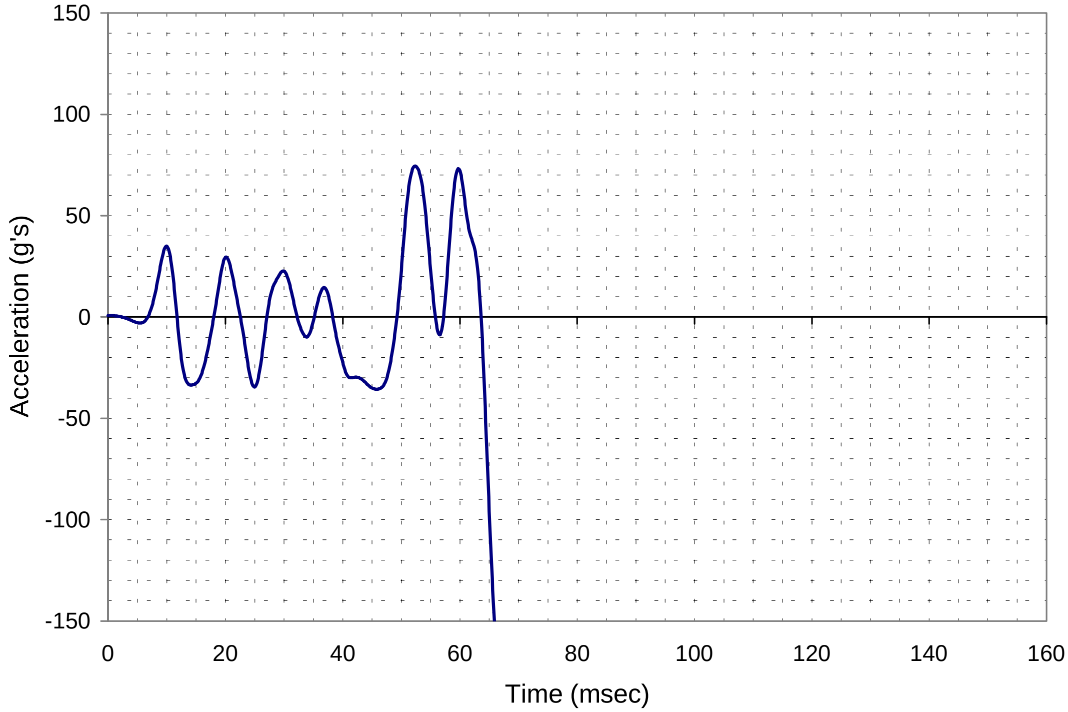

FIGURE B-55. FS 420 LEFT SIDEWALL, ACCELEROMETER Z-DIRECTION
(NEFF Channel 101)

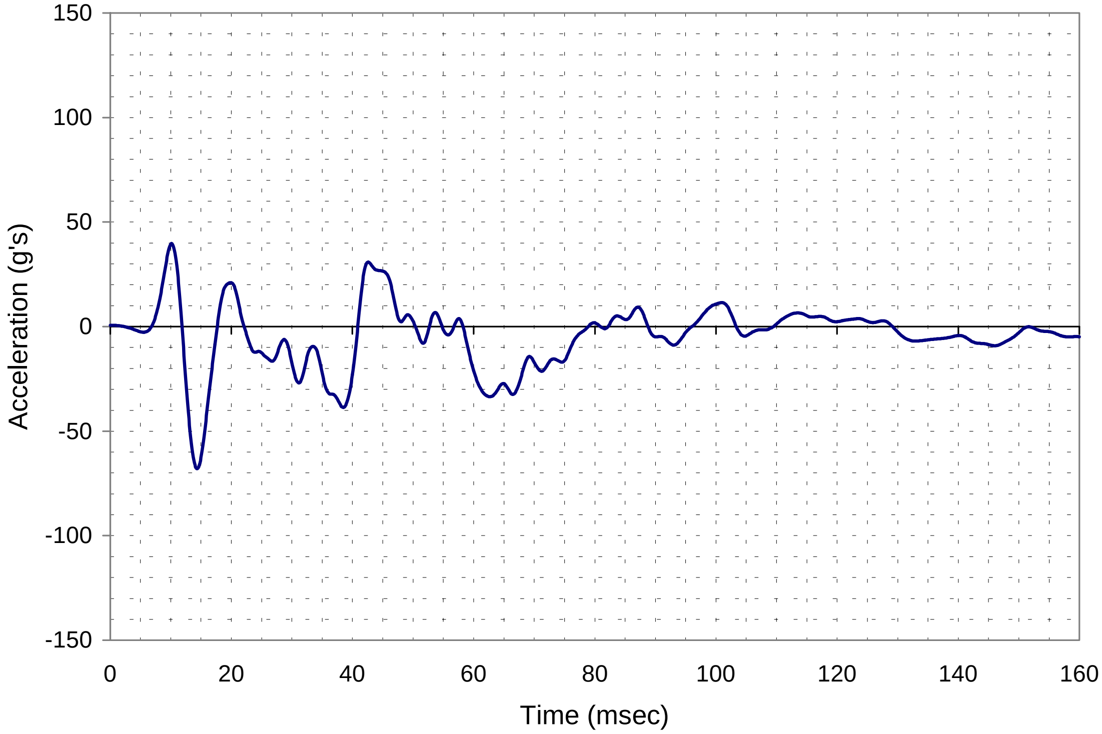

FIGURE B-56. FS 420 RIGHT SIDEWALL, ACCELEROMETER Z-DIRECTION
(NEFF Channel 104)

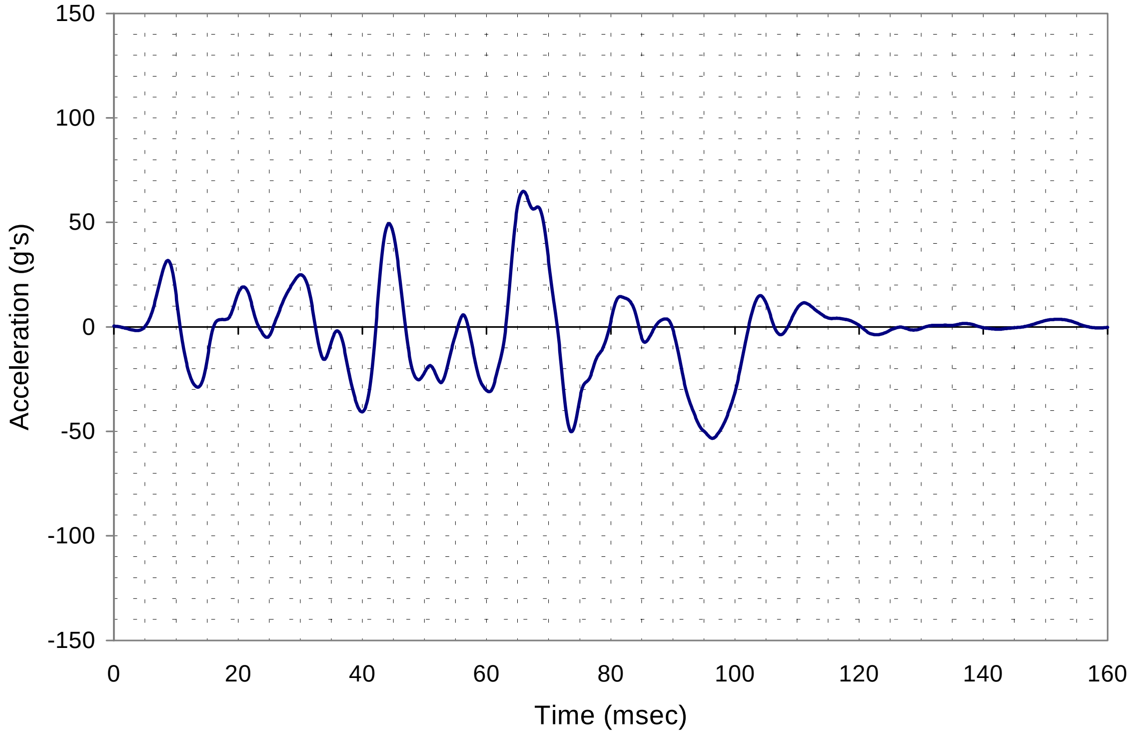

FIGURE B-57. FS 460 LEFT SIDEWALL, ACCELEROMETER Z-DIRECTION
(NEFF Channel 109)

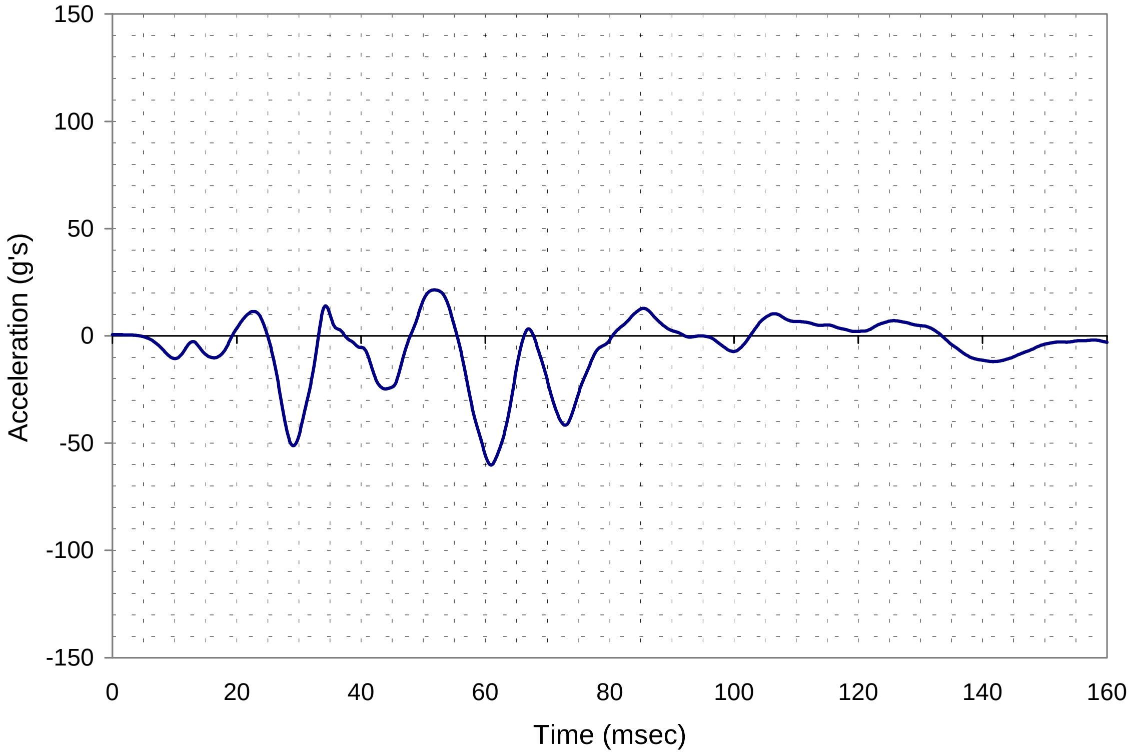

FIGURE B-58. FS 456 RIGHT DOOR, ACCELEROMETER Z-DIRECTION
(NEFF Channel 416)

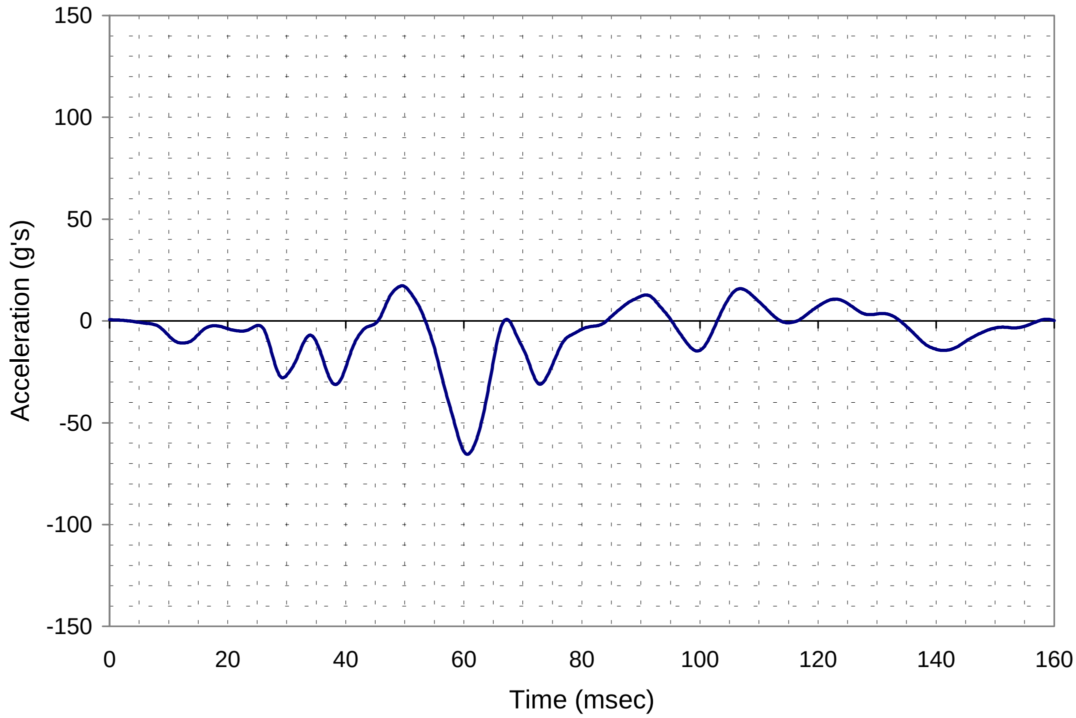

FIGURE B-59. FS 476 RIGHT DOOR, ACCELEROMETER Z-DIRECTION
(NEFF Channel 417)

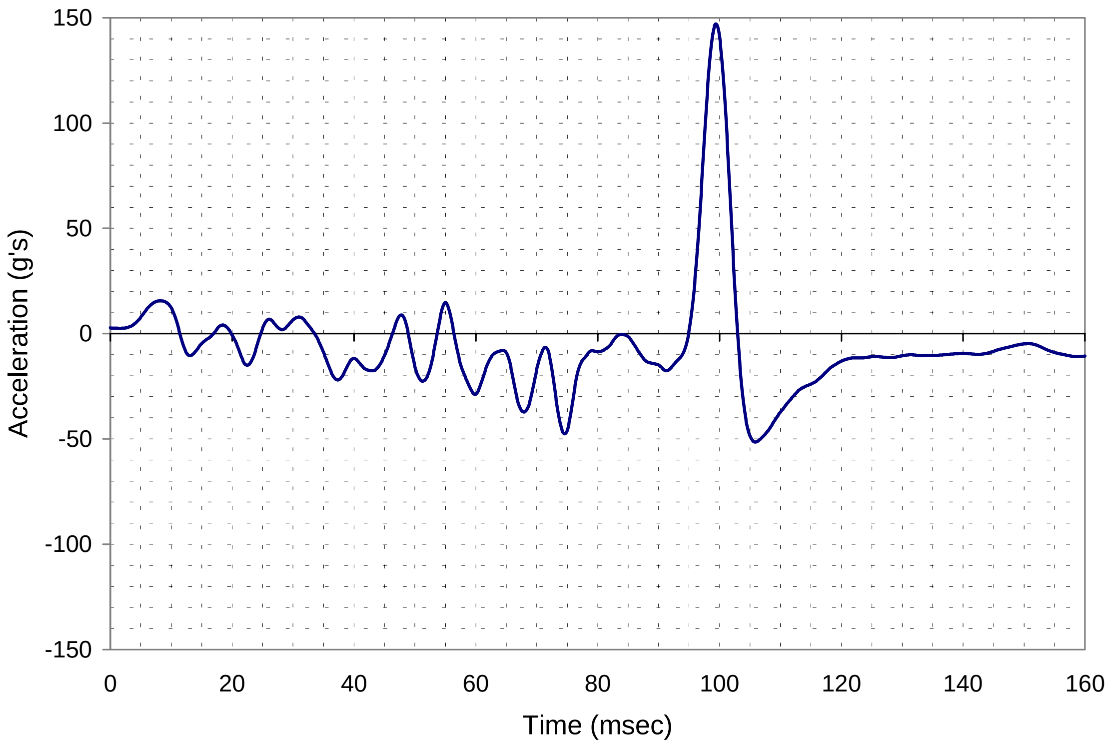

FIGURE B-60. FS 500 LEFT SIDEWALL, ACCELEROMETER Z-DIRECTION
(DAS-48S Channel 25)

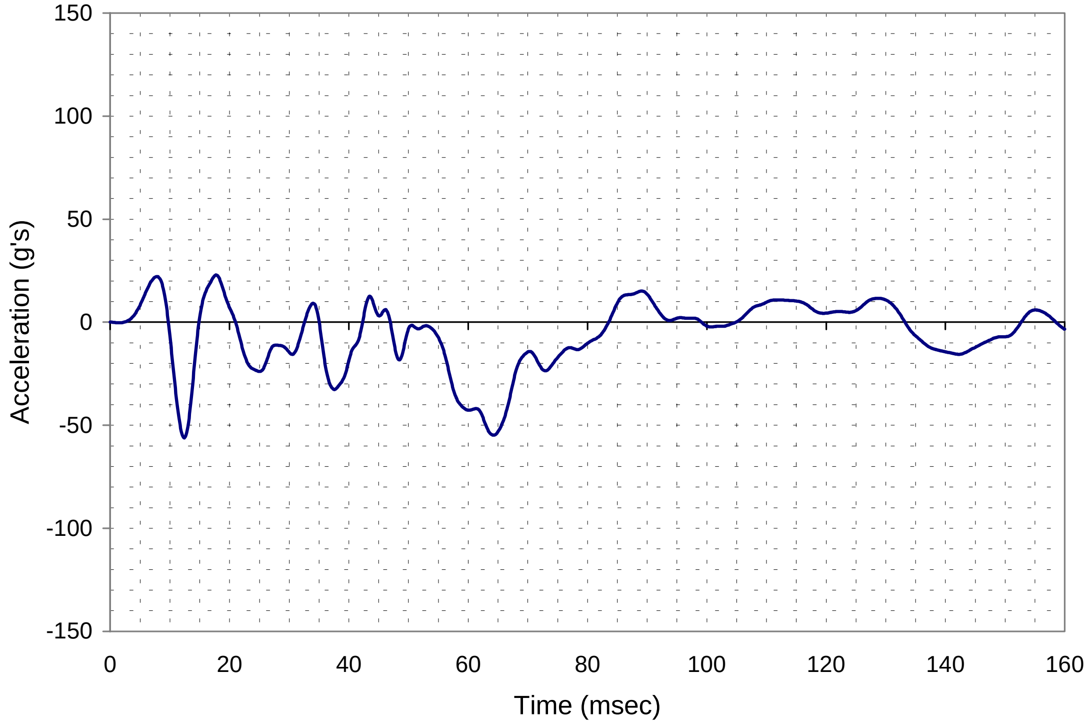

FIGURE B-61. FS 500 RIGHT SIDEWALL, ACCELEROMETER Z-DIRECTION
(NEFF Channel 418)

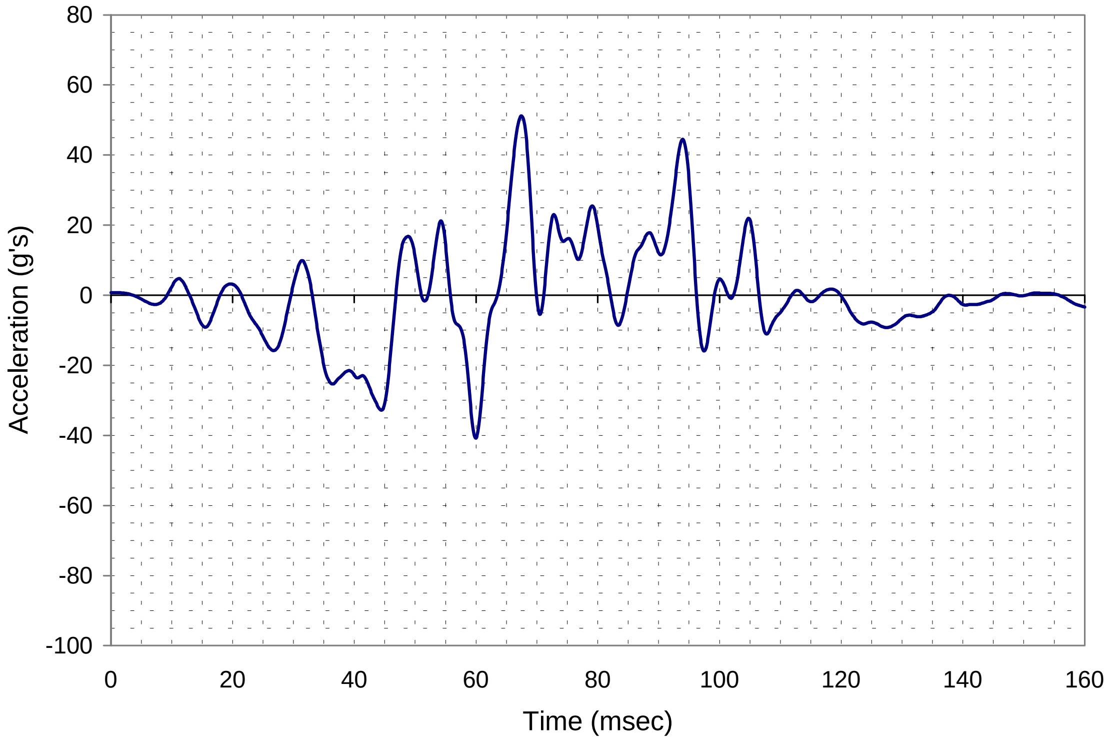

FIGURE B-62. FS 446 LEFT TANK RAIL, ACCELEROMETER Z-DIRECTION
(DAS-48S Channel 22)

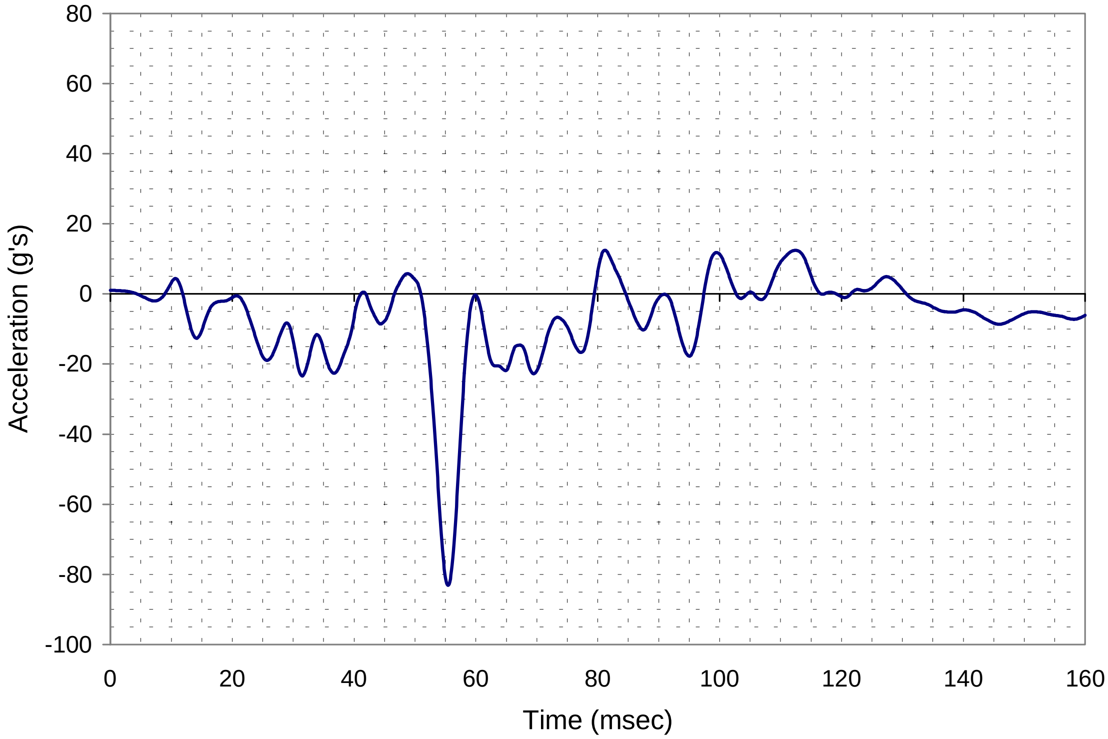

FIGURE B-63. FS 446 RIGHT TANK RAIL, ACCELEROMETER Z-DIRECTION
(NEFF Channel 422)

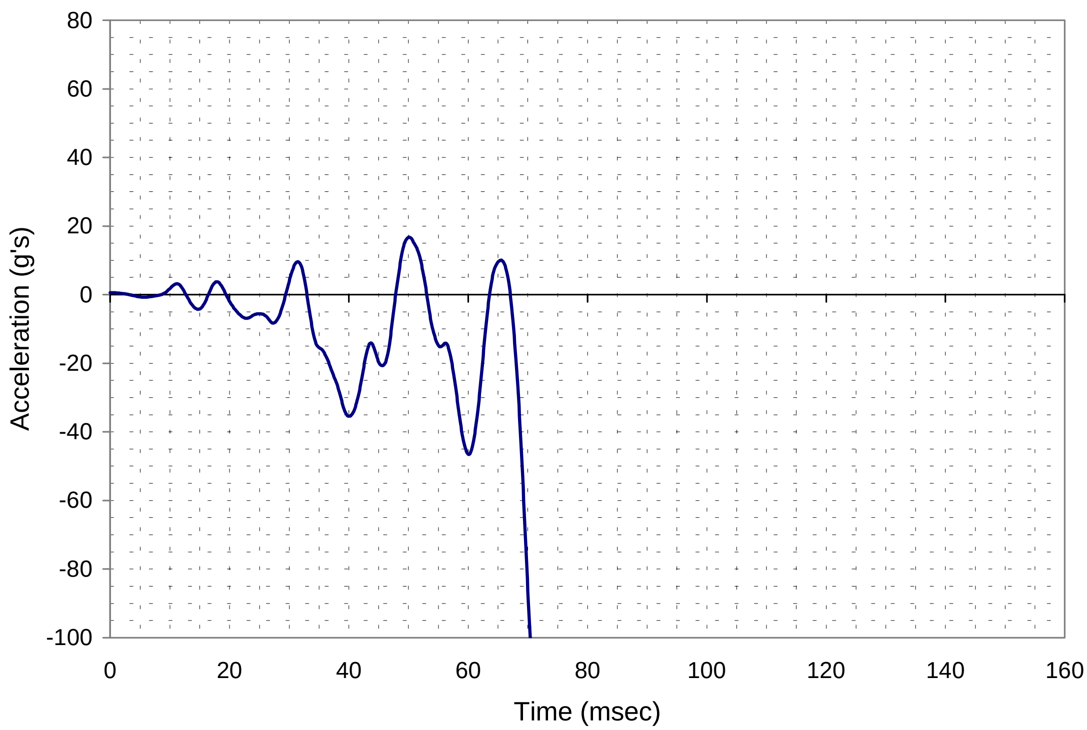

FIGURE B-64. FS 487 LEFT TANK RAIL, ACCELEROMETER Z-DIRECTION
(NEFF Channel 110)

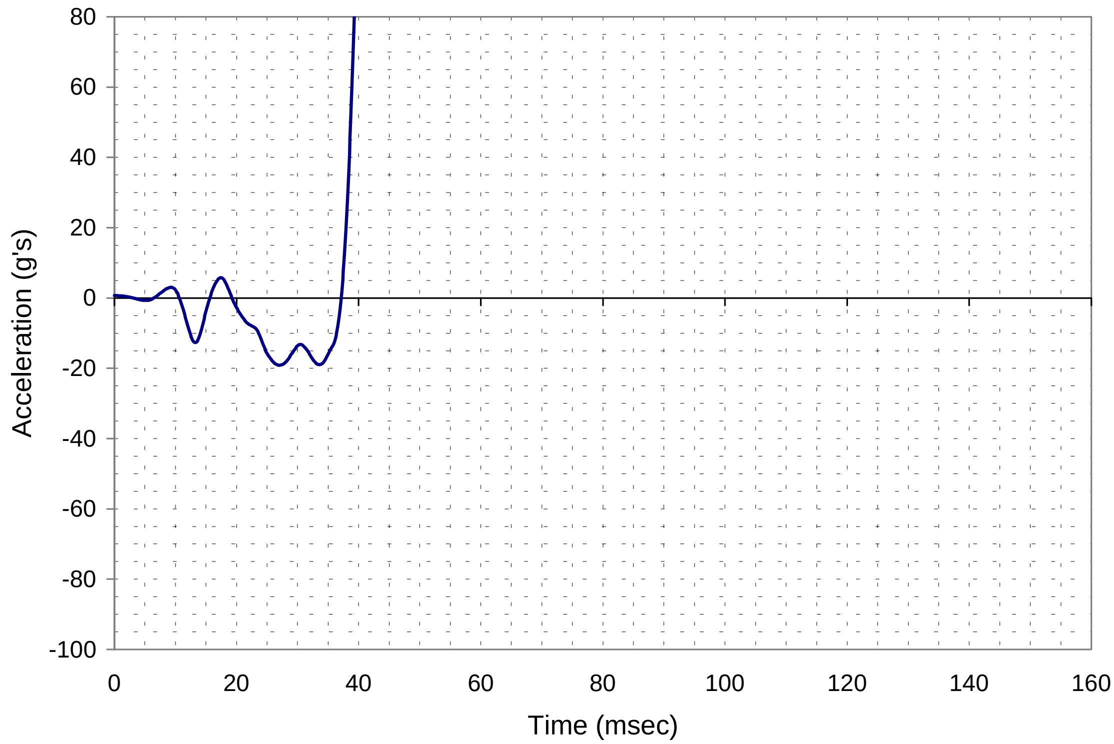

FIGURE B-65. FS 487 RIGHT TANK RAIL, ACCELEROMETER Z-DIRECTION
(DAS-48S Channel 24)

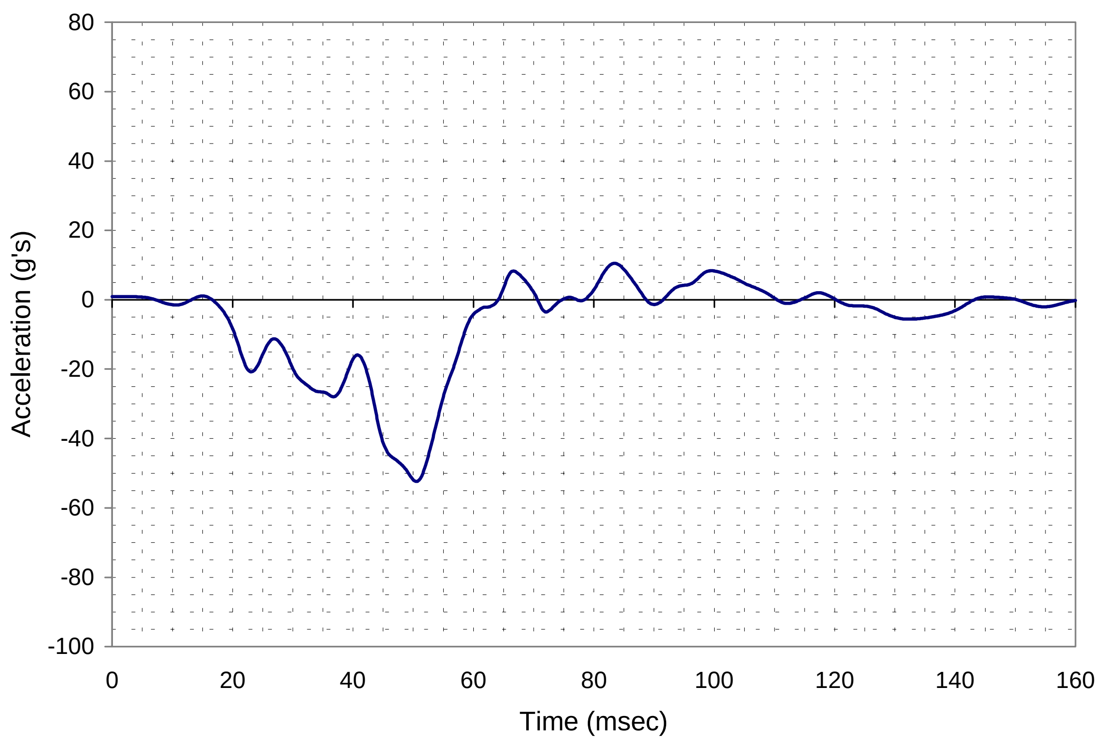

FIGURE B-66. FS 446 LEFT FRONT TANK, ACCELEROMETER Z-DIRECTION
(NEFF Channel 112)

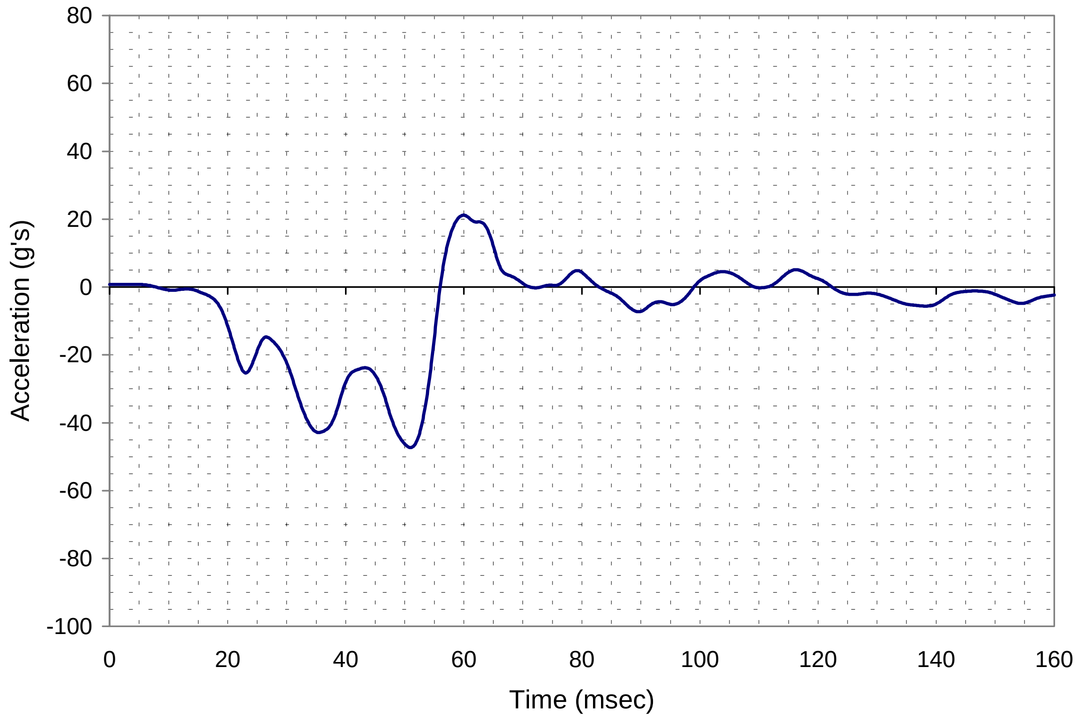

FIGURE B-67. FS 446 RIGHT FRONT TANK, ACCELEROMETER Z-DIRECTION
(DAS-48S Channel 28)

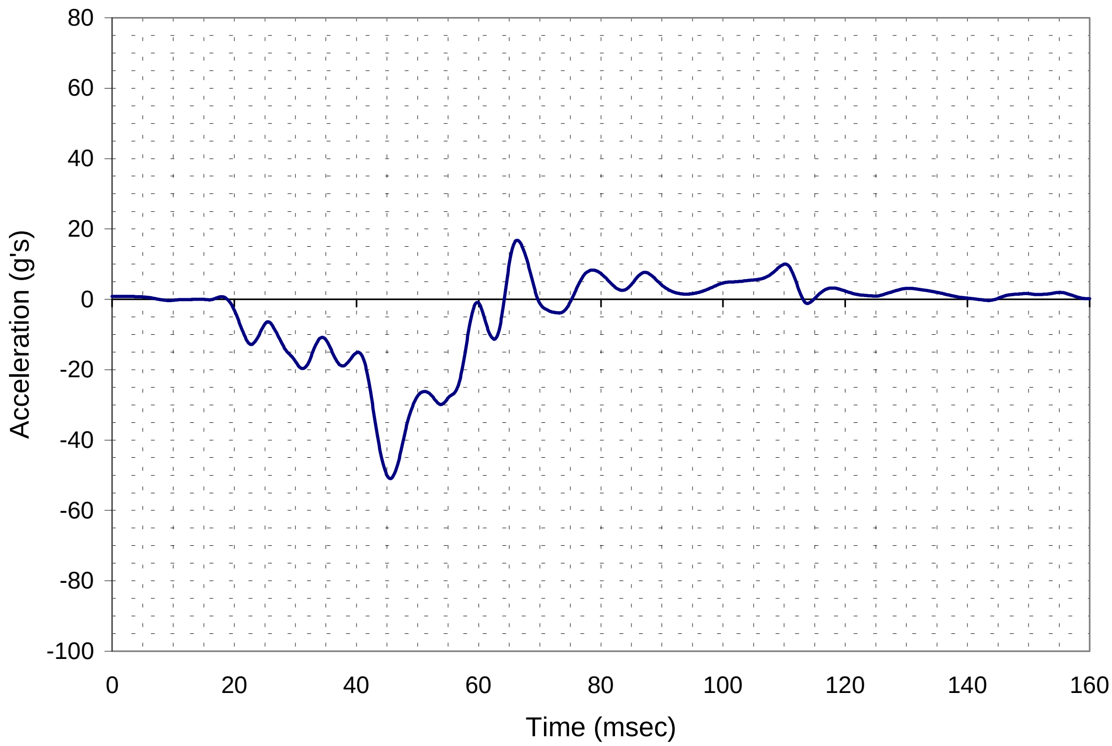

FIGURE B-68. FS 457 LEFT SIDE TANK, ACCELEROMETER Z-DIRECTION
(DAS-48S Channel 29)

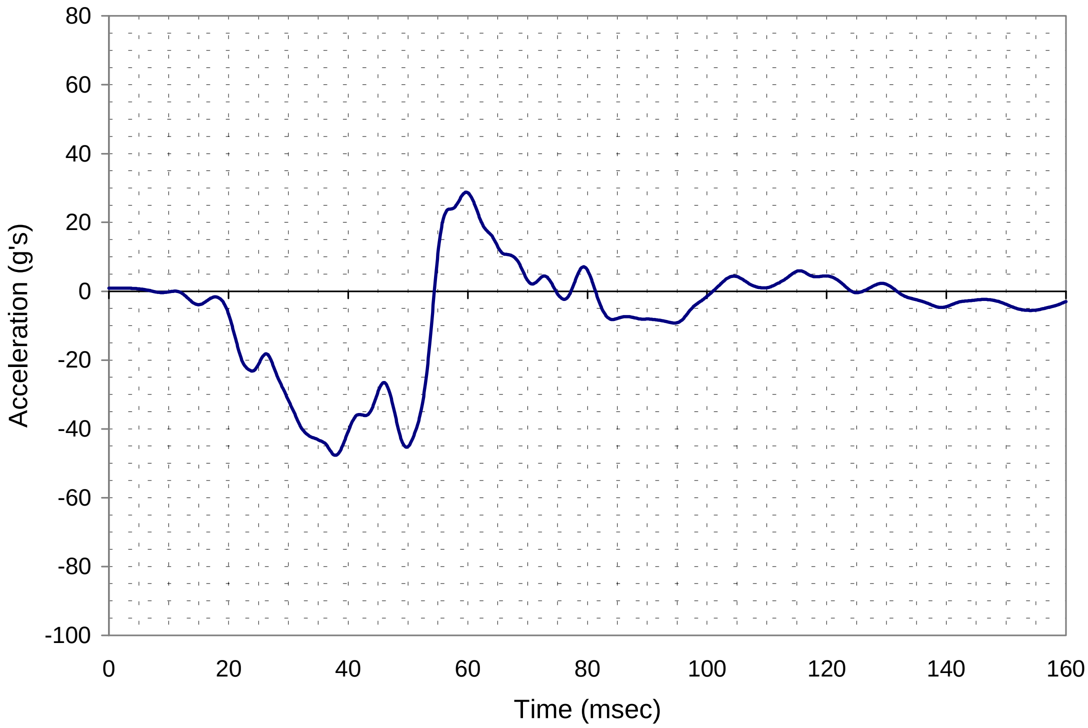

FIGURE B-69. FS 457 RIGHT SIDE TANK, ACCELEROMETER Z-DIRECTION
(NEFF Channel 113)

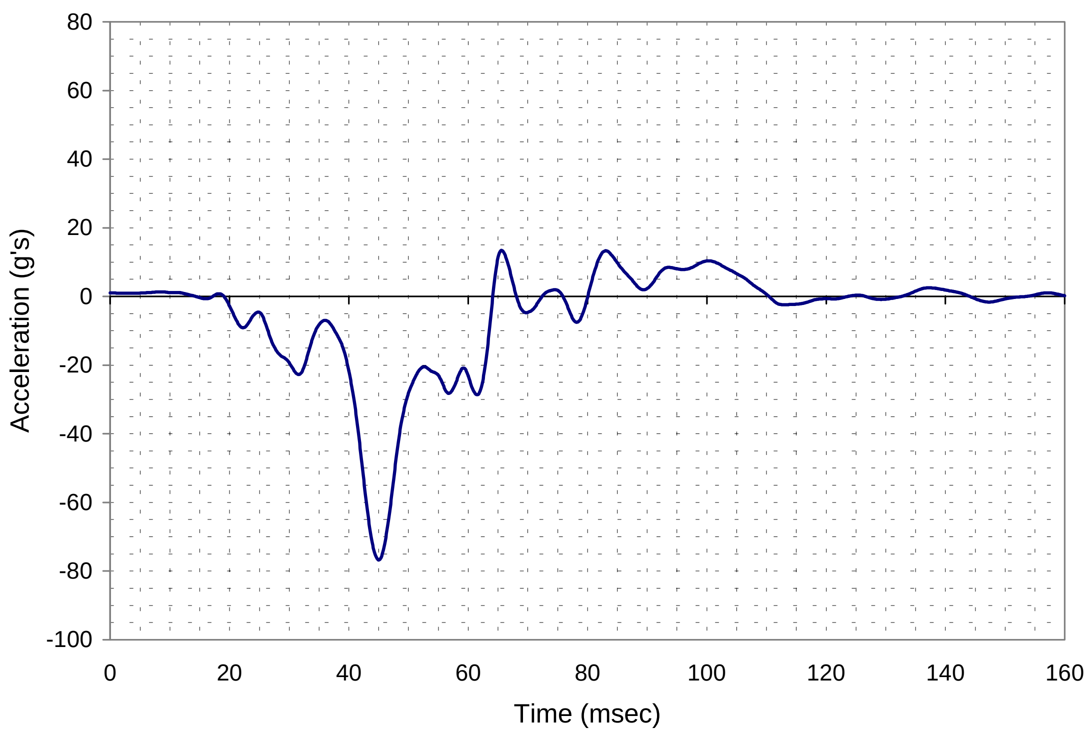

FIGURE B-70. FS 478 LEFT SIDE TANK, ACCELEROMETER Z-DIRECTION
(NEFF Channel 114)

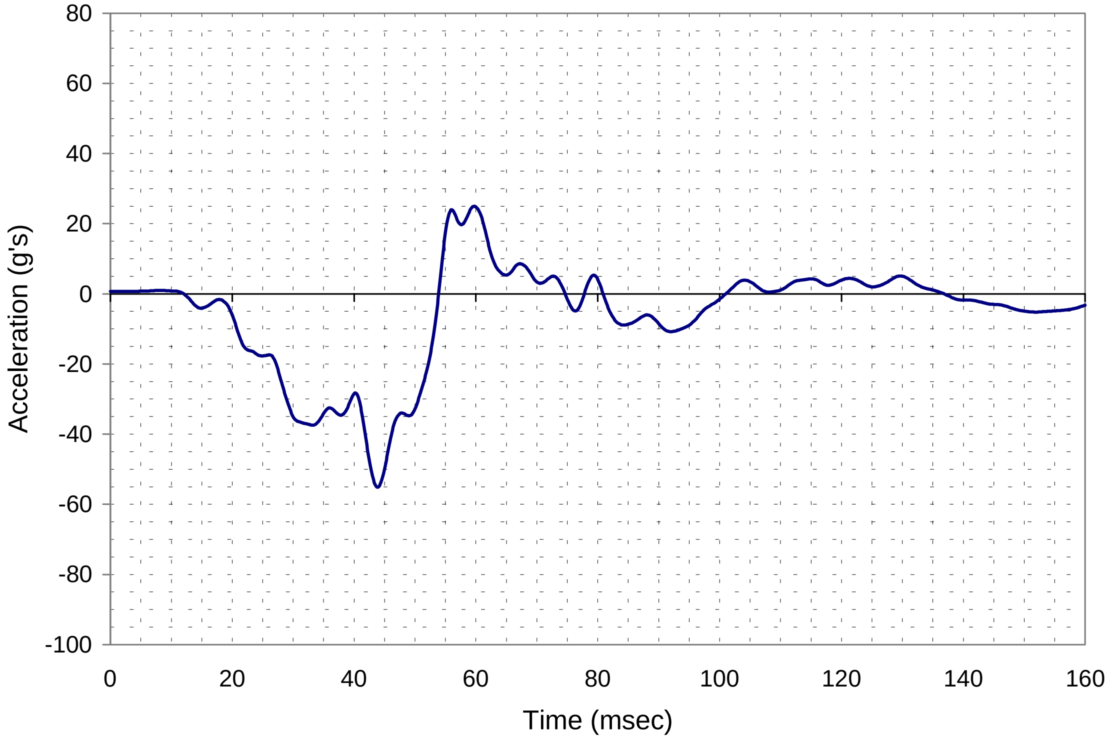

FIGURE B-71. FS 478 RIGHT SIDE TANK, ACCELEROMETER Z-DIRECTION
(DAS-48S Channel 30)

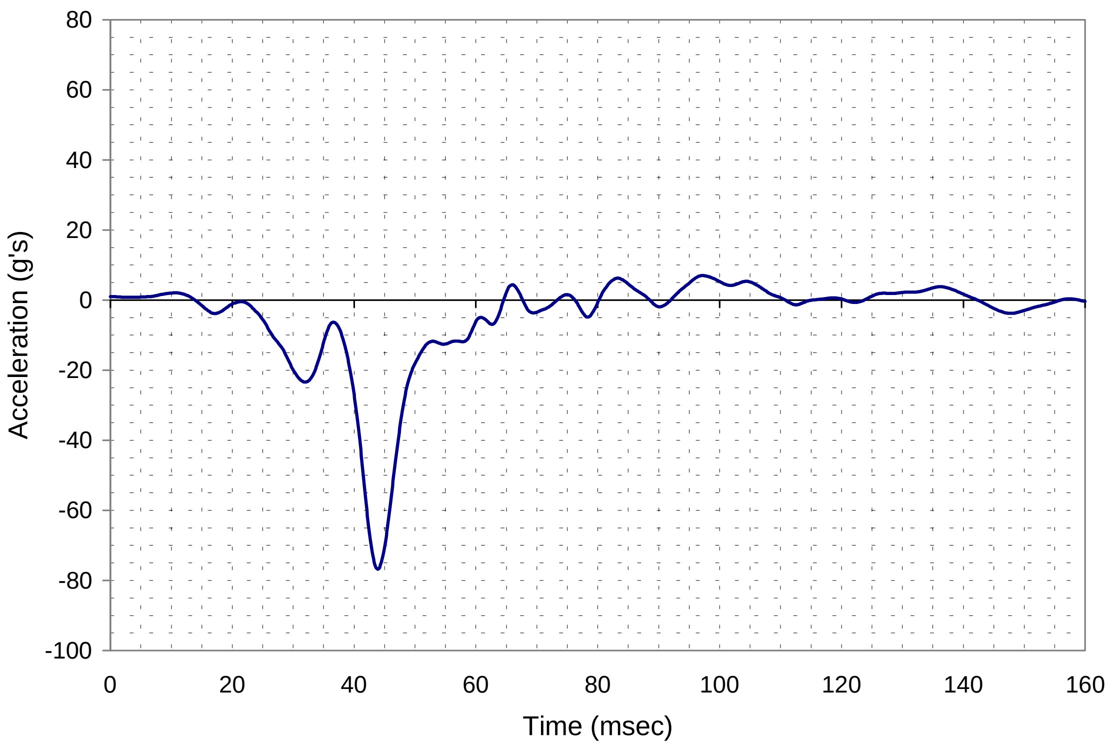

FIGURE B-72. FS 489 LEFT REAR TANK, ACCELEROMETER Z-DIRECTION
(DAS-48S Channel 31)

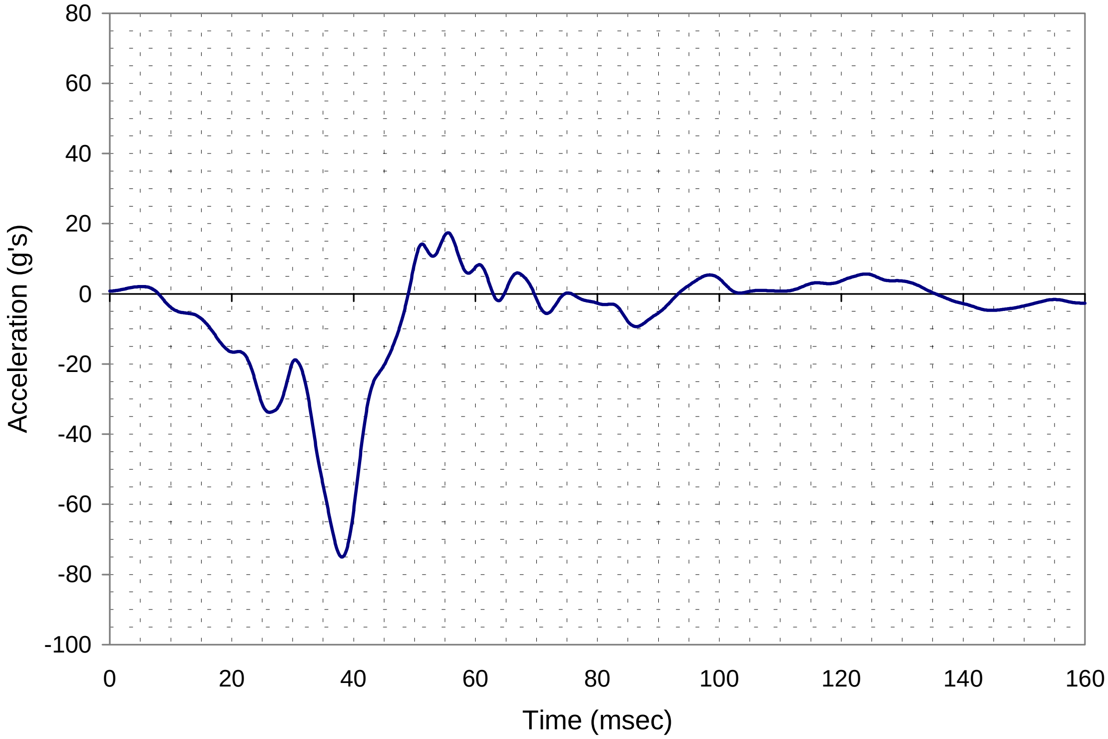

FIGURE B-73. FS 489 RIGHT REAR TANK, ACCELEROMETER Z-DIRECTION
(NEFF Channel 115)

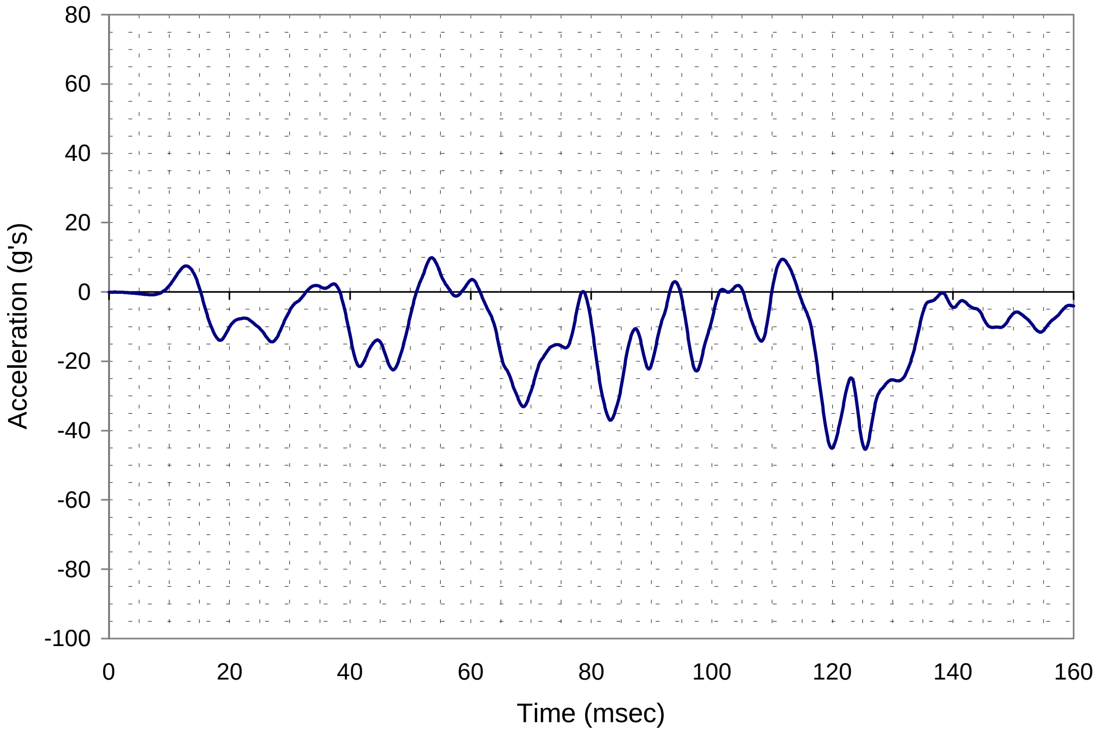

FIGURE B-74. FS 420 LEFT CEILING, ACCELEROMETER Z-DIRECTION
(NEFF Channel 420)

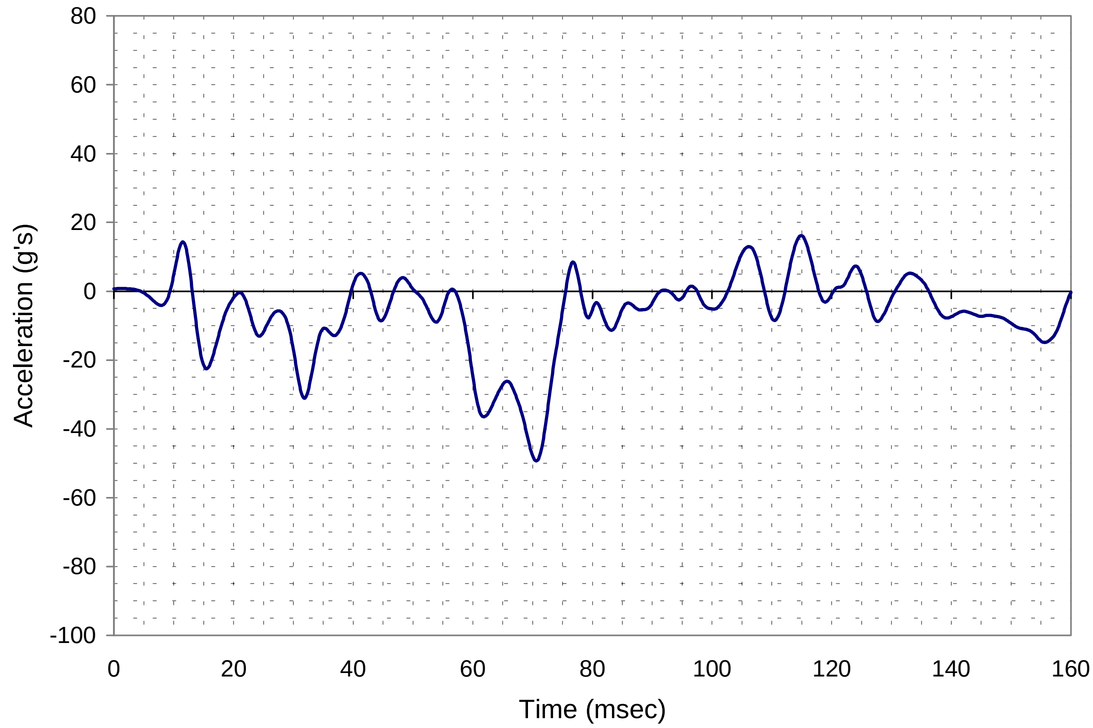

FIGURE B-75. FS 420 RIGHT CEILING, ACCELEROMETER Z-DIRECTION
(NEFF Channel 421)

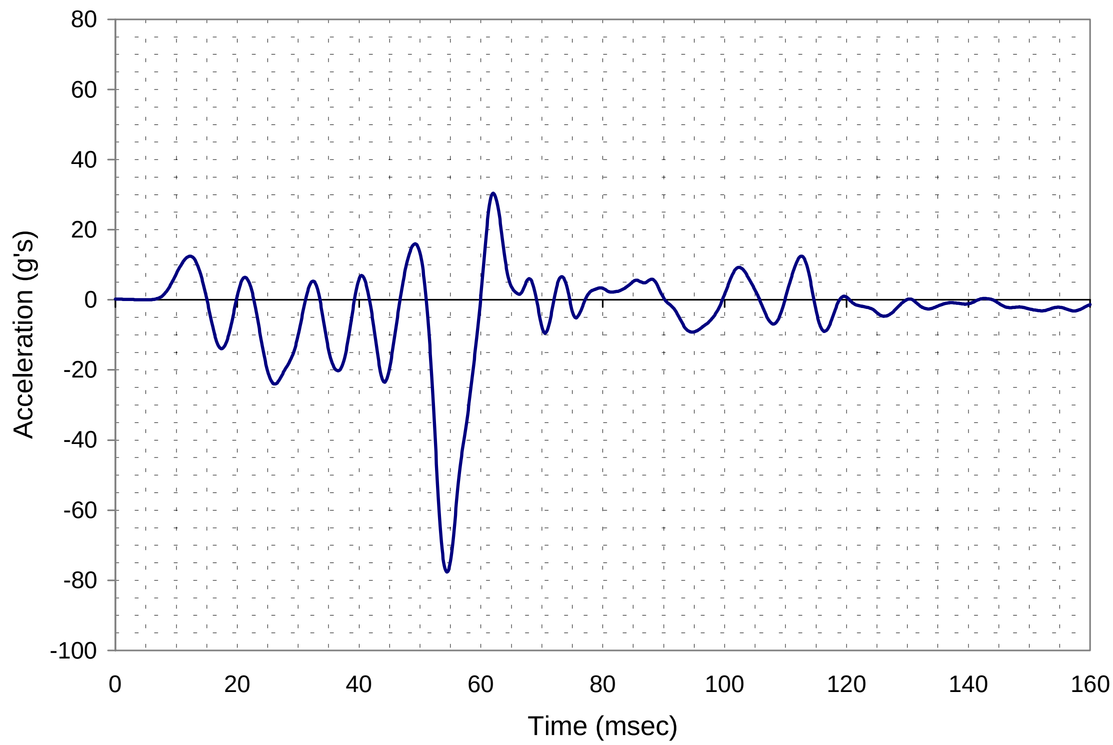

FIGURE B-76. FS 460 CENTER CEILING, ACCELEROMETER Z-DIRECTION
(NEFF Channel 423)

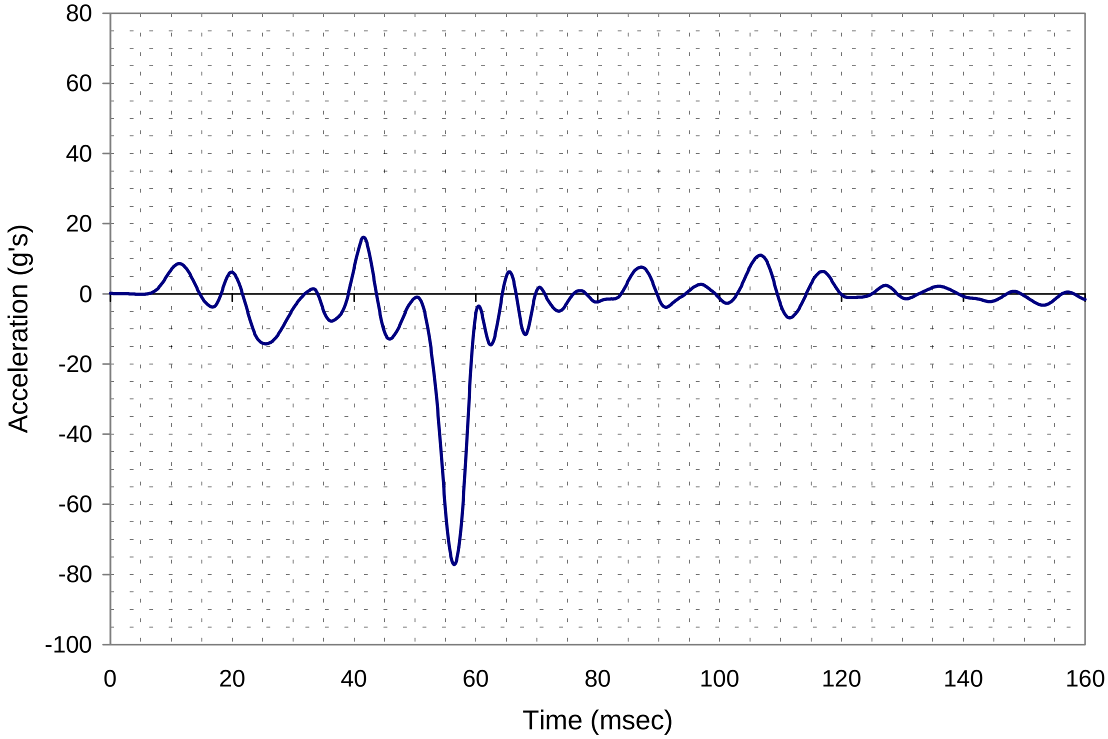

FIGURE B-77. FS 480 CENTER CEILING, ACCELEROMETER Z-DIRECTION
(DAS-48S Channel 23)

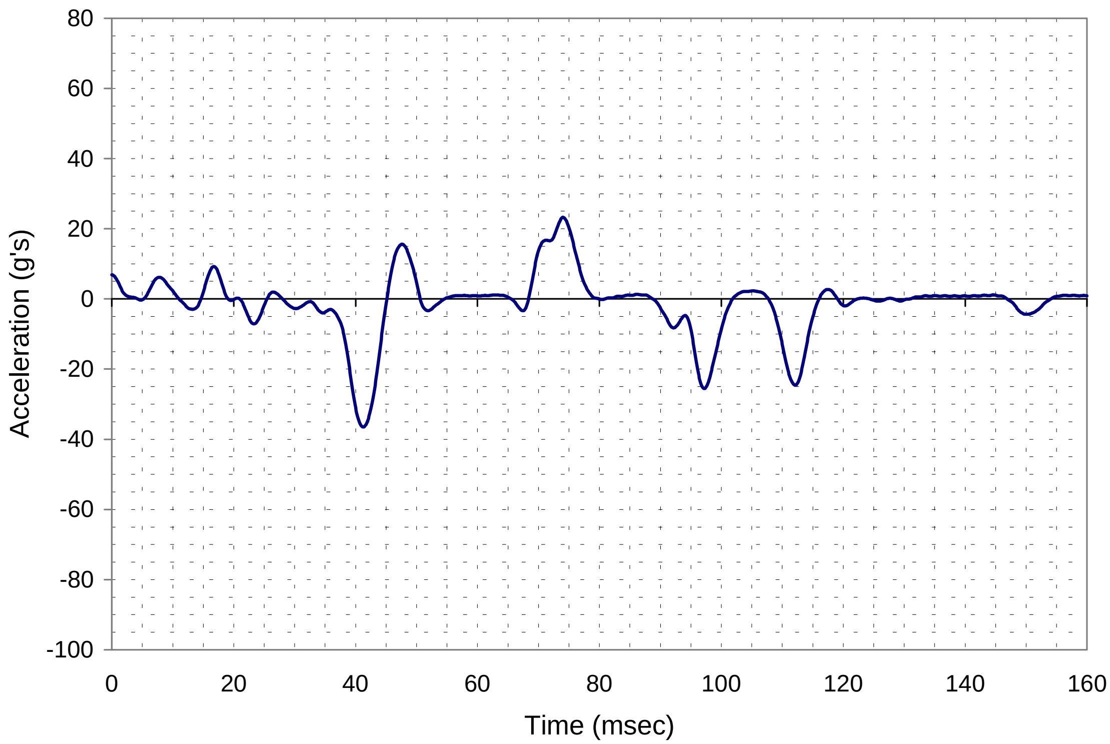

FIGURE B-78. FS 500 LEFT CEILING, ACCELEROMETER Z-DIRECTION
(NEFF Channel 111)

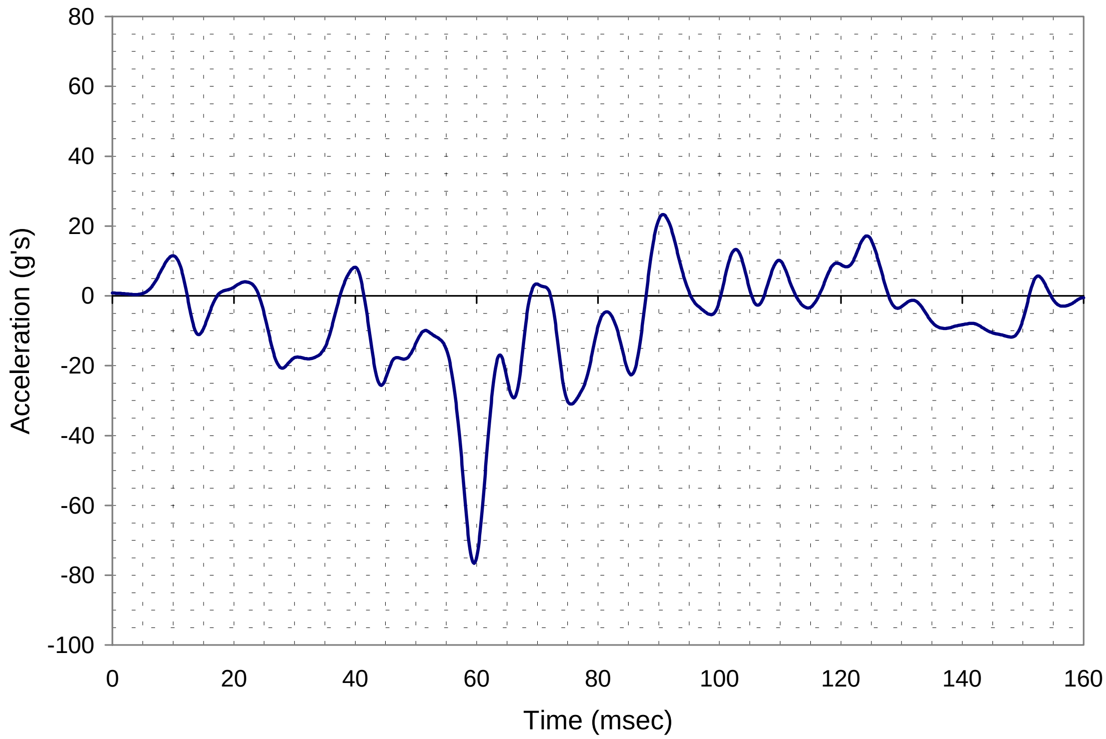

FIGURE B-79. FS 500 RIGHT CEILING, ACCELEROMETER Z-DIRECTION
(DAS-48S Channel 27)

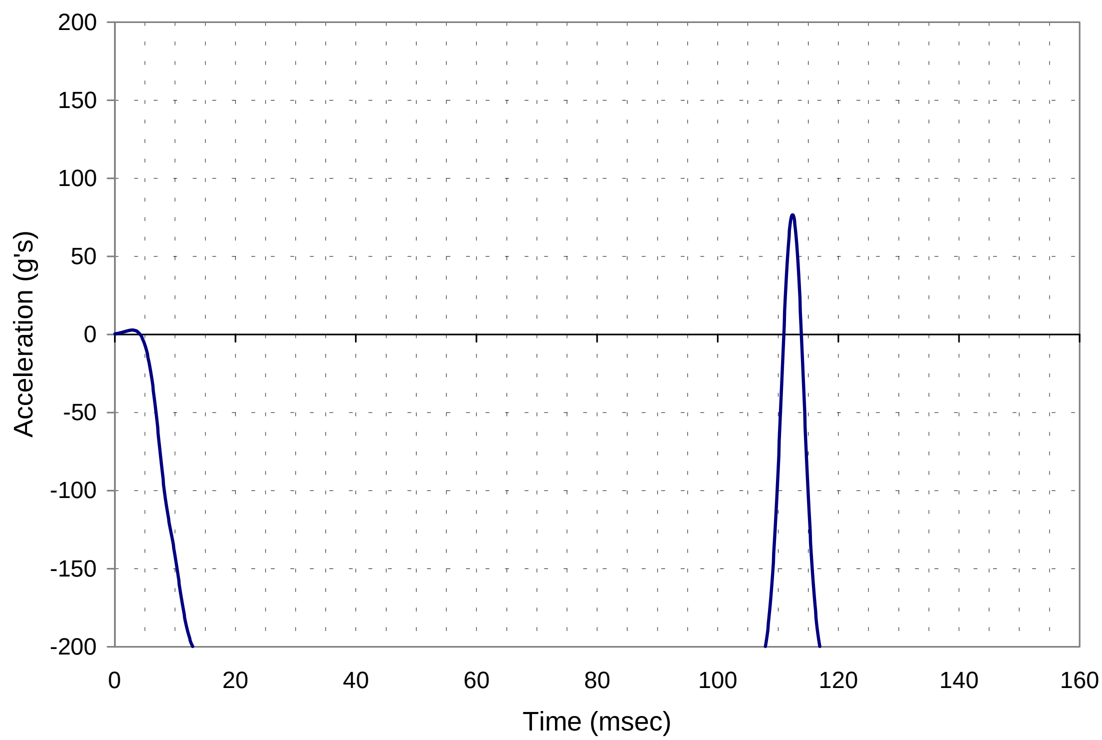

FIGURE B-80. FS 420 CENTER FLOOR, ACCELEROMETER Z-DIRECTION
(NEFF Channel 102)

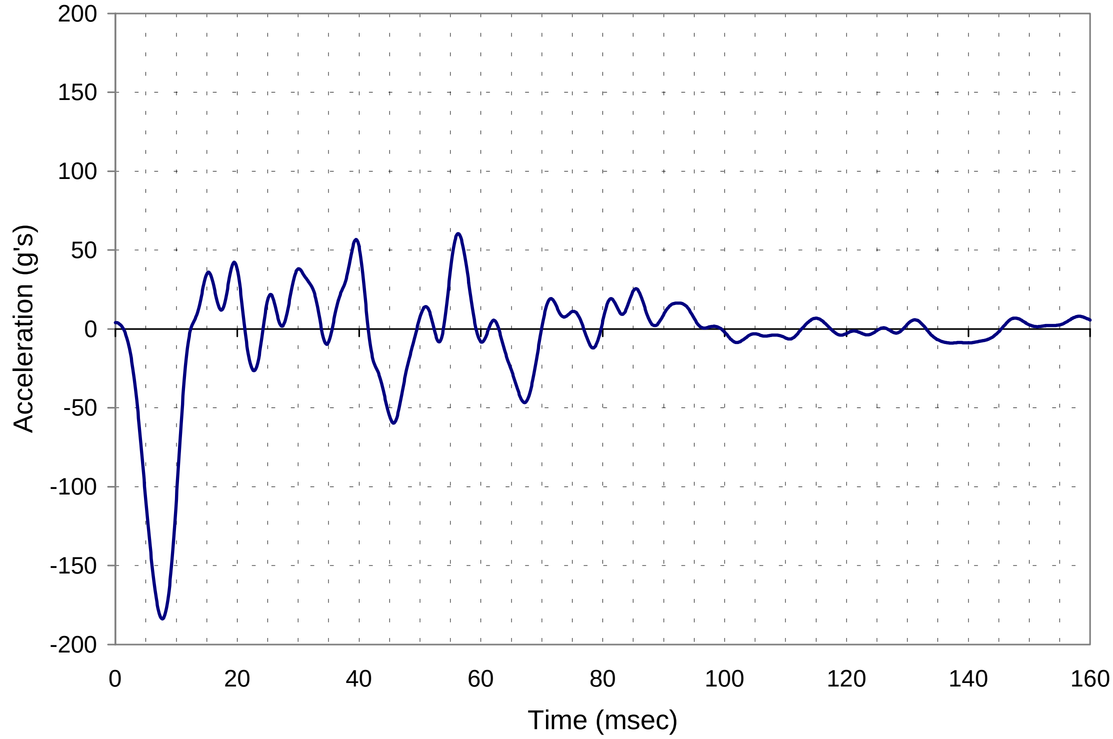

FIGURE B-81. FS 500 CENTER FLOOR, ACCELEROMETER Z-DIRECTION
(DAS-48S Channel 26)

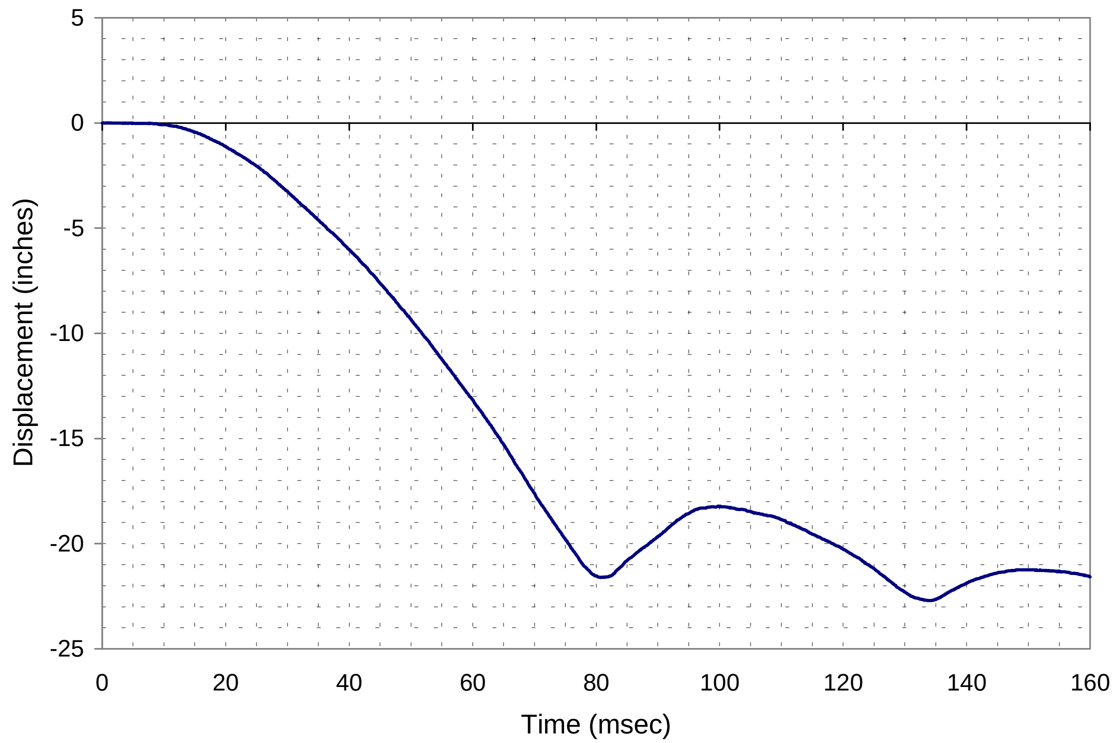

FIGURE B-82. FS 420 CENTER STRING POTENTIOMETER
(NEFF Channel 103)

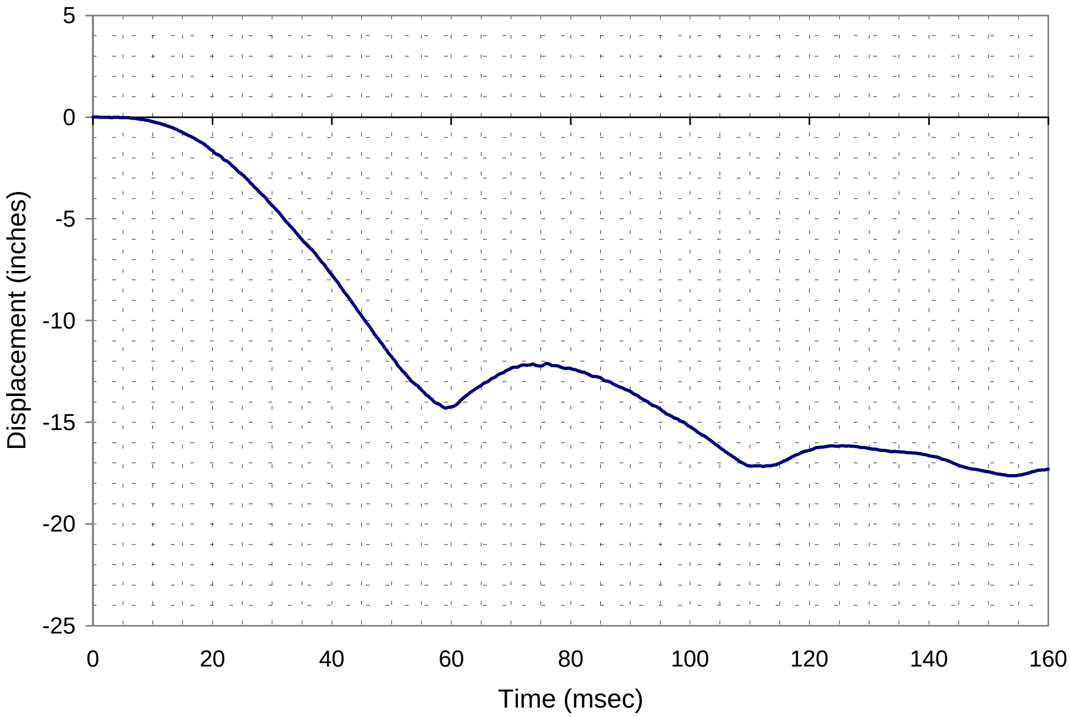

FIGURE B-83. FS 500 CENTER STRING POTENTIOMETER
(DAS-48S Channel 103)

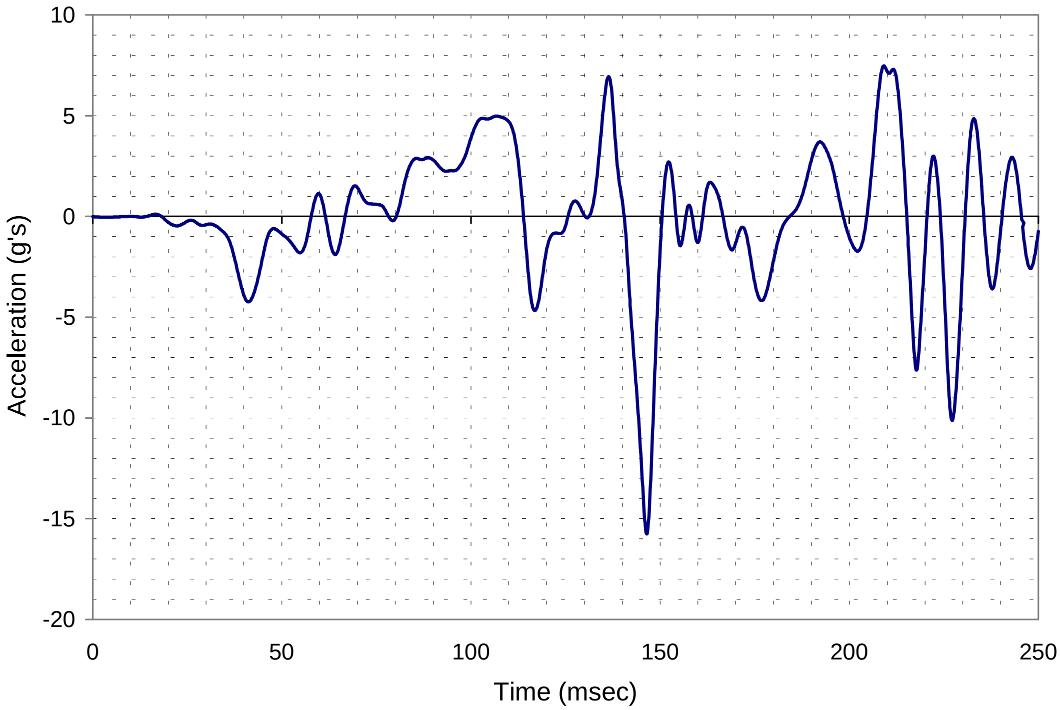

FIGURE B-84. PLATFORM ACCELEROMETER #1 Z-DIRECTION
(NEFF Channel 201)

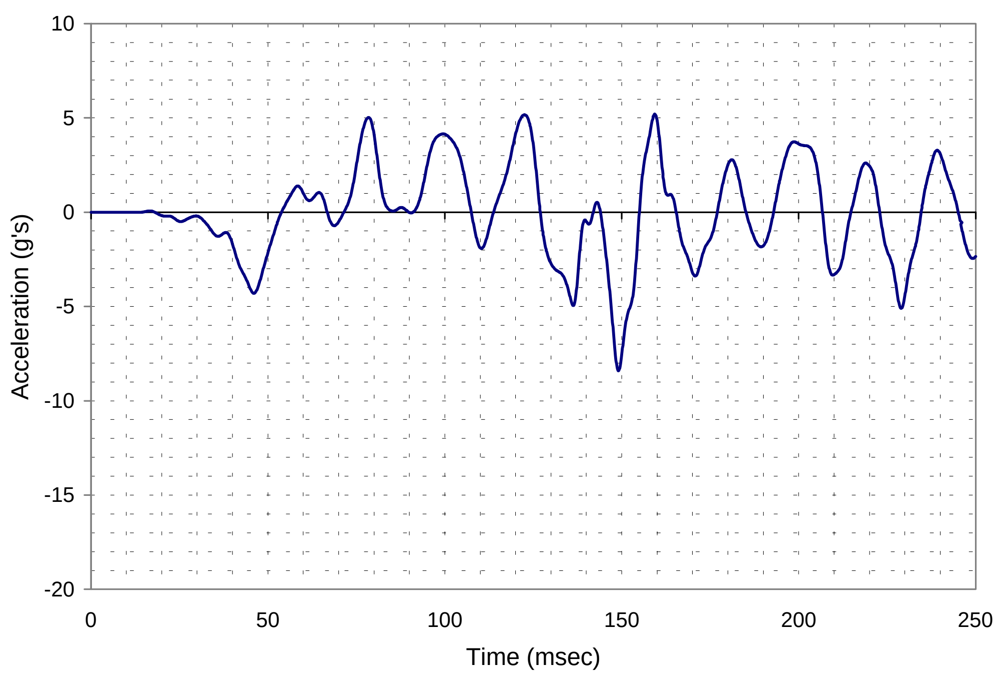

FIGURE B-85. PLATFORM ACCELEROMETER #2 Z-DIRECTION
(NEFF Channel 204)

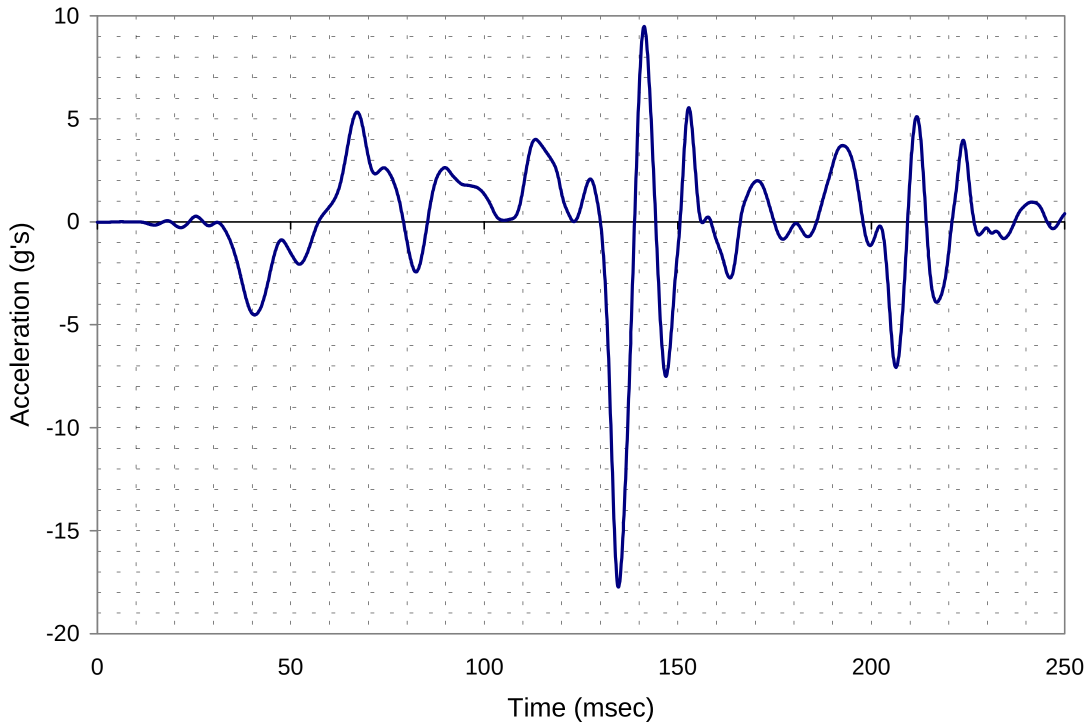

FIGURE B-86. PLATFORM ACCELEROMETER #3 Z-DIRECTION
(NEFF Channel 205)

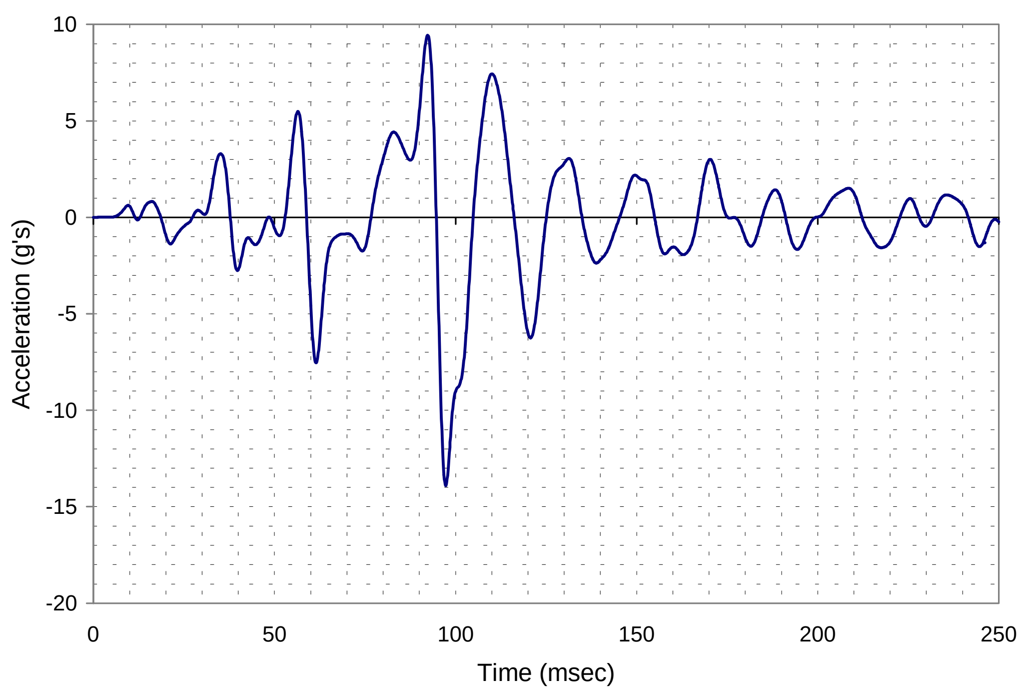

FIGURE B-87. PLATFORM ACCELEROMETER #4 Z-DIRECTION
(NEFF Channel 213)

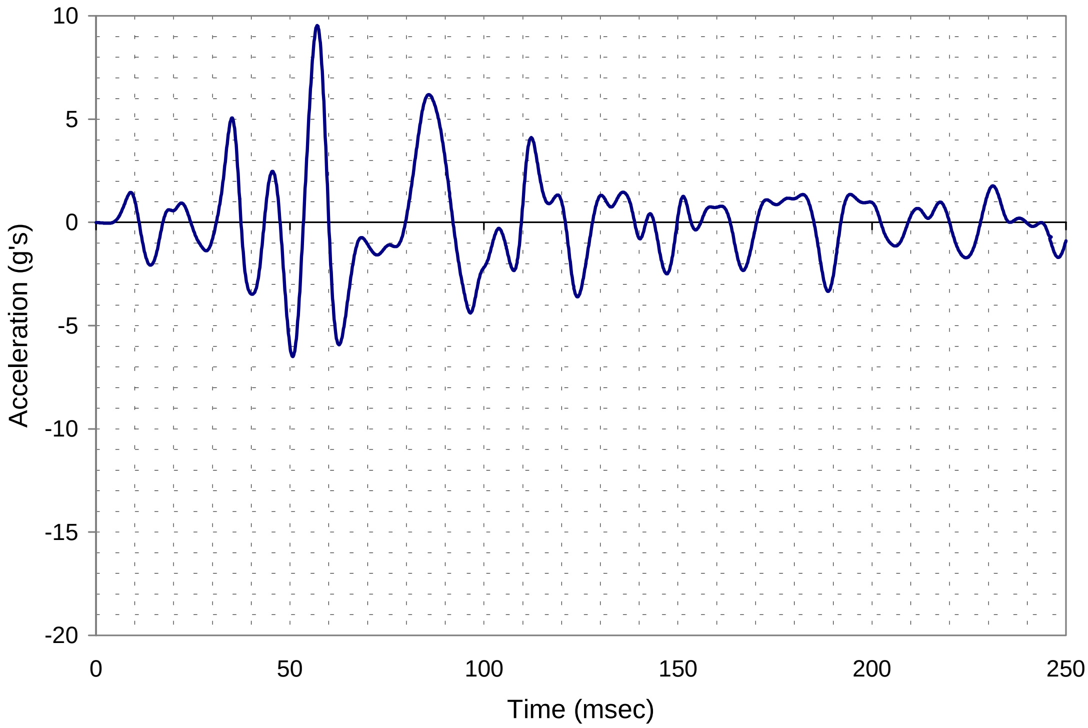

FIGURE B-88. PLATFORM ACCELEROMETER #5 Z-DIRECTION
(NEFF Channel 216)

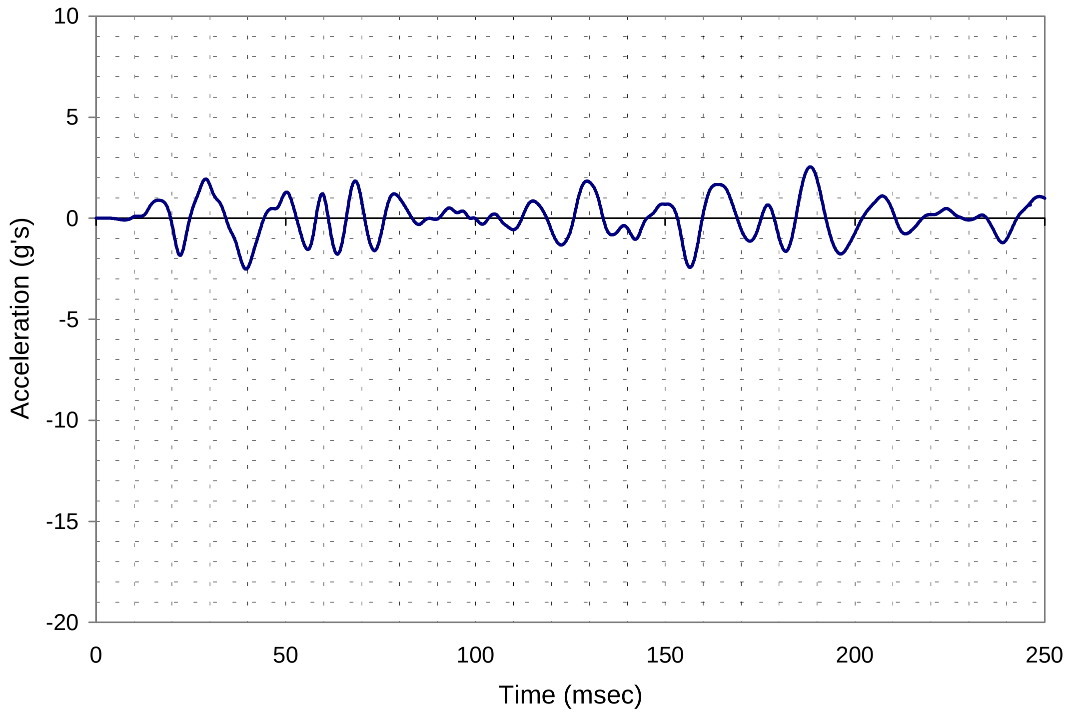

FIGURE B-89. PLATFORM ACCELEROMETER #6 Z-DIRECTION
(NEFF Channel 209)

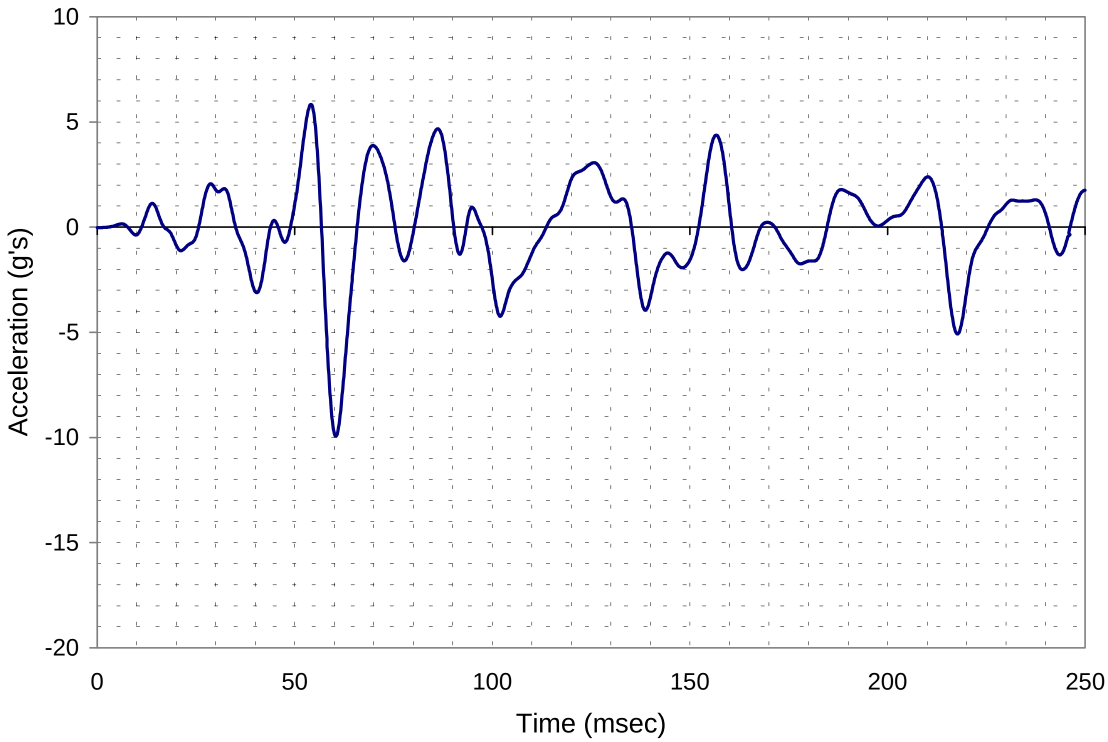

FIGURE B-90. PLATFORM ACCELEROMETER #7 Z-DIRECTION
(NEFF Channel 224)

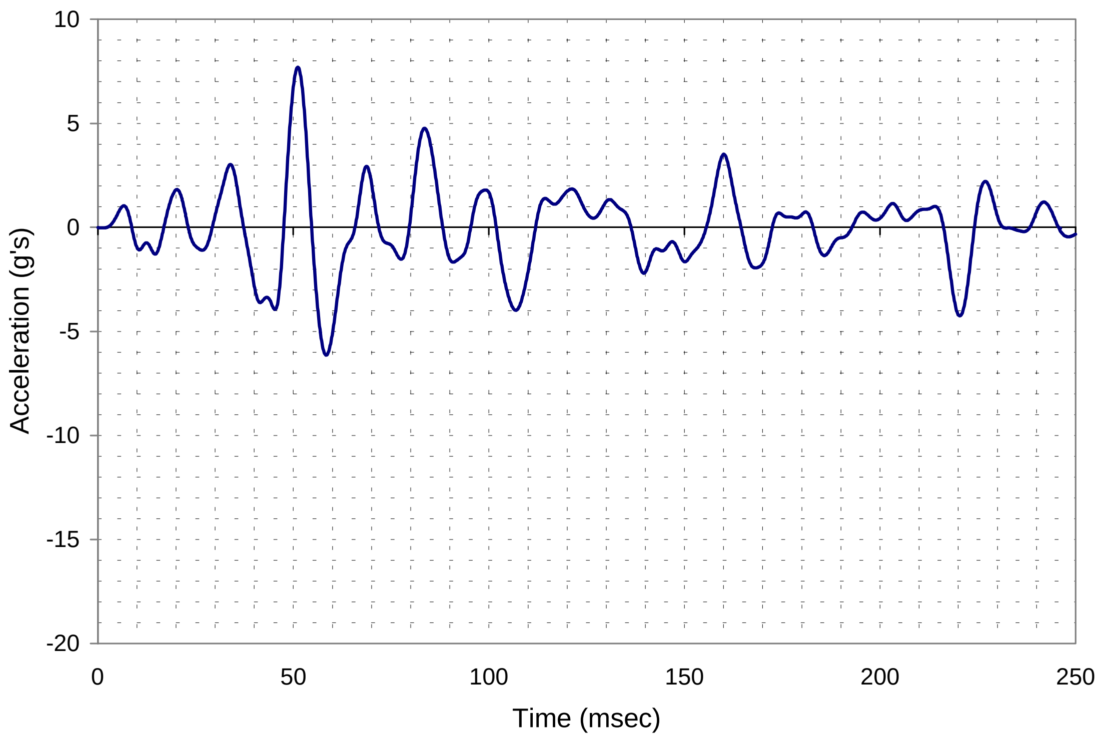

FIGURE B-91. PLATFORM ACCELEROMETER #8 Z-DIRECTION
(NEFF Channel 220)

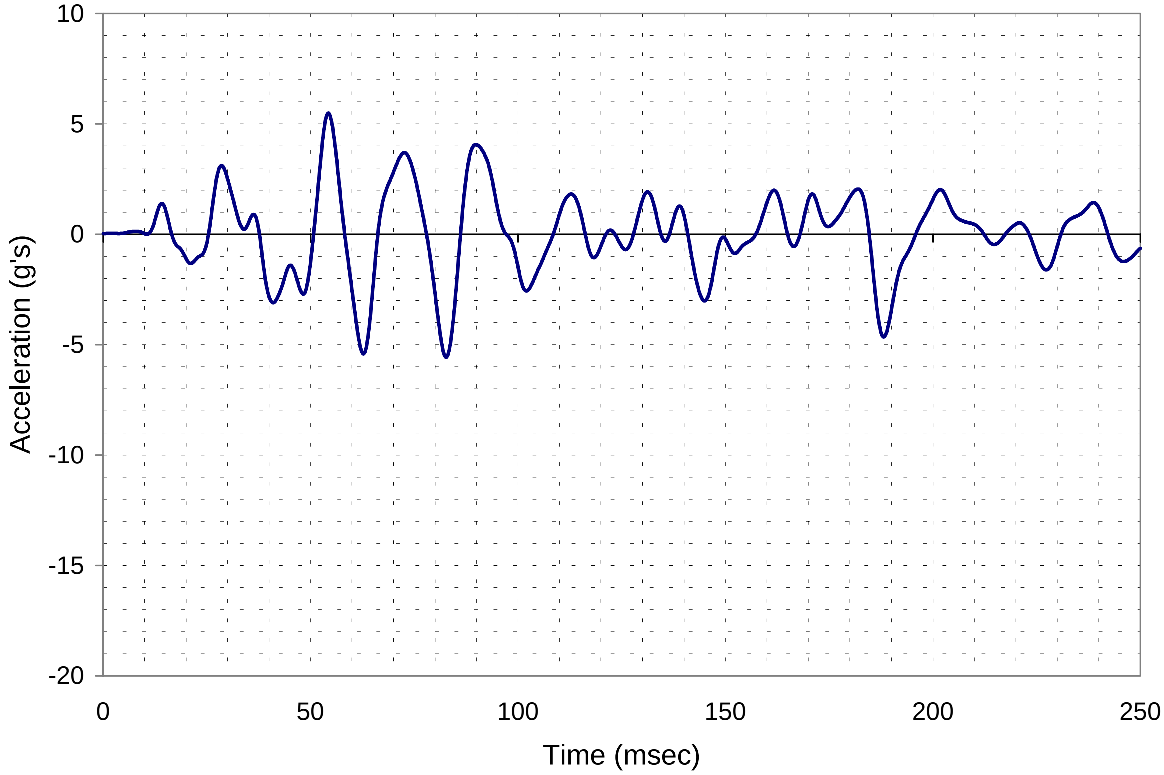

FIGURE B-92. PLATFORM ACCELEROMETER #9 Z-DIRECTION
(NEFF Channel 212)

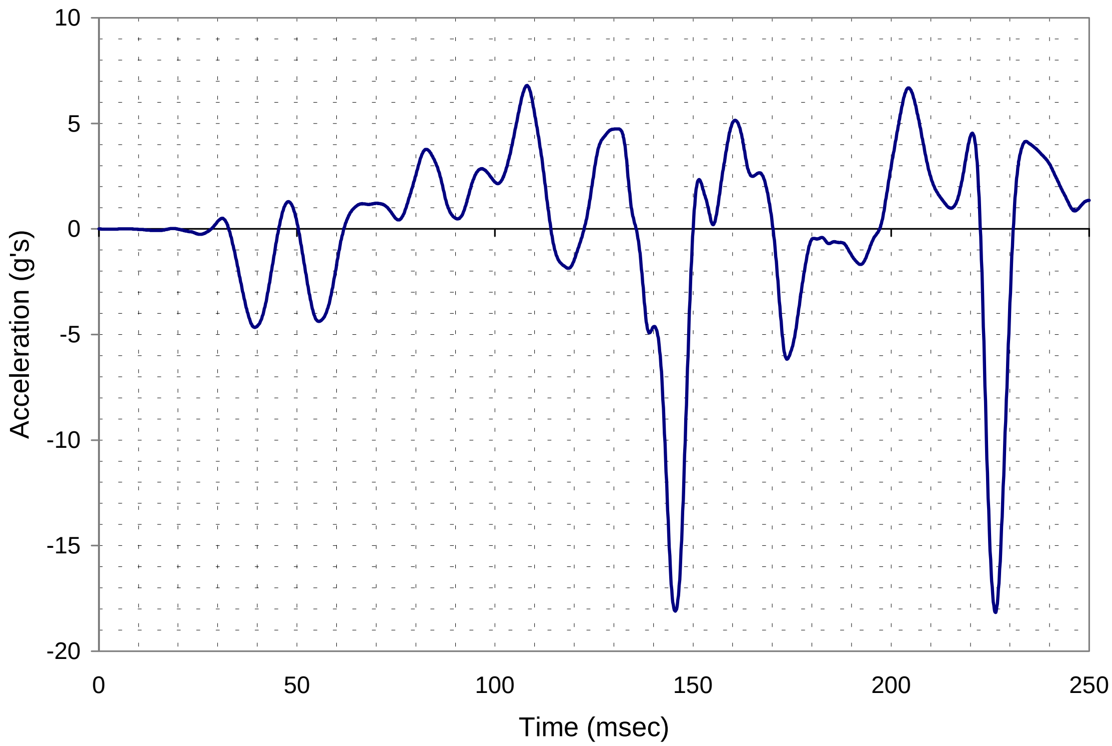

FIGURE B-93. PLATFORM ACCELEROMETER #10 Z-DIRECTION
(NEFF Channel 428)

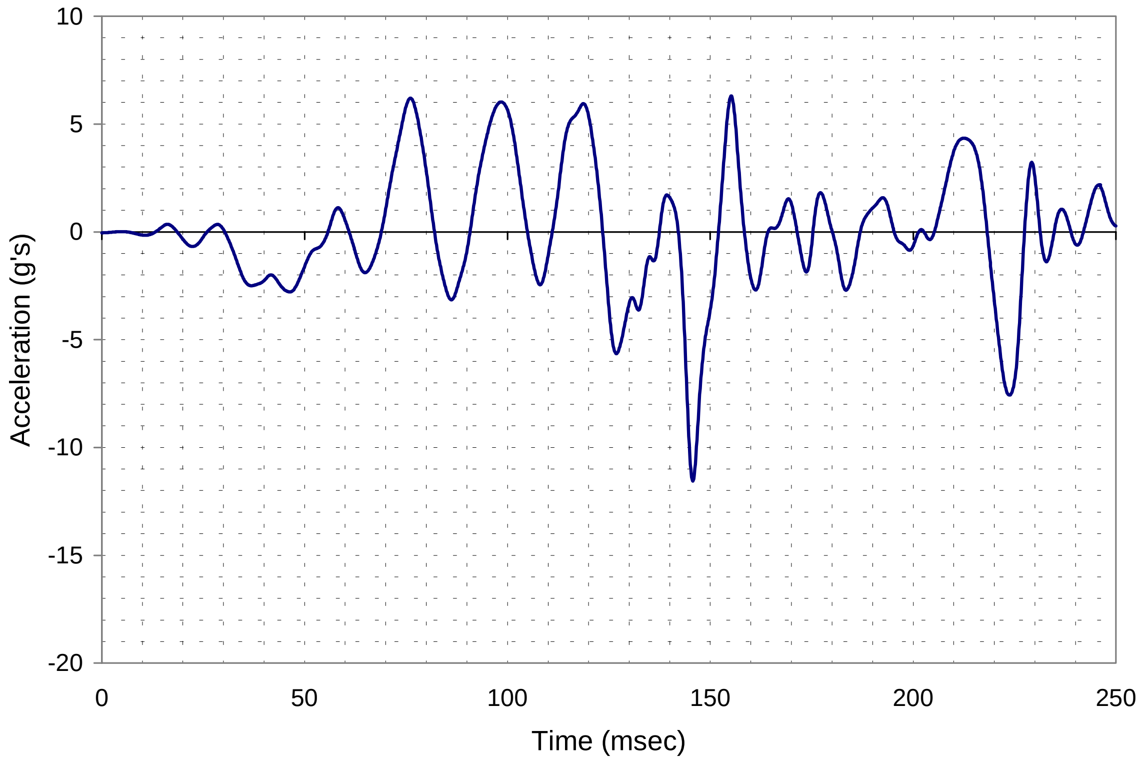

FIGURE B-94. PLATFORM ACCELEROMETER #11 Z-DIRECTION
(NEFF Channel 431)

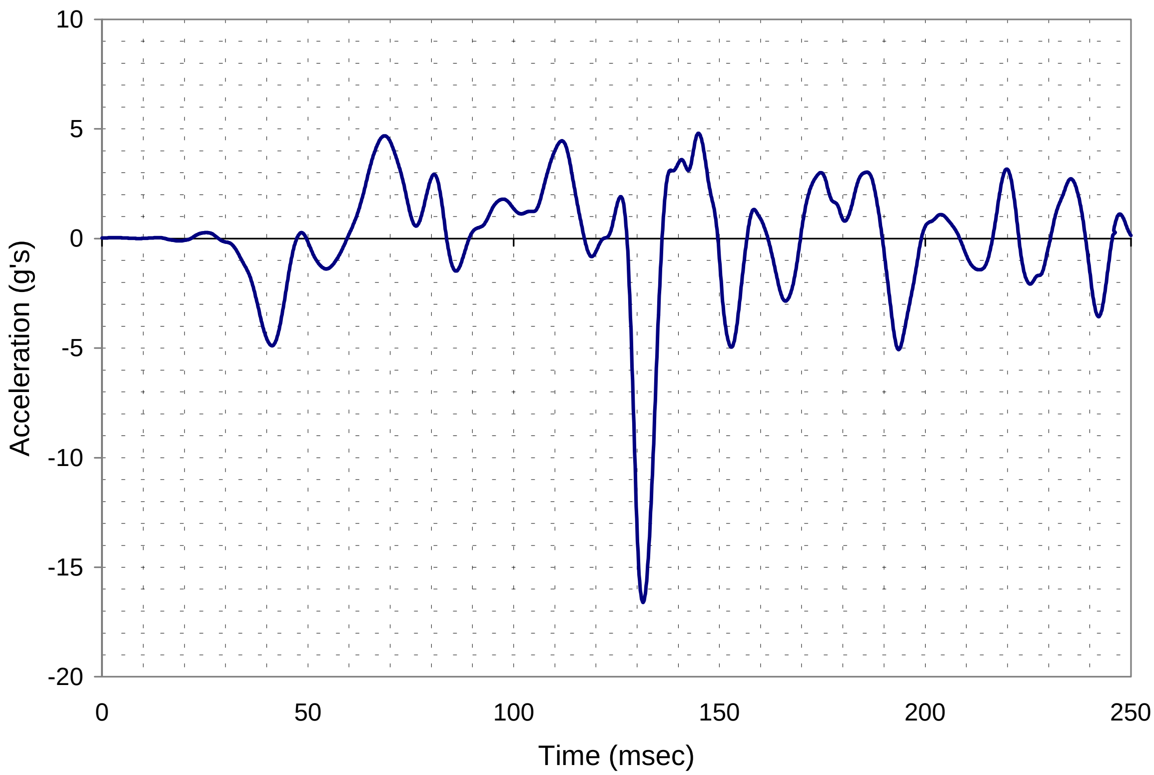

FIGURE B-95. PLATFORM ACCELEROMETER #12 Z-DIRECTION
(NEFF Channel 424)

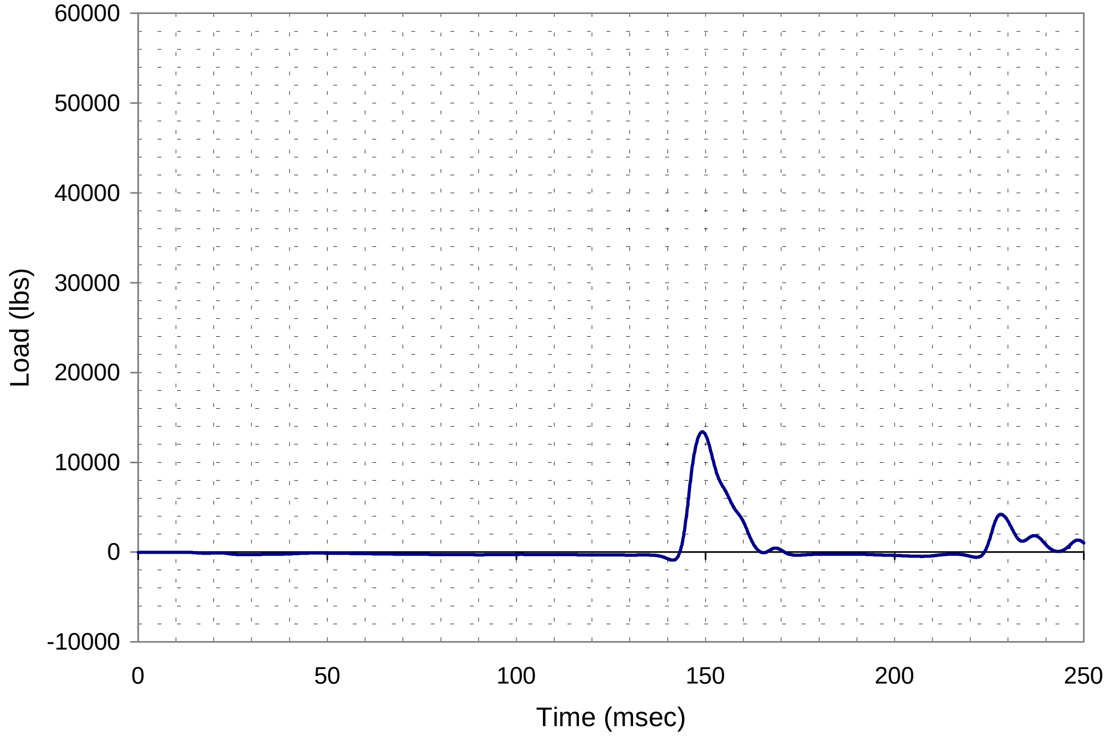

FIGURE B-96. PLATFORM LOAD CELL #1
(NEFF Channel 203)

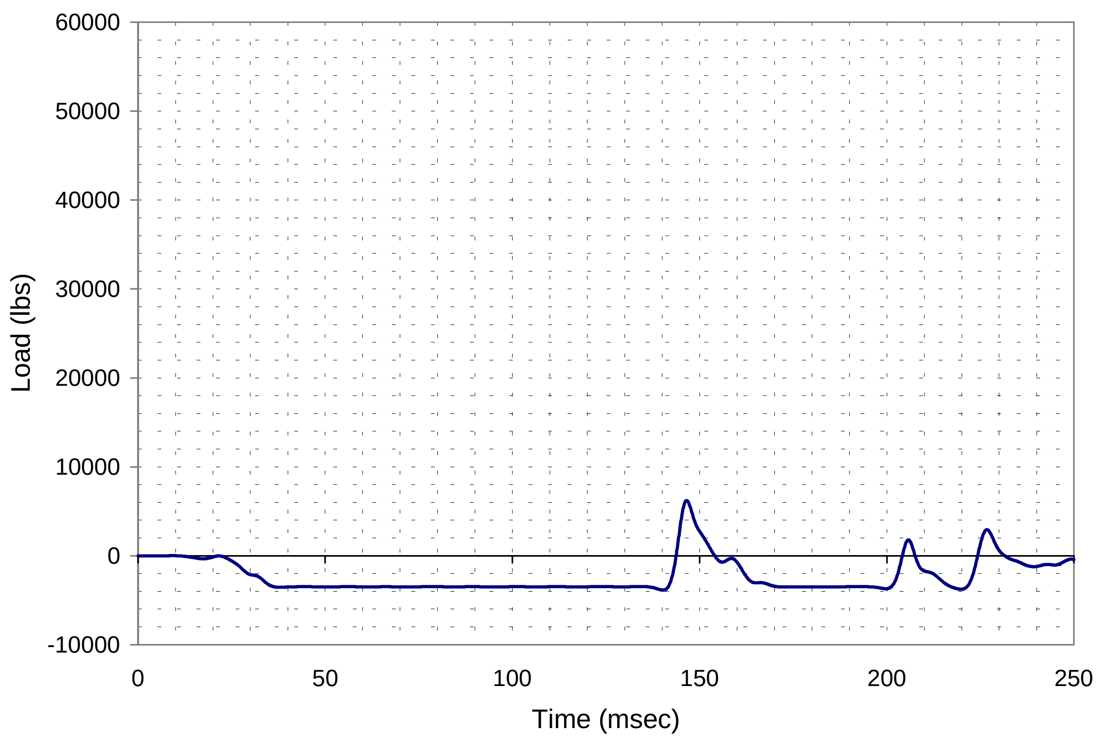

FIGURE B-97. PLATFORM LOAD CELL #2
(NEFF Channel 208)

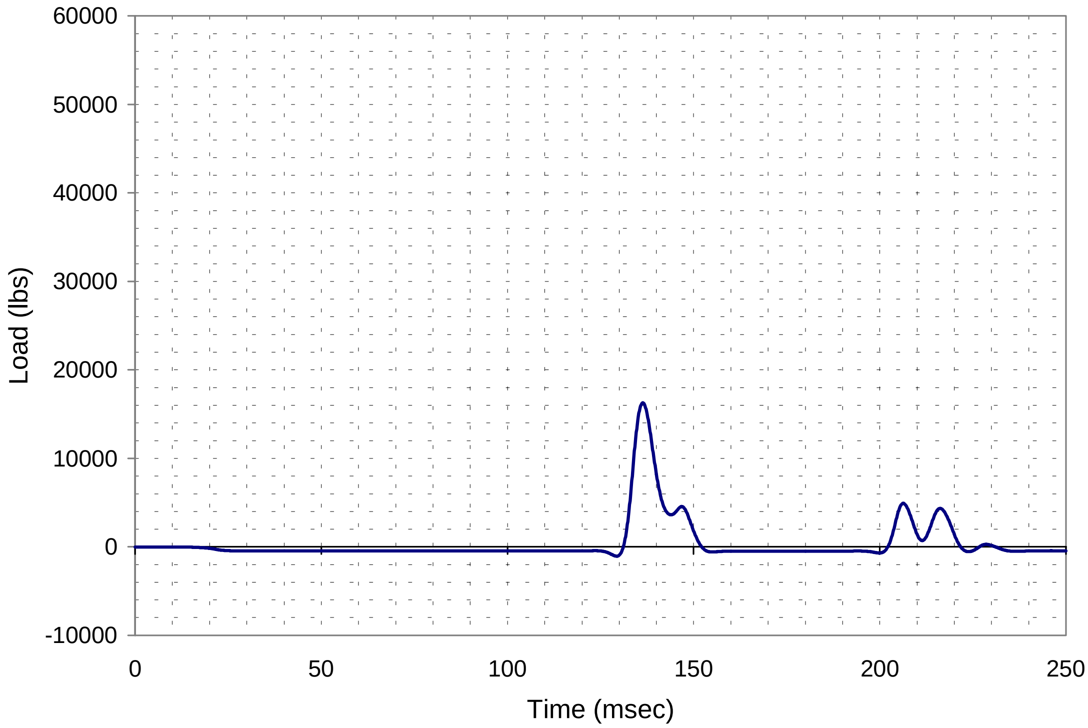

FIGURE B-98. PLATFORM LOAD CELL #3
(NEFF Channel 207)

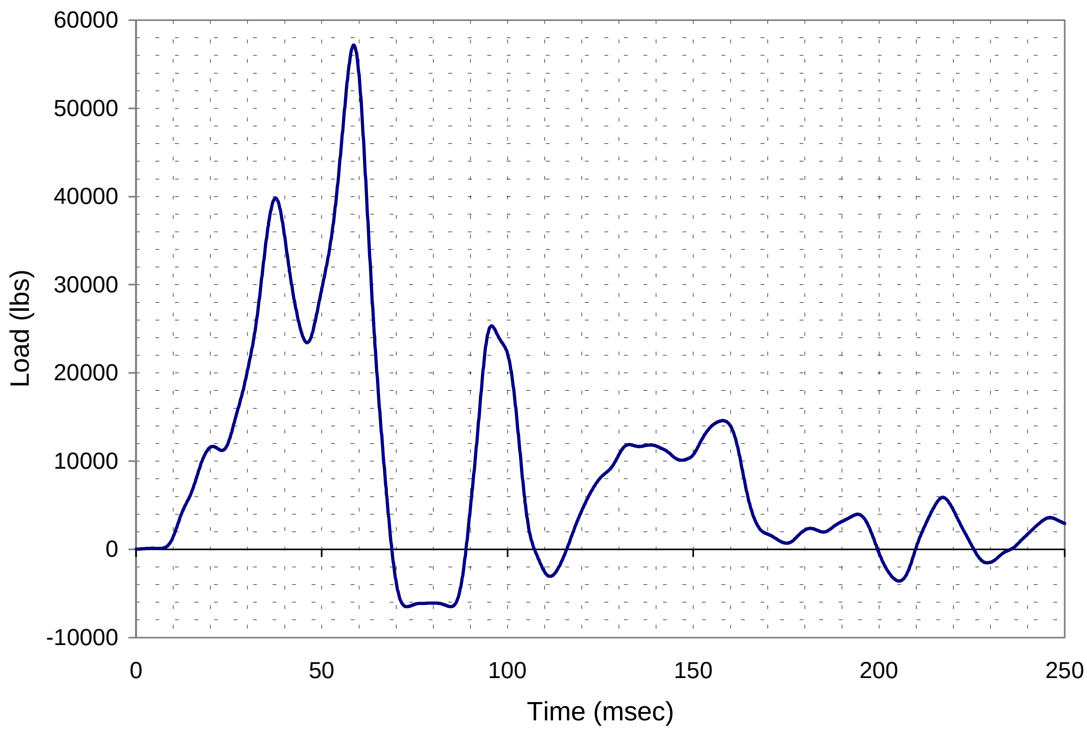

FIGURE B-99. PLATFORM LOAD CELL #4
(NEFF Channel 215)

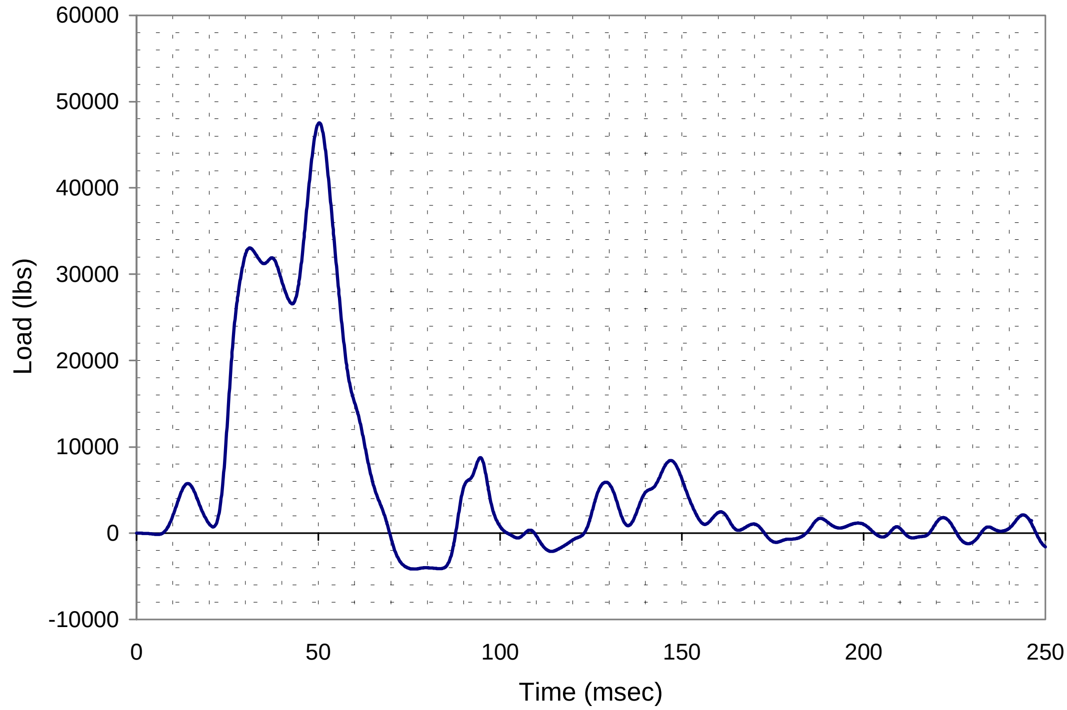

FIGURE B-100. PLATFORM LOAD CELL #5
(NEFF Channel 219)

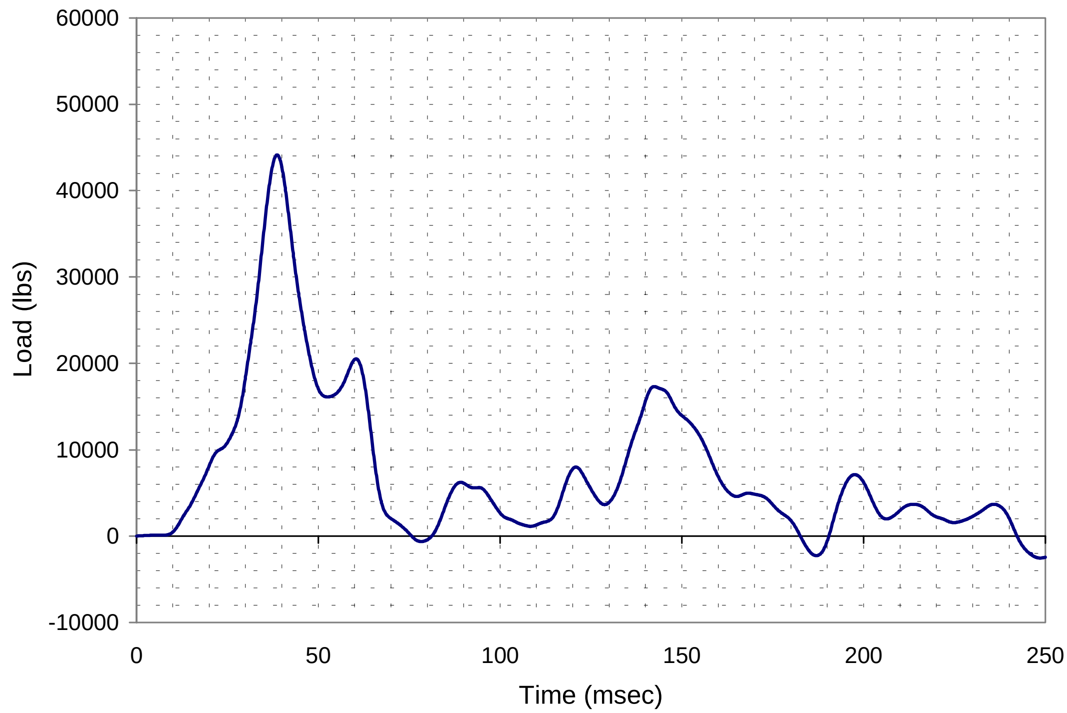

FIGURE B-101. PLATFORM LOAD CELL #6
(NEFF Channel 211)

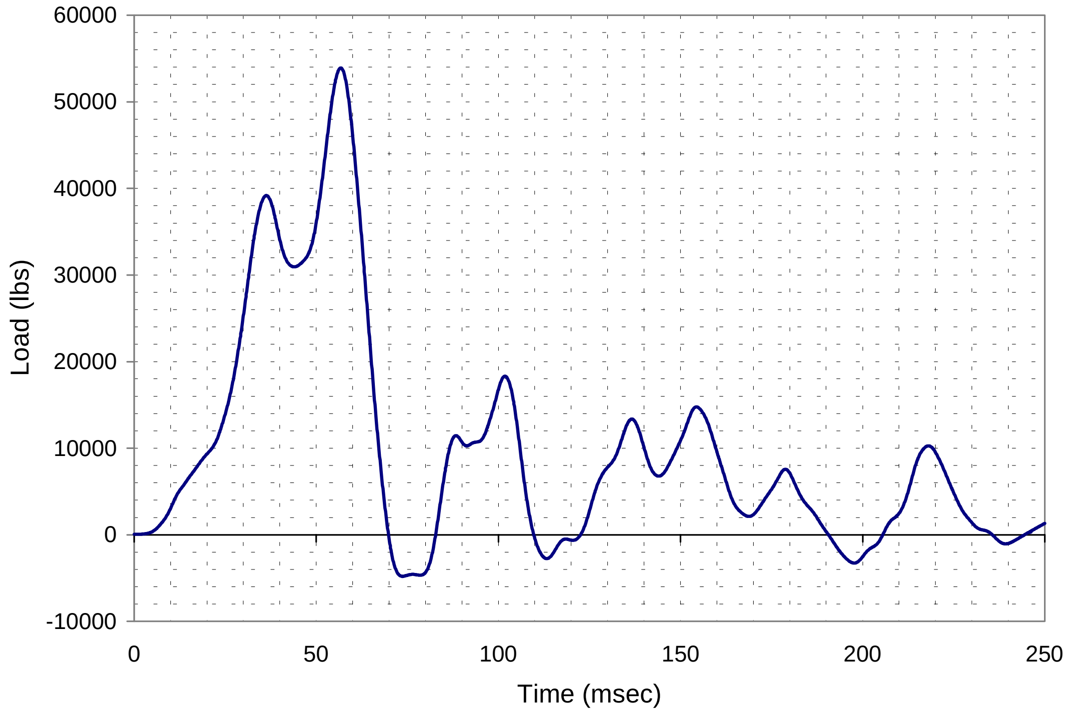

FIGURE B-102. PLATFORM LOAD CELL #7
(NEFF Channel 226)

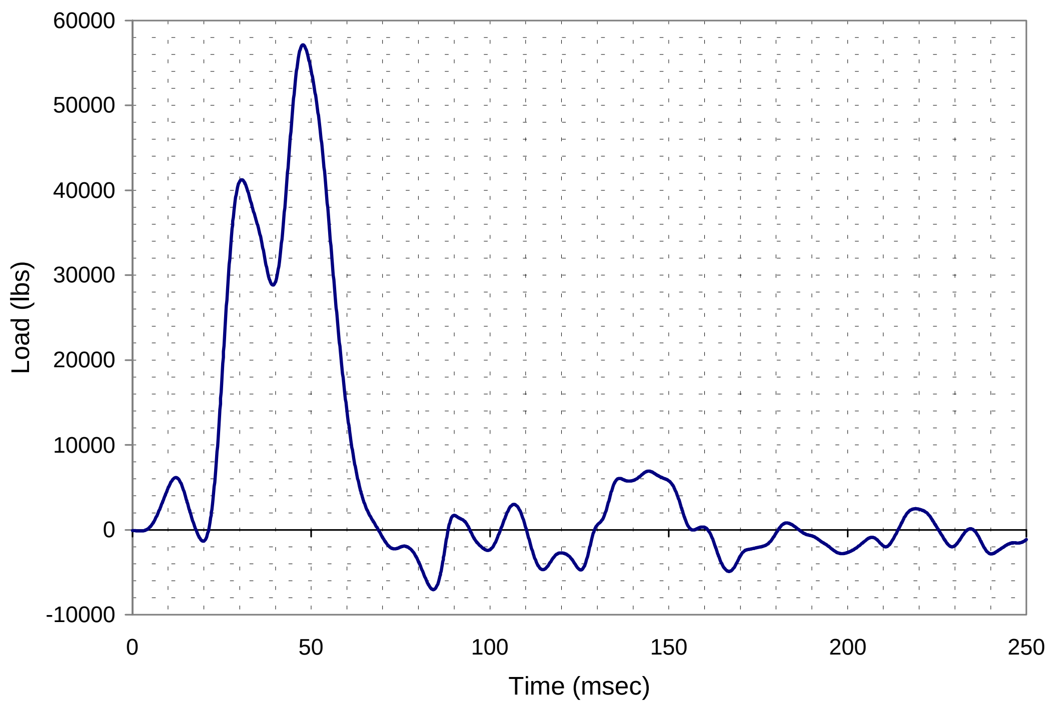

FIGURE B-103. PLATFORM LOAD CELL #8
(NEFF Channel 223)

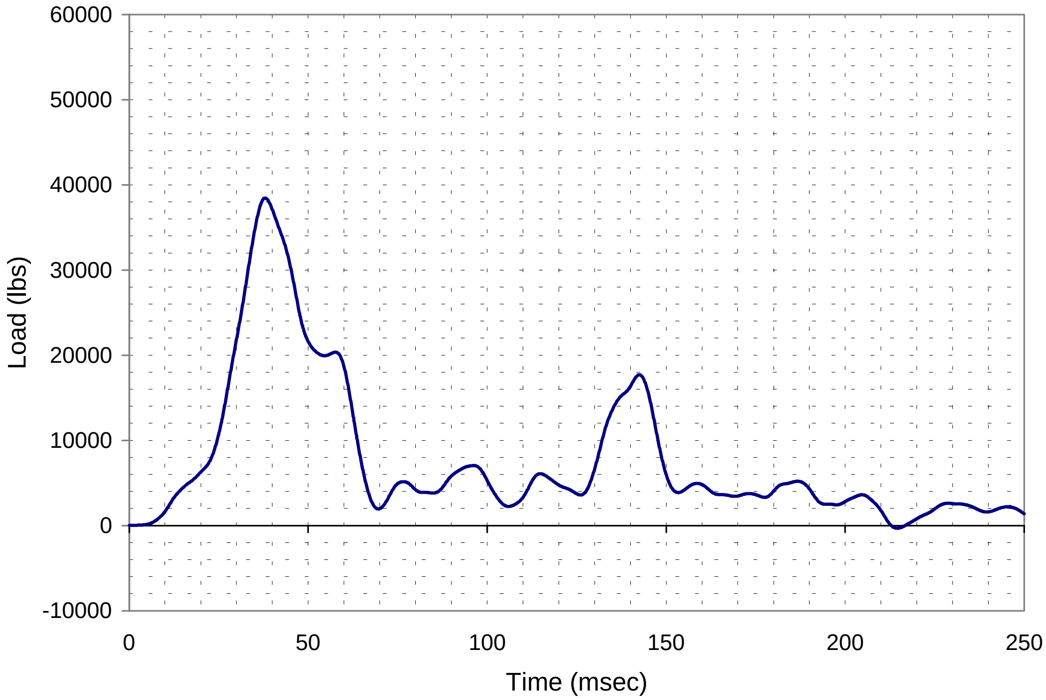

FIGURE B-104. PLATFORM LOAD CELL #9
(NEFF Channel 225)

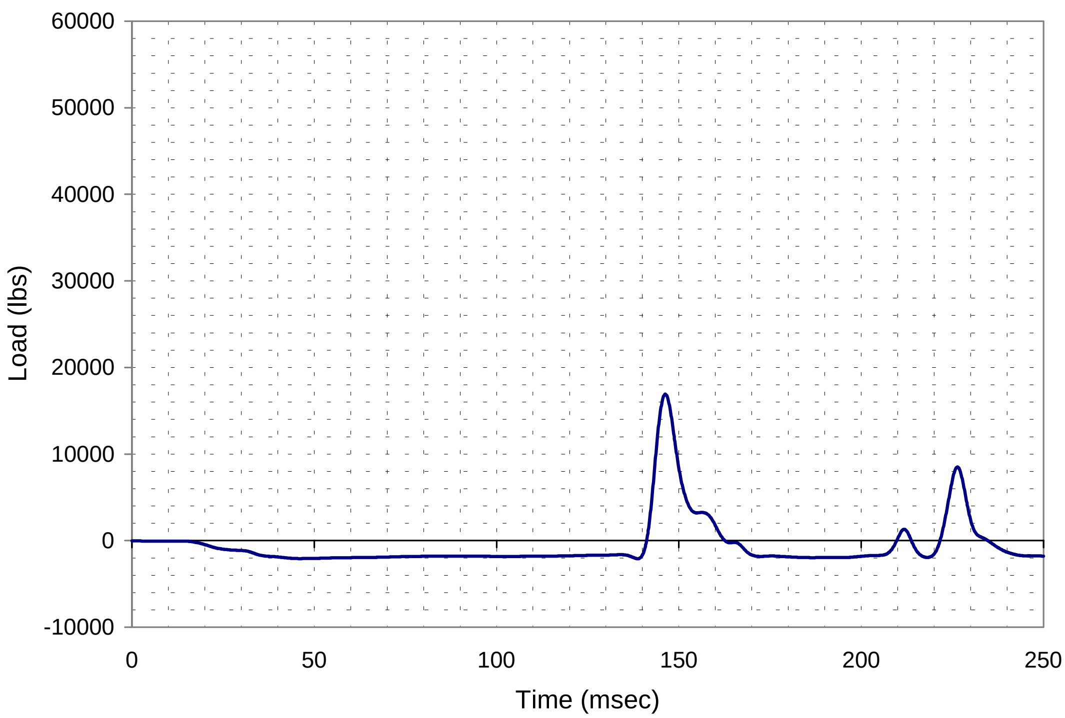

FIGURE B-105. PLATFORM LOAD CELL #10
(NEFF Channel 430)

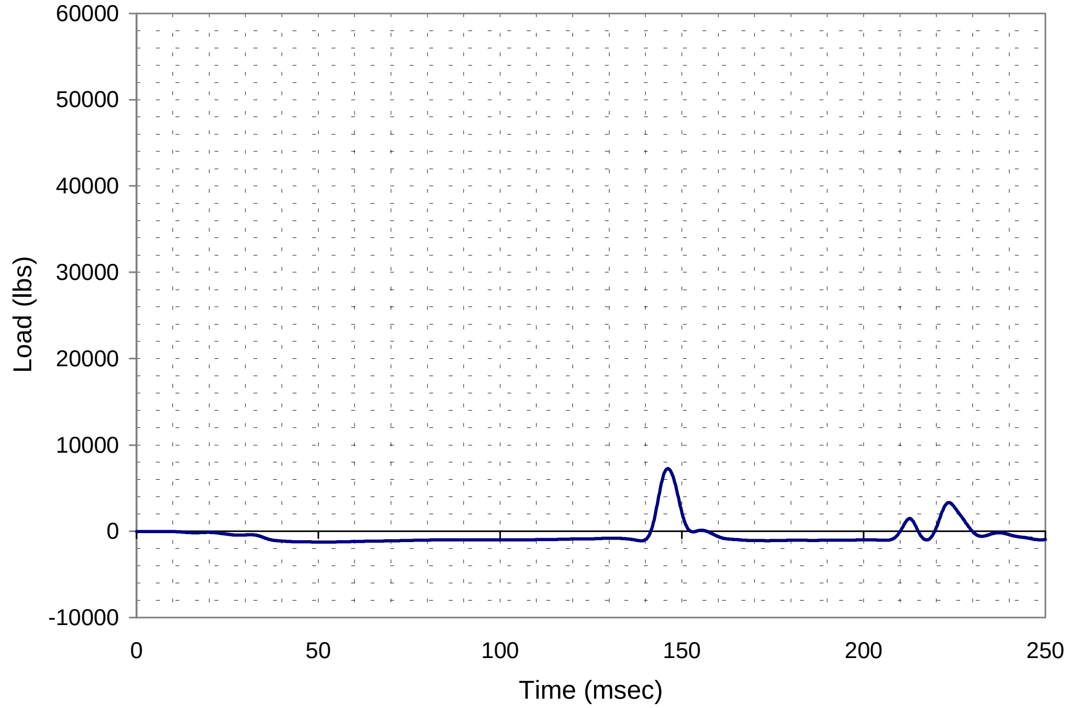

FIGURE B-106. PLATFORM LOAD CELL #11
(NEFF Channel 427)

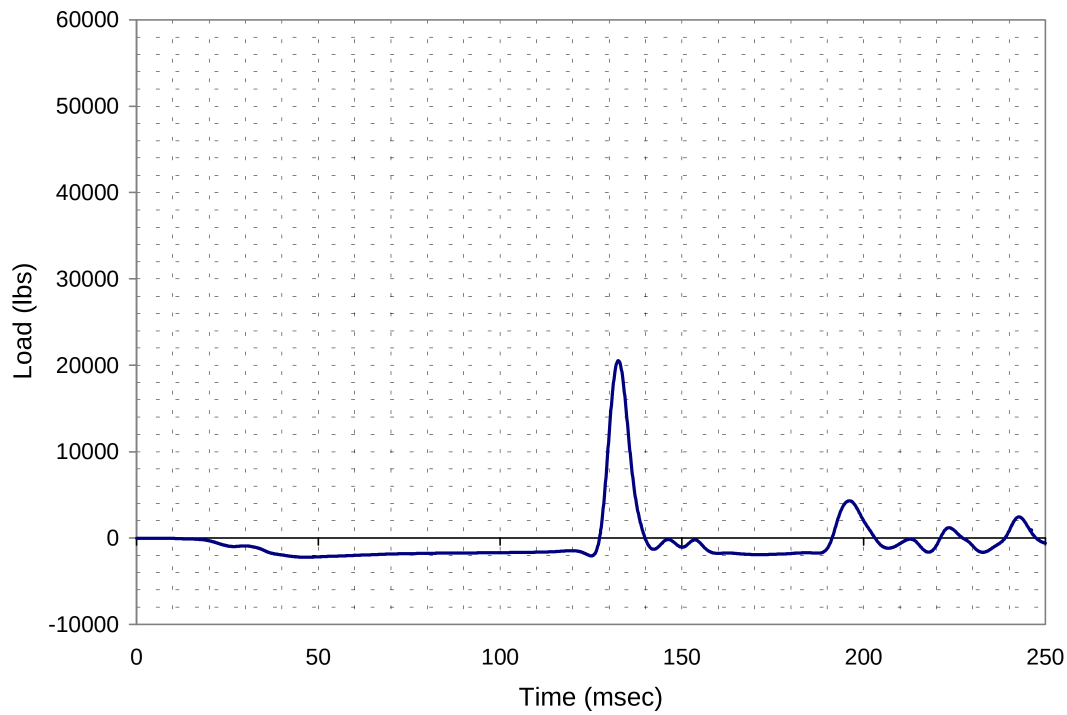

FIGURE B-107. PLATFORM LOAD CELL #12
(NEFF Channel 426)

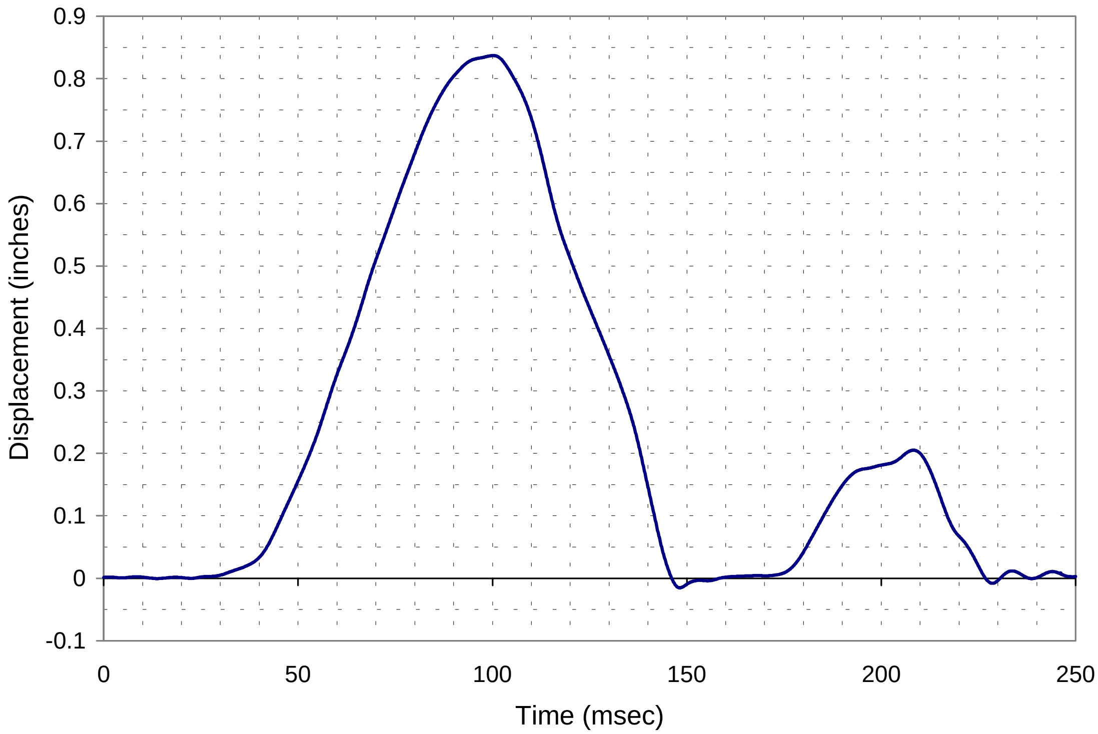

FIGURE B-108. PLATFORM STRING POTENTIOMETER #1
(NEFF Channel 202)

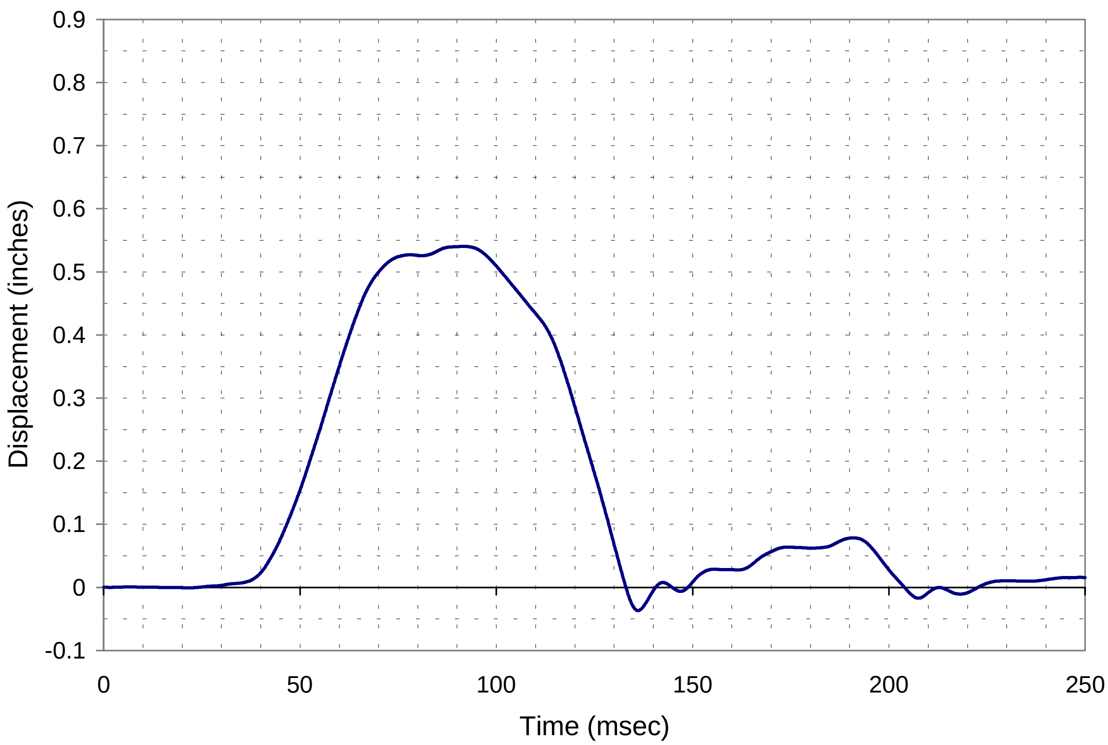

FIGURE B-109. PLATFORM STRING POTENTIOMETER #2
(NEFF Channel 206)

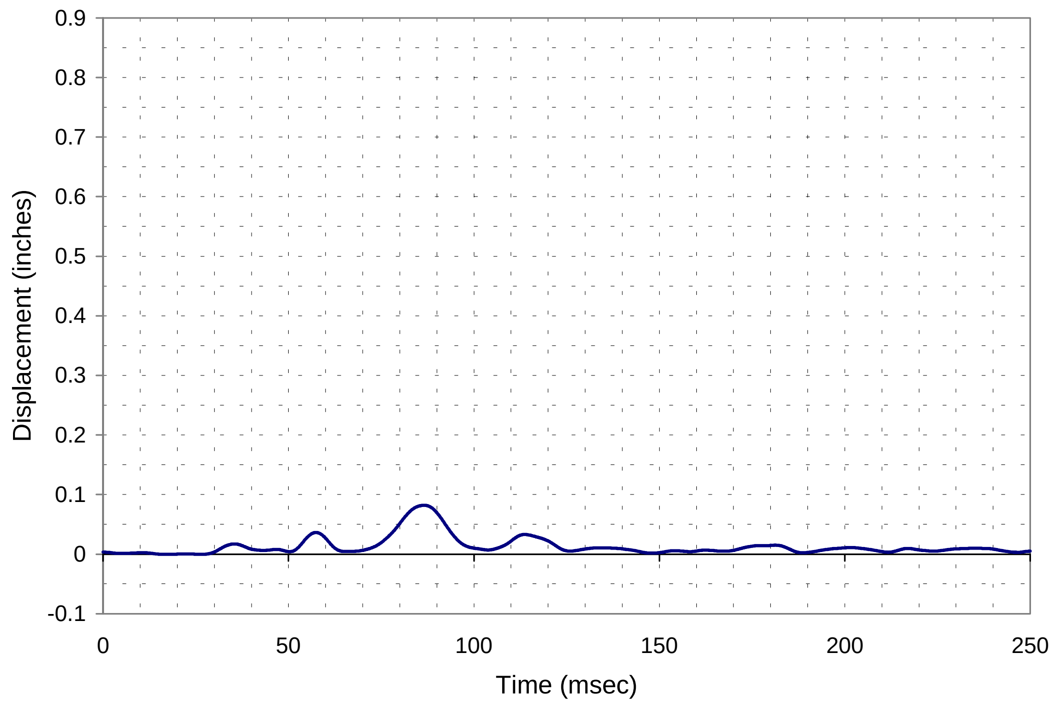

FIGURE B-110. PLATFORM STRING POTENTIOMETER #3
(NEFF Channel 217)

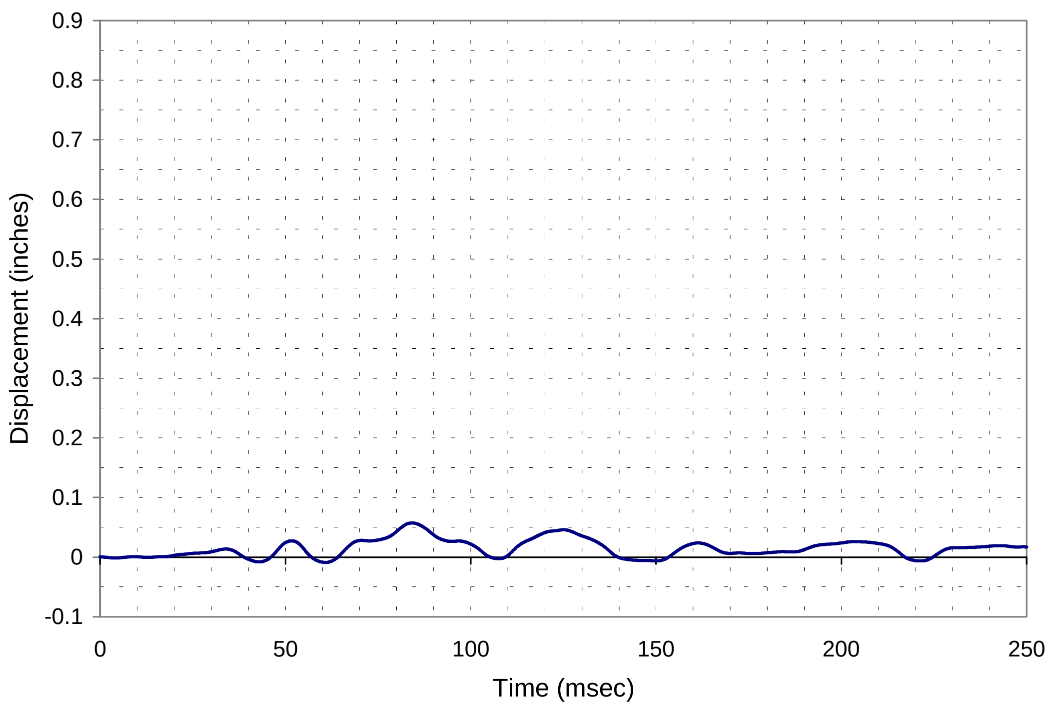

FIGURE B-111. PLATFORM STRING POTENTIOMETER #4
(NEFF Channel 221)

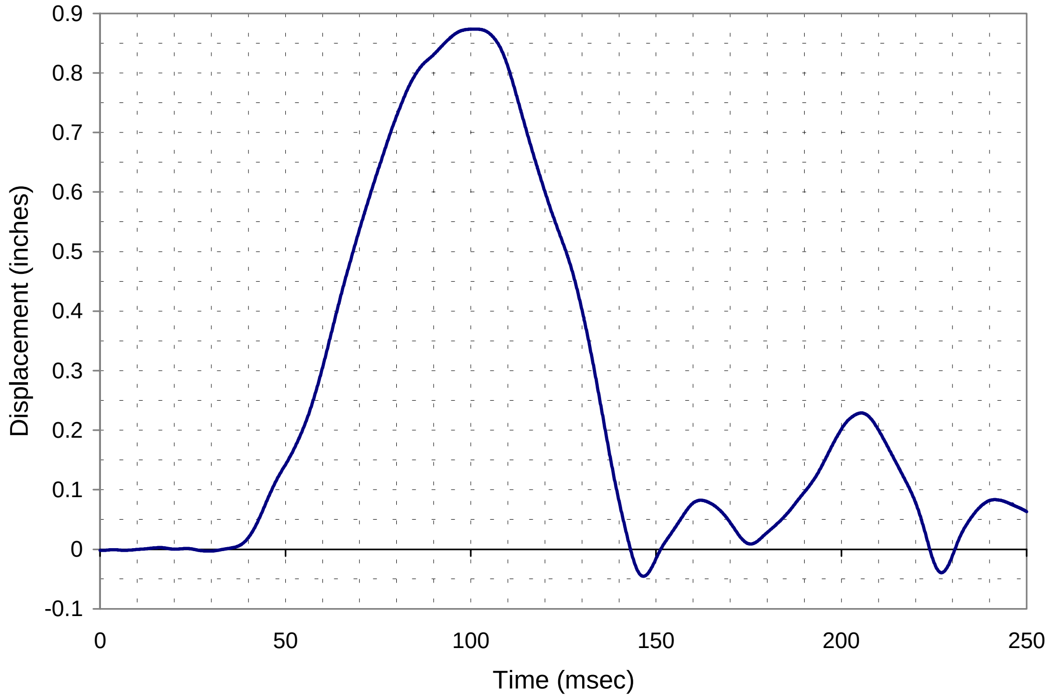

FIGURE B-112. PLATFORM STRING POTENTIOMETER #5
(NEFF Channel 429)

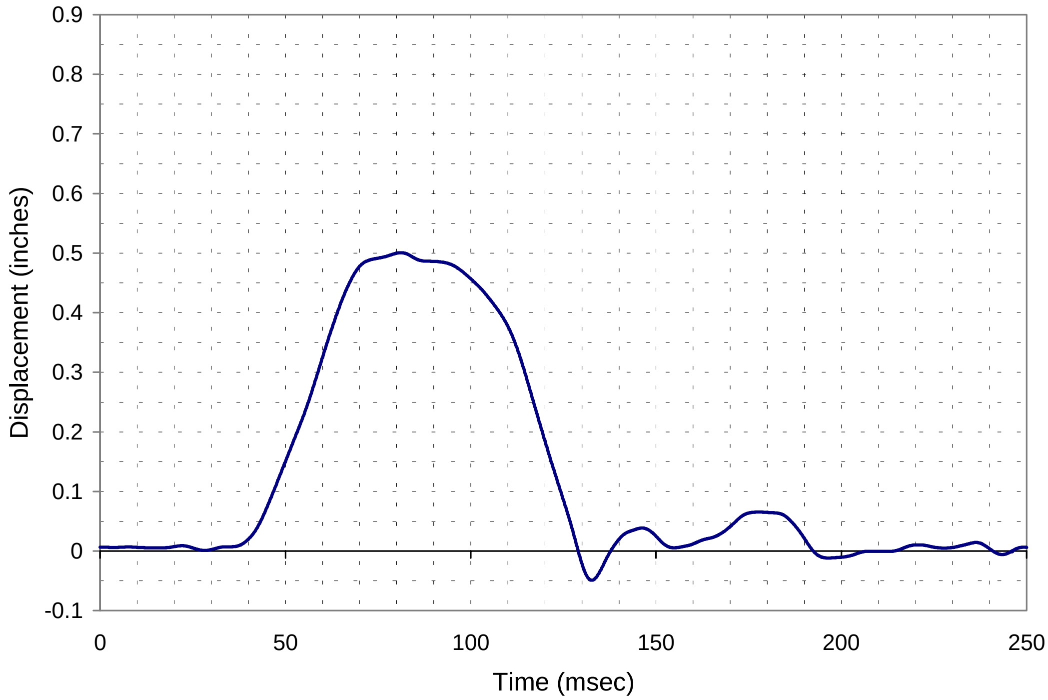

FIGURE B-113. PLATFORM STRING POTENTIOMETER #6
(NEFF Channel 425)